UNIVERSITY OF SOUTHAMPTON

ABSTRACT

FACULTY OF ENGINEERING AND APPLIED SCIENCE

DEPARTMENT OF ELECTRONICS AND COMPUTER SCIENCE

Doctor of Philosophy

SUBSTATION EARTHING

By Miszaina Osman

Good substation earthing is essential for safe and reliable power systems. The main objective of this research is to study and develop a safe substation site, within not only the substation but also its immediate vicinity, with particular attention to the impedance of substation earthing mats and the distribution of the surface potentials. CDEGS MALT software package is used to model the earthing system, and the results obtained are analysed with other methods, namely the analytical model, numerical method, and experimental technique where applicable. CDEGS MALT software has a high reputation throughout the world. This has been verified in hundreds of technical papers published in the most reputed international journals to prove its reliability and accuracy. An electrolytic tank is also used throughout this research. Part of the initial study shows that the experimental results and the computational results compares very well with less than 1% difference in most cases. The computer software CDEGS MALT and the experimental tank are used to investigate some issues regarding substation earthing. The first issue investigated is regarding an earthing standard widely used in the UK, which is the S34, and some other common theoretical formulae relating to the resistance and surface potential of simple earthing systems. The second issue involves the resistance of an earthing disc with varying depth. The resistance and surface potential is greatly affected as the buried depth of the disc is changed. The next aspect is the effect of an insulating barrier to the earthing system. Using an insulating barrier can decrease the surface potentials in the vicinity outside the barrier significantly. However, this is at the expense of a slight increase in the resistance of the earthing system and an increase in surface potential between the grid and the barrier. However, the percentage increase is far less than the percentage decrease in surface potential that can be achieved outside the barrier. When the barrier is made of plates with varying gap spacing, the spacing of the plates is very critical. However, it was found that a barrier made of insulating plates at a specified spacing is fit to act as a solid barrier. This can reduce costs and is easier to drive into the ground. Although CDEGS MALT proves to be reliable and accurate, as with all software, there are bound to have some defects. It was discovered that the percentage of difference between CDEGS MALT and experimental results increases when potentials measured are very close to the earthing grid. This proximity effect reduces as the earthing grid is buried at approximately 12 times the rod diameter.

CONTENTS

List of Figures

List of Tables

Acknowledgements

First, I would like to express my utmost gratitude to God, The Almighty, for all the blessings and guidance He has bestowed on me.

My grateful thanks to my project supervisors, Dr. George Chen and the late Professor Tony Davies for their constant encouragement and support throughout this project.

My special thanks and appreciation to Dr. Richard Stoll for his kind concern, help and advice. His help has been most invaluable in this project.

Special appreciation and thanks to the late Mr. Rolland Caldecutt, for his great ideas and assistance in the laboratory. Also, many thanks to Mr. Brian Rogers and Mr. Neil Palmer for their help.

My gratitude is also extended to the National Grid Company plc, the funding company for this project, and in particular to Dr. Neil Pilling.

Last but not least, special thanks to my husband, my daughter, my parents, my family and friends for their support and encouragement.

Definitions

A	area of grid
a	spacing between two adjacent electrodes (Wenner, Schlumberger and S34)
bd	buried depth
C_1	current probe 1
C_2	current probe 2
C	foot resistance reduction factor
c	spacing between two barrier plates
c'	spacing between two earthing rod
d	distance from centre of grid
d'	rod diameter
d''	$\sqrt{2} \times$ rod diameter
E	electric field
E_t	overall error in experimentation
h	top layer soil thickness
I	current
I_{BODY}	body current
J	current density
K'	a point on the earth surface x_k distance away from the earthing grid for Fall-of-Potential method
k	factor to calculate resistance of grid in S34
L	length of buried conductor
L_1	length of cylindrical tube (water resistivity measurement)
l	rod length
N	number of vertical rods
P_1	potential probe 1
P_2	potential probe 2
P	a point on the earth surface x_p distance away from the earthing grid for Fall-of-Potential method
ρ	resistivity
ρ_S	resistivity of the top soil layer

R	resistance
R_B	body resistance
R_{ext}	external resistor in experimental circuit
R_{FT}	parallel resistance of the feet, for touch voltage situations
R_{FS}	series resistance of the feet, for step voltage situations
R_g	grid electrode earthing resistance
r	rod radius
r_1	radius of cylindrical tube (water resistivity measurement)
r_2	radius of the experimental tank
t	maximum expected shock duration
V	voltage
Vs	surface potential
V_{TOUCH}	touch voltage
Vx	potential of any point at a distance x from the axis of a grid
x	distance of barrier from edge of grid
x'	distance from the axis of the grid (S34)
x''	distance from an earthing rod
x_p	the distance between the voltmeter reading and the earthing grid for Fall-of-Potential method
x_k	the distance between the current electrode and the earthing grid for Fall-of-Potential method
y	depth of barrier from water surface
z	spacing between two potential probes in Shlumberger method
σ	conductivity

Abbreviations

AC	alternating current
DC	direct current
GPR	ground potential rise
S.D.	standard deviation

CHAPTER 1

Introduction

Power plants and substations are extremely vulnerable to hazards of lightning strikes, electrical and mechanical equipment malfunctioning, and of course, human errors in which surge current in the order of kiloamperes is impressed on the plant or is generated from within. Hence, earthing has become one of the dominant problems of system design.

1.1 Purpose of earthing

Adequate earthing of electrical substations is of significant importance to increase the reliability of the supply service as it helps to provide stability of voltage conditions, preventing excessive voltage peaks during disturbances, and a means of providing a measure of protection against lightning. Earthing generally means an electrical connection to the general mass of earth, the latter being a volume of soil/rock etc., whose dimensions are very large in comparison to the electricity system being considered. It should be noted that in Europe and UK, the term 'earthing' is used, whilst in America, the term 'grounding' is more common.

Some of the reasons for having an earthed system are [1, 2]:

- To provide a sufficiently low impedance path and means to carry and dissipate electric currents into ground under normal and fault conditions without exceeding any operating and equipment limits or adversely affecting continuity of service.
- To assure such a degree of human safety that a person working or walking in the vicinity of grounded facilities is not exposed to the danger of a critical electric shock.
- To retain system voltages within reasonable limits under fault conditions (such as lightning, switching surges or inadvertent contact with higher voltage systems), and ensure that insulation breakdown voltages are not exceeded.
- Custom and practice.
- Graded insulation can be used in power transformer.

- To limit the voltage to earth on conductive materials which enclose electrical conductors or equipment.
- To stabilise the phase to earth voltages on electricity lines under steady state conditions, e.g. by dissipating electrostatic charges which have built up due to clouds, dust, sleet, etc.
- A means of monitoring the insulation of power delivery system.
- To eliminate persistent arcing ground faults.
- To ensure that a fault which develops between the high and low voltage windings of a transformer can be dealt with by primary protection.
- To provide an alternative paths for induced current and thereby minimise the electrical "noise" in cables.
- Provide an equipotential platform on which electronic equipment can operate.

The earthing system must generally have a low impedance in order to perform successfully in fulfilling any of the above functions, so that in dispersing or collecting current from the ground, an excessive voltage rise does not occur.

1.2 Safety functions of earthing

Safety is the main concern of any earthing of electrical installations. Basically, an earthing system is designed to provide two safety functions. Firstly, it is called bonding. Any exposed conductive metalwork, that is likely to be touched, is connected together by bonding conductors. Metal enclosures are usually used to house electrical equipment, and the enclosure will temporarily become live if there is a live conductor that touches it. Hence, if there is such a fault, the potential on all exposed conductive metalwork will virtually be the same, due to the bonding conductors. In other words, the resulting potential difference can be lowered to a minimal value as the bonds equalise potential within the site. An equipotential platform is thus created. A bonding conductor will ensure that if a person is in contact simultaneously with two different pieces of exposed metalwork, the person does not receive a shock, as the potential difference is minimal or insufficient for this to take place.

The second function of the earthing system is to ensure that any fault current can return to source in a controlled manner, in the event of an earth fault. 'Controlled manner' means that the return path is provided and predetermined so that damage to equipment or injury to individuals can be avoided. Sufficient earth fault current should flow to operate protective devices correctly, which will in turn initiate the operation of circuit breakers or fuses to interrupt the flow of current. Hence, the earthing system should be designed to have impedance low enough to ensure the earth fault current can pass through. In addition, the earthing system will experience a rise in potential while the fault current is flowing and this should also be limited to a predetermined value.

These are the purpose of the earthing system. However, they are also required to overcome a wide range of different problems encountered. Some of them are listed below:

a) Conventional Fault: Faults that arise from damage to a cable or breakdown of the phase to earth insulation in a piece of equipment. This is termed 'power frequency' faults because most of the energy dissipated in the fault will be at mains frequency (50 Hz).

b) High frequency faults: These faults usually take place at sites where large amounts of power are rectified or capacitor banks are switched, such as radio or television transmitters. Hence, energy will be available at higher frequencies than normal. The earthing system must be designed to provide low impedance at these frequencies.

c) Lightning protection: Many electrical installations are prone to the risk of damage from lightning strike, such as windfarms [2-4]. Hence, an adequate earthing system is a fundamental part of the electrical installations.

During some types of maintenance or construction, the earthing system is also used as a means of achieving safe working conditions. Before any work can commence, plant that was previously energised has to be switched off and its previously live components connected to earth. This allows any stored energy to be discharged safely to ground and

helps to prevent dangerous voltages arising on the equipment being worked on. Places like a paper manufacturing plants or when explosives or volatile chemicals are present, the earthing system is required to continuously discharge the build up of static charge.

Indeed, the earthing system performs a wide range of functions throughout all the stages of providing electricity, i.e. at the generating station, the electricity company substation through to the electrical installations in homes, offices, and factories.

1.3 Aims and objectives of research

The general aim of this research is to improve the existing earthing practice in industry, and to decrease the percentage of fatal accidents in or outside the substation. More specifically, the objectives of this research are as follows:

i) To improve the accuracy with which the impedance of a substation earthing system to "remote" earth may be calculated.
ii) To analyse the surface potential distributions in and around the substation.
iii) To analyse the different methods used in earthing calculations and computations.
iv) To decrease the surface potentials outside the substation to ensure better safety to the public by using a highly resistive barrier.

The following chapter descriptions outline how and where these objectives were met during the course of this study.

1.4 Summary of Chapters

This thesis is divided into nine chapters with appendices. Chapter 1 gives the introduction and overview of the research.

Chapter 2 provides background information on power systems earthing, and is intended for electrical engineers who may not be familiar with some of the aspects of power system earthing.

Chapter 3 outlines the method of analysis used throughout the research. It covers various methods available ranging from analytical method, methods developed by other researchers, British and American Standards, computational method and experimental technique. A general overview of the computer software used in this research, which is CDEGS MALT, is also included. The electrolytic tank used in this research is explained and history of electrolytic tanks used in earthing researches is given.

In Chapter 4, a comparison of CDEGS MALT and other theoretical methods are given. This chapter can be divided into two distinct sections. The first section deals with comparing CDEGS MALT with existing formulae for the resistance and surface potentials of vertical rod(s). The next section investigates part of the S34 Standard, by comparing with the computer software, CDEGS MALT.

In Chapter 5, the measured resistance and surface potentials of multi rod array are investigated. Comparisons are made between computed (CDEGS MALT) and experimental results. The S34 standard formulae are also used for comparison where applicable. This comparison will give more assurance of the accuracy and reliability of the experimental results.

Chapter 6 investigates on the variation of DC resistance of an earthing disc with increasing burial depth.

In Chapter 7, the effect of an insulating barrier on one side of the earthing system is investigated. Two different types of barrier is used, one being a solid barrier and the

other is a barrier made of plates with varying gaps. The effect of these barriers on the resistance and surface potential of the earthing system is studied.

Chapter 8 details the limitation found in the computer software CDEGS MALT. It was found that percentage difference between CDEGS MALT and experimental results increases as the surface potentials measured are very close to the earthing rod. Various types of grids are tested, with particular attention given to measurements in and around the grid.

Chapter 9 outlines the conclusions obtained from this research and gives recommendations for future work.

CHAPTER 2

Literature Review

2.1 Earth Resistance

'Earth Resistance' means the resistance of the earth to the path of an electrical current. The earth is not a good conductor of electricity, when compared to conductors such as metals. It so happens that, in general, the cross section of the path taken by the current is very large, and this means that, despite the poor conductive qualities of the soil, the actual resistance may be quite small. The earth has long been used as a conductor; very often for safety reasons and its resistance is a matter of considerable importance.

The condition and content beneath the surface of the soil is sometimes an important aspect to a certain number of cases. Many methods have been developed by which investigations can be made on the surface of the soil. These are usually based on the measurement of one of the physical properties of the soil, and one such property is the electrical resistance. This resistance varies with the type of soil and in particular with the moisture content. By measurements made on the surface, vital information can be obtained, from which deductions can be made as to the nature of the underlying soil.

In electricity-supply systems, it is common practice to connect the system to "earth" at suitable points, the idea since in the event of a fault, sufficient current will flow through the fault path so that the protective gear will operate and isolate the faulty circuit. It is therefore essential that this "connection to earth" be of a sufficiently low resistance.

2.2 Conduction through the soil

The soil has been used as a conductor of electricity since the earliest days of electric supply. It was thought that, because the dimensions of any current path through the earth would be very large, the resistance of any such path would be negligible. The point which was overlooked was that means had to be provided to pass current into and out of

the earth, and that these means, in the form of plates, rods or pipes, will have a finite resistance to the passage of current from them into the earth.

The electrical properties of the soil are in themselves of interest and importance, particularly the specific resistance or resistivity. The resistivity is one of the factors in determining the resistance of any earth electrode and is of importance in connection with the problems of interference between power lines and telecommunication circuits.

Most soils and rocks when completely dry are non-conductors of electricity, exceptions to this are certain mineral bodies, which are conductors because of their metallic content. Sands, loams, and rocks are, however, in themselves of such high resistance that they can be considered as non-conductors. When they contain water, the resistivity drops considerably and they must then be considered as conductors, although very poor ones when compared with metals. The resistivity of soil would be determined by the quantity of water held in the soil, and on the resistivity of the water itself. In other words, conduction through the soil becomes conduction through the water held in the soil and so the conduction must be electrolytic.

Thus, the main factors that determine the resistivity of soil are [5]:

(a) Type of soil
(b) Chemical composition of salts dissolved in the contained water
(c) Concentration of the salts dissolved in the contained water.
(d) Moisture content
(e) Temperature
(f) Grain size of the material and distribution of grain size
(g) Closeness of packing and pressure

2.3 Soil resistivity measurements

Accurate soil resistivity measurements are essential, particularly when electricity companies are faced with having to establish substations in sites on reclaimed land usually with non uniform soil, having limited area and/or close to third party equipment (especially telecommunications and gas). These conditions complicate the design task,

and accurate measurements are essential if the most effective, economic solution is to be found.

The purpose of earth resistivity tests related to power system design is to assist in the determination of an appropriate soil model which can be used to predict the effect of the underlying soil characteristics on the performance of an earthing system during ground faults. The electrical characteristics of the earth are usually sufficiently uniform over horizontal distances to permit the soil beneath typical sites to be considered uniform over horizontal dimensions. In such cases, vertical variations in resistivity can often be described by one, two, or more frequently, three or more distinct horizontal layers of earth. Sometimes, however, earth resistivity variations over horizontal dimensions are significant and can therefore not be neglected. In such instances, the horizontal variations in resistivity can often be modelled as two or more distinct vertical layers of earth.

The first stage in designing an earthing system is to take a series of earth resistivity measurements and in order to do this, it is necessary to pass current through the earth by inserting electrodes into it so that current can be fed in and out. Some of the most frequently used methods for determining the resistivity of the soil are described in the next few sub sections. From these methods, a representative model of the ground can be constructed. It can comprise of horizontal and/or vertical soil layers having significantly different electrical resistivity values. Ideally, these measurements should be taken before the installation of electrical equipment, and the measurements should be taken in an environment free of electrical interference.

2.3.1 Wenner Method

The measurement configuration most widely used in the electric power industry to measure soil resistivity is a four-electrode (probe) method developed by F. Wenner [6]. As shown in Figure 2.1, four uniformly spaced electrodes are inserted into the earth surface along a straight line, with the outer pair being used as current input probes and the inner pair as potential references.

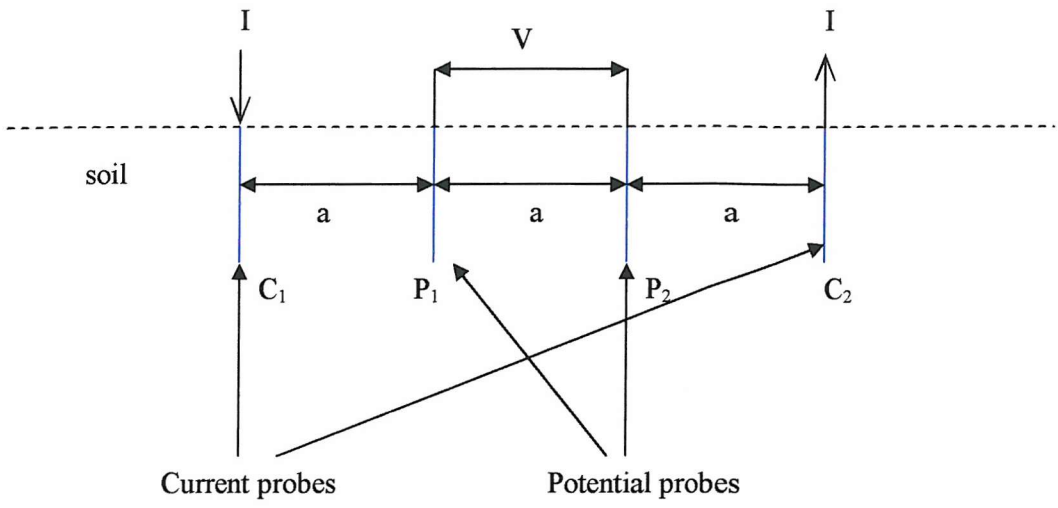

Figure 2.1: Wenner method

Using the Wenner geometry, the apparent measured resistivity is:

$$\rho = 2 \pi a R \ (\Omega m) \qquad (2.1)$$

where ρ is the apparent soil resistivity in ohm-meters, 'a' is the spacing between two adjacent electrodes in meters and R is the measured apparent resistance (ratio of measured voltage to test current in ohms). 'Apparent resistivity' is the term used here since the formula assumes the soil is uniform within a hemisphere to a depth approximately 'a' metres below the centre of the measurement array.

When the electrode penetration depth is small compared to electrode spacing, equation 2.1 effectively describes the variation in measured resistivity as a function of electrode separation 'a'. Physically, the greater the electrode spacing, the greater the volume of earth encompassed by the test current in its traverse from C_1 to C_2 and hence, the greater the depth of earth involved in the measurement. In practice, the depth of each electrode should not normally exceed 'a' divided by 20 and usually the depth does not exceed 0.3m [7].

Information regarding the soil layering can be obtained by taking a series of readings, where 'a' is increased in steps. Thus, a plot of apparent resistivity against 'a' spacing can

be drawn to provide information on the general structure of the soil. Measurements should be taken over several traverses, which are representative of the site of interest, and up to a sufficiently long 'a' spacing (typically 30m to 60m). The test instrument used should be sufficiently accurate to measure quite small resistance values at these large spacing, i.e. in the order of 0.01 ohm to 0.002 ohm [7]. Also, the instrument should ideally be able to filter or reduce the effect of 'noise', due to 'natural earth' and any induced current present. Ideally, soil resistivity measurement should be made in the absence of buried metallic conductors or structures [8].

The simplest interpretation of a soil model problem is when the measured apparent resistivities, ρ, vary minimally around an average value. This indicates that the earth around the measurement site is reasonably uniform and has the resistivity equal to that average value. Generally, apparent resistivity curves change smoothly and do not exhibit abrupt changes. When there is a sudden change in the curve, it is an indication that the measurement array has just crossed a vertical fault or a local discontinuity close to earth surface. Also, the presence of buried pipes or other metallic structures close to the surface of the earth will also cause sudden changed in the apparent resistivity.

The results from the measurement of apparent resistivities against electrode spacing can be translated into an equivalent soil model using graphical or computerised method. The graphical method is described by Tagg [5]. Several computer programmes are available to help produce and interpret data to give the equivalent soil model. Generally, they follow a curve fitting process, and the unknowns are the individual layer thickness and resistivity. Examples of such programs are the CDEGS program (RESIST module) [9, 10] and the SPEF (Soil Parameters Estimation using Finite Expressions) [11].

2.3.2 Schlumberger Method

An important variation of the Wenner method, which is widely used in geophysical prospecting, is the unequally spaced symmetrical configuration, called the "Schlumberger" arrangement (Figure 2.2) [7]. This method circumvents a shortcoming of the Wenner method often encountered at large probe spacing whereby the magnitude of the potential between the potential probes becomes too small to give reliable

measurements. By increasing the distance between the potential probes, the potential value is increased and the sensitivity limitations encountered using the Wenner method may be overcome. This method is generally more accurate for measurement of soil resistivity for small areas. The apparent resistivity according to the Schlumberger method is given by:

$$\rho = \pi R a (a+z)/z \qquad (2.2)$$

where a is the spacing between adjacent potential and current electrodes (in meters), z is the spacing between potential electrodes (in meters) and *R* is the measured apparent resistance.

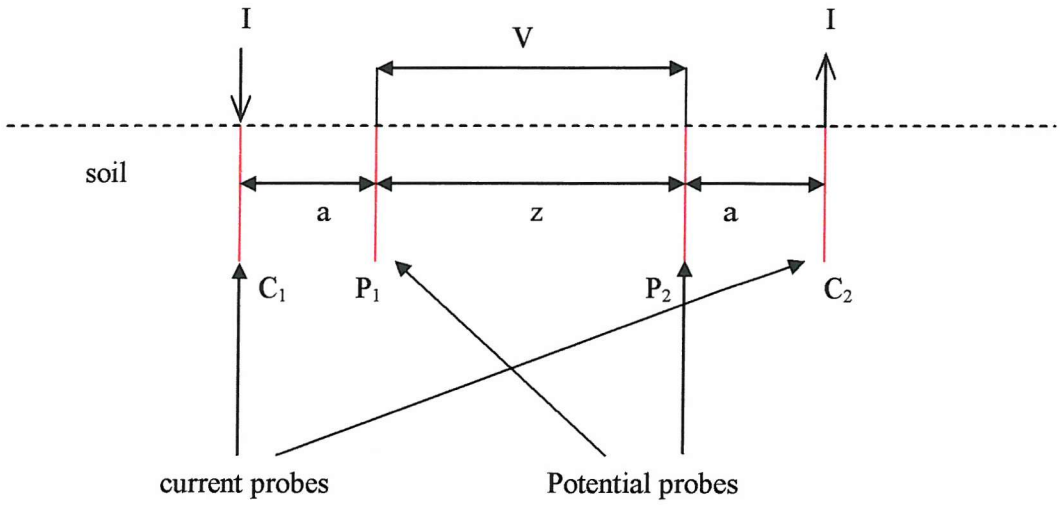

Figure 2.2: Schlumberger method

2.3.3 Rod Resistance Measurement

The next available method to measure soil resistivity is by using rod resistance measurement [7, 12]. A vertical rod is inserted, say for one metre, into the soil and its resistance measured. It is then inserted at a further one metre and the resistance measured again. This process is repeated until the rod has been installed to the required or maximum achievable depth and at several representative locations within the site of interest. One formula which expresses the resistance of a rod of length 'l' and diameter 'd'' in uniform soil of resistivity 'ρ' is as below [5]:

$$R = \frac{\rho}{2\pi l}\left(\ln\frac{8l}{d'} - 1\right) \qquad (2.3)$$

The apparent uniform soil resistivity 'ρ' is calculated using this formula, which will provide the measured resistance value at each depth. A graph of the resistivity measured against depth can be drawn and by examining the graph, it is possible to estimate where significant changes in soil resistivity are occurring. Once again, computer software can be used to derive an equivalent soil model.

2.4 Fundamental concepts of an Earthing System

A simple earthing system consists of horizontal conductors (also called "mesh" or "grid" conductors) buried at a certain depth below the earth's surface and long vertical conductors (also called "earthing rods") that are connected to the grid formed by the horizontal conductors. The horizontal grid is usually rectangular and is subdivided into a number of rectangular loops or "meshes".

When the fault current is injected into the earthing system, it flows throughout the earthing system and leaks into the surrounding earth from the bare metallic conductors. The earthing system and all metallic structures connected to it will be at a relatively high electrical potential because of its energization by the fault current; as current flows through the earth away from the earthing system, the potential drops and eventually reaches zero at a great distance from the earthing system. This zero potential zone is usually referred to as "remote soil" [2].

Figure 2.4 shows electrical potentials, which occur at the earth's surface when the earthing system (with 4 meshes, earthing rods at every corner) is energised. Note that these potentials are plotted as a percentage of the electrical potential of the energised earthing system. This electrical potential of an energised earthing system is usually termed "ground potential rise" or simply "GPR".

From Figure 2.3, it can be seen that earth surface potentials are lower than the GPR and vary greatly from one location to another. Location directly above a grid conductor,

earth surface potentials are closest to the GPR but, on the other hand, potential "valleys" occur in the middle of grid meshes and the difference between the GPR and the earth surface potential is maximum at these centre points. This means that a person standing at the centre of a mesh and contacting any metallic structure (e.g., a switch handle, the housing of a piece of equipment, a ladder, etc.) which is connected to the earthing system, will be subjected to the greatest "touch voltage" available anywhere within the earthing system. A touch voltage is the type of potential difference which could cause current to flow through the arm-body-leg path of a person, e.g. a person standing on the ground and touching earthed metal equipment in the substation (assumed to be at the same potential as the earthing system) [13]. UK standards define the worst case touch potential as the difference between the GPR and the ground potential one metre diagonally outwards from the grid corner.

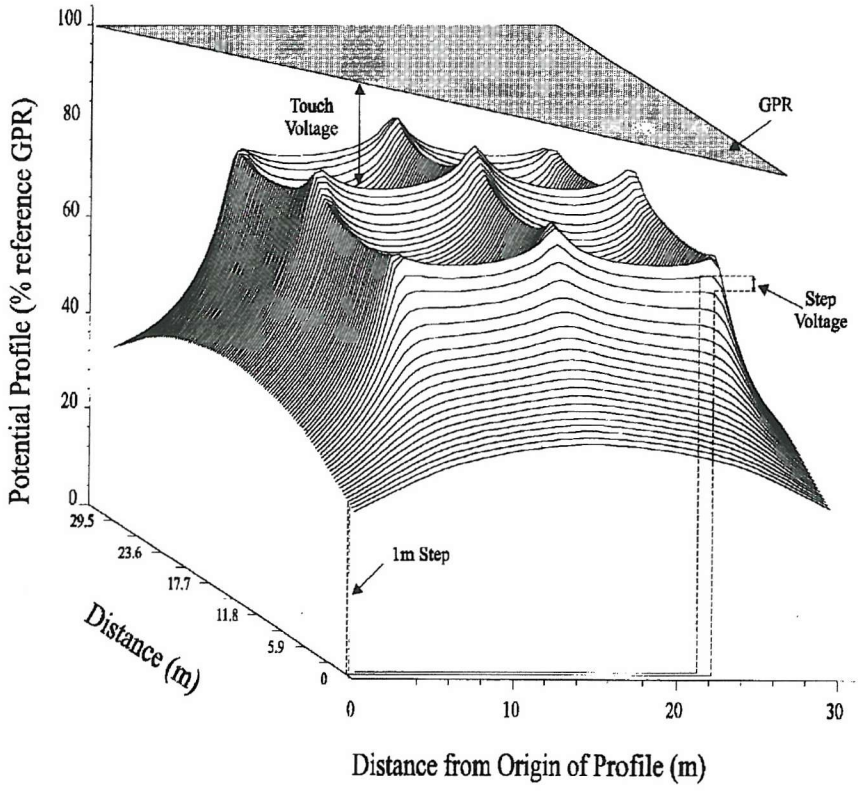

Figure 2.3: 3-D Plot of Earth Surface Potentials above Earthing System

Due to the sharp drop in earth surface potentials outside the perimeter of the earthing system, large touch voltages could also be possible. However, when substations are involved, it is normal practice to install a boundary fence 1 m within the earthing system

perimeter to ensure that no substation metallic structures are present outside the earthing system area, where large touch voltages would otherwise be present.

Although a person should normally not be exposed to touch voltages outside the earthing system perimeter, "step voltages" are possible. As Figure 2.4 shows, the steep potential gradient outside the earthing system perimeter could result in a significant potential difference appearing between two earth surface locations at which a person's feet are positioned. A step voltage is the type of potential that would cause a current flow through the legs of a person. The worst case step potential is defined as the voltage of 1 metre of ground surface diagonally outwards from above a grid corner [13]. The ground above the grid is normally covered with crushed rock to increase the ground surface resistivity, but the ground outside would normally have a low surface resistivity and so the acceptable touch and step potentials there would be lower.

When an electrical current is injected into the earth by an earthing system, the current is met by a resistance, which depends directly upon the properties of the soil, and more particularly upon the resistivity of the soil. Due to the effect of current flowing through this resistance, the electrical potential of the earthing system and all metallic structures connected to it rises. When the interconnected system of metallic structures is small, the potential rise throughout the system is approximately the same and is termed "GPR".

For a given injection current, the GPR is directly proportional to the soil resistivity. It is therefore very important, when designing an earthing system, to make soil resistivity measurements at the substation site to ascertain the soil structure; otherwise, the performance of the earthing system cannot be predicted. Similarly, seasonal variations in soil structure (e.g., change in soil structure when the top layer freezes) must also be taken into account to ensure an adequate design.

For a given injection current, the GPR is approximately inversely proportional to the area of the grid. Note that the shape and burial depth of the grid also affect the GPR to some extent.

The ground potential rise is defined with respect to a point in the earth a great distance away from the substation, as shown in Figure 2.4. The GPR is therefore the reading that would be seen on a voltmeter one of whose leads is connected to the substation earthing system, and the other connected to a ground very far away. This can be seen in another way. If one end of a well insulated cable is grounded far away from the substation, and the other end is brought into the substation area during a fault, then the GPR is the voltage, existing between the cable conductor and any other conductor, that is connected electrically to the substation earthing system (this generally means all metallic structures within the substation perimeter). This illustrates the principle of a transfer voltage (low voltage transferred from the remote grounding point); it can also mean a high voltage transferred to a remote point which can endanger both personnel and equipment.

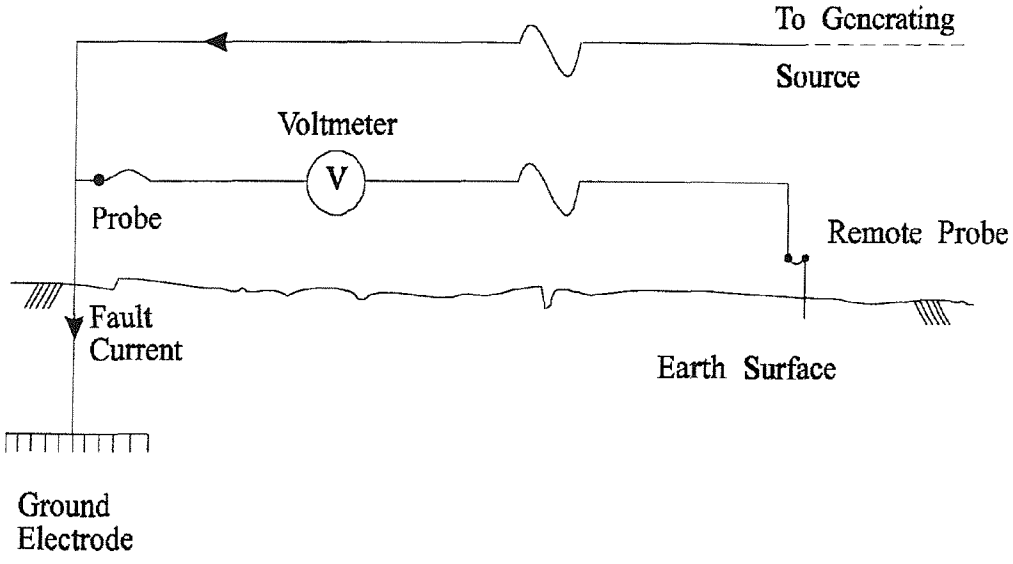

Figure 2.4: Theoretical measurement of GPR of a ground electrode

Existing UK practice terms a substation as "hot" if its GPR exceeds 430V or 650V, depending on whether the protection is normal or high speed. If telecommunication equipment, which is remotely earthed, enters the zone, then mitigation is required. This could require redesigning the grid to reduce the GPR and hence the area of the hot zone, providing additional insulation, imposing safe working procedures, bonding or physically diverting the equipment such that it does not enter the hot zone.

2.5 Earthing System Impedance/Resistance Measurement and Interpretation

The two main methods for measuring the impedance of the earthing system at a medium or large substation are:

a) Fall-of-Potential

b) Current Injection

The earthing system will consist of mechanical parts above ground, metallic components within the soil and the surrounding soil itself. On top of that, there are the parallel paths, such as cables and tower lines. Each of these will have a specific resistance value, and also contact resistances for example at joints and at material interfaces. In a new installation, the most significant contact resistance would be at the interface between the earth conductors and the surrounding soil.

2.5.1 Fall-of-Potential Method

The Fall-of-Potential method is the most common method for electrode systems measurement. This method employs two auxiliary electrodes, one being the earth-current return (current electrode), the other (the potential electrode) allowing measurement of the voltage drop between the electrode under test and a point P of the soil surface (see Figure 2.5)

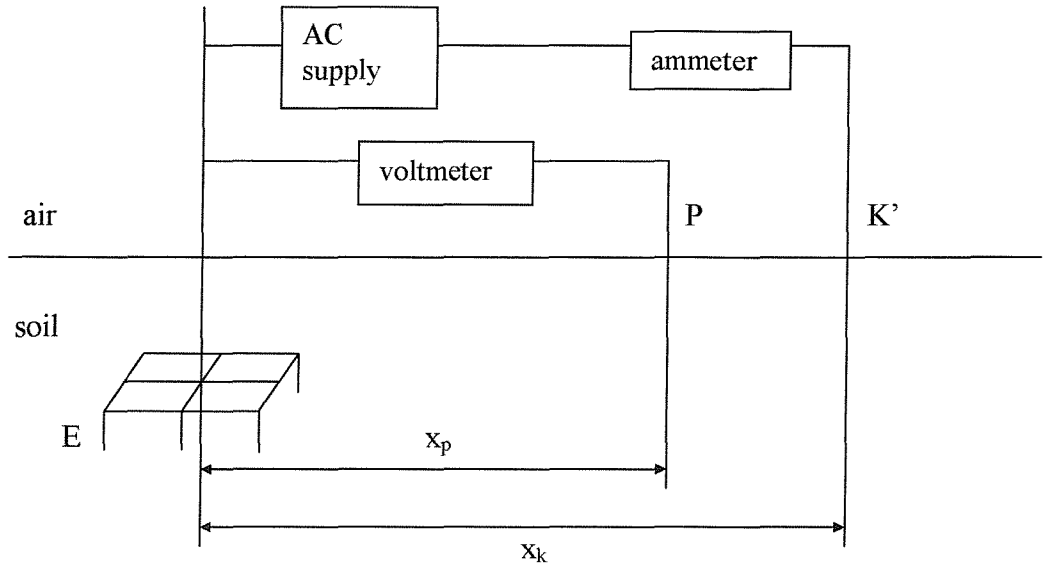

Figure 2.5: Fall-of-Potential method arrangement

In this way, it is possible to measure the earth resistance of only the electrode under test, and it does not include the earth resistance of the current electrode. Unfortunately, the fall-of-potential method involves difficulties and errors in the measurements when it is applied to large earthing systems. In fact, in this case, it is necessary to increase the distance 'x_k' between the system under test and the current electrode (see Figure 2.5). Some of the difficulties resulting from doing this are [14-16]:

a) The effects due to the stray currents over a wide area. Such stray currents may be due to nearby traction and other electrical installations.
b) The effects of the electromagnetic coupling between the test lead. For long stretched wires, the inductance and capacitance to earth and between them can cause considerable error.
c) The probability that the current electrode cannot be located at the above-mentioned distance x_k.

It is well known that by using a frequency which is not present in the stray currents or by using filters, the effects of stray current may be lessened [5, 14]. Regarding the difficulties caused by the electromagnetic coupling, some suggested methods to overcome this are:

a) The use of direct current will eliminates the coupling effects but causes unwanted electrolytic effects [14].
b) The use of periodically reversed direct current but in this way the measured value of the earth resistance cannot be accurate in AC applications [5, 14].
c) The placement of the potential electrode at the side opposite to the current electrode [14]. In this way, the coupling effects are eliminated, but the measured value of the earth resistance is always smaller than the true value. Moreover, this arrangement of the electrodes cannot always be carried out [15].

In order to avoid the difficulty of inaccessible areas, Tagg [15] showed that, for hemispherical electrodes, the distance x_k between E and K' can be made as small as is practicable, and yet true resistance can be obtained if the distance x_p between E and P is 61.8% of x_k. Although this conclusion is based on the analyses of hemispherical electrodes, it is found that it gives excellent results for rod electrodes as well, provided that $x_k \geq 10$ rod length, and assuming the soil is homogeneous [15, 16].

However, by using this 61.8% rule, it is necessary to know the exact point from which the measurements of the separation of the current and potential electrodes should be made. In other words, the centre of the equivalent hemisphere must be known. This becomes very difficult in a complex earthing system. A special method to do this was developed by Tagg [15].

If the soil is assumed to be represented by a two-layer model, the value of x_p is no longer 61.8% of x_k. The value of x_p now is a function of the geometric variables describing the electrodes E and K', and of the parameters ρ_1 (top layer resistivity), ρ_2 (bottom layer resistivity) and h (depth of the top layer). The bottom layer is assumed to extend to infinity. Determination of the parameters ρ_1, ρ_2 and h is by means of resistivity measurements [5, 6, 14, 17, 18]. Analytical formulae allowing the calculation of x_p as a function of all the above-mentioned variables have not yet been found and therefore, the calculation of x_p is only possible using suitable computer programs [19]. A general digital procedure to determine x_p is given by Amoruso, Savino and Sylos Labini [20].

2.5.2 Current Injection

In this method, a reasonable amount of current (typically 50 to 200A) is passed directly through the test earth grid and back to a return electrode via the soil [7]. The potential on the earth grid will rise in relation to true earth. The grid impedance can then be calculated by the voltage rise measured and the current obtained. The voltage is normally measured by reference to a remote earth which is provided via a telephone line.

The main difficulty with this method is due to its cost and can be difficult to carry out. In most urban type substations, an underground circuit has been used in the past to provide the current injection route. This would typically be an 11kV cable, earthed at the remote location with the cable ends available at the test position for the injection of current. The measured values often will indicate the impedance of the cable sheaths between the test and source sites, rather than the earth resistance of the test site. Another option that will likely provide a more reliable result is an unearthed overhead line [21]. This type of test can become expensive because of the additional equipment needed and the time taken, during which the test circuit is not available for service.

Sources of error includes [21]:

a) Difficulty in obtaining a sufficiently long metallic telephone circuit.

b) Interaction with telecommunication system earths. The telephone circuit may be connected to other nearby earths which interact with that under test and hence will give a lower voltage measurement than the actual one.

c) The test current that actually flows via the earth grid to ground might be less due to parallel paths which will divert this current.

d) Difficulty in obtaining a circuit through which to pass the test current.

2.6 Effects of Electrode Shape, Size and Position

A dominant part of the impedance is that due to the physical orientation of the earthing electrodes. Earthing rods or electrodes can be made from solid copper, stainless steel or copper bonded steel. The rods are supplied by most manufacturers in various different diameters from 10 mm to 25 mm and in lengths from 1.2 m to 3m. The most common size used nowadays is 15 to 16 mm in diameter, and 3 to 4 m in length. Typical buried depth of the main earth grid is 0.6 m [22]. Some of the methods to reduce the earthing impedance are:

a) Increasing the buried length of a vertical rod

As the rod length increases the overall resistance falls progressively more quickly. This is due to deeper soil with better electrical properties being reached. In some soil conditions, particularly where there is a limited area available, use of vertical rods may prove to be the most effective option, but it does depend on the soil structure. The vertical rods give a degree of stability to the impedance of an earthing system. Normally they should be of sufficient length that they are in or near the water table and below the freezing line. This means that the impedance should be less influenced by seasonal variations in water content or temperature [23].

b) Increasing the length of a horizontal conductor

Horizontally laid strip is generally considered to be a good option, particularly when it is possible to route this in several directions. However, it was found that for approximately the same length of conductor, vertical rods are more effective in terms of reducing the grid resistance than adding horizontal conductors [23].

c) Increasing the side length of a square earth grid/plate

This is one of the most effective way to reduce the resistance of the earthing electrode [23].

d) Increasing the radius of the earth rod

Usually there is little to be gained by extending the radius of earth electrodes beyond that necessary to deal with the mechanical and corrosion requirements. Tubes can be used instead of solid conductors to increase the external surface area, whilst moderating the increase in volume of the metal used. However, the increased installation cost may outweigh the value of the performance increase. In rocky condition it may be advantageous to increase the effective diameter of the electrode by surrounding it with material which has a lower resistivity then the surrounding rock [23].

e) Increasing the buried depth

This only provides a marginal reduction in impedance, but at a relatively high cost, so is not normally considered. It should be remembered that the greater the burial depth, the smaller the voltage gradients on the surface of the soil. Within a substation, a high voltage is required above the electrode, to minimise touch voltages. However, if an earth electrode extends into a field, then a low surface voltage is required to reduce step potentials. In some cases, it is advantageous to increase the depth of electrodes to reduce the risk of electrocution to horses, cattle and other animals [23].

2.7 Driving Methods

In essence, there are two ways of installing earthing rods. They are [22]:

a) driving either with a sledge hammer or a mechanical hammer.

b) boring and back filling with a soil conditioning medium.

The first method is dependent on the soil conditions and the depth of the installation. However, it is the quickest and cheapest method. The use of sledge hammer is not recommended for depths greater than 4m because it would be very difficult to drive the rods vertically and sometimes gives rise to poor resistance readings due to inadequate rod to soil contact. The sledge hammer is more suitable for small rods and when the soil is

very soft. The use of a mechanical hammer gives better results than a sledge hammer and allows installation of longer rods.

The second method, boring holes to install earth rods, is necessary in very poor ground conditions. However, this method is very expensive. A large hole needs to be drilled in order for the rod to be backfilled with a soil conditioning medium such as Bentonite or Marconite. These substances will reduce the resistance to earth of the earth rods.

2.8 Soil Conditioning Materials

The resistivity of the soil is an important aspect in earthing problems. As mentioned earlier, one of the methods in reducing the overall grid resistance is by adding additional earth rods. However, if this does not have the required effects, then methods of modifying the soil resistivity can be a possible solution. Some of the methods to reduce soil resistivity are:

a) Addition of Electrolytes [22]

Soil without electrolytes is a poor conductor. Soluble substances such as salt (sodium chloride), washing soda (sodium carbonate), and Epsom salts (magnesium sulphate), can reduce the soil resistivity. However, these substances are only short lived as the salt will become diluted in time. Another substance which have been found to be one of the best for this type of application is Gypsum (calcium sulphate). This is because Gypsum has a low solubility and provides adequate conductivity.

b) Improving moisture retention

The soil surrounding the earth conductors may become extremely dry for example, at places which suffer prolonged period of drought. Material such as Bentonite, which is added locally to the conductor will prevent excessive moisture loss. Bentonite is a natural clay containing the mineral montmorillionite [24]. By adding water, Bentonite resistivity becomes very low. Unlike a salt bed, Bentonite will not gradually leach out, because it is part of the clay itself. Bentonite can swell up to 13 times its dry volume and it adheres to nearly any surface it touches [25, 26].

c) Improving the contact surface of the earth electrodes

Although the moisture and material content of the native soil can give lower resistivity, a stony soil can cause problem due to the lack of contact between the electrode and soil. There are a few ways to overcome this. First, the area around the conductor can be backfilled with a suitable fine loam type soil which is cheap to obtain and can have low resistivities. Bentonite may also be used as it will expand to make good contact with the conductor and will fill any voids at its interface with the soil. However, these two methods have its setback in extremely dry conditions. Another alternative is to encase the conductor in conductive concrete [22]. Conductive concrete is made by using a crystalline form of carbon as the aggregate, and this material is called Marconite.

2.9 Electrical Safety Criteria

Figure 2.6 depicts a typical touch voltage situation. A man is standing near to an energised metallic structure, which he is touching with one hand. Due to the potential difference between the structure and the location on the earth's surface where the man is standing, a current will flow through his body. The magnitude of this current will depend upon the electrical resistance of the man's body and the resistance of the earth between his feet and the earthing system [27]. Equation 2.4 gives the exact relationship between body current I_{BODY}, touch voltage V_{TOUCH}, body resistance R_B, and foot resistance R_{FT}. Note that foot resistance is not the resistance of the man's feet, but the resistance of the earth beneath his feet.

$$I_{BODY} = \frac{V_{TOUCH}}{R_B + R_{FT}} \qquad (2.4)$$

Equation 2.4 does not account for the protection that could be provided by rubber gloves or boots. Although this protection is present in typical situations, earthing systems are designed assuming the worst possible scenario: bare hand contact and wet shoes with negligible insulating value [28].

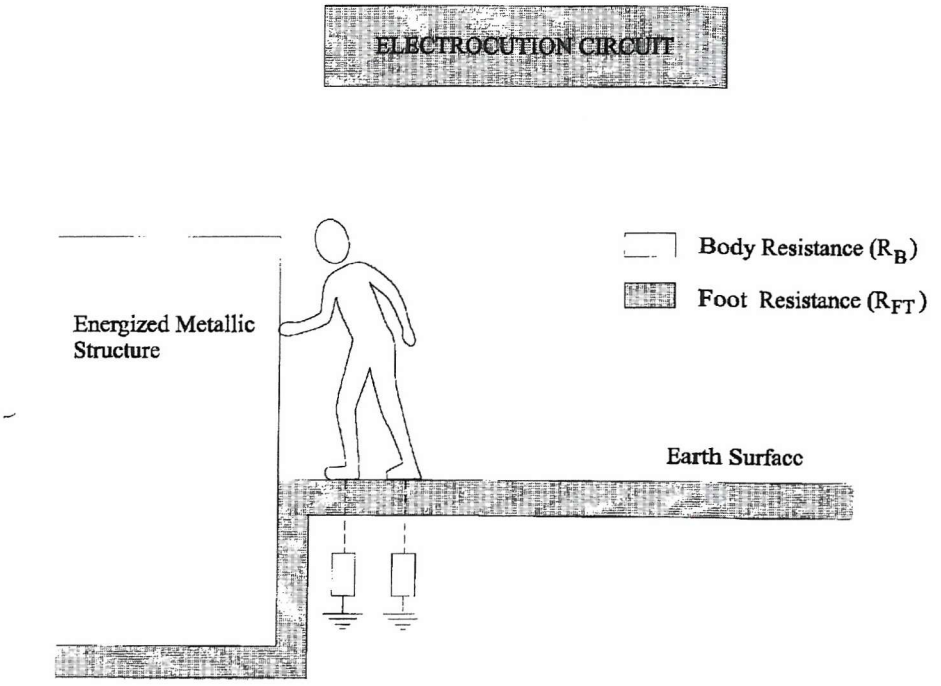

Figure 2.6: Typical touch voltage situation

The maximum body current, $I_{BODY-MAX}$, indicates the threshold where a person experiencing a current below this value has a very low probability of experiencing ventricular fibrillation[1]. For currents above $I_{BODY-MAX}$, ventricular fibrillation becomes more and more likely.

One milliampere is generally recognised as the threshold of perception, a value of current at which a person is just able to detect a slight tingling sensation in his hands or fingertips, caused by the passing of current [29].

The maximum acceptable touch voltage, $V_{TOUCH-MAX}$, is clearly the value which results in a body current of $I_{BODY-MAX}$:

$$V_{TOUCH-MAX} = I_{BODY-MAX} * (R_B + R_{FT}) \qquad (2.5)$$

A similar equation results for step voltage situations (Equation 2.6):

$$V_{STEP-MAX} = I_{BODY-MAX} * (R_B + R_{FS}) \qquad (2.6)$$

[1] Ventricular fibrillation is the major cause of death due to electric shock and is a state of the heart in which the heart muscle cells lose their synchronism, resulting in the interruption of the heart's pumping action. Human beings cannot recover spontaneously from this condition.

In this case, current flows into one foot, through the body, and out of the other foot into the earth. The current path in the step voltage situation is quite different from the current path in the touch voltage situation, hence the values of maximum body current, body resistance, and foot resistance are not all the same for the two shock scenarios. Typically, a lower percentage of the body current flows in the heart region for a step-type shock than for a touch-type shock; $I_{BODY-MAX}$ is therefore larger for step voltage situations. Also, the foot resistance in Equation 2.6, R_{FS}, is defined as the resistance, through earth, between the two feet, rather than the resistance between the feet and the earthing system. Thus, R_{FS} is often regarded as a series combination of two resistances, each represents the resistance of the earth local to each foot, while R_{FT} is regarded as a parallel combination of these two resistances. In this way, R_{FS} is approximately four times greater than R_{FT}.

2.10 Maximum Body Current

The maximum acceptable body current is a function of the duration of the shock: the longer the shock duration, the lower the current level required to induce ventricular fibrillation. Presently, Dalziel's equation (Equation 2.7) is used almost exclusively in North America to determine maximum acceptable body current levels as a function of shock duration. Dalziel's equation is recommended by ANSI/IEEE Standard 80 [28].

$$I_{BODY-MAX} = \frac{0.116}{t^{\frac{1}{2}}} \qquad (2.7)$$

where

$I_{BODY-MAX}$ is the maximum acceptable body current or "fribillation current" in amperes

t is the maximum expected shock duration in seconds (this is usually the substation fault clearing time)

0.116 is a constant related to the weight of the shock victim: 0.116 corresponds to a weight of 50 kg and is used for locations accessible to the general public.

Dalziel's equation is not applicable for shock durations in excess of 3 seconds or shorter than 0.03 seconds. Equation 2.7 is plotted in Figure 2.7 on a log-log graph. In Europe, however, another curve based on more recent research is gaining widespread acceptance. This curve, which is to be found in Report 479-1 [30] of the International Electrotechnical Commission (IEC), the European counterpart of IEEE, is also plotted in Figure 2.7.

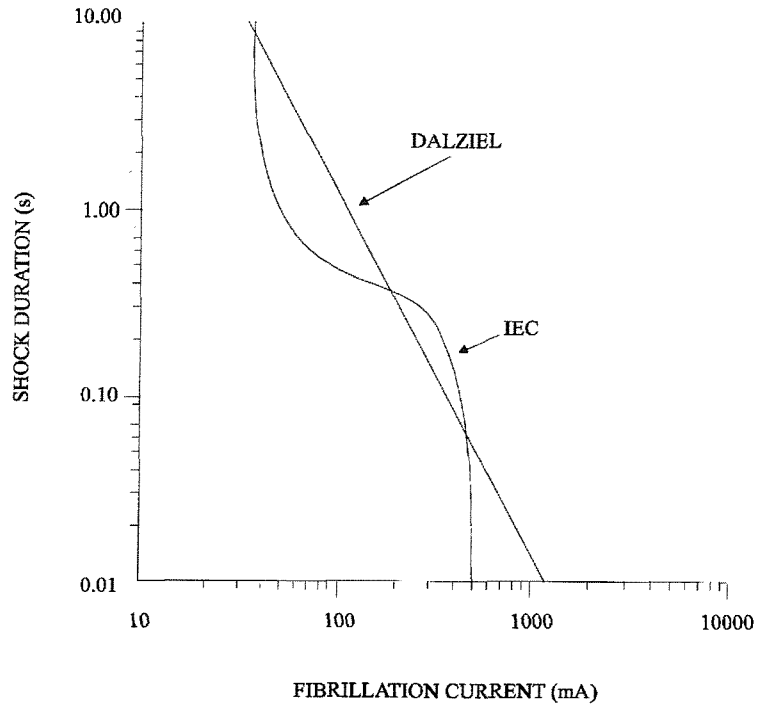

Figure 2.7: Maximum acceptable body current as a function of shock duration

2.11 Body Resistance

ANSI/IEEE Standard 80 suggests that a body resistance value of 1000 ohms is appropriate in most instances. On the other hand, IEC Report 479-1 asserts that body resistance is a function of the contact voltage, a fact recognised by ANSI/IEEE Standard 80, and presents a plot of body resistance versus contact voltage. Figure 2.8 is based on this plot and depicts body resistance as a function of body current, for a hand to hand or hand to foot contact, and dry conditions. The IEC curve is a lower limit on body resistance and is assumed to be valid for 95% of a given population.

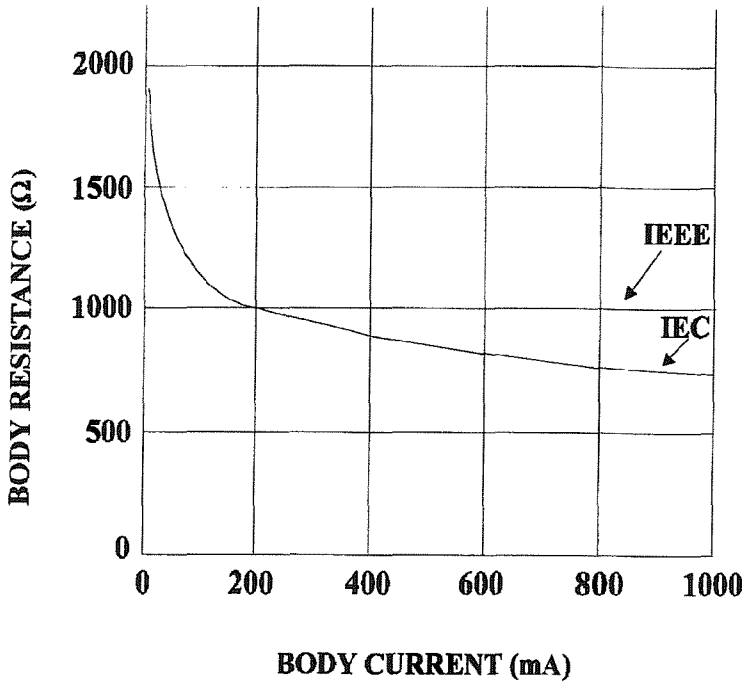

Figure 2.8: Body resistance as a function of body current

2.12 Foot Resistance

Foot resistance, in touch voltage situations, is defined as the resistance, through earth, between a person's feet and the energised earthing system. However, there is such a large portion of the foot resistance concentrated in the soil closest to the feet, that for most practical purposes, the effect of the earthing system configuration on the foot resistance can be ignored [27]. As a result, the foot resistance to be used in determining the maximum acceptable touch and step voltages is a function only of the soil characteristics near the earth's surface.

When the earthing system to be evaluated is buried in a homogeneous soil with a resistivity ρ and no earth surface covering layer such as crushed rock or asphalt is present, then the following Equations 2.8 and 2.9 can be used to determine the foot resistance for touch and step voltage situations, respectively. These equations are based on a metal plate model of the foot with a 0.08m radius. This foot model, which is

proposed in ANSI/IEEE Standard 80 [28], results in a foot resistance of about 3 ρ. If mutual resistance is neglected between the two feet, then:

$$R_{FT} = 0.5\ (3\ \rho) = 1.5\ \rho \qquad (2.8)$$

$$R_{FS} = 2.0\ (3\ \rho) = \mathbf{6.0}\ \rho \qquad (2.9)$$

where

R_{FT} is the parallel resistance of the feet, in ohms, for touch voltage situations

R_{FS} is the series resistance of the feet, in ohms, for step voltage situations

ρ is the resistivity, in ohm-m, of the uniform soil

When the soil is not uniform or when an earth surface covering layer is present for added safety (see Section 2.13), then more general equations must be used. In most instances, it will be possible to model the soil with a 2-layer structure as shown in Figure 2.9. This model consists of a top layer with thickness h and resistivity ρ_s, and a semi-infinite bottom layer with resistivity ρ.

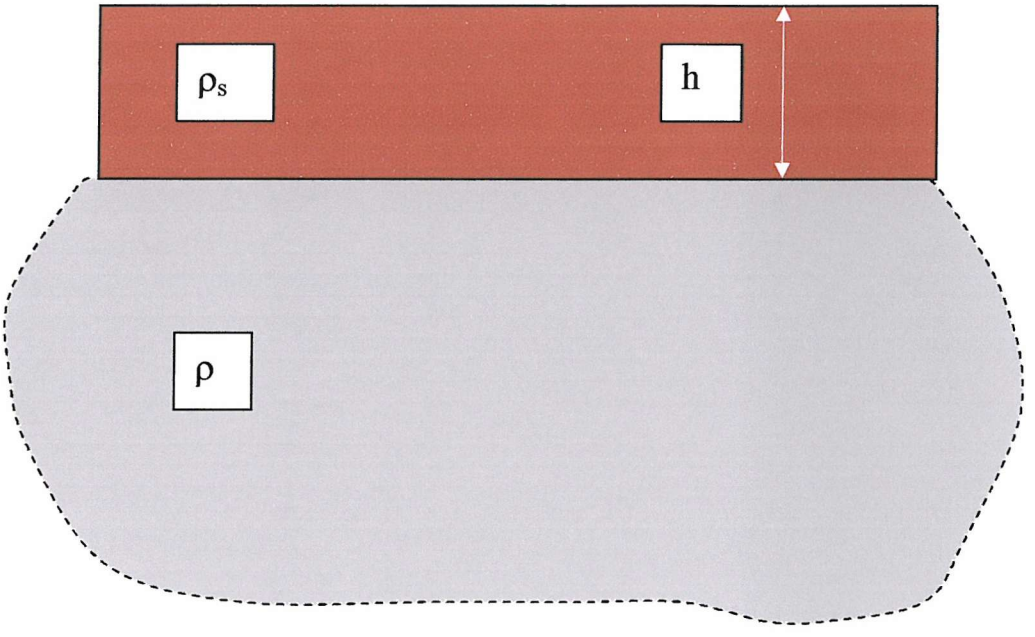

Figure 2.9: Two-layer soil structure

Note that soil composition nearest to the earth surface is the most critical, so changes in soil structure at great depths need not be taken into account for determining foot

resistance. Equations 2.10 and 2.11 can be used in conjunction with Figure 2.9 (adapted from [28]) to determine foot resistances for 2-layer soils.

$$R_{FT} = 1.5C\,\rho_s \qquad (2.10)$$

$$R_{FS} = 6.0C\,\rho_s \qquad (2.11)$$

where

ρ_s is the resistivity of the top soil layer

C is the foot resistance reduction factor given by Figure 2.10

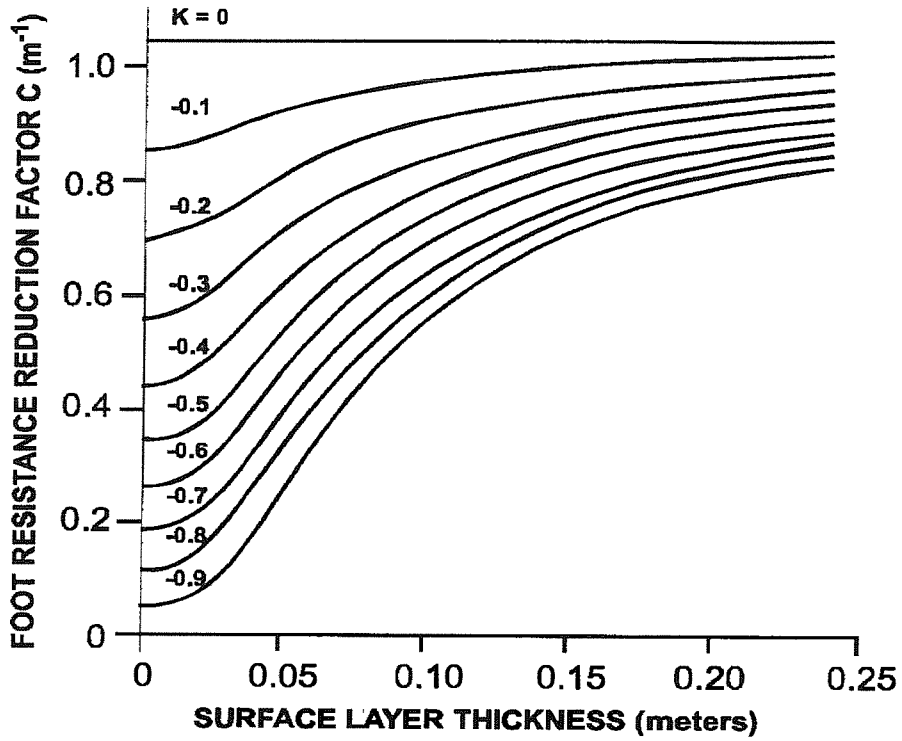

Figure 2.10: Foot resistance reduction factor

Note that use of Figure 2.10 requires calculation of the soil reflection factor, K. This is done using Equation 2.12:

$$K = \frac{\rho - \rho_s}{\rho + \rho_s} \qquad (2.12)$$

The constant C used in Equations 2.10 and 2.11 is obtained when the foot is modelled as a 0.08 m radius circular plate lying on the surface of a thin layer (resistivity ρs and thickness h) overlaying a uniform soil of resistivity ρ.

2.13 Earth Surface Covering Layer

In order to increase safety in and around substations, it is common practice to spread a layer of high resistivity material, such as crushed rock or gravel, over the earth's surface [13, 31]. This increases foot resistance and therefore the maximum touch and step voltage values, which can safely be tolerated. The rock layer does not act as part of the normal earth path but forms a high-resistance barrier between earth and the equipment area. The barrier provides some additional resistance in series with an individual standing on the rock and touching substation equipment, thus reducing the possible body current. The use of rock or gravel for surfacing may have some merit when the surface is dry, but moisture in conjunction with certain contaminations reduces the resistance to a relatively low value.

In order to make effective use of an earth surface covering layer, it is of course important to know the approximate resistivity of the material. Table 2.1, based on a similar table in Reference [32], shows wet resistivities of several commonly used materials. Noting that permissible touch and step voltage levels can be very sensitive to the resistivity of the earth surface layer, Reference [32] recommends that samples of the surface material be tested for their wet resistivity before use.

Earth surface covering layer	**Resistivity of material when wet (ohm-metres)**
Concrete	20-100
Crushed aggregate base granite (with fines)	500-1000*
Washed granite similar to pea gravel	5000*
#57 washed granite similar to ¾" gravel	8000**
asphalt	Over 10000*

* based on water resistivity of 500 ohm-metres

** based on water resistivity of 43 ohm-metres

Table 2.1: Wet Resistivities of Typical Earth Surface Covering Layer Materials

When selecting an earth surface covering layer material, resistivity is not the only factor which must be considered: it is equally important to ensure that the integrity of the layer will be maintained throughout the lifetime of the substation. For example, crushed rock can become contaminated with windblown debris and can be washed away by wind and rain. In this case, regular inspections and maintenance are required.

It should be noted that the high resistivity layer must extend beyond the earthing system area if step voltages during fault conditions are expected to be larger than the voltages that can be tolerated by a person standing on the native soil.

Finally, Table 2.1 indicates that wet concrete can have a very low resistivity when wet. As a result, if a substation earthing system relies on a high resistivity layer to achieve safe touch and step voltages, concrete walkways or operator pads can represent a safety hazard if proper precautions are not taken. Appropriate measures, which can be implemented to overcome this problem, include earthing the steel mesh reinforcing wires in the concrete or providing an appropriate insulating coating on the concrete.

CHAPTER 3

Method of Analysis

In order to achieve the aims and objectives outlined, various methods were implemented in the analysis as listed below:

I. Analytical method.

II. British and other Standards, such as S34, BS7430, BS7354 (Section 7), EA TS 41-24, and IEEE Std 80-2000.

III. Formula developed by other researchers in the Literature.

IV. Computer software CDEGS (MALT).

V. Electrolytic tank.

3.1 Analytical Method [33, 34]

An analytical solution for the ground resistance of a single vertical rod in homogeneous soil was developed which is believed to be more accurate than any other existing model. The main assumption made is that, because the rod radius r is much less than the length l, the current is injected into the soil from the cylindrical surface only (i.e. the tip is ignored) with a density that varies linearly with height. The solution involves a truncated series of modified Bessel functions and is rather cumbersome, although the resistance and surface potential distribution can be computed in a few seconds. Details are given in Appendix 1.

It was realised at the outset that the Bessel series model would not be suitable for more than one rod. However, it was required to have a reliable way of checking some of the simple analytical models that have been proposed in the literature and which express the resistance to ground and surface potential in simple closed form. If confidence can be placed in one of these models then it becomes possible to handle an array of vertical rods in homogeneous soil with relative ease. One such model is the so-called cylindrical rod with hemispherical tip. This sounds ideal until it is realised that all the surrounding equipotentials are constrained to follow the same shape, i.e. become cylinders with

closing hemispheres of increasing diameter. Not only is the local current density forced to cross these equipotential surfaces at right angles but also with uniform density over the surface. The resulting current flow almost certainly suffers considerable distortion.

On the other hand, it was discovered that, for rods of length more than 100 times radius, the resistance obtained from the Bessel function series solution can be reproduced almost exactly by a thin ellipsoidal model with its minor axis given by $d'' = \sqrt{2} \times$ rod diameter ($2r$). This is a modified version of the existing model in which the more obvious value $d' = 2r$ is assumed. An ellipse is a co-ordinate surface in the prolate spheroidal co-ordinate system, and it can be shown by separation of variables that the ground resistance is given by

$$R_{el} = \frac{1}{2\pi\sigma l} \ln \frac{4l}{d'} \qquad (3.1)$$

where σ is conductivity of soil (provided $d'/l < 0.1$ which is more than satisfied by original requirement $l > 100r$). The surface potential is given by

$$V = V_0 \frac{\ln\left(\coth\frac{\eta}{2}\right)}{\ln\frac{4l}{d'}} \qquad (3.2)$$

where V_0 denotes the potential of the rod and η is the co-ordinate describing the dimension of the elliptical equipotential on which the field is required. The outwardly-directed electric field on the surface is then

$$E = \frac{2V_o}{l \sinh(2\eta) \ln\frac{4l}{d'}} \qquad (3.3)$$

Equations 3.2 and 3.3 can be written in terms of the injected current I by replacing V_0 by IR. At a large distance x'' from the axis of the rod where $2\eta >> 1$, eqn.3.3 yields

$$E = \frac{4V_0 \exp(-2\eta)}{l \ln \frac{4l}{d'}} \qquad (3.4)$$

Now the Cartesian co-ordinate x'' $\cong l \sinh(\eta) \cong 0.5\, l \exp(\eta)$, so that, in terms of the injected current I, $E \cong I / (2\pi \sigma x''^2)$. But this expression can also be derived from the simple hemispherical model of a rod, which is not surprising because the distant equipotentials in a prolate spheroidal co-ordinate system tend to become spherical in shape. On the other hand, the surface potentials yielded by the popular hemispherical model, even with its radius r selected to give the correct resistance to earth, are only acceptable at a horizontal distance of more than three rod lengths from the axis of symmetry. This is not surprising when it is realised that r may be about half the original rod length. The conclusion is that the modified ellipsoidal model of a cylindrical rod is almost certainly of sufficient accuracy for the analysis of multiple arrays of closely spaced vertical rods, and will always yield the correct earth resistance. However, the hemispherical model can only be used for distant fields and widely separated rods.

Eqn.3.2 for the surface potential at distance x'' from the axis of a single rod can be written in terms of the injected current as

$$V = I \frac{\ln\left[\coth\left(0.5 \sinh^{-1} \frac{x''}{l}\right)\right]}{2\pi\sigma l} \qquad (3.5)$$

This expression assumes the rod to be a thin half-ellipsoid with its length (i.e. half the major axis) at least 10 times the minor axis d'' (=$\sqrt{2}$ times rod diameter). This will be satisfied in practice, and the resistance can be obtained within about 1% (low) from eqn.3.1 if the length $\geq 100 \times$ rod radius.

We can begin to illustrate the relative ease with which rods can be combined by considering two rods in homogeneous soil separated by distance c'. First let the current I be injected at one rod and extracted from the second. The surface potential (relative to true earth zero) at any point can be found by superposition and will of course be zero at points equidistant from both rods, i.e. on the plane of symmetry. The total potential V_1 at

the first rod is the sum of the isolated potential IR, due to the injected current, and the potential

$$V_{12} = -I\frac{\ln\alpha}{2\pi\sigma l} \tag{3.6}$$

set up by the current $-I$ in the second rod (assuming c' >> a), where

$$\alpha = \coth\left(0.5\sinh^{-1}\frac{c'}{l}\right) \tag{3.7}$$

Thus $V_1 = IR + V_{12}$, and, by symmetry, the potential at the second rod is $V_2 = -IR - V_{12}$. The potential difference is therefore $\Delta V = V_1 - V_2 = 2\,(IR + V_{12})$, so that we have

$$0.5\Delta V = IR + V_{12} = I\frac{\ln\frac{4l}{d'} - \ln\alpha}{2\pi\sigma l} \tag{3.8}$$

But in a practical situation both I and ΔV can be measured, so we have a possible method of obtaining σ, the local value of the "homogeneous" soil conductivity. This method is tested in Section 3.5.3. The rods should be closely spaced, subject only to the condition that the spacing should be much greater than the radius of the rods.

The same technique can be used to determine the theoretical value of the ground resistance of a system consisting of two vertical rods solidly connected together above ground level. The rods share the current I equally (by symmetry), and so we have

$$V_1 = V_2 = 0.5I\left(R + \frac{\ln\alpha}{2\pi\sigma l}\right) \tag{3.9}$$

where α is defined in eqn.3.7 and R is, as usual, the ground resistance of an isolated rod. The combined resistance is therefore 0.5 [R + ln(α) / ($2\pi\sigma$ l)] which tends to R/2 as c'/ l increases because the interference between the electric field distributions of the two rods (which dictate the individual current flow patterns) becomes negligible.

A practical earthing system will consist of an array of N vertical rods with an adjacent spacing of only a few metres. We will consider the situation where only the rods, and not the interconnecting links, are in direct contact with the ground because at present only the vertical rods can be modelled. The superposition technique can be used to take into account the interference between the rods; an effect that increases the overall resistance substantially above the minimum value of R/N. The method is considerably simplified if the array is fairly small and symmetrical. For example, consider three rods arranged in a line and numbered in sequence 1,2,3. Equations for V_1, V_2, and V_3 can be obtained in terms of the individual currents I_1, I_2, and I_3. From the fact that all three potentials must be equal to the same value, V say, two equations with the three currents as the only unknowns can be formed. In addition, symmetry imposes the condition $I_3 = I_1$, and so all the currents can be determined. The ground resistance is finally given by V/ΣI.

This technique, but used with rods modelled as cylinders with hemispherical tips has been used by Datta, Basu and Chowdhury [16] for several simple arrays. Apart from the two-rod case mentioned earlier, the simpler example considered by Datta et al is for three rods situated at the corners of an equilateral triangle, where symmetry dictates that the current injected by each rod is one third of the total. The resistance ratio (actual resistance divided by the value for a single rod, R) is given by (1+2m)/3, where

$$m = \frac{\ln \frac{l+j}{j}}{\ln \frac{l}{r}} \qquad (3.10)$$

and j is the length of the sides of the triangle. On the other hand, using the ellipsoidal model, it can be shown that the value of m in eqn.3.10 becomes

$$m = \frac{\ln \alpha}{\ln \frac{4l}{d'}} \qquad (3.11)$$

For the useful case of four vertical rods placed at the corners of a square, the resistance ratio is (1+2m+q)/4, where m is given by equations 3.10 or 3.11, and q has the same form as m but with j replaced by $\sqrt{2}$j to allow for the diagonal separation between rods in opposite corners of the square.

3.2 British and other Standards

The Standards referred to in this research are the ones commonly used by industry and other researchers.

3.2.1 Engineering Recommendation S34 (1986)

The *Engineering Recommendation S34 (1986)* [35] is a guide for assessing the rise of earth potential at substation sites. This Guide outlines the methods which should be used to assess the maximum rise of earth potential and the local ground potential profile which can occur at transmission, bulk supply point and primary and distribution substations operating at 6.6kV and above. The Guide also prescribes methods for determining the value of the resistance/impedance of earth electrode systems. The Guide does not deal with the effects of such potentials or with measures of protection that might be considered necessary if the potentials exceed certain limits which may be specified elsewhere.

3.2.2 *BS7430 (1998)*

This British Standard Code of Practice for Earthing [36] gives guidance on the methods that may be adopted to earth an electrical system for the purpose of limiting the potential (with respect to the general mass of earth) of current-carrying conductors forming part of the system, and non-current-carrying metalwork associated with equipment, apparatus, and appliances connected to the system.

BS7430 applies only to land-based installations; it does not apply to ships, aircraft, or offshore installations, nor does it deal with the earthing of medical equipment or the special problems encountered with solid-state electronic components and equipment due

to their sensitivity to static electricity. This standard does not address electromagnetic compatibility requirements for earthing, nor does it give recommendations for functional earthing.

3.2.3 *BS7354 (Section 7,1990)*

Section 7 of BS7354 [37] supplements the information in CP1013 and includes a procedure for the design of the earthing system for switching stations. CP1013 is code of practice 1013 and is titled 'Earthing', last published in 1965. It no longer exists and is superseded by BS7430 & BS7354.

BS7354 was rewritten in 1990 to be compatible with CENELEC and IEC standards at the time. It provides guidance on system earthing and equipment earthing.

3.2.4 *EA TS 41-24* [38]

This specification relating to main earthing systems in substations is a companion document to BS Code of Practice 1013 (1988) and supersedes Engineering Recommendations S5/1 (1966). This specification was issued in 1992, although much of the work on which it is based was completed some years previously. It includes the voltage limits used within the electricity supply industry, which differ from those of BS 7354, even though the two documents can be considered to apply to many of the same installations.

3.2.5 *IEEE Std 80-2000* [39]

This Guide is primarily concerned with outdoor ac substations, either conventional or gas-insulated. Distribution, transmission, and generating plant substation are included. The intent of this guide is to provide guidance and information pertinent to safe earthing practices in ac substation design.

3.3 Formulae developed by other researcher in the Literature

These formulae will be quoted and used in the next chapter, as a comparison with other methods.

3.4 Computer Software CDEGS MALT

The application of computer-assisted design techniques to the solution of complex engineering problems can result in substantial cost savings, both in engineering and construction. It can also improve accuracy and reduce design time. This is particularly true for earthing problems, which cannot generally be solved accurately using conventional simplified or empirical methods. The software used in this research is the CDEGS software, in particular the MALT module.

3.4.1 Background information on the creator of CDEGS

SES states that [40]:

"The CDEGS (**C**urrent **D**istribution, **E**lectromagnetic Fields, **G**rounding and **S**oil Structure Analysis) software package was developed by the world leader in Grounding/Earthing, Lightning and Electromagnetic Interference, which is the Safe Engineering Services and Technologies Ltd. or better known as SES. SES' primary focus is helping its customers to assess and mitigate the effects of grounding & electromagnetic interference on people, equipment and the environment, safely, efficiently, and economically."

"Since its foundation in 1978, SES has been recognized as an undisputed world authority on the effects of soil on the interaction between electrical installations and other utilities such as gas and oil pipelines, communication industries, and railway electrification. SES holds the distinction of being the only company worldwide totally dedicated to providing the engineering community with expertise, software and training for the solution of complex problems related to earthing and electromagnetic interference. SES has earned an international reputation for pioneering work in earthing and in electromagnetic and

conductive interference analysis involving electrical networks. Typical areas of application for its research and development work include electrical system networks and neighbouring utility installations such as oil and gas pipelines, telecommunications cables, and railway tracks."

"Its leadership is maintained through an aggressive and ongoing research and development program, regular involvement in the analysis of a wide variety of practical and challenging industrial problems, and its support of a superior and growing line of engineering applications software modules."

3.4.2 Documentation and Validation Reports

On this issue, SES states that [40]:

"Engineers and scientists are now more and more relying on engineering software developed by independent professionals or specialized firms outside of their own organizations as was usually the case a decade or more ago. Consequently, some critical questions need to be answered before selecting a specific engineering software package. One important question is whether the software is accurate and how this can be verified. This is an important question because it is crucial for the safety and integrity of any engineering study or design. Another important aspect is whether the software is well documented. This question addresses the fundamental requirement for insuring adequate understanding of the subject and usage of the technical software. In other words, a satisfactory engineering software must have sufficient documentation and an adequate validation report. This implies necessarily that the software producer is competent and has the necessary resources to conduct and document its software validation tests."

"SES' engineers and scientists conduct their own research and development and offer advanced consulting services on a continuous basis in the marketplace. This unique combination allows SES to develop and maintain state-of-the-art, industry applications-oriented software. SES' scientific publications, in the most reputable journals, are an excellent indication of how SES is viewed in the scientific community."

"Extensive scientific validations of the software using field tests and comparisons with analytical or published research results have been conducted for over twenty years. The validation conducted by SES as well as other independent researchers is documented in hundreds of technical papers published in the most reputed international journals."

"Each module in CDEGS has been tested to insure that it produces the correct results for a large number of cases. These cases are tested for every release of the programs and the results are validated by comparing them to the existing ones, which in turn have been continuously validated over the years using the following three well-documented mechanisms [40] with some of the published documents listed:

a) Comparisons with field tests and experimental scale models. References [9, 41-49] provides the comparisons between measured and computed results.
b) Comparisons with scientific published results. References [8, 9, 19, 44, 46, 48, 50-90] are technical publications and research and development reports which describe scientific validation studies using CDEGS results. Essentially, computed results produced by the CDEGS engineering modules are compared to analytical results already published by other researchers. The comparisons often involve classical cases or simple models for which exact analytical results exist already.
c) Comparison with other similar programs using completely different techniques. References [73, 85, 91, 92] provides technical publications and research and development reports which gives scientific validation studies using CDEGS results. Essentially, computed results produced by the CDEGS engineering modules are compared to known analytical results obtained using computer models based on completeley different techniques. The comparisons often involve complex cases for which no exact analytical results exist."

3.4.3 Overview of CDEGS

The CDEGS software package is a powerful set of integrated engineering software tools designed to accurately analyse problems involving earthing, electromagnetic fields, electromagnetic interference including AC/DC interference mitigation studies and various aspects of cathodic protection and anode bed analysis with a global perspective, starting literally from the ground up. CDEGS computes conductor currents and

electromagnetic fields generated by an arbitrary network of energized conductors anywhere above or below ground for normal fault, lightning and transient conditions. CDEGS models simple and multi-component conductors, including bare, coated pipes and pipe-enclosed cable systems buried in complex soil structures [10].

CDEGS itself is composed of eight individual modules, which are RESAP, MALT, MALZ, TRALIN, SPLITS, HIFREQ, FCDIST AND FFTSES. Each of theses modules caters for a particular type of analysis. CDEGS modules are enabled on the installation of hardware protection key on the parallel port of the computer. A brief explanation of each module is given below, except for the MALT module, which will be explained in the next section [10]. The modules are:

a) RESAP: This program interprets measured soil resistivity data and determines equivalent earth structure models. The users enter apparent resistance or resistivity values which have been measured using Wenner, Schlumberger or arbitrary electrode arrays and RESAP determines a multilayered or exponential soil structure which most closely matches the measured results.

b) MALZ: This program analyses the frequency domain performance of networks of buried, current-carrying conductors and computes the following quantities:
   - Magnetic field in the air,
   - Conductor and earth potentials,
   - Current distribution in the conductors

   It is particularly suited for analysing extensive ground networks which cannot be considered to be equipotential surfaces or which interact with nearby coated pipelines. MALZ is also an excellent tool for analysing conductor networks energized by current at frequencies varying from 0 to about 1 MHz or for studying the cathodic protection of coated structures. Finally, using FFTSES, the transient response of any network of conductors is easily determined using program MALZ.

c) TRALIN: This program analyses electric line cross sections to determine conductor line parameters, electrostatic and electromagnetic induction effects on undergrounded conductors, and electric fields in the air. TRALIN can be applied to

industrial, distribution, and transmission lines with any number and type of conductors or phases configured in any arbitrary positions. Computations take into account the non-uniform nature of soil structure characteristics. The most usual application of TRALIN is to compute series and shunt impedance of electric line conductors and nearby non-energised conductors such as pipelines and communications cables. These impedances are then used to create a circuit model, which can be analysed by the SPLITS program to compute currents flowing in all parts of the systems (including metallic return paths) and potentials throughout the system.

d) SPLITS: This program determines the distribution of load and short-circuit currents in every section or span of a multi-conductor, multi-phase electric transmission, distribution, or industrial network. It is also used to investigate the electromagnetic interference effects caused by such conductors on neighbouring facilities such as pipelines, communication lines, rails, and fences.

e) FCDIST: This program computes the distribution of fault currents between a earthing system and the overhead ground wires or neutral wires which are connected to it.

f) HIFREQ: This program analyses the performace of networks of buried and above-ground current-carrying conductors and computes the following quantities:

- Magnetic field in the air and in the earth
- Electric field in the air and in the earth
- Conductor and earth potentials
- Current distribution in the conductors
- Self and mutual impedances and capacitances of conductors and arbitrary shaped circuits

HIFREQ is particularly suited to analyse extensive conductor networks including earthing systems energized at frequencies ranging from DC to hundreds of MHz. Using appropriate software such as FFTSES, the transient response of any network of conductors is easily determined.

g) FFTSES: This program performs Forward and Inverse Fast Fourier Transforms on waveforms to be studied by frequency domain programs such as the MALZ, SPLITS, and HIFREQ programs and on waveforms generated by theses programs.

3.4.4 MALT module

This research involves bare rods as conductors and is undertaken at 50 Hz, hence the MALT module is used. Abbreviation MALT stands for Mise-a-la-Terre (in French). This French expression in general means grounding. MALT is the oldest and most widely known program of the CDEGS software package. It is generally used to analyse electric system earthing networks and is often used to investigate transferred potentials and currents diverted to uncoated pipelines or other bare metallic structures.

MALT can be used to determine the distortion effects caused by the proximity of two earthing networks carrying currents in opposite directions. MALT can also solve cathodic protection problems involving non-extensive uncoated buried structures. Finally, it can be used to interpret ground resistance measurements in non-uniform soils when carried out using the well-known fall-of-potential method. MALT assumes low-frequency harmonic current excitations similar to those existing during normal or fault power conditions [10].

The most common application of MALT is to model electric substation, plants, factory or power line structure earthing systems in uniform, horizontally, vertically or hemispherically multi-layered soils and to determine the ground resistance and GPR, potentials at user-defined points in the soil and at the earth surface, and touch and step voltages at user-defined points throughout the earthing system area. Transfer potentials to nearby, bare non-energised structures are also computed.

MALT is used mainly when all conductors to be modelled are bare and when the size of the various energised buried systems (e.g. a substation earthing system and a nearby return electrode) modelled is small enough that the potential difference between two locations on the same system is expected to be small, i.e. each system is an equipotential

surface. If these conditions are not satisfied, MALZ (Cathodic Protection & Frequency Grounding) should be used instead.

In MALT, the program energises the earthing system as a whole (not a specific conductor). Thus, for example, if there are 2 symmetrically located rods of the same length and radius, the current injected will be equally distributed between them. MALT is designed in such a way that it does not take into account the longitudinal impedance of earthing conductors. Thus, in this situation the location of the current injection points within the ground network do not play a significant role. It is as if the conductors from the main electrode have a 'zero resistance' link to an imaginary injection point.

3.4.5 Theoretical approach outline used in MALT

The sources of electric field in the case of an earthing network located in a soil are charges located on the surfaces of conductor segments. Each conductor is subdivided into small conductor segments. Each conductor segment is assumed to have a uniform surface charge distribution. The method of images is applied for all the elements of the soil interfaces and all the conductor segments, to take into account the presence of the earth surface. The charge distribution in the system is determined by numerically solving integral equations expressing the boundary conditions on the conductor segments. Finally, the earth potentials anywhere is computed by considering the contributions from all the charges on the conductor segments.

3.4.6 Input and Output Data in MALT

MALT is relatively simple to use due to its user-friendly structure. However, some tasks may be a bit complicated, but it gets the job done very well. Upon entering CDEGS, the working directory must be specified, and then a string is entered to identify the series of simulations that are about to run. Figure 3.1 shows CDEGS main screen. CDEGS main screen consist of three main panels, which are *Data Entry, Engineering,* and *Plot/Report.* It can be seen that from the central panel, CDEGS consists of eight engineering modules. Data entry session for these programs is started by clicking on the "Toolbox" button at the top of the left panel (highlighted in red). After all the data is ready, the appropriate

module button in the central panel is launched, in this case, the MALT module (highlighted in blue). Finally, the "Toolbox" button at the top of the right panel will give the results of the computations (highlighted in green).

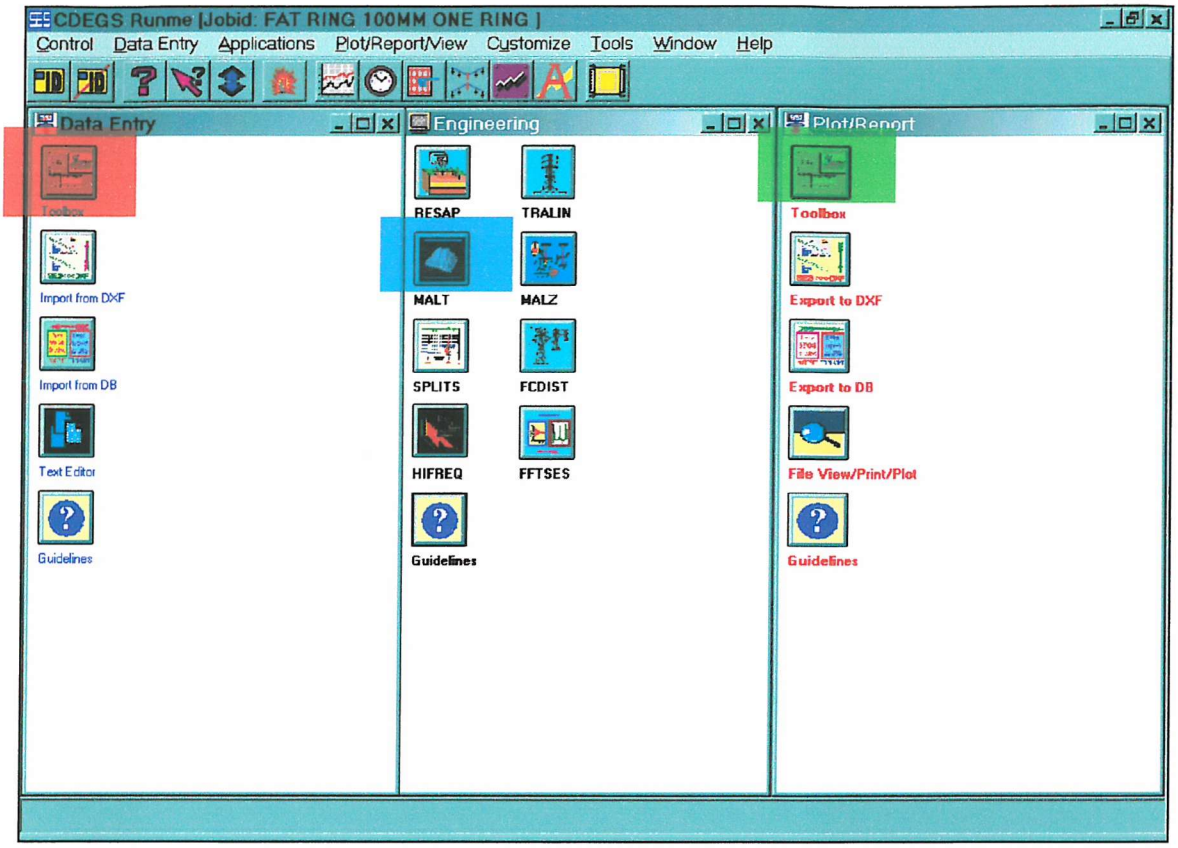

Figure 3.1 : CDEGS Main Screen

The input data task of MALT is straightforward. See Figure 3.2 for the master data entry screen for MALT. The data can be entered using the buttons at the bottom left hand corner, which consists of:

a) *Soil Type*: type, resistivities, and location of layer interfaces.
b) *System* (Electrode configuration): physical location of the conductors that constitute the electrodes (i.e., the ground network and other directly energised or non-energised buried structures, if any).
c) *Computations* (Profile data): pertinent data about the directions in which potential profiles are to be calculated.

d) *Advanced* (Codes and options): this data allows a flexible and efficient use of program MALT capabilities for each particular problem to be studied.

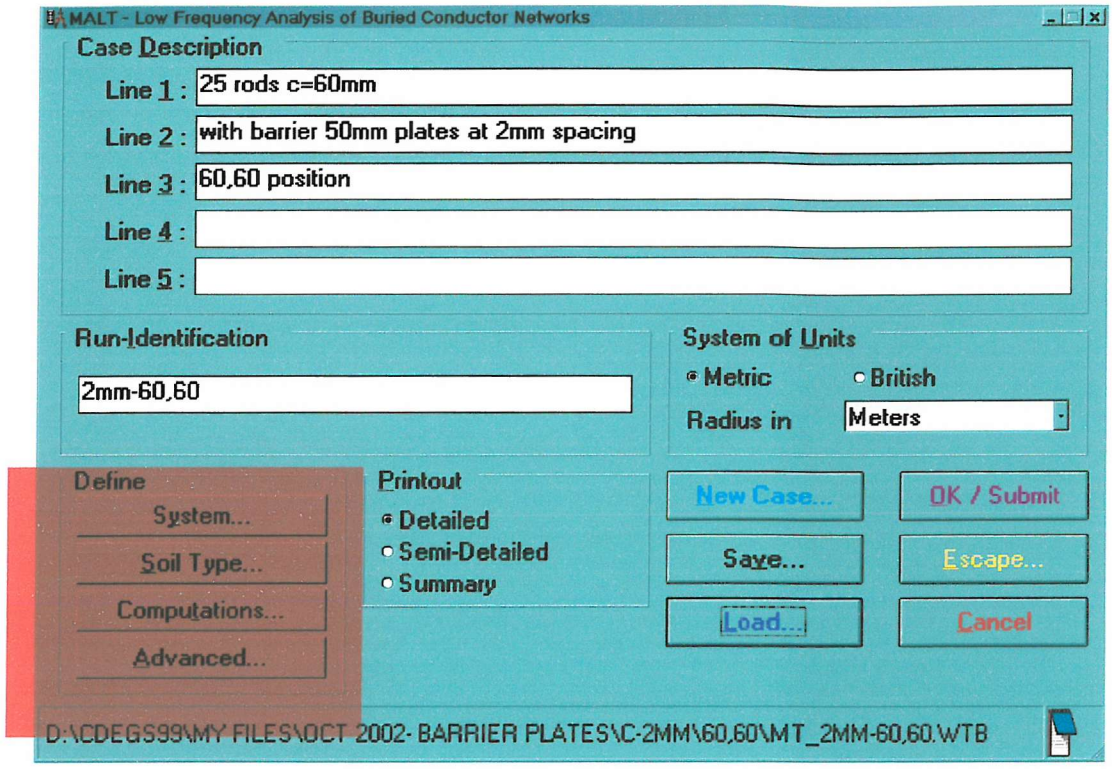

Figure 3.2 : MALT main input screen

Figure 3.3 shows the MALT *System* screen. The top left of the screen (highlighted in red) suggests, more than one earthing system can be entered, which are a main earthing system, an optional return electrode, and any number of buried structures, each one consisting of as many conductors as desired and each one energised by a voltage, a current, or left floating. As the illustration shows, the conductors can be oriented in any way you wish, in three-dimensional space. The conductor coordinates can be specified by a number of means, alone or combined.

Figure 3.4 illustrates the SesCAD screen. SesCAD is an important tool in drawing the earthing grid. There are many features in SesCAD, which will make drawing the earthing grids easier.

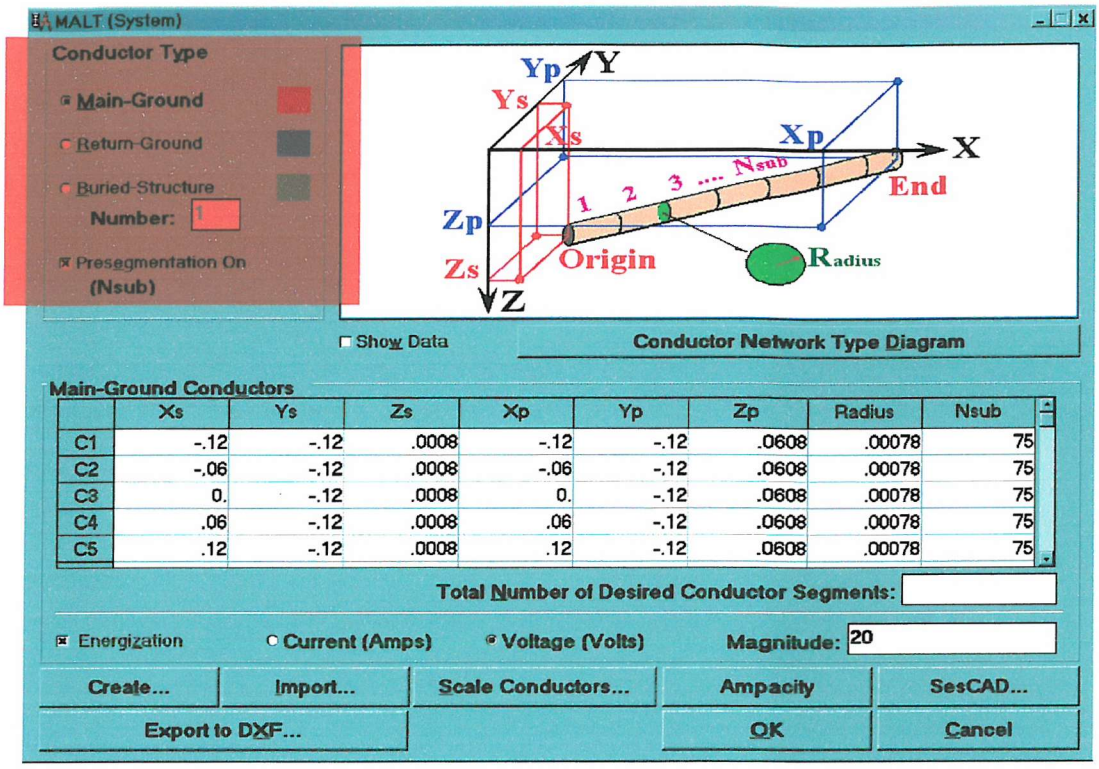

Figure 3.3 : MALT *System* screen

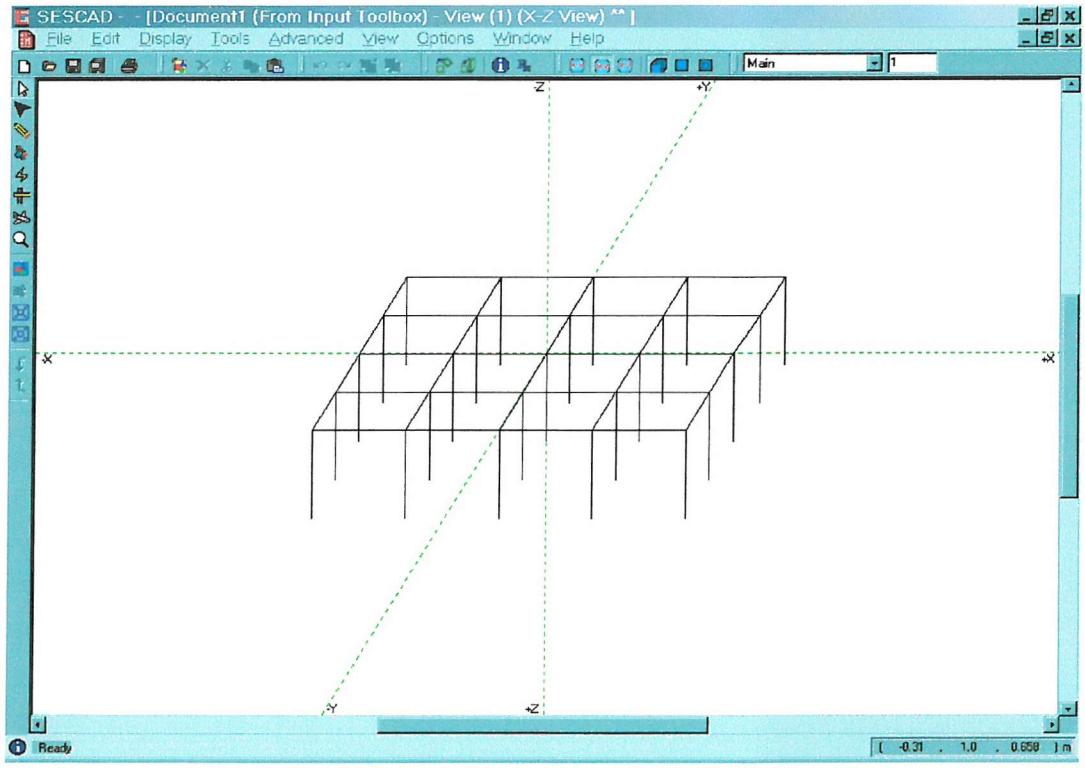

Figure 3.4: *SesCAD* screen

After drawing the earthing system and entering the appropriate data, the next step would be to enter the soil structure characteristics. If RESAP has been run, MALT will automatically use the model proposed by RESAP if one is not entered here. MALT offers a great variety of soil models as can be seen from Figure 3.5. The most commonly used in practise is the horizontally layered soil. Other soil structures include vertical layering, multiple finite volumes of soil with different resistivities (useful for modeling backfill or multi-tiered sites), cylindrical and hemispherical volumes of soil (to model rivers, lakes, etc.).

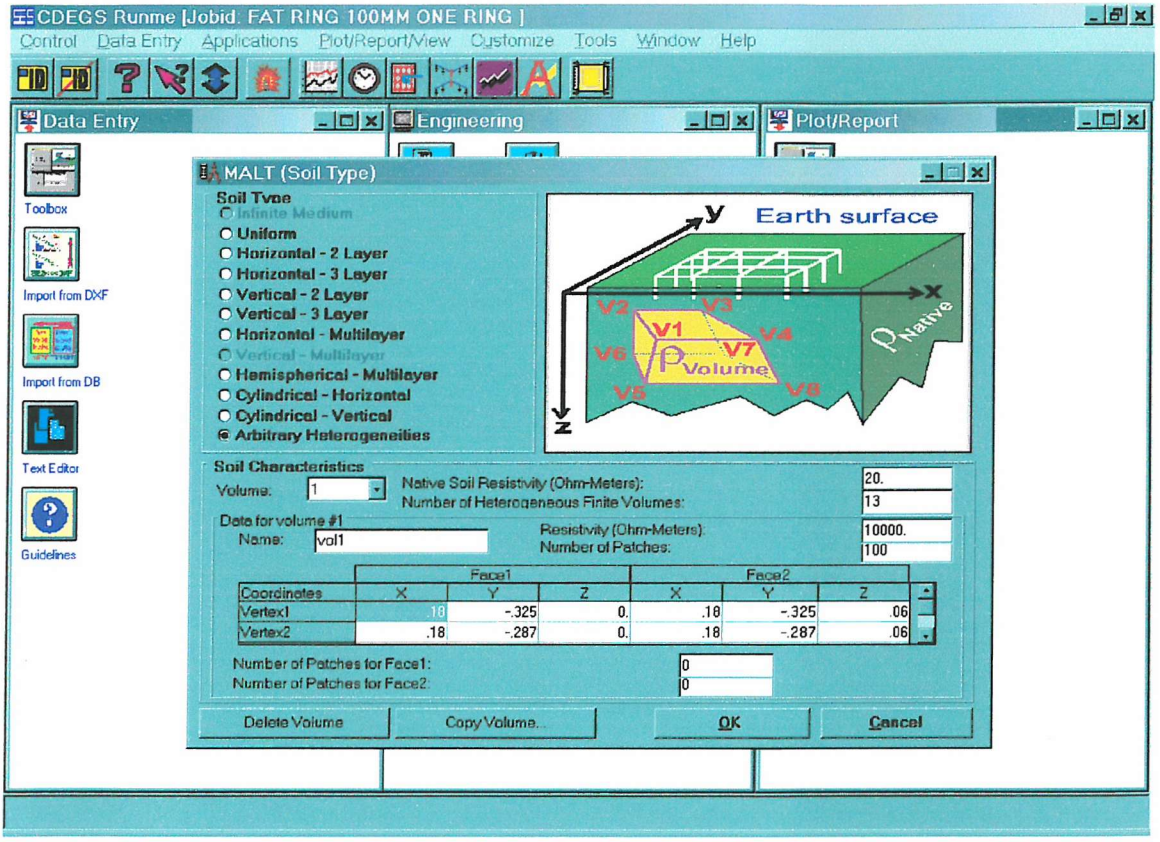

Figure 3.5: *Soil Type* screen

The *Computation* screen (see Figure 3.6) is where the points for touch voltages, step voltages and earth surface potentials will be specified. This can be done with SesCAD (highlighted in red), in which one or more rectangular arrays of points can be drawn with the mouse; simple lines of points or "profiles" can also be specified. Alternatively, this information can be entered in the table shown on this screen (highlighted in green).

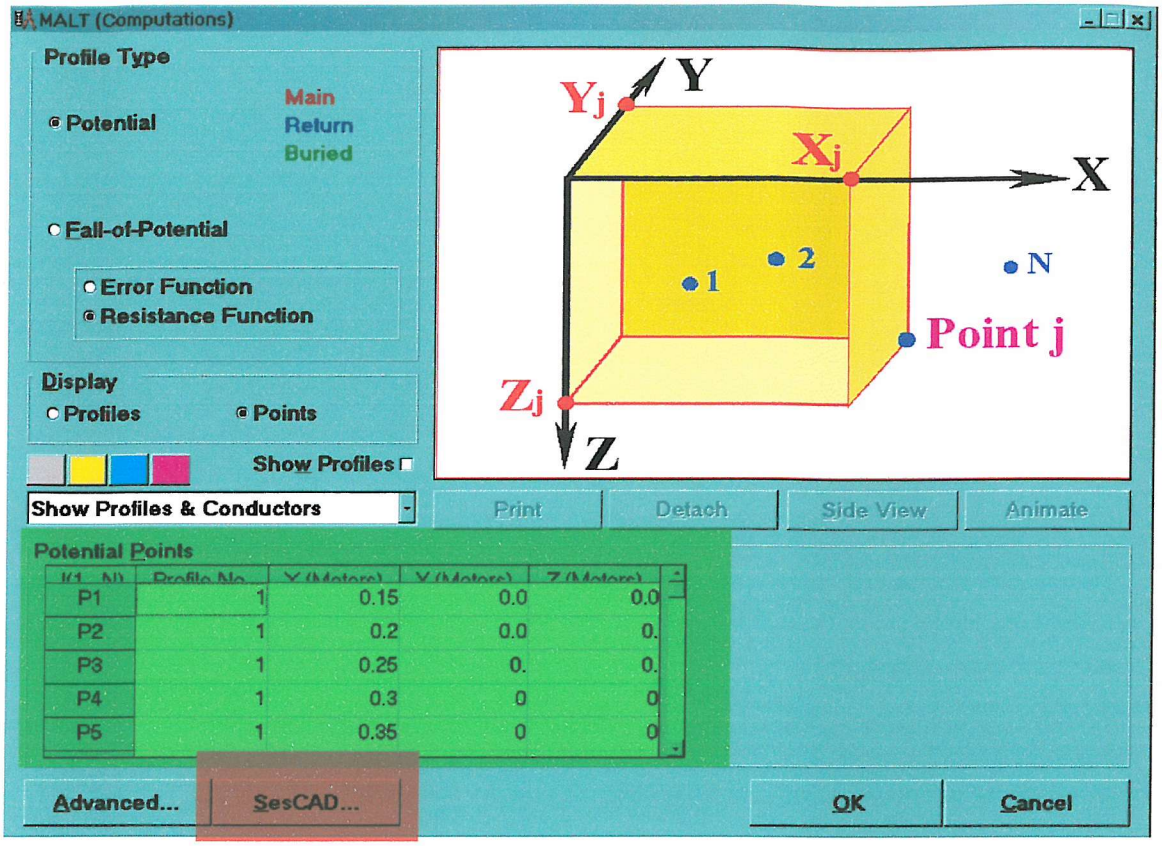

Figure 3.6: *Computation* screen

A large variety of graphs and reports can be generated by MALT. The data that can be plotted includes: touch voltages, step voltages, earth potentials, fall-of-potential apparent impedances, conductor potentials, and conductor leakage currents. Figures 3.7 and 3.8 show a couple of examples of output screens that can be obtained after the computations have been done.

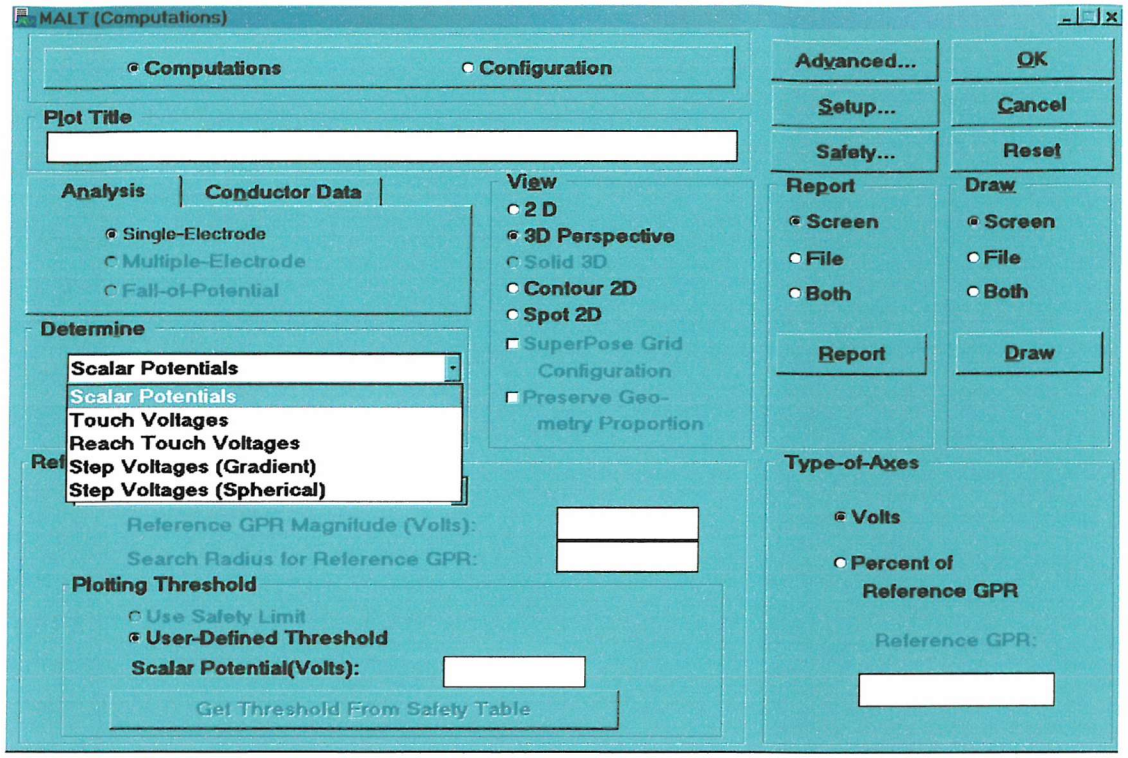

Figure 3.7: A large variety of graphs and reports can be generated by MALT.

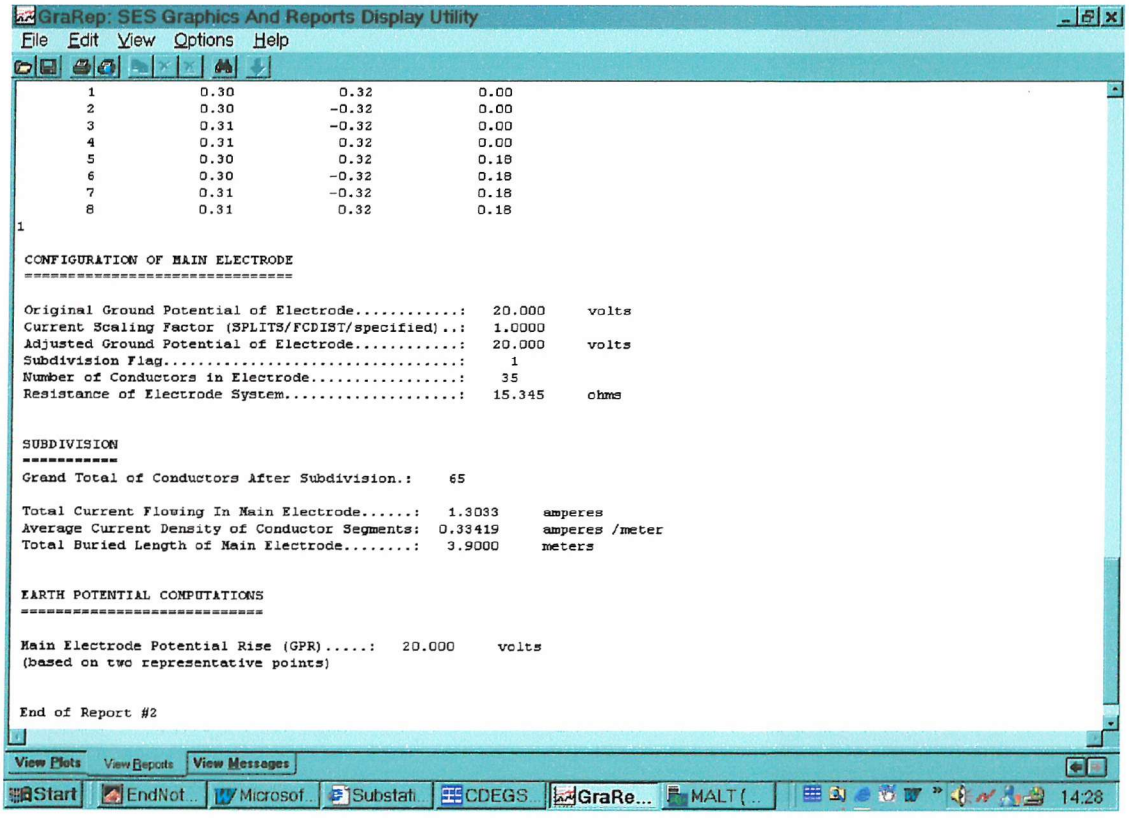

Figure 3.8: Numerical values from the output panel giving the grid resistance and GPR.

3.5 Electrolytic Tank

The need for accurate design procedures for the earthing system becomes more important both from a safety point of view and from financial considerations, as the number and complexity of AC substations increase. When all the physical dimensions of an earthing grid system are reduced in size by the same scale factor (this includes the conductor diameter and the depth to which the grid is buried), the pattern of current flow and the shape of the equipotential surfaces are unaltered. Some further changes are necessary in order for modeling to be of practical value. The full-scale grid is buried in semi-infinite earth, but a solid medium is inconvenient both from the measurement standpoint and when delicate model grids must be frequently removed for modifications and replaced. Hence, the obvious alternative is an electrolytic tank. The electrolyte presents no particular problem for the homogeneous case, as water is a convenient choice.

In essence there are only three methods for evaluating the performance of an earthing grid. These are the measurements on a full-scale grid, numerical computation (see Chapter 3), and measurement on a scale model grid. Full-scale tests are both costly and difficult to perform, hence they are very unattractive. Numerical methods, on the other hand, are very convenient to use once the necessary programs are available and thoroughly verified. Creation of these programs, however, is not without its problem. In all but the simplest cases, it is necessary to make some simplifying assumptions.

Scale modelling provides a valuable alternative method. It requires only a very modest investment in equipment. It can be used to verify numerical methods during the development phase. Once an electrolytic tank has been set up, it is possible to make changes on grid models quickly and easily.

3.5.1 Researchers using Electrolytic Tank and Scale Models

In a 1950 paper by Koch, the concept of using scale models and an electrolytic tank to simulate the performance of earthing grids was introduced [93]. This paper may have had the most impact on the IEEE-80 Guide [94]. A number of other researchers published papers in the 1950's on the use of scale models, for example, McCrocklin and Wendlandt

[95] and Amstrong [96] in the United States, Schmidt [97] in Germany, and Faletti, Rossignani and Malaman [98] and Rossignani and Rostagno [99] in Italy. The use of scale models continued world wide in the 1960's with work by Amstrong and Simpkin [31], Thapar and Puri [100], and Voronina [101]. A number of papers have been published in the last decade on research work related to scale models performed at Ecole Polytechnique, Montreal, Canada [42, 90, 102]; the researchers include Dawalibi, DeJean, Gervais and Mukhedkar.

The size of the electrolytic tank is directly related to the minimum scale factor, which can be used. In the initial work by Koch, the model size was limited to 120mm with a scale factor of 115. The tank was a metal container. Many researchers utilized a rectangular tank either made of concrete or of wood construction and lined with plastic with one of the larger being 6 x 15 feet by 1.5 feet deep (1.83m x 4.57m by 0.46m deep) [96]. There are a few researchers who use a hemispherical tank. Kouteynikoff [103] used a 2.7m diameter hemisphere while a 20m diameter hemisphere was used by Amstrong and Simpkin [31] and Thapar and Puri [100]. The researchers in reference [95] report the use of a large lake as the electrolytic tank in which case grids up to 2.44m x 2.44m were tested.

The physical return electrode varied significantly among the various researchers. Koch used the metal container which was the electrolytic tank as the return electrode [93]. In one case a hemispherical return electrode was used [103] and in another the return electrode was a copper bar located around the periphery of the tank just below the water level [104]. Most researchers report the use of a return electrode that was a small plate or simply an electrode located at one edge of the tank.

3.5.2 Experimental Arrangement

The experimental tank used in this research is cylindrical and measures 2m in diameter and 1.2 m in depth. It also has a plastic liner that covers the inner part of the tank. The model-earthing mat is mounted on a central platform suspended from a rigid arm attached to one of the vertical steel wall struts. The potential on the surface of the water is measured by a probe suspended by a plumb-bob arrangement from a horizontal arm

that is free to rotate about the axis of the tank through 360^0. Only the tip of the wire is touching the surface of the water. Surface measurements within the platform area are obtained by inserting fixed probes through 1.5 mm holes in the platform. The platform is made from hard clear Perspex that will not absorb water and it provides a horizontal configuration with the minimum distortion and sag.

The true earth plane is a flat zinc-coated steel mesh, containing very small holes, whose height from the tank bottom can be adjusted. The resistance of a single vertical rod was measured with the mesh between 0.8m and 1.1m below the surface. No significant difference was found and so the earth plane is sufficiently distant at 1.0m. The inner circular side of the tank is also conducting; it is covered using the same material as the flat mesh.

The model rods are made of brass and are 1.56 mm in diameter and 60 mm in length. In addition, two thin copper discs were manufactured (diameters 50 mm and 100 mm) as a simple approximation to a horizontal earthing mat that can be modelled theoretically (although not by CDEGS MALT).

The AC source consisted of a variac and an isolating transformer. The isolating transformer was for safety purposes and allows earthing of the outer electrode of the tank. A variable resistor was used between the conducting tank lining and one side of the power supply to simulate approximately the resistance between the outer tank wall and infinity (see Appendix 2). The applied voltage thus simulated that which would exist between the earthing electrode being tested and infinity. A high impedance voltmeter was used to monitor this voltage and a digital multimeter measures the current through the tank and external resistor. The ratio of these two readings is a measure of the effective grid resistance when buried in a semi-infinite earth. The multimeter also measures the potential of the voltage probe with respect to "infinity". Figure 3.9 below illustrates the electrolytic tank circuit.

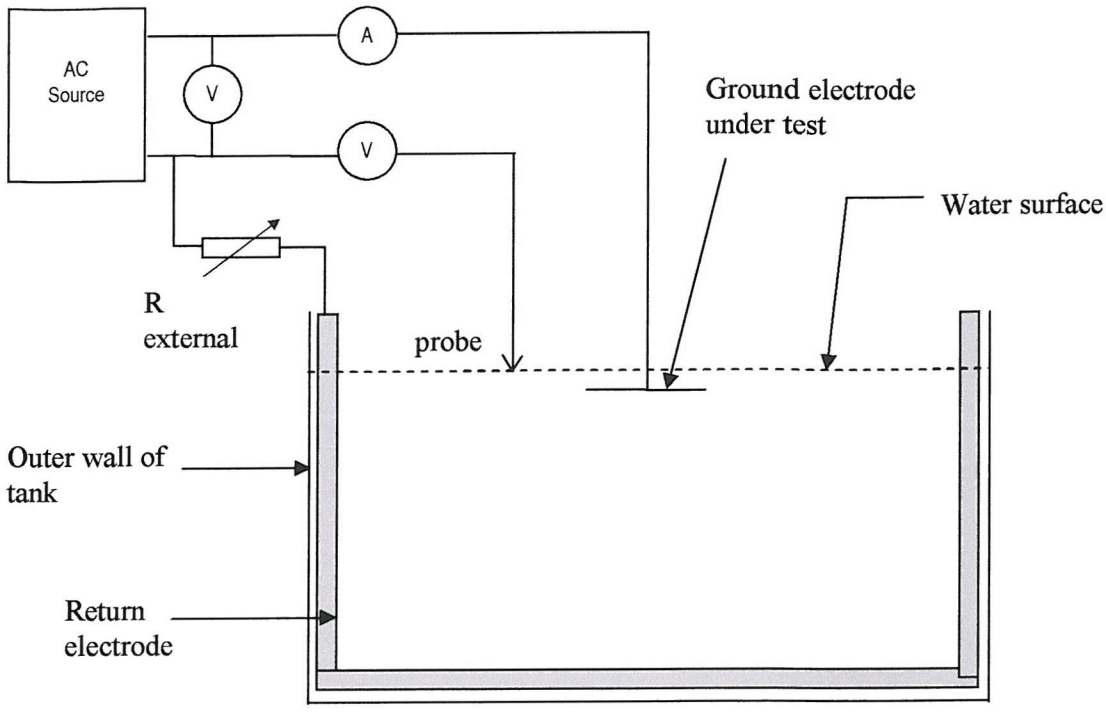

Figure 3.9: Electrolytic tank circuit

The figures below show some of the experimental set up.

Figure 3.10: Earthing grids 1 – horizontal mesh, combined grid, disc and hemispherical electrode

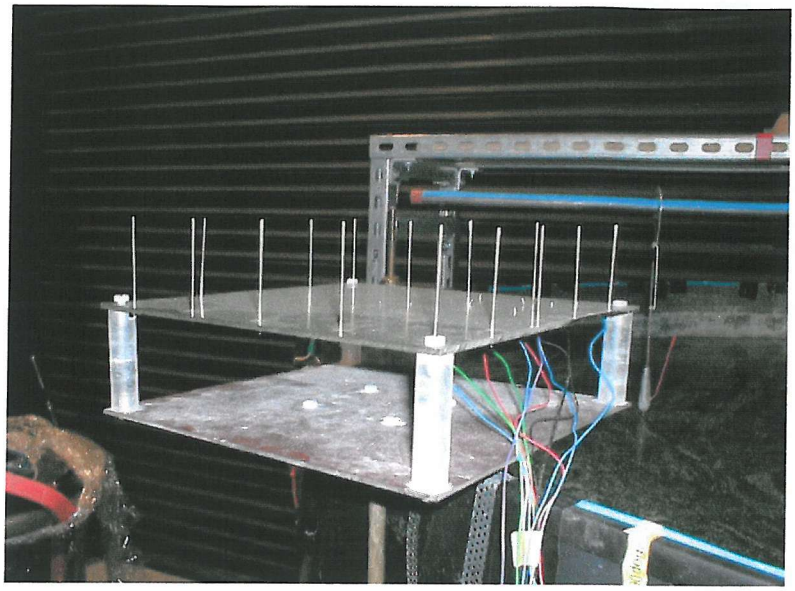

Figure 3.11: Earthing grids 2 – 16 vertical rods

Figure 3.12: Voltage probe

Figure 3.13: Side view of electrolytic tank

3.5.3 Water Resistivity Measurement

The resistivity of the electrolyte (tap water) used in the scale models, which represents soil in real situation, plays an important role in the accuracy of the measurements obtained. The value of the external resistor, which simulates approximately the resistance between the outer tank wall and infinity, depends on the resistivity of the water used. Hence, these four methods have been conducted when measuring the water resistivity in the electrolytic tank:

a) Conductivity meter

- Two *Hanna Instruments* conductivity meters were used. These meters were calibrated using the appropriate calibration solution at least once a week, or before any experiment takes place. These meters provide a quick and accurate way to measure water resistivity. Figure 3.14 shows the conductivity meters used throughout this research.

Figure 3.14: Conductivity meters

b) Equation 3.8 (Section 3.1)

- Two rods in homogeneous soil separated by a distance c' has been discussed in Section 3.1 (Analytical Method). Equation 3.8 obtained can be used to calculate σ, the value of the soil resistivity or the tank water in this case. Equation 3.8 is as follows:

$$0.5\Delta V = IR + V_{12} = I\frac{\ln\frac{4l}{d'} - \ln\alpha}{2\pi\sigma l}$$

where l = length of rod

d'=rod diameter

$\alpha = \coth\left(0.5\sinh^{-1}\frac{c'}{l}\right)$

c'= spacing between two earthing rods

- In practical, both I and ΔV can be measured. This experiment is done in the electrolytic tank itself. Hence, the resistivity of the water in the tank can be obtained.

c) Passing Current through a Cylindrical Tube

- Using Ohms Law, the resistivity of the water inside the cylindrical tube can easily be obtained when voltage is applied at both ends of the tube. Figure 3.15 illustrates the experimental set-up. The formula used is as shown below [105-108]:

$$R = \frac{V}{I} = \frac{EL_1}{J\pi r_1^{\,2}} = \rho \frac{L_1}{\pi r_1^{\,2}} \qquad (3.12)$$

$$\therefore \rho = \frac{V}{I} \frac{\pi r_1^{\,2}}{L_1} \qquad (3.13)$$

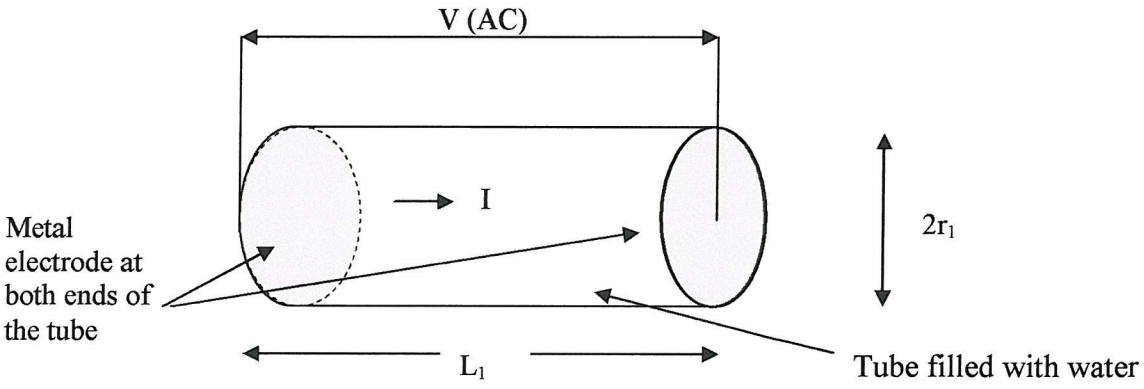

Figure 3.15: Passing current through a cylindrical tube

d) Modified Wheatstone Bridge

- The resistance of an electrolyte is usually determined with the aid of a modified Wheatstone bridge [109, 110]. The circuit diagram is shown diagrammatically in Figure 3.16.

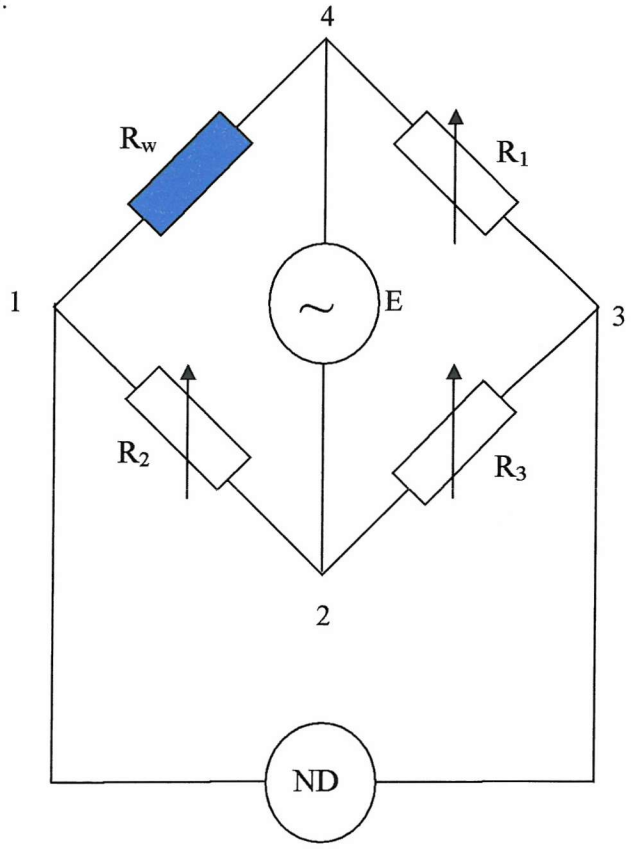

Figure 3.16: Modified Wheatstone Bridge

- R_1, R_2, and R_3 are calibrated variable resistance (i.e. resistance box), R_w is the cylindrical tube filled with water as in 3.5.3 (c), E is a source of current (i.e. an oscillator), and ND is a null detector.
- The current at E is turned on and the variable resistances are adjusted until no current passes through the Null Detector. At this point of balance, the total fall in potential in the branches 412 and 432 must be the same, and also point 1 and point 3 must be at the same potential, since no current passes through ND. Therefore,

$$\frac{R_w}{R_w + R_1} = \frac{R_3}{R_3 + R_2} \qquad (3.14)$$

$$R_w = \frac{R_1}{R_2} R_3 \qquad (3.15)$$

- This is an outline of the method developed by Kohlrausch [109, 110] and commonly used at the present day.

Method (b), (c) and (d) are done to check the accuracy and reliability of the conductivity meters. These three methods gave similar reading with less than 2% difference when compared with the conductivity meter reading. Hence, for simplicity, only the calibrated conductivity meters were used in the experiments.

3.5.4 Experimental Measurement Errors

With a working system developed, the next objective was to establish the validity and any experimental errors from the results obtained. Several approaches were taken to this. The bottom earth plane was made in such a way that it could move up and down, hence altering the depth of the tank. By measuring the same model grid in various tank depths, it was possible to establish that the finite size of the tank did not prevent correct potential profiles being measured. As a second check, comparisons were made between measured results and those obtained by numerical computation in the limited number of cases when computed values were obtainable from outside sources. Comparisons with theoretical methods can be obtained in Chapter 4.

Most if not all experiments have one thing in common, which is each measurement that is made is subject to experimental uncertainties [111-115]. This means that if a repeated measurement of a particular quantity is to be made, there is likely to be a variation in the observed value. Although it may be possible to reduce an uncertainty by improved experimental method or the careful use of statistical techniques, it can never be eliminated.

In this research, all of the experiments are done at least three times at different days to ensure its reliability and reduce any unintentional errors. The results presented in this thesis are the mean values and the standard deviations (S.D.) are quoted in each result in

the Appendix. All conclusions drawn are based on the mean values. The standard deviation was found to be very small, less than 1% for resistance measurement and surface potentials measurements in most cases. This shows that the results are reproducible. Standard deviation is calculated using the following formulae [111-115]:

$$\sigma = \sqrt{\frac{\Sigma\left(x_i - \bar{x}\right)^2}{n}} \tag{3.16}$$

where x_i is the ith measured value, $\bar{x}$ is the mean value, and n is the number of times the experiment is being repeated.

An experiment may require the determination of several quantities, which are later to be inserted into an equation. For example, the resistance of a system is obtained by applying the voltage, V (measured by a voltmeter), and the current through the system, I, is measured. Using Ohm's Law, V=IR, the resistance can then be obtained. Hence, the uncertainties in the measured quantities, V and I, can be combined to give an uncertainty in the calculated resistance, R. This is called propagation of uncertainties or error propagation [111].

Referring back to the experimental circuit in Figure 3.9, the equation to obtain the resistance of the earthing system (scaled to 0.1S/m) is as follows:

$$R_g = \frac{V}{I_{no\ R_{ext}}} + R_{ext} \tag{3.17}$$

And the equation to obtain the external resistor, R_{ext} is:

$$R_{ext} = \frac{1}{2\pi\sigma r_2} \tag{3.18}$$

$I_{no\ Rext}$ is the current obtained when there is no external resistor. The simpler way is to insert the external resistor when doing the experiment to get the actual current when the tank is simulated to be infinite in size. However, by doing this, one cannot determine the errors produced by the R_{ext} as it will be deleted from the equation.

R_{ext} value is dependent upon the radius of the cylindrical tank, r_2 and the conductivity of the water, σ (see Appendix 2). These two values are measured using a meter ruler and a conductivity meter (see Figure 3.10) respectively. The quantities to obtain R_g, the earthing system resistance, are measured using the analogue voltmeter and a multimeter to measure the current.

As for the surface potential measurements, the equation is as shown:

$$V_s = V_{wrt\ \text{tank}} + I(R_{ext}) \tag{3.19}$$

Where $$I = \frac{V}{R_g} \tag{3.20}$$

$V_{wrt\ tank}$ is the surface potential with respect to tank lining (i.e. no external resistor present). In order to obtain the surface potential with respect to infinity, the voltage across the external resistor is included. Again, it would be simpler to add the external resistor during the experimentation to get the surface potential with respect to infinity directly, but one cannot determine the errors produced by the R_{ext} as it will be deleted from the equation.

Hence, according to Kirkup [111], the maximum experimental error can be calculated by inserting the maximum and minimum values for the uncertain quantities. For example,

$$\frac{V_{\max}}{I_{\min}} = R_{g\max} \tag{3.21}$$

$$\frac{V_{\min}}{I_{\max}} = R_{g\min} \tag{3.22}$$

$$\frac{R_{g\max} - R_{g\min}}{2} = \Delta R_g \tag{3.23}$$

ΔR_g is the error in obtaining the resistance taking into account the uncertainties produced by the voltmeter and the multimeter.

Table 3.1 shows the accuracy of equipment involved in the experiment.

Equipment	Accuracy
Meter ruler	± 0.5 mm
Conductivity meter	± 1% of the full scale (± 0.001999S/m)
Analogue Voltmeter	¼ of 1% of the full scale deflection (± 0.075V)
Multimeter (measuring current)	0.1% of the reading + 0.04% of the range (1A range)
Multimeter (measuring voltage)	0.04% of the reading + 0.02% of the range (750V range)
Resistance box (for the external resistance)	1Ω knob (±0.03%+2mΩ), 0.1Ω knob (±0.1%+2mΩ), 0.01Ω knob (±2%+2mΩ)

Table 3.1: Accuracy for each instrument used

For example, for the 4 vertical rods with 60mm spacing arranged in a square, the voltage applied is 20V ± 0.075V. The current measured through the earthing system without the external resistor is 0.247A ± 6.39 x 10^{-4} A. The conductivity of the water at that time was measured to be 0.0580 ± 0.001999 S/m. Hence, the maximum and minimum resistance obtained (from equation 3.17 and 3.18) when taking into account the uncertainties in the experimental equipment (refer to Table 3.1) are (scaled to 0.1 S/m):

$$R_g = \left(\frac{V}{I_{no\ \mathrm{Re}\,xt}} + \frac{1}{2\pi\sigma r_2} + \text{resistance box error} \right)\left(\frac{\sigma}{0.1} \right) \tag{3.24}$$

$$R_{g\max} = \left(\frac{20.075}{0.246} + \frac{1}{2\pi(0.056001)(0.95)} + 8.1m\Omega \right)\left(\frac{0.059999}{0.1} \right) = 50.63\,\Omega \tag{3.25}$$

$$R_{g\min} = \left(\frac{19.925}{0.248} + \frac{1}{2\pi(0.059999)(1.05)} - 8.1m\Omega \right)\left(\frac{0.056001}{0.1} \right) = 46.42\,\Omega \tag{3.26}$$

$$\therefore \quad \Delta R_g = \frac{50.63 - 46.42}{2} = 2.11\,\Omega \tag{3.27}$$

8.1 mΩ is the error from the resistance box, calculated as follows (for $R_{ext} = 2.74\Omega$):

$$\Delta R_{box} = [(0.03\% \times 2) + 2m\Omega] + [(0.1\% \times 0.7) + 2m\Omega] + [(2\% \times 0.04) + 2m\Omega] = 8.1\, m\Omega \quad (3.28)$$

An example in calculating the experimental uncertainties in surface potential measurement is shown below. This measurement is at angle 0°, and distance 0mm for the same rod configuration as in the resistance measurement (4 rods with 60mm spacing). The voltage applied is 20V ± 0.075V and the current measured through the earthing system without the external resistor is 0.247A ± 6.39 x 10^{-4} A. The conductivity of the water at that time was measured to be 0.0580 ± 0.001999 S/m. The multimeter error when measuring the surface potential is ±0.155 V. Hence, the maximum and minimum surface potential obtained when taking into account the uncertainties in the experimental equipment (refer to Table 3.1) are:

$$V_s = \left(V_{s\ wrt\ tan\ k} + multimeter\ \ error\right) + \left(\left(\frac{V}{R_g + \Delta R_g}\right)\left(\frac{1}{2\pi\sigma r_2}\right)\right) \quad (3.29)$$

$$V_{s\max} = (11.31 + 0.155) + \left(\left(\frac{20.075}{48.5 - 2.11}\right)\left(\frac{1}{2\pi(0.056001)(0.95)}\right)\right) = 12.7576V \quad (3.30)$$

$$V_{s\min} = (11.31 - 0.155) + \left(\left(\frac{19.925}{48.5 + 2.11}\right)\left(\frac{1}{2\pi(0.059999)(1.05)}\right)\right) = 12.1485\,V \quad (3.31)$$

$$\therefore \quad \Delta V_s = \frac{12.7576 - 12.1485}{2} = 0.3\,V \quad (3.32)$$

These measurement uncertainties together with the standard deviation are included in the results in the Appendices. To improve clarity of the graphs, these uncertainties are not shown in the graphs of results.

CHAPTER 4

Comparison of CDEGS MALT with Theoretical Methods

Many formulae have been developed to calculate the resistance and surface potentials for some rod configurations. The analytical model explained in Chapter 3 (Section 3.1) is one of them. Tagg [5] lists several common formulae for a single vertical rod. Surprisingly, the circular cylindrical shape is difficult to handle, especially if a rounded or pointed tip is included, and so either a more mathematically tractable shape is taken, or assumptions are made about the distribution of the surrounding current flow pattern.

4.1 Existing Formulae for the Resistance and Surface Potentials of Vertical Rod(s)

a) **single electrode**

i) Cylinder with hemispherical tip [16, 116]

$$R_{cyl} = \frac{\rho}{2\pi l} \ln \frac{l}{r} \qquad (4.1)$$

where ρ = resistivity of soil (Ωm)

l = length of rod (m)

r = radius of rod (m)

$$Vx' = \frac{I\rho}{2\pi l} \ln\left(\frac{l + x'}{x'}\right) \qquad (4.2)$$

where Vx'= potential of any point at a distance x' from the axis with respect to the zero potential point.

The formula for 'cylinder with hemispherical tip' has been derived by Datta et al [16] under the assumption that the current has uniform density over each equipotential surface, and that all such surfaces maintain the same shape as the rod surface. Neither of these assumptions is necessarily true in practice.

ii) Ellipsoid [5, 16, 34, 116]

The following equations use the normal assumption that the minor axis of the ellipse is the diameter of the rod (d'). However, the value has been found to be more accurate if d''= √2 x d' is employed (see Chapter 3, Section 3.1).

$$R_{el} = \frac{\rho}{2\pi l} \ln \frac{4l}{d'} \tag{4.3}$$

$$Vx' = IR_{el} \frac{\ln\left\{\coth \frac{\eta}{2}\right\}}{\ln\left(\frac{4l}{d'}\right)} \tag{4.4}$$

where d' = 2r

sinh η = x'/l

x' = distance from axis of rod (m)

ρ = resistivity of soil (Ωm)

l = length of rod (m)

r = radius of rod (m)

iii) S34 Vertical Rod Formula [35, 116]:

$$R_{S34} = \frac{\rho}{2\pi l}\left(\ln \frac{8l}{d'} - 1\right) \tag{4.5}$$

$$Vs = \frac{\rho I}{2\pi l} \ln\left(\frac{l}{x'} + \sqrt{1 + \frac{l^2}{x'^2}}\right) \tag{4.6}$$

where x' = distance from axis of rod (m)

d' = 2r

ρ = resistivity of soil (Ωm)

l = length of rod (m)

r = radius of rod (m)

b) **Two electrodes**

i) From reference [16]:

$$R = \left(\frac{1+m}{2}\right) R_{cyl} \tag{4.7}$$

$$m = \frac{\ln\frac{l+c'}{c'}}{\ln\frac{l}{r}}$$

where c' = spacing between rods (m)

R_{cyl} = resistance of an isolated rod for cylinder with hemispherical tip

l = length of rod (m)

r = radius of rod (m)

ii) From reference [34]:

$$R_{el} = 0.5\left[R_{el} + \frac{\ln(\alpha)}{2\pi\sigma l}\right] \tag{4.8}$$

$$\alpha = \coth\left\{0.5\sinh^{-1}\frac{c'}{l}\right\}$$

where R_{el} = resistance of an isolated rod for ellipsoid model

c' = spacing between rods (m)

l = length of rod (m)

σ = conductivity of soil (S/m)

c) **Four electrodes**

From reference [16],

$$R = \left(\frac{1 + 2m + q}{4} \right) R_{cyl} \qquad (4.9)$$

where

$$m = \frac{\ln \frac{l + c'}{c'}}{\ln \frac{l}{r}} \qquad q = \frac{\ln \frac{l + \sqrt{2}c'}{\sqrt{2}c'}}{\ln \frac{l}{r}}$$

c' = spacing between rods (m)

R_{cyl} = resistance of an isolated rod

l = length of rod (m)

r = radius of rod (m)

From reference [34],

$$R = \left(\frac{1 + 2m + q}{4} \right) R_{el} \qquad (4.10)$$

where:

$$m = \ln \left[\frac{\coth \left\{ \frac{1}{2} \sinh^{-1} \frac{c'}{l} \right\}}{\ln \frac{4l}{d'}} \right] \qquad q = \ln \frac{\coth \left\{ \frac{1}{2} \sinh^{-1} \frac{\sqrt{2}c'}{l} \right\}}{\ln \frac{4l}{d'}}$$

c' = spacing between rods (m)

R_{el} = resistance of an isolated rod

l = length of rod (m)

d' = 2 x r (radius of rod) (m)

4.2 Results of comparison

Using the same parameters as the initial proposed design for the experimental tank, the resistance and surface potential for each electrode configuration discussed above are computed. The parameters used in the computations for both the theoretical formula and in MALT are as follows:

Rod radius = 0.7 mm

Rod length = 60 mm

Soil resistivity = 10 Ωm

Injected current = 1A

The results for resistance of various rod configurations and surface potentials for one rod are as shown in the Tables 4.1 and 4.2 below respectively and compared with the results obtained by CDEGS MALT.

Rod configuration	**Model**	**Spacing, c (mm)**	**Resistance of the electrode system (ohms)**	
			Formula	**MALT (Uniform soil)**
1 rod	Analytical solution	-	127.8	126.4
	Cylinder with Hemispherical tip	-	118.1	
	Ellipsoid	-	127.3	
	Vertical rod (S34)	-	128.3	
2 rods	Reference [16]	30	73.6	80.1
		60	68.2	73.9
		120	64.4	69.3
	Reference [34]	30	82.8	80.1
		60	75.3	73.9
		120	70.0	69.3
4 rods	Reference [16]	60	42.3	46.5
		120	36.9	40.0
		180	34.5	37.4
		240	33.6	36.0
	Reference [34]	60	47.9	46.5
		120	40.5	40.0
		180	37.7	37.4
		240	36.3	36.0

Table 4.1: Resistance of different electrode systems

MALT seems to agree very well with the theoretical formulas with percentage difference less than 1.5% for most cases. This is because MALT uses the most commonly used method for earthing analysis which is based on the method of images and assumes that the earthing system is an equipotential structure [117].

The cylinder with hemispherical tip model has about 6-8% error when compared to MALT and also other formula. The cyclindrical rod with hemispherical tip sounds ideal until it is realised that all the surrounding equipotentials are constrained to follow the same shape, i.e. become cylinders with closing hemispheres of increasing diameter. The local current density is not only forced to cross these equipotential surfaces at right angles but also with uniform density over the surfaces. The resulting current flow almost certainly suffers considerable distortion. This could be the cause of the substantial error when compared with other methods.

Table 4.2 below shows the comparison of surface potential for one rod using the various theoretical formulae and MALT. As for the resistance calculations before, the model 'cylinder with hemispherical tip' gives the worst percentage difference, when compared with MALT. MALT, S34 and ellipsoidal model gives identical results. With the very good agreement, it is thought that MALT and S34 might employ the ellipsoidal model in the computations.

Model	**Vx' (volts) (x'= distance from axis of rod)**								
	4mm	6mm	8mm	10mm	12mm	14mm	16mm	18mm	20mm
Analytical	86.47	76.41	69.26	63.72	59.20	55.39	52.11	49.22	46.66
Cylinder	73.55	63.61	56.77	51.62	47.53	44.17	41.33	38.90	36.77
Ellipsoid	90.25	79.53	71.95	66.10	61.34	57.34	53.91	50.90	48.24
S34	90.25	79.53	71.95	66.10	61.34	57.34	53.91	50.90	48.24
MALT	90.25	79.53	71.95	66.10	61.34	57.34	53.91	50.90	48.24

Table 4.2: Surface potential for one rod using various methods

Table 1 (page 20) of S34 [35] gives the recommended expression for the earth resistance of a single vertical rod as

$$R_{S34} = \frac{\ln \frac{4l}{r} - 1}{2\pi\sigma l} \qquad (4.11)$$

It is interesting that equation 4.11 give results within 1% of those for the modified ellipsoidal model (eqn. 3.1). This is in contrast to the models that either assumes the current to leave the cylindrical surface of the rod with uniform density or have equipotentials formed of cylinders closed with hemispheres (see Section 3.1).

The feature of particular interest, however, is the expression for the surface potential given in Table 3 of S34, namely

$$V_{S34} = I \frac{\ln\left[\frac{l}{x'} + \sqrt{1 + \left(\frac{l}{x'}\right)^2}\right]}{2\pi\sigma l} \qquad (4.12)$$

If this is compared with eqn.3.5 for the ellipsoid (see Section 3.1) it can be shown after some work that the expressions are identical. This fact follows from the identities

$$\sinh^{-1} y = \ln\left\{y + \sqrt{1 + y^2}\right\} \qquad \text{and} \qquad \coth Y = \frac{e^{2Y} + 1}{e^{2Y} - 1}$$

where $y = x'/l$ and $Y = 0.5\ sinh^{-1}(x'/l)$ (see equation 3.5). It is almost certain that the rod model proposed in S34 is also based on the ellipsoid, as shown by the results here.

4.3 Comparisons with S34: More complex grid

CDEGS MALT is used here to compare with three of the cases given in S34 [35]. They are the 'Buried Grid', 'Groups of Rods in Hollow Square' and 'Combined Grid with Rods connected around the Periphery'. For each case, different random test parameters are applied.

4.3.1 Buried Grid

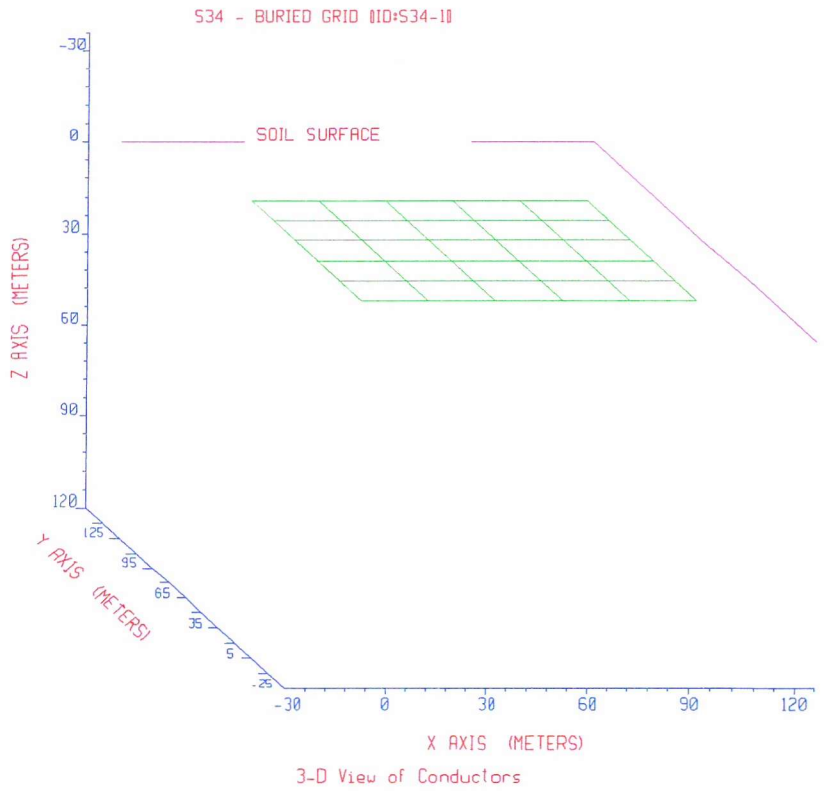

Figure 4.1: Buried grid

Parameters used:

Case No.	Grid area (m^2)	Grid dimension (m)	ρ soil (Ωm)	Burial depth (m)	Radius (m)	Current (A)	Length (m)
1	10000	100x100	100	1	0.01	100	1200
2	100	10x10	20	1	0.017	100	180
3	400	20x20	200	2	0.03	150	200
4	10000	100x100	100	0.05	0.01	100	1200
5	100	10x10	20	0.05	0.017	100	180
6	400	20x20	200	0.05	0.03	150	200

Formulae given in S34 (page 20, Table 1, column 5) [35]

$$R = \frac{\rho}{4r} + \frac{\rho}{L}$$

where

L = length of buried conductor

$$r = \sqrt{\frac{A}{\pi}}$$

A= area of grid

Formulae given in S34 (page 22, Table 3, column 3) [35]

$$Vs = \frac{\rho I}{2\pi r'} \arcsin \frac{r}{x'}$$

$$r' = \frac{\rho}{4\,Rg}$$

Rg = grid electrode earthing resistance (ohm)

4.3.2 Group of rods in hollow square

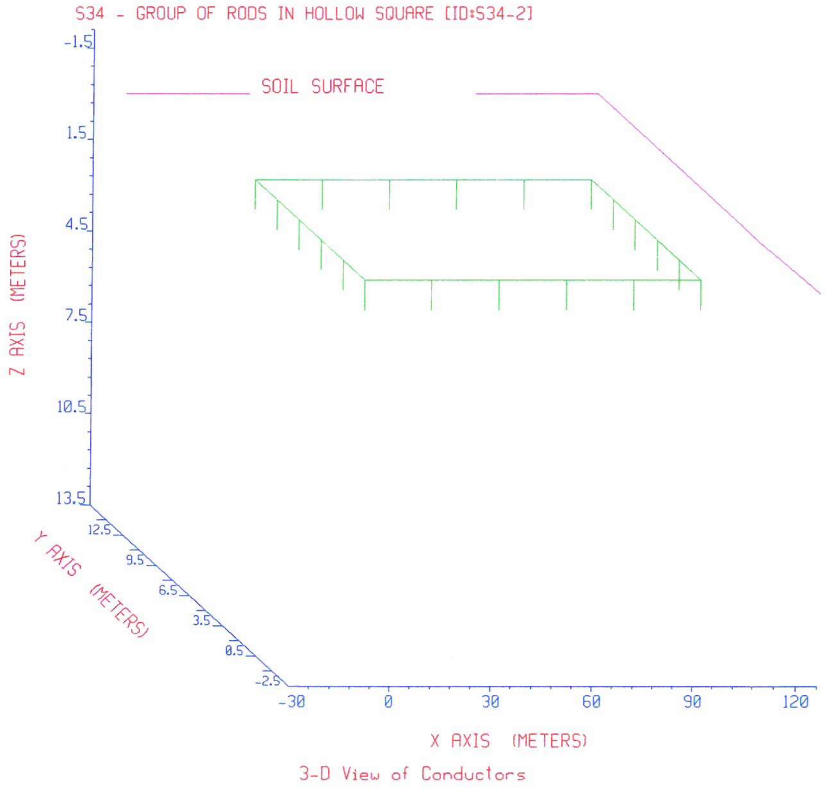

Figure 4.2: Groups of rods in hollow square

Parameters used:

Case No.	Length of rods (m)	Grid dimension (m)	ρ soil (Ωm)	Burial depth (m)	Radius (m)	Current (A)	N	k	a
1	1	100x100	100	1	0.01	100	20	6.5	20
2	1.5	10x10	20	1	0.017	100	32	7.5	1.25
3	1	20x20	200	2	0.03	150	16	6	5
4	1	100x100	100	0.05	0.01	100	20	6.5	20
5	1.5	10x10	20	0.05	0.017	100	32	7.5	1.25
6	1	20x20	200	0.05	0.03	150	16	6	5
7	3	100x100	100	0.05	0.01	100	20	6.5	20
8	3	10x10	20	0.05	0.017	100	32	7.5	1.25
9	3	20x20	200	0.05	0.03	150	16	6	5
10	10	100x100	100	0.05	0.01	100	20	6.5	20
11	10	10x10	20	0.05	0.017	100	32	7.5	1.25
12	10	20x20	200	0.05	0.03	150	16	6	5

Formulae given in S34 (page 20, Table 1, column 6) [35]

$$R = \frac{R'}{N}(1 + k\alpha)$$

where

$$R' = \frac{\rho}{2\pi l}\left(\ln\frac{8l}{d'} - 1\right)$$

N = number of rods
k = factor (Figure 18, S34 – Appendix 3) = 6.5

$$\alpha = \frac{r_h}{c'} \qquad r_h = \frac{\rho}{2\pi R'}$$

c' = spacing between vertical rods

4.3.3 Combined grid with rods connected around periphery

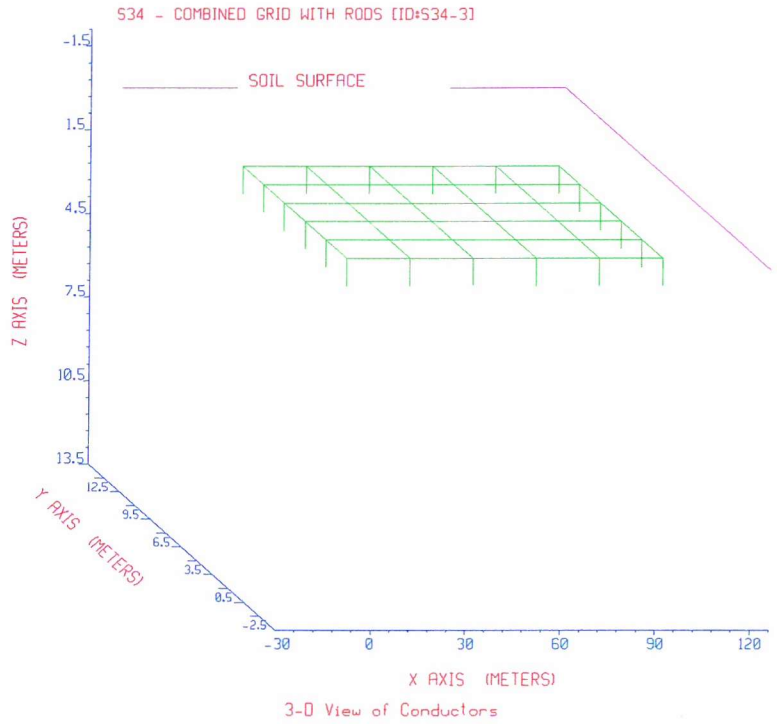

Figure 4.3: Combined grid with rods connected around periphery

Parameters used:

Case No.	Length of rods (m)	Grid dimension (m)	ρ soil (Ωm)	Burial depth (m)	Radius (m)	Current (A)	W
1	1	100x100	100	1	0.01	100	1
2	1.5	10x10	20	1	0.017	100	1.5
3	1	20x20	200	2	0.03	150	1.7
4	1	100x100	100	0.05	0.01	100	1
5	1.5	10x10	20	0.05	0.017	100	1.5
6	1	20x20	200	0.05	0.03	150	1.7
7	3	100x100	100	0.05	0.01	100	1
8	3	10x10	20	0.05	0.017	100	1.5
9	3	20x20	200	0.05	0.03	150	1.7
10	10	100x100	100	0.05	0.01	100	1
11	10	10x10	20	0.05	0.017	100	1.5
12	10	20x20	200	0.05	0.03	150	1.7

Formulae given in S34 (pg 20, Table 1, col. 7) [35]

$$R = \frac{R_1 R_2 - R_{12}^2}{R_1 + R_2 - 2R_{12}}$$

where
R_1 = resistance of grid (buried grid)
R_2 = resistance of rods (rods in hollow square)

$$R_{12} = R_1 - \frac{\rho}{\pi L}\left(\ln\frac{l}{b} - 1\right)$$

$$b = \frac{W}{\pi}$$

W = width of strap

4.3.4 Discussions

Results of the computations can be seen in Appendix 4 (all scaled to 0.01 S/m soil conductivity). An interesting point to note here is that two out of the three sets of parameters used gives a fairly large percentage difference between MALT and the S34 formula for the resistance of the electrode system for the situation of '*group of rods in hollow square*'. This is shown by the highlighted values in bold (Tables 1 - 4 in Appendix 4).

Further investigation showed that the formula for '*group of rods in hollow square*' is very dependent on the rod length. By increasing the rod length to 10m, as expected the resistance value is decreased, and hence the percentage difference with MALT is reduced (Table 4, Appendix 4). Also, it can be seen that for cases 2, 5, 8 and 11 for '*group of rods in hollow square*', the percentage difference between the S34 formula and MALT is smaller, than the other cases of this same category. In these cases, the 'k' factor (see Appendix 3), which is dependent on the number of rods, is the highest. It can be deduced that the higher the 'k' factor, the better the agreement between S34 and MALT. Sullivan [118] in his paper mentioned that the 'k' curve in S34 is a satisfactory fit within reading errors except at four and eight rods, i.e. low 'k' factor. The methods and theory behind this 'k' factor is unknown, and no explanation is given in S34.

The formula given in S34 does not include the depth of the buried grid, and the injected current. When computing with CDEGS, these two parameters are taken into consideration. Further tests conclude that, as the buried depth of the grid is decreased, the resistance value generated by CDEGS approaches the values computed by the S34 formula (Appendix 4, Table 2, depth=0.05m). However, the injected current value has no effect on the overall resistance, but the GPR (Ground Potential Rise) will increase as the injected current is increased.

Hence, it is deduced that the formula given in S34 assumes that the grid is buried just below the ground level, i.e. 10cm depth or less. Furthermore, S34 formula dictates that there is a limit to how short the rod length should be.

To conclude, overall it can be seen that CDEGS MALT gives good and reliable results.

CHAPTER 5

The Measured Resistance and Surface Potentials of Multi-Rod Array

Following the good agreement between CDEGS MALT and some theoretical formula investigated in Chapter 4, verification was also done using the electrolytic tank. Overall, the configurations investigated consist of arrays of rods without horizontal links (Table 5.1), and with horizontal links (Table 5.2). All the arrays shown in Table 5.1 have been investigated experimentally and the results compared with CDEGS MALT and the ellipsoid model. The latter is not applicable when horizontal rods are involved (Table 5.2) but results from the same empirical formulas listed in S34 have been included where appropriate.

Electrode Description	Electrode Configurations	Rod Configuration
Rods without links	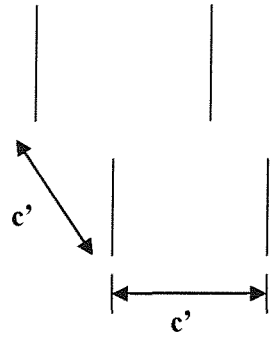	a) 4 rods, c' = 60 mm b) 4 rods, c' = 120 mm c) 4 rods, c' = 180 mm d) 8 rods, c' = 60 mm e) 8 rods, c' = 90 mm f) 8 rods, c' = 120 mm g) 12 rods, c' = 60 mm h) 16 rods, c' = 60 mm

Table 5.1: Configurations of selected cases for rods without links.

Electrode Descriptions	Electrode Configurations	Cases selected
(1) Hollow square	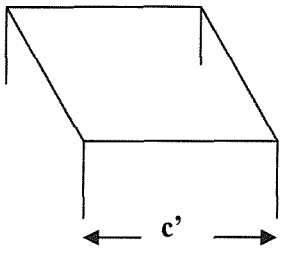	a) 4 rods, c' = 120 mm b) 4 rods, c' = 240 mm c) 8 rods, c' = 60 mm d) 8 rods, c' = 120 mm e) 16 rods, c' = 60 mm
(2) Combined grid and rods connected around the periphery	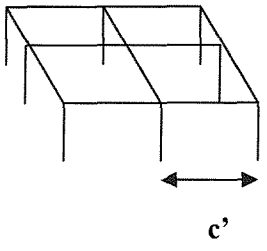	a) 8 rods, c' = 60 mm b) 8 rods, c' =120 mm c) 16 rods, c' = 60 mm
(3) Buried grid	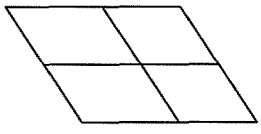	a) 120 x 120 mm^2 b) 240 x 240 mm^2
(4) Others	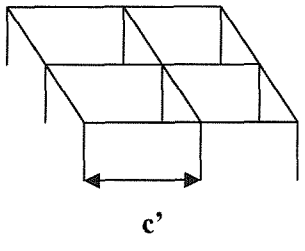	a) 25 rods, c' = 60 mm b) 21 rods, c' = 60 mm c) 17 rods, c' = 60 mm

Table 5.2: Configurations of selected cases for rods with links.

S34 provides formulae to find the resistance of electrode descriptions (1), (2) and (3), and the surface potentials for (3) only. Hence, apart from these, experimental results will be compared to that obtained from CDEGS MALT.

For rods with or without links, surface potential measurements and calculations were made at two different angles, 0° and 45°, with reference to the centre of electrode system (the first point). This is as illustrated in Figure 5.1 (red circles denote rod positions).

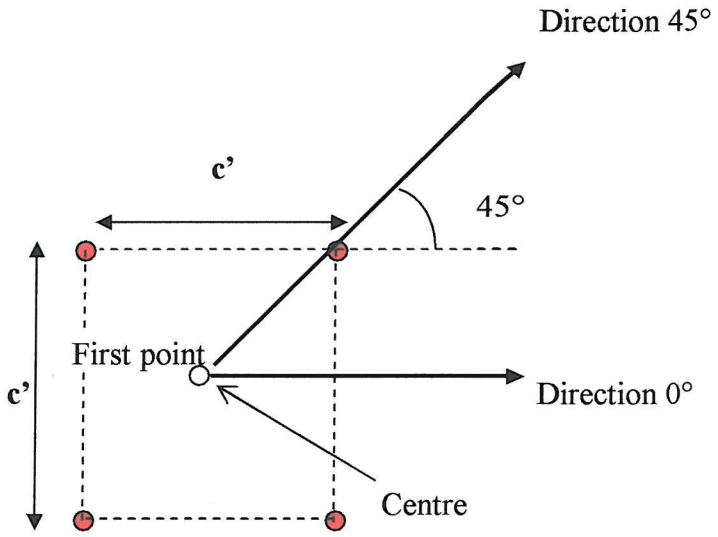

Figure 5.1: Directions of the surface potential measured.

All results obtained are scaled to a conductivity of 0.1 S/m for comparison purposes.

5.1 Rods without horizontal links

Table 5.3 below shows the results obtained.

Electrode Configuration	Resistance, R (Ohm)		
	CDEGS MALT	Ellipsoid	Experiment
4 rods (c' = 60mm)	47.77	47.15	48.50
4 rods (c' = 120 mm)	40.95	39.78	41.40
4 rods (c' = 180 mm)	38.27	36.99	38.77
8 rods (c' = 60 mm)	29.57	29.37	30.10
8 rods (c' = 90 mm)	25.61	25.14	26.01
8 rods (c' = 120 mm)	23.44	22.87	23.90
12 rods (c' = 60 mm)	21.85	21.72	22.03
16 rods (c' = 60 mm)	17.49	17.39	17.70

Table 5.3: Resistance values for rods without horizontal links

The experimental resistance results obtained have good agreement with the MALT values with percentage error of less than 2%. Also, comparison between experimental and the ellipse model gave percentage error of less than 4% for most cases.

For surface potential distribution the agreement is much better. From the results obtained, the agreement between the experiment and CDEGS MALT is very good with percentage error of less than 1% for most cases. MALT and the ellipsoid model gave less than 1 % error as well.

The experimental resistances and surface potentials were higher than the MALT and the ellipsoid values. This might be due to the equipment uncertainties as explained in Chapter 3. Other than that, the external resistor assumption could give the rise in resistance and surface potentials giving a slightly higher reading than the computed ones.

The graphs in Figures 5.2-5.7 show the typical shape and results for some of the electrode configuration. Full results are given in Appendix 5.

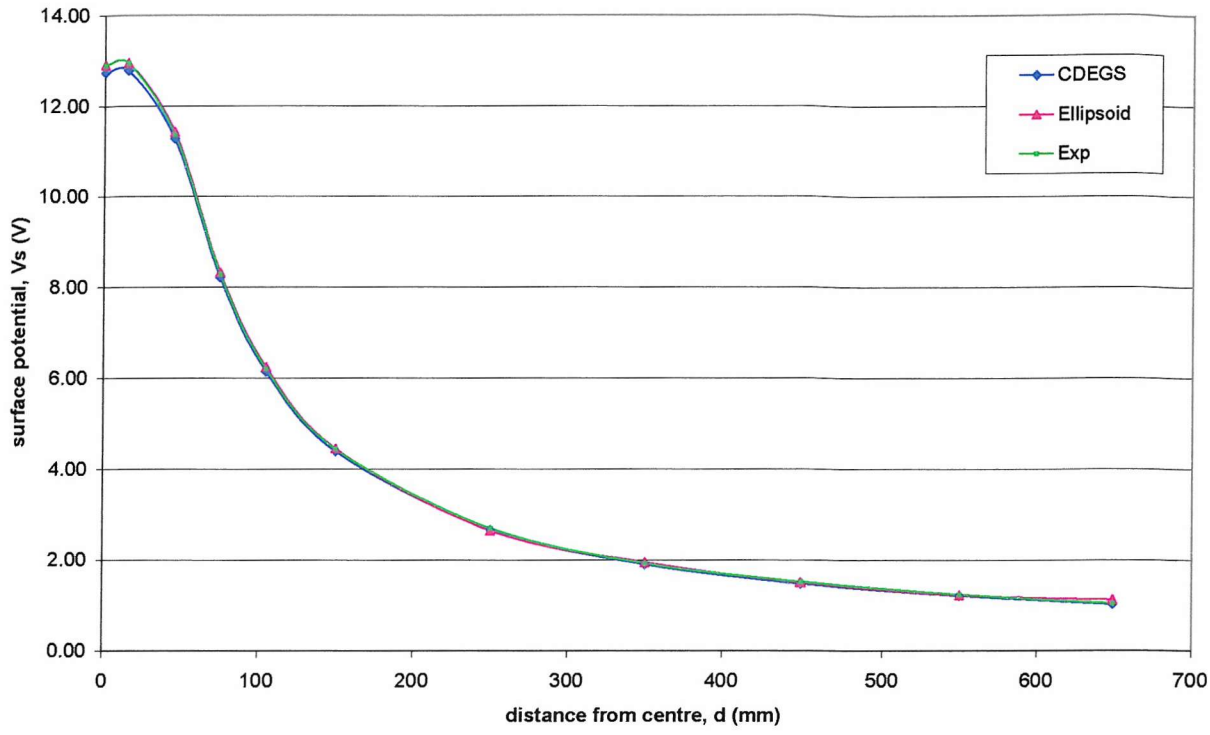

Figure 5.2: Surface potential, Vs (V) against distance, d (mm) at 0 degree from centre of grid for 4 rods without horizontal links (c'=60 mm)

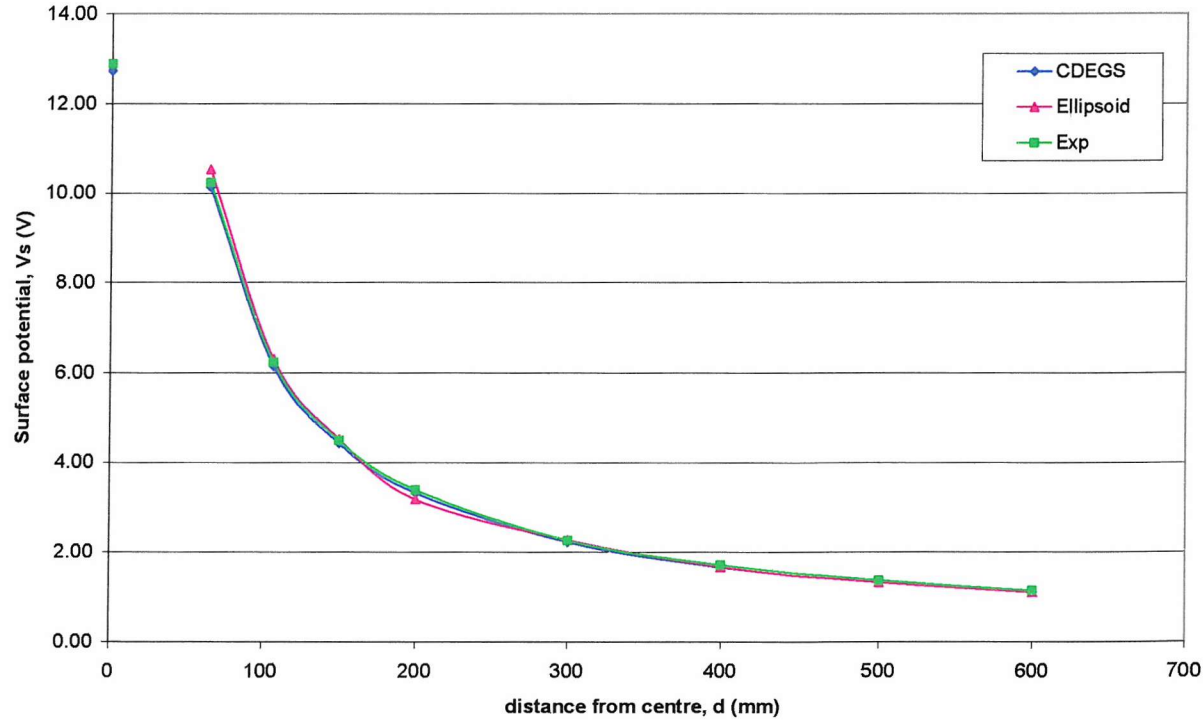

Figure 5.3: Surface Potential, Vs (V) against distance, d (mm) at 45 degree from centre of grid for 4 rods without horizontal links (c'=60 mm)

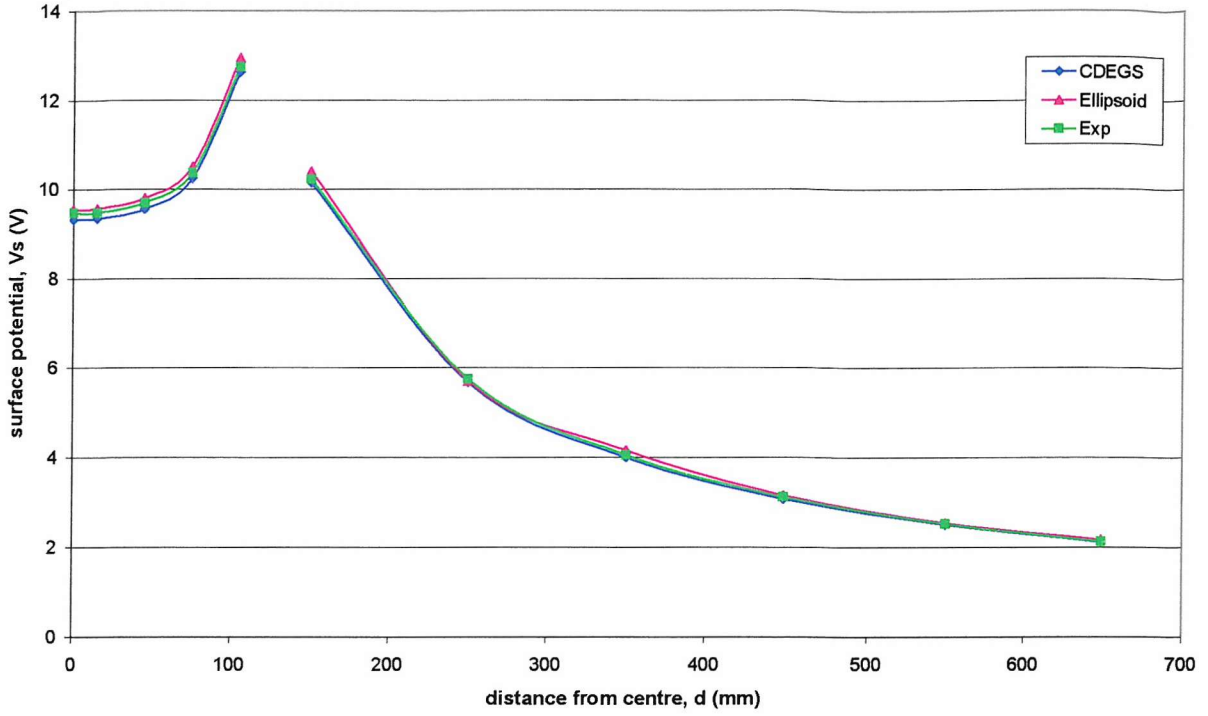

Figure 5.4: Surface potential, Vs (V) against distance, d (mm) at 0 degree from centre of grid for 8 rods without horizontal links (c'=120 mm)

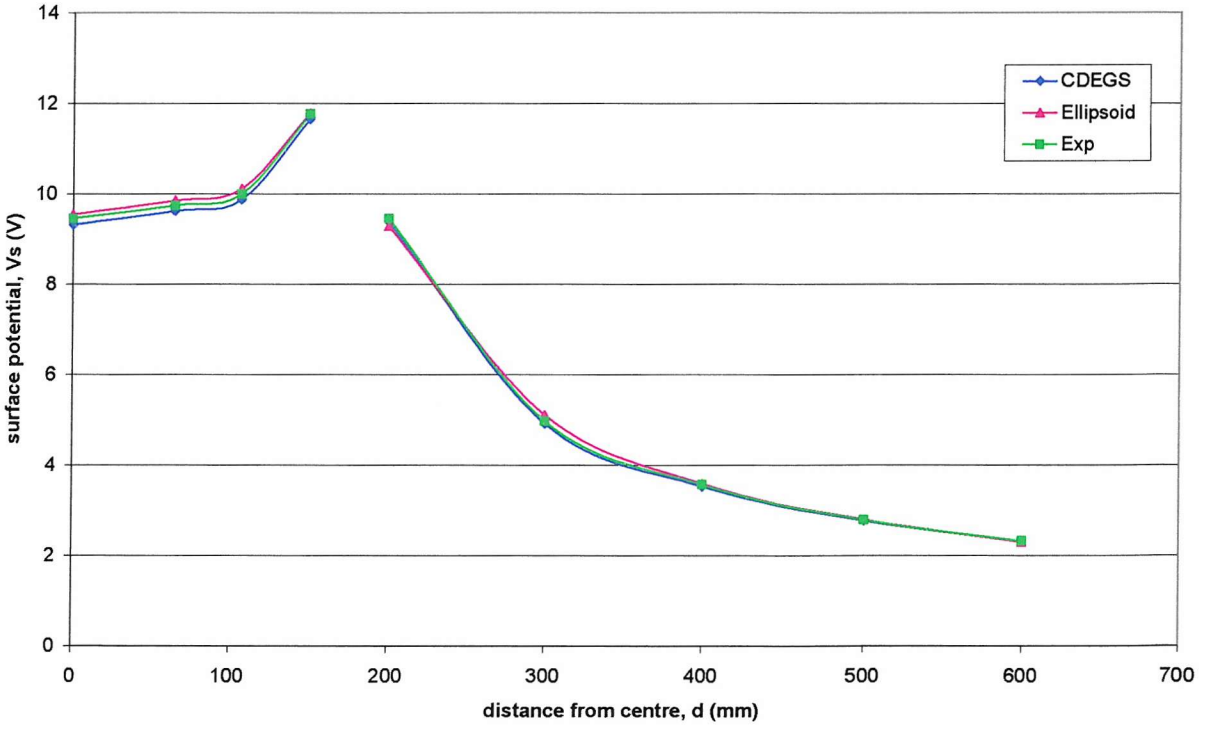

Figure 5.5: Surface potential, Vs (V) against distance, d (mm) at 45 degree from centre of grid for 8 rods without horizontal links (c'=120 mm)

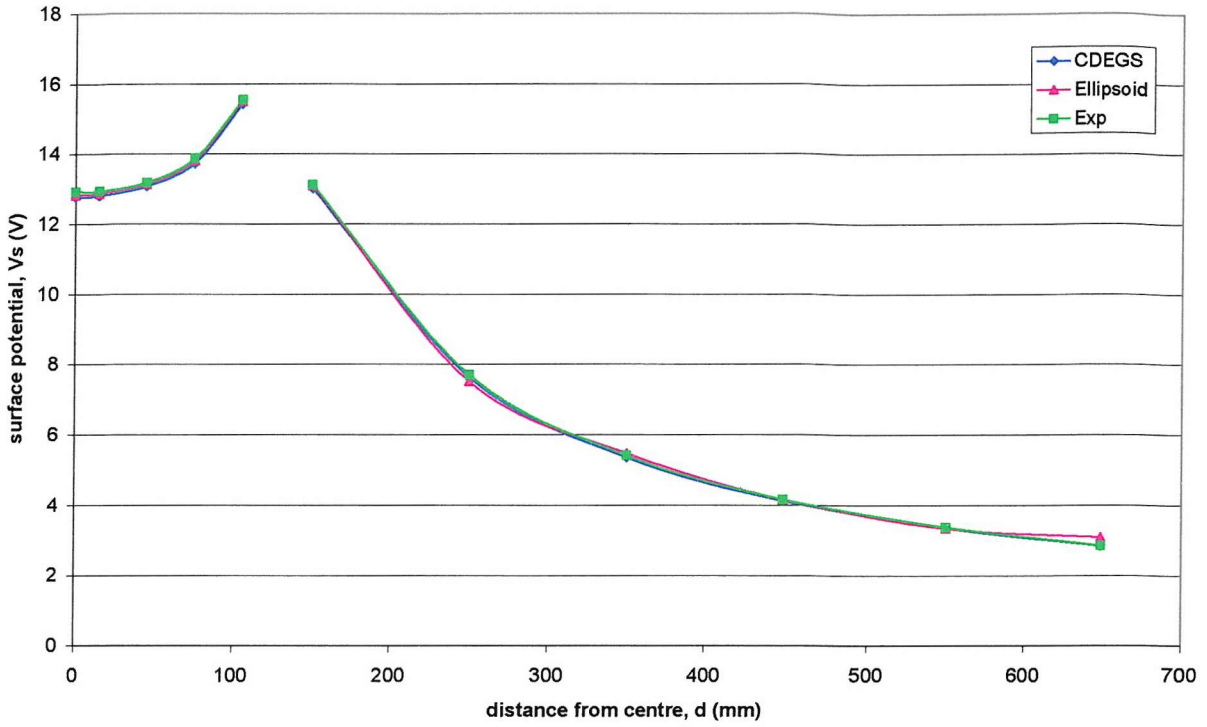

Figure 5.6: Surface potential, Vs (V) against distance, d (mm) at 0 degree from centre of grid for 16 rods without horizontal links (c'=60 mm)

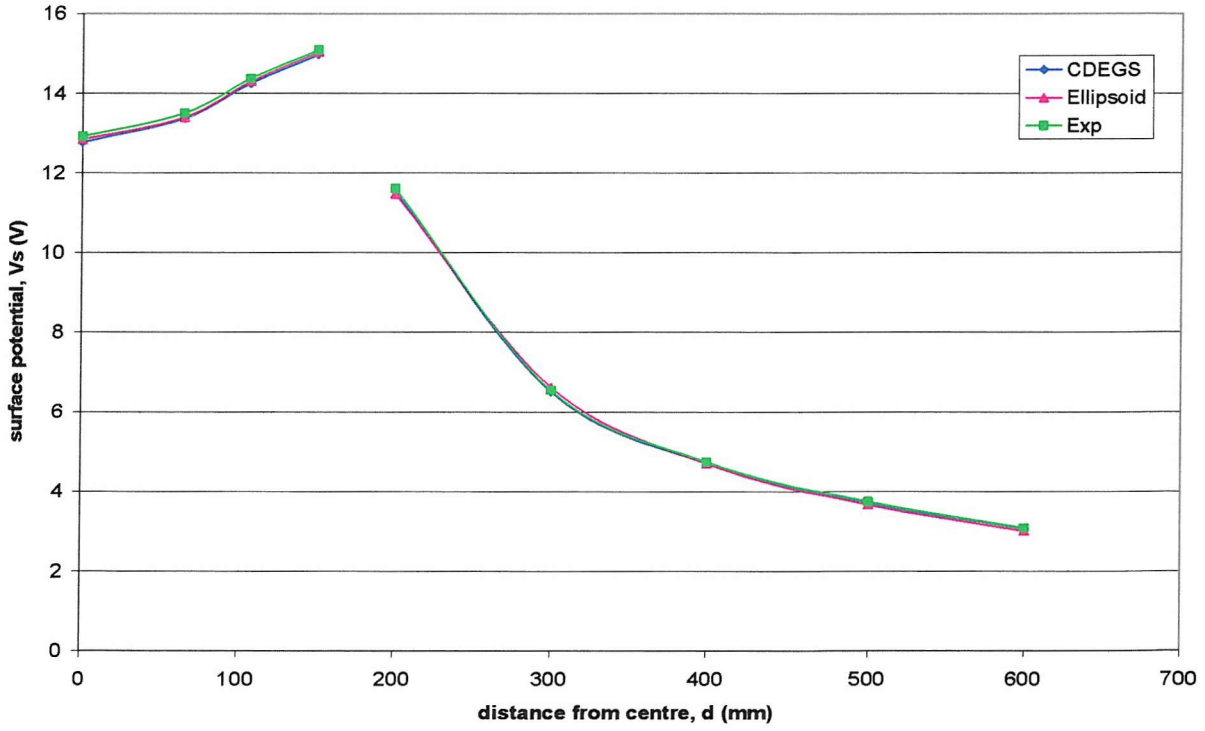

Figure 5.7: Surface potential, Vs (V) against distance, d (mm) at 45 degree from centre of grid for 16 rods without horizontal links (c'=60 mm)

5.2 Rods with horizontal links

For this section, the configurations can be classified into different types, as in the S34:

- *Group of rods in hollow square*
- *Combined grid with rods connected around periphery*
- *Buried grid*
- Other configurations (this is not in S34)

The results with the three different methods are shown in Table 5.4 below:

Electrode Configuration	Resistance, R (Ohm)		
	CDEGS MALT	Experiment	S34
4 rods in hollow square (c' = 120mm)	30.03	30.52	39.99
4 rods in hollow square (c' = 240mm)	19.33	19.65	35.67
8 rods in hollow square (c' = 60mm)	26.78	27.20	29.95
8 rods in hollow square (c' = 120mm)	17.74	18.01	22.81
16 rods in hollow square (c' = 60mm)	16.02	16.30	17.80
Combined grids with 8 rods connected in periphery (c' = 60 mm)	26.38	26.80	28.61
Combined grids with 8 rods connected in periphery (c' = 120 mm)	16.85	17.11	19.70
Combined grids with 16 rods connected in periphery (c' = 60 mm)	14.42	14.66	17.78
Buried grid (120 x 120 mm^2)	38.00	38.60	50.82
Buried grid (240 x 240 mm^2)	18.84	19.16	22.63
25 rods with 240 x 240 mm^2 grid (c' = 60 mm)	14.91	15.10	-
21 rods with 240 x 240 mm^2 grid (c' = 60 mm)	15.05	15.29	-
17 rods with 240 x 240 mm^2 grid (c' = 60 mm)	15.20	15.45	-

Table 5.4: Results for resistance of rods with horizontal links system

For the 4 rods in a hollow square configuration, S34 gave the highest resistance value, whereas MALT provides the lowest. The difference between MALT and experimental results is about 1.6% (with respect to MALT values). The percentage difference between MALT and S34 decreases as the rod spacing gets smaller. Further tests with MALT and S34 using smaller and larger rod spacing than the ones tested here confirms that the latter statement is true. Referring back to Section 4.3 (Comparisons with S34: More complex grid), this trend can be seen as well.

As for the 8 rods in a hollow square results, the percentage of differences for MALT is almost the same as before, i.e. about 1.5%. However, the S34 results decreases in percentage (with respect to MALT) when compared with the previous rod configuration of 4 rods. The percentage of difference reduces by almost one third of the value from the 4 rods' results. This is due to the influence of the 'k' factor in the formula of S34, as discussed in Section 4.3. The 8 rods combined grid configuration gave a lower percentage of difference when compared to the 4 rods combined grid because the 'k' factor (in the S34 formula) is larger.

The '*Combined Grid with Rods connected around the periphery*' configuration for the experimental results agrees quite well with the MALT values with percentage of difference less than 1.7%. As for the S34 results, the scenario is almost the same as with the rods in a hollow square configuration.

It can also be seen from Table 5.4 that the S34 formula gives the highest values of resistance for all configurations. The 'Buried Grid' in particular has quite a significant difference in the results obtained between the three methods. Further examinations using CDEGS and the S34 formulae indicate that as the buried grid area increases, the smaller the difference between CDEGS and S34. This is shown in Table 5.5 below. Also, for the buried grid formulae, S34 does not take into account the radius of the rods.

Buried Grid Area (m^2)	S34 resistance (ohms)	CDEGS resistance (ohms)	Difference (ohms)
60	115.42	75.72	39.70
120	50.82	38.00	12.82
240	22.63	18.84	3.79
360	14.30	12.48	1.83

Table 5.5: Comparison of resistance as buried grid area increases

Furthermore, for all the formulae, S34 does not include the buried depth. This factor surely affects the results obtained compared to CDEGS, as the latter is very sensitive to the burial depth of the earthing system.

Figures 5.8-5.13 show the potential distributions for some of the different types of electrode systems for rods with links. Full results for all the configurations tested as in Table 5.4 can be seen in Appendix 6. Only Figure 5.10 and Figure 5.11 (for buried grid case) show curves from all three methods, as the S34 formulae for surface potentials are not available for other configurations. These two graphs show how S34 results differ from the computed and experimented results. Of all the three methods, S34 again gives the lowest surface potential. This can lead to a higher touch voltage assumption and hence can over design a substation earthing system.

It is also observed that for all the results, the potential distribution from CDEGS MALT is slightly lower than that of experimental values. This is also the case for the resistance measurements. Overall, the percentage error for surface potentials between MALT and experimental values are on average less than 1%. The experimental resistances and surface potentials were higher than CDEGS MALT. This might be due to the equipment uncertainties as explained in Chapter 3. Other than that, the external resistor assumption could give the rise in resistance and surface potentials giving a slightly higher reading than the computed ones.

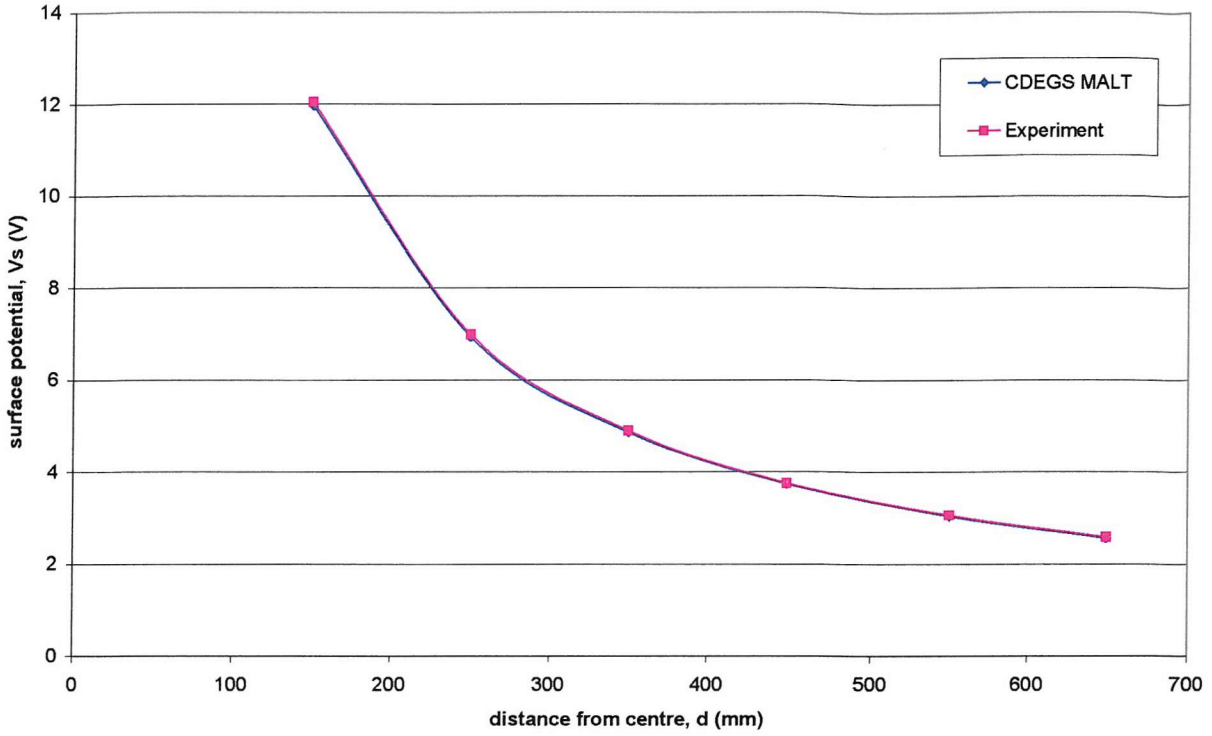

Figure 5.8: Surface potential, Vs (V) against distance from centre of grid, d (mm) at 0 degree traverse from centre for 4 rods in hollow square (c'=240 mm)

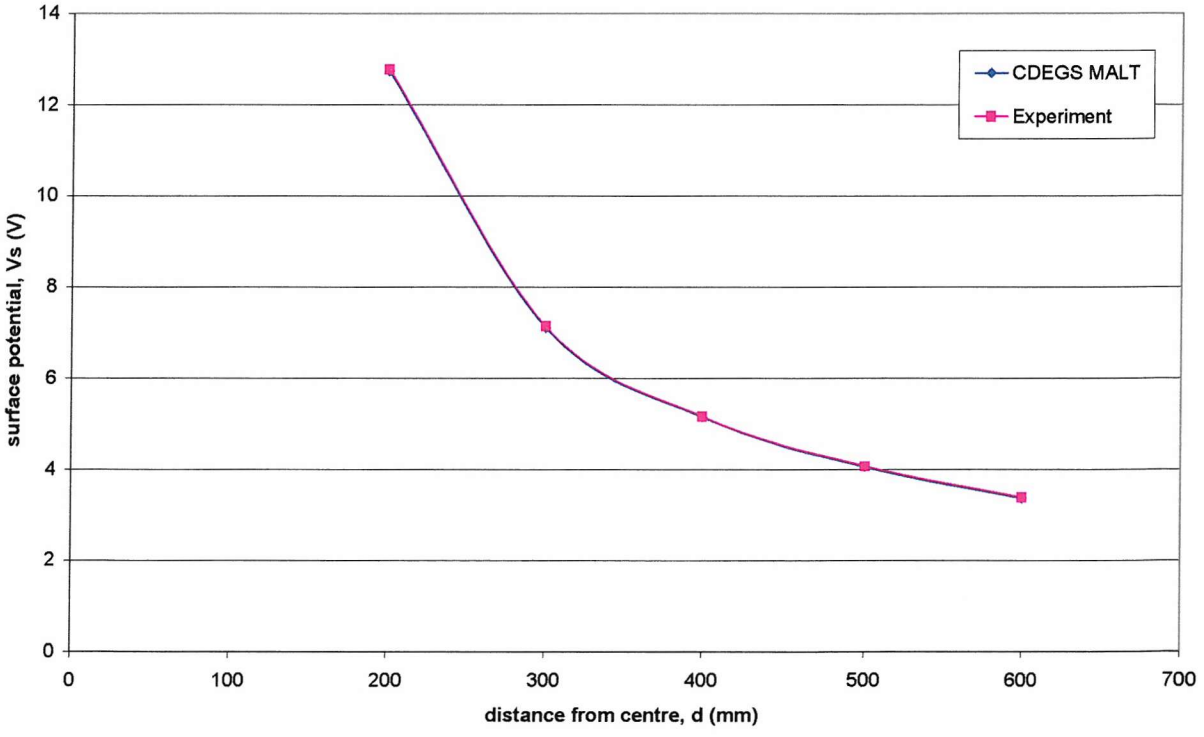

Figure 5.9: Surface potential, Vs (V) against distance, d (mm) at 45 degree from centre for 16 rods in hollow square (c'=60 mm)

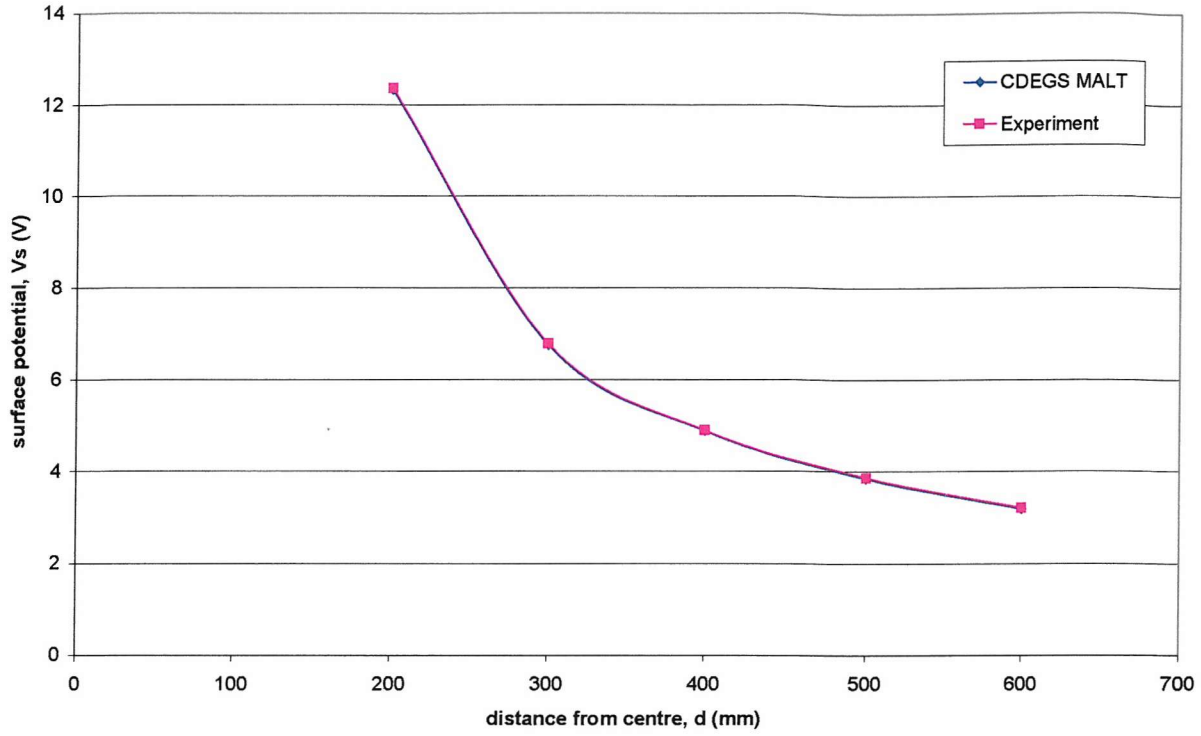

Figure 5.10: Surface potential, Vs (V) against distance from centre of grid, d (mm) at 45 degree traverse from centre for combined grid with 8 rods connected around the periphery (c'=120 mm)

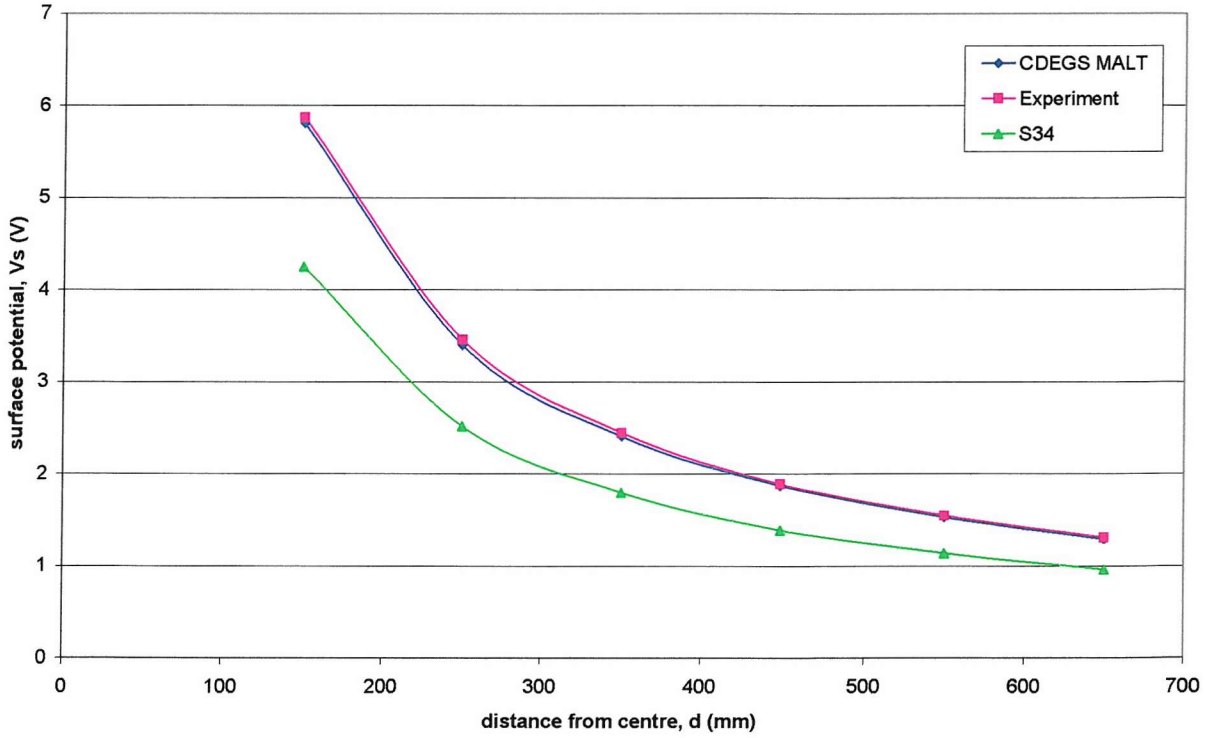

Figure 5.11: Surface potential, Vs (V) against distance from centre of grid, d (mm) at 0 degree traverse from centre for buried grid (120 x 120 mm square)

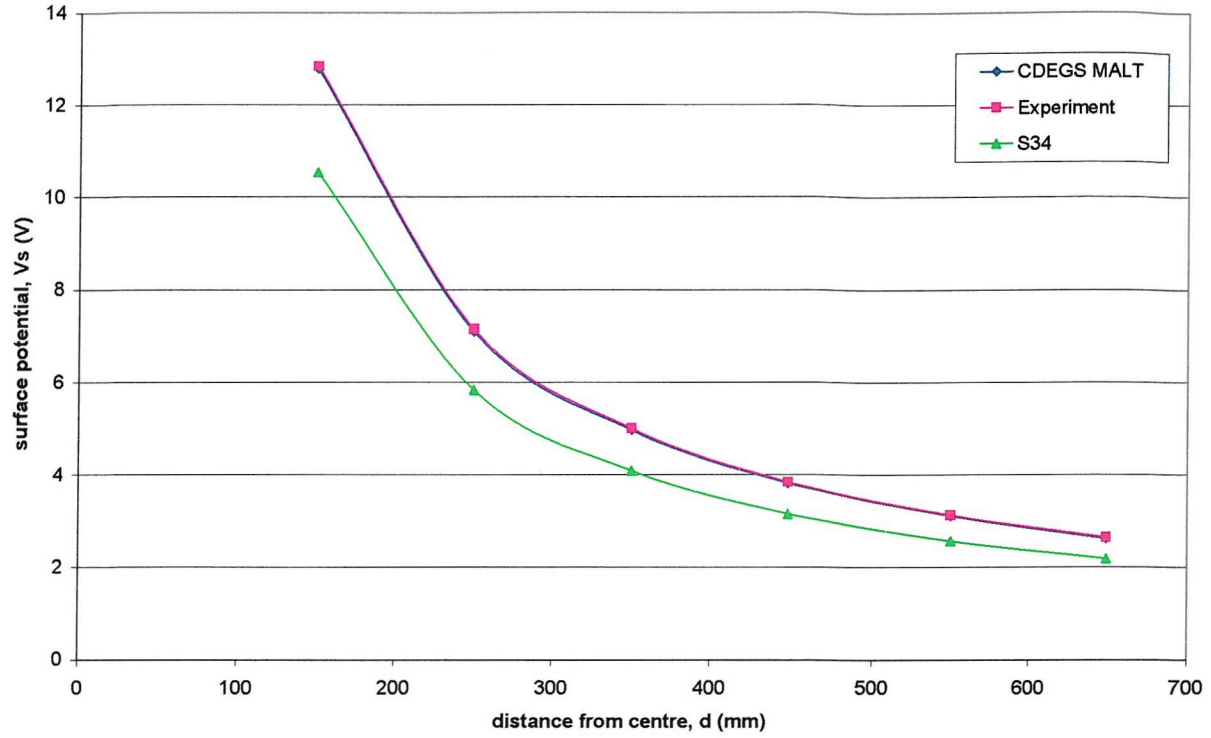

Figure 5.12: Surface potential, Vs (V) against distance from centre of grid, d (mm) at 0 degree traverse from centre for buried grid (240 x 240 mm square)

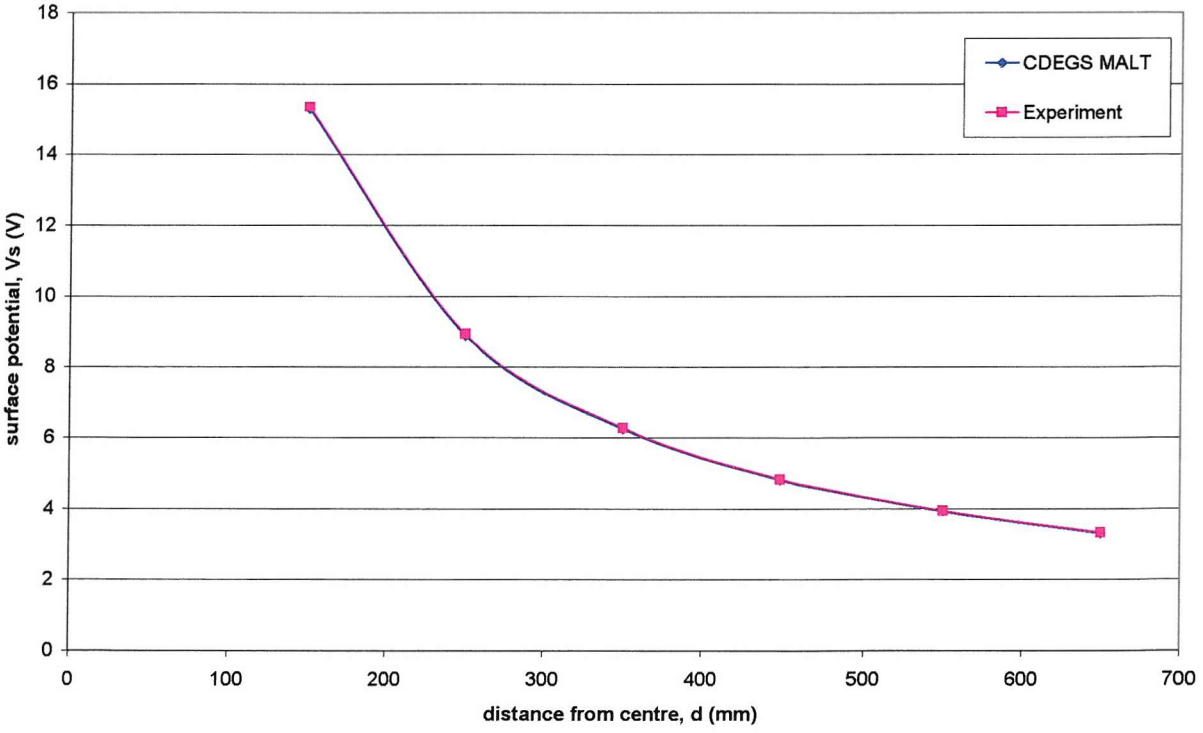

Figure 5.13: Surface potential, Vs (V) against distance, d (mm) at 0 degree from centre for 25 rods with horizontal links (c'=60mm)

5.3 Conclusions

MALT was compared with some simple vertical rod formula in Chapter 4 with some of the available formula in journals and Standards. Here, more complex grids were tested and compared with the electrolytic tank's results. The comparison is very good. The earthing resistance values are within less than 2% and the surface potential values are on average less than 1% difference between MALT and experimental values. Hence, the MALT program and the experimental tank prove to be reliable and compare well with each other. S34 gave the same errors as have been found in Chapter 4 and some of the the S34's grid configurations tested here are found to be unreliable due to the large percentage difference when compared with CDEGS MALT and the experimental results.

CHAPTER 6

Variation of Resistance of a Disc with Increasing Depth

Besides using electrodes driven into the earth or horizontal electrodes, conducting plates can also be used to disperse fault current into the earth. The conducting plate is buried in the earth and connected to an earthing electrode, to increase the surface area for current dispersion. On the one hand, earthing grids are used extensively in manufacturing plants and power stations, and have been broadly studied in recent years, but on the other, earthing plates are sometimes preferred in domestic and office situations [119].

An earthing plate is usually made of steel, aluminium, or other inexpensive conducting material (although aluminium is very susceptible to corrosion). The plate is buried beneath and parallel to the surface of the earth. Circular and rectangular plates are the most prevalent, although the shape of an earthing plate could be made to conform to a given physical environment. During an emergence of a surge current, current injected into an earthing electrode is free to flow into the earthing plate because both are good conductors. Since the conductivity of an earthing plate is much higher than that of the surrounding earth, charges are accumulated on the plate. Eventually the current input into the plate is equal to the current dissipated into its surrounding earth [119].

6.1 Resistance Measurement of the Disc

In this section a disc was used to investigate its resistance with variation in depth. Previously, all the work has been concentrated on horizontal electrodes or vertical rods systems. Finite element method was tested initially, but to no success. In addition, CDEGS MALT could not model a disc accurately; hence a finite difference program developed by Dr. R. L. Stoll [120] is used to compare with the experimental results.

A brass disc of 50 mm radius and 3 mm thickness was set up in the water tank and its resistance measured as the depth of the upper surface of the disc below the water level is increased. This is illustrated in Figure 6.1 below:

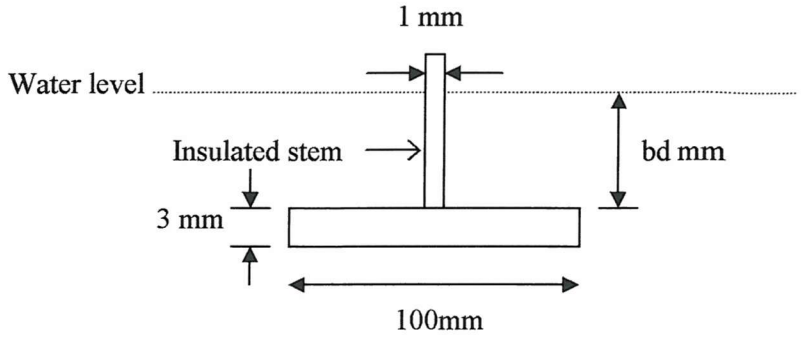

Figure 6.1: 50 mm radius Disc Electrode

The conductivity of the water has been scaled to 0.1 S/m as usual. It can be seen in Figure 6.2 that burying the disc at a depth equal to its radius causes a substantial reduction of the resistance by over 30%. These measurements have been confirmed using the finite-difference program based on a scalar electric potential.

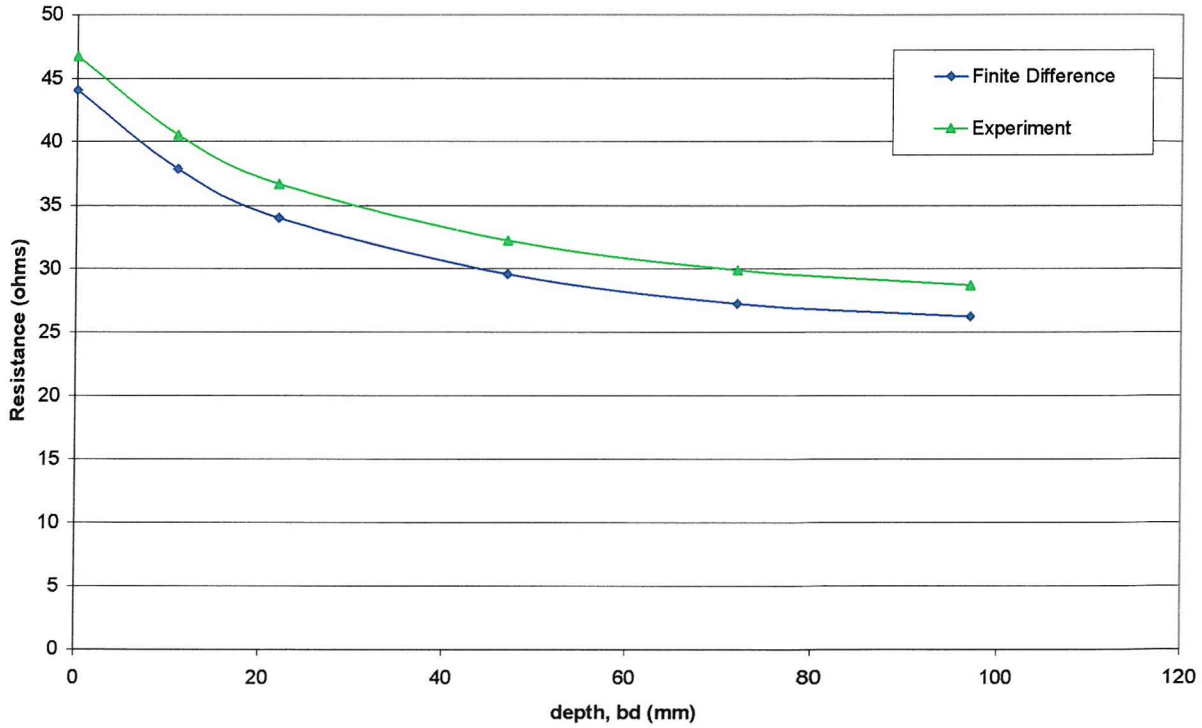

Figure 6.2: Graph of Resistance (ohms) of 100mm diameter disc at various depth, bd (mm)

The computed values are all about 2.6 Ω below the measured ones (~5-8% difference). Investigation has shown that this is not due to numerical discretization errors, or to the position assumed for the true earth plane (1m depth and 1m radius). It is interesting to

note that the analytical solution based on the collapsed oblate-spheroidal solution, that takes the conducting surface to be an equipotential, gives a resistance of 47.17Ω if a radius of 53mm is assumed to allow for the 3mm thick edges of the real disc. This value is still three ohms higher than the numerically computed result. The same analytical solution yields 24.27Ω for a fully immersed disc, if we now allow only 1.5 mm for the thickness. It will not be possible to investigate further because CDEGS is not suited for the representation of a disc.

6.2 Surface Potential Measurements of the Disc

Figure 6.3 gives the results for the measured surface potential distribution for several depths of disc when the potential applied to the centre of the disc is 20V. Only within three or four radii of the axis of symmetry does the depth of the disc significantly influence the surface potential.

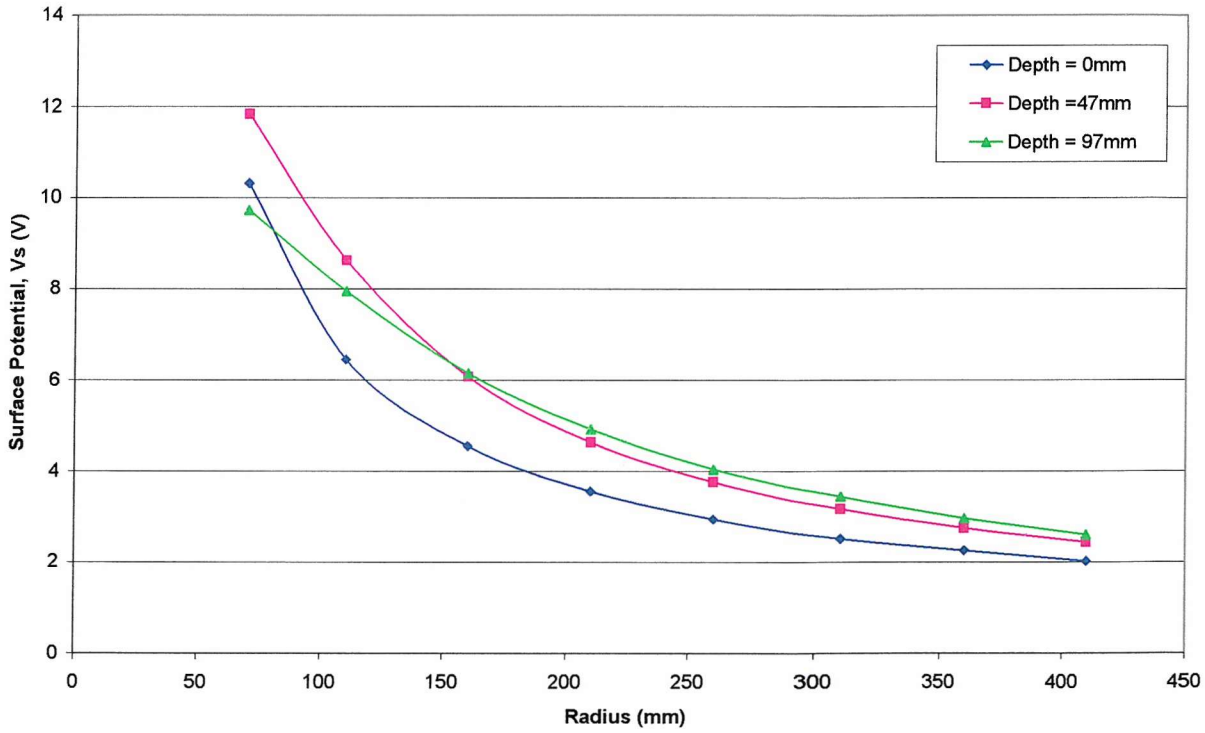

Figure 6.3: Measured surface potentials for 100 mm diameter disc at various depths

Figure 6.3 indicates some unexpected behaviour, especially close to the edge of the disc. This can be clarified by examining the surface potential at a fixed radius as a function of depth (see Figure 6.4). As the disc is lowered, the potential initially rises above the value

corresponding to a disc at the surface. This is due to the fact that current can now leave the top of the disc and thus current flow lines leave the highly conducting surface at right angles and travel up towards the surface of the water before eventually turning back towards the distant true earth plane.

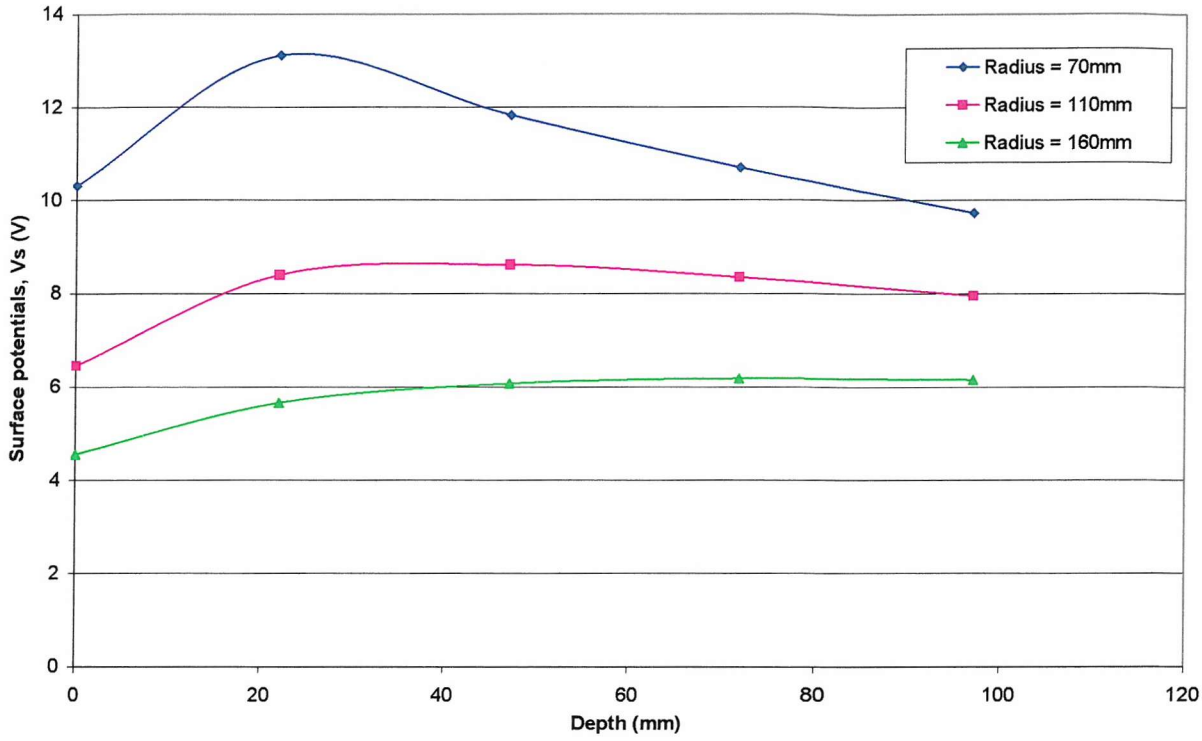

Figure 6.4: Measured surface potentials for 100 mm diameter disc with various radius

6.3 Conclusions

The charges at the disc are uniformly distributed in the central region and highly concentrated at the perimeter [119]. The earthing resistance is dependant on the radius of the circular plate, its depth and the conductivity of the earth. It is observed that the earthing resistance decreases with the increase in the depth of burial. If the disc is close to the earth surface, charges are pushed to the lower side of the disc, and the upper side is under utilised. Therefore, the earthing resistance is increased. On the other hand, if the disc is buried deep in the earth, charges would be evenly distributed on both sides of the disc, and the dispersion of currents into the surrounding earth would be optimised.

CHAPTER 7

The Effect of an Insulating Barrier on One Side of an Earthing System

A barrier, as its name implies, is an obstacle barring advance or access. In an earthing system point of view, a highly resistive barrier can be used to reduce surface potentials outside the vicinity of the substation. However, the penalty is a higher earthing resistance because the current path is being interrupted.

Two different structures of barriers (with the same length, width and height) have been investigated. The first one is a solid rectangular barrier made of Tufnol (insulating material). The second one is a plate barrier made of perspex plates (insulating material) arranged at a specified spacing to form a 'rectangular barrier'. These two arrangements are illustrated in the figures below:

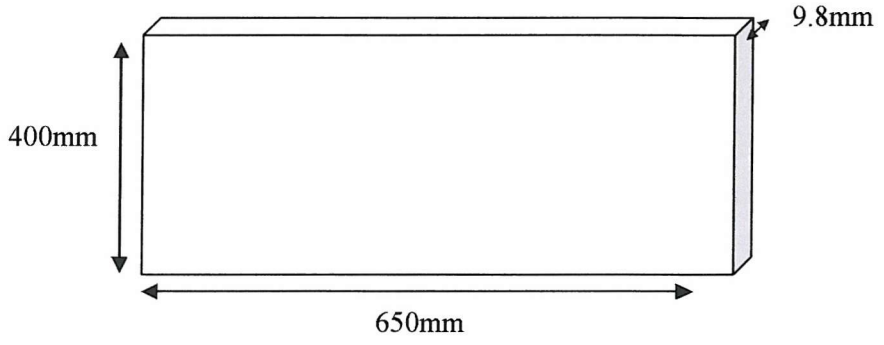

Figure 7.1 : solid barrier (not to scale)

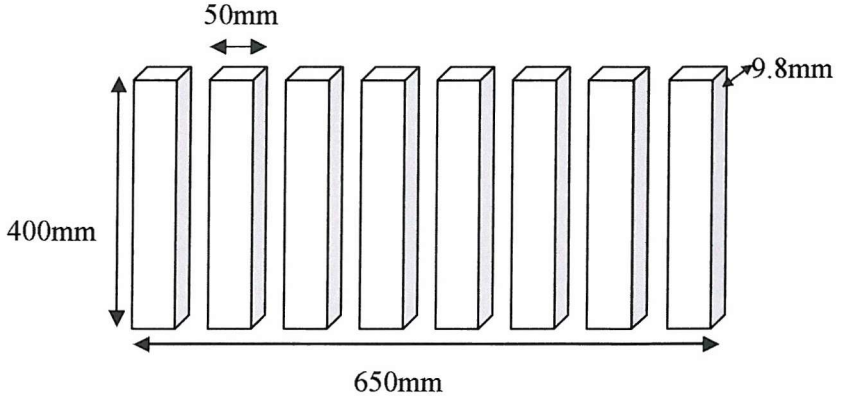

Figure 7.2: plate barrier (not to scale)

7.1 Solid Barrier

In the experiment done, the length of the insulating barrier running parallel to one side of the earthing electrode array was 650 mm and the distance between the inner surface of the barrier and the edge of the array was varied between 60 mm and 180 mm in steps of 60 mm. The depth of the barrier below the surface of the water ranged from 60 mm and 180 mm in steps of 60 mm, having been arranged to be lowered on two supporting wires in increments of 60mm. Figure 7.3 and Figure 7.4 illustrate the top view and side view of the system under examination.

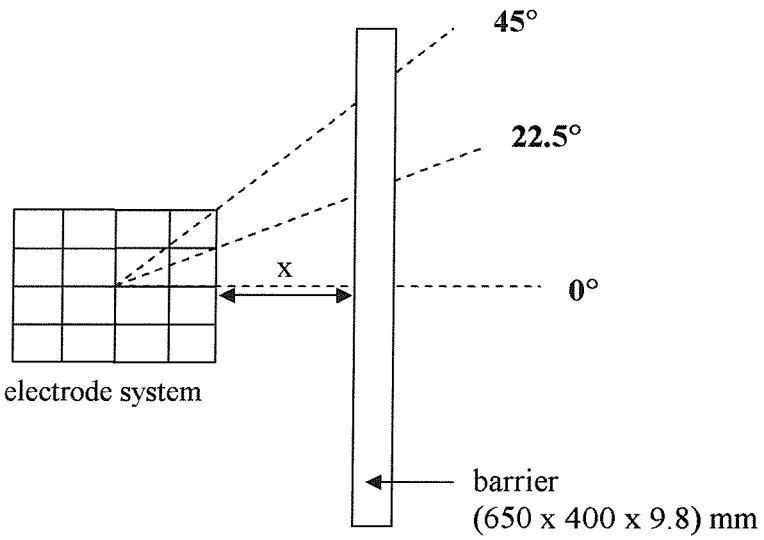

Figure 7.3: Top view of barrier system

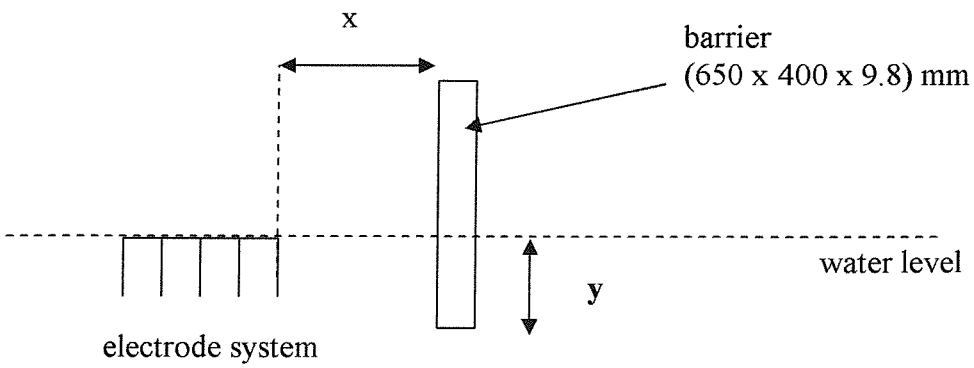

Figure 7.4: Side view of barrier system

The configuration of the electrode system used is the 'Combined Grid with 16 rods connected around the periphery and 9 internal rods', i.e. 25 rods with horizontal links. The grid size is 240 mm x 240 mm and each rod is 60 mm long. The rod size is the same as before, that is 1.56 mm in diameter.

7.1.1 Resistance Measurements for Solid Barrier

The measured curves of resistance against barrier depth for CDEGS MALT and experimental results are shown in Figures 7.5 and 7.6 respectively, together with the line indicating the original resistance before the barrier was lowered. Figure 7.7 shows the CDEGS MALT and experimental results together. All values are scaled to a water conductivity of 0.1 S/m. The difference between the experimental and CDEGS MALT results are well within experimental error, i.e. less than 1.04% difference.

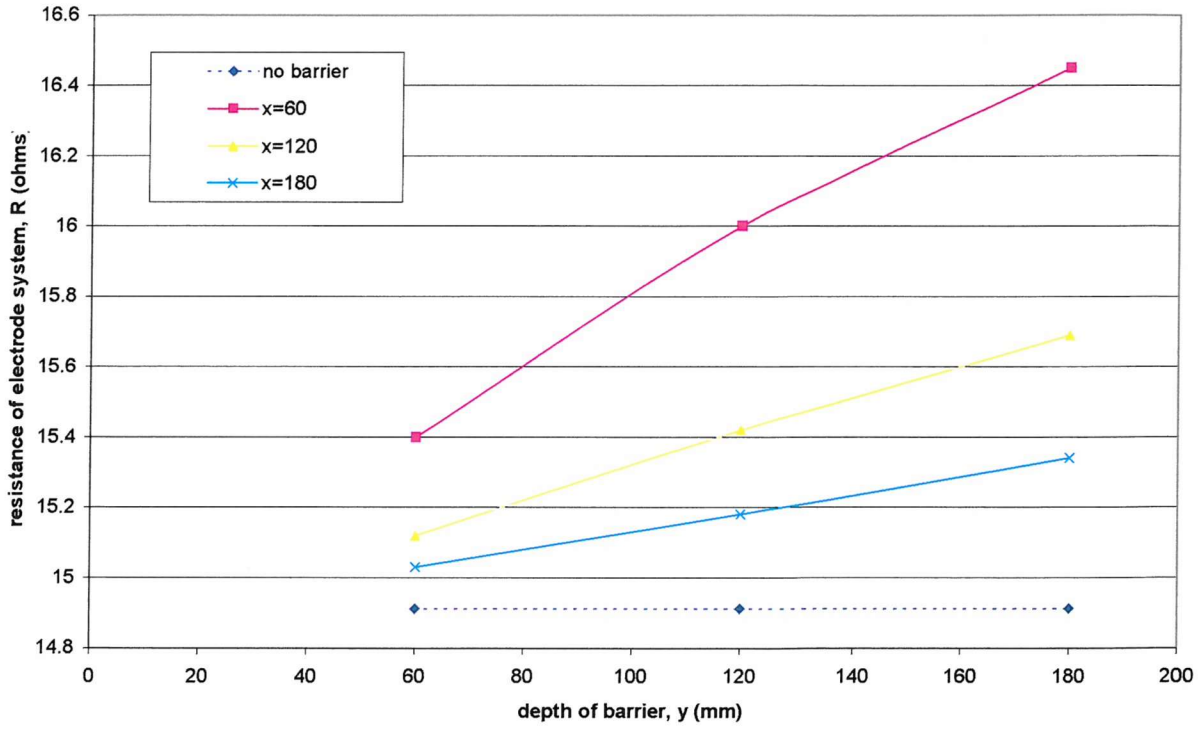

Figure 7.5: CDEGS MALT Computations: Resistance of electrode system, R (ohm) with the solid barrier against depth of barrier, y (mm)

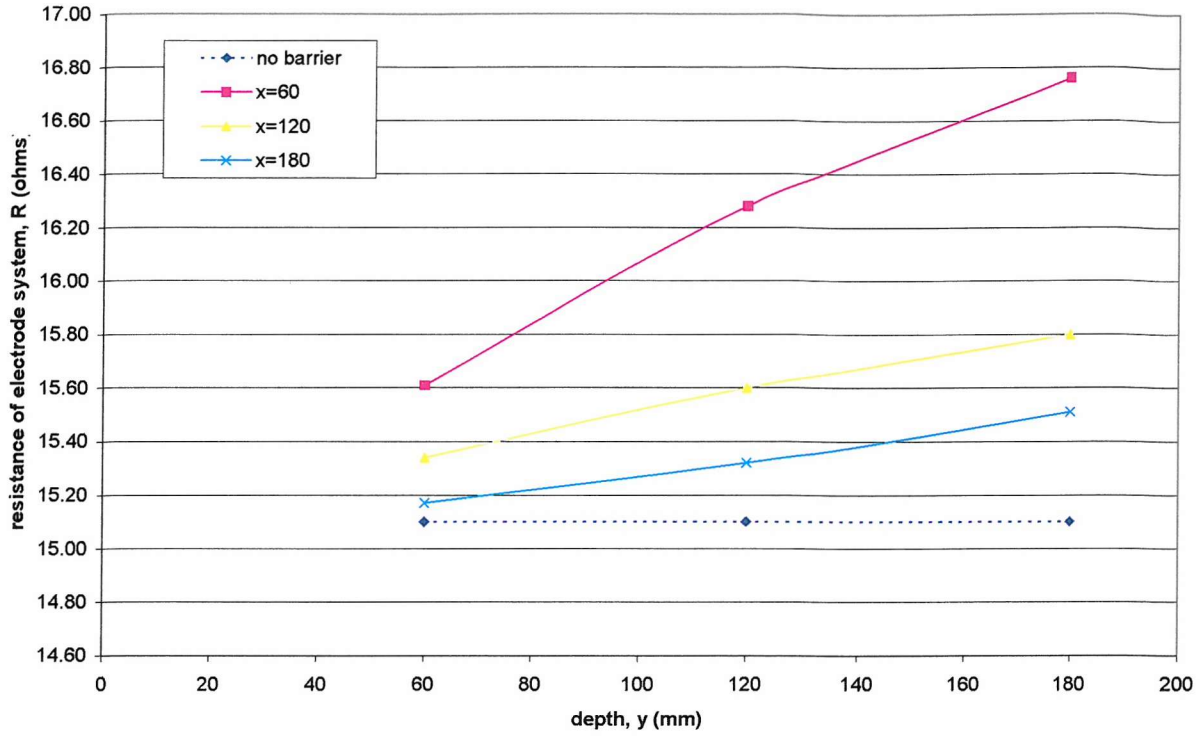

Figure 7.6: Experimental Results: Resistance of electrode system, R (ohms) with the solid barrier against depth of barrier, y (mm)

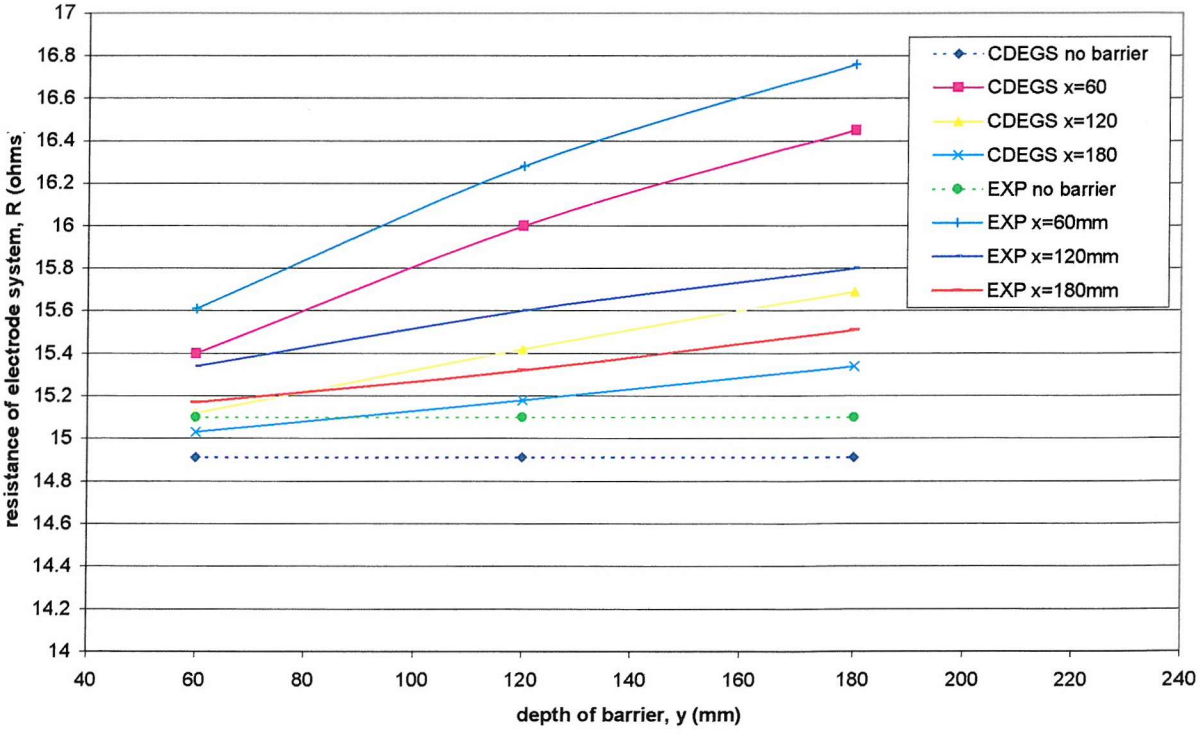

Figure 7.7: Comparison between MALT and Experimental Results for the Resistance of the electrode system with the solid barrier

The resistance rises due to the fact that the length of the current path on one side of the array is increased by the presence of the barrier, but even in the worst case shown (a deep barrier close to the array) the increase is between 10.3% and 11% for both cases (CDEGS MALT and experimental results). Typically, for a sensible barrier depth and spacing in the region of two vertical rod lengths, we have an increase of earthing resistance of less than 3.5%. From figures 7.5 – 7.7 it is clear that if the barrier distance from the grid is less than two rod length, the increase in resistance is quite significant.

7.1.2 Surface Potential Measurements for Solid Barrier

The surface potential distribution was measured along radii at angles of 0° (perpendicular to the edge of the array and through the centre of the barrier), 22.5° and 45°. Being an insulator, it was only necessary to have a thin barrier of 9.8 mm thickness. Figures 7.8 to 7.24 show the potential distribution results in graphical form. Not all the results are shown in the graphs here due to space limitations (using the experimental results, there can be up to 27 graphs of different combinations). Full-tabulated results are in Appendix 7 (B). Figures 7.8 to 7.16 show the comparison between CDEGS MALT and experimental results for all barrier positions for 0° traverse. Figures 7.17 to 7.24 depict the CDEGS MALT surface potential results for varying barrier positions, angles and depths. For all the different configurations of barrier position, the results obtained from the experiments are higher then the computed results by less than 1% outside the barrier. For readings in between the barrier and the grid, depending on the position where the reading is taken, the percentage of difference between CDEGS and experimental results (with respect to the energizing voltage, 20V) is between 1-2%. The nearer the reading position is to the grid, the higher is the percentage difference. This is due to the limitation of the computational methods CDEGS MALT, and this will be discussed in Chapter 8.

As expected, the results obtained here show that in the presence of a high resistivity barrier, the surface potential between the earthing grid and the barrier increases, whilst that outside the barrier decreases, compared to the values in the absence of a barrier. The latter must have a depth of at least twice the length of the earthing rods used in the grid before the external reduction is significant, especially close to the back of the barrier, as

can be seen from the graphs using CDEGS MALT results (Figures 7.18-7.24) for all three measured angles. Figure 7.24, where the spacing is such that the 45° line passes close to the edge of the barrier, shows that even with a depth of three rod lengths, the screening performance has deteriorated. Also, when the barrier is positioned at more than two rod lengths, the screening performance is almost constant.

The barrier is intended to lower the surface potentials outside the vicinity of the substation for public safety. However, although the surface potential within the substation vicinity increases, the increase is not more than 30% (for all three measured angles) compared to when no barrier is present, even with a barrier positioned one rod length away and three rod lengths deep (see Figure 7.10).

Also, the percentage increase of the inner surface potentials is still less compared to the decrease in surface potentials that can be obtained outside the barrier, even at positions relatively very far away from the barrier. For example, when the barrier is at position x=120 mm and y=120 mm, at 0° traverse, the surface potential increase of the barrier compared with no barrier is 17% on the substation side. However, at the same distance outside the barrier, the percentage decrease is 33% (see Figure 7.12).

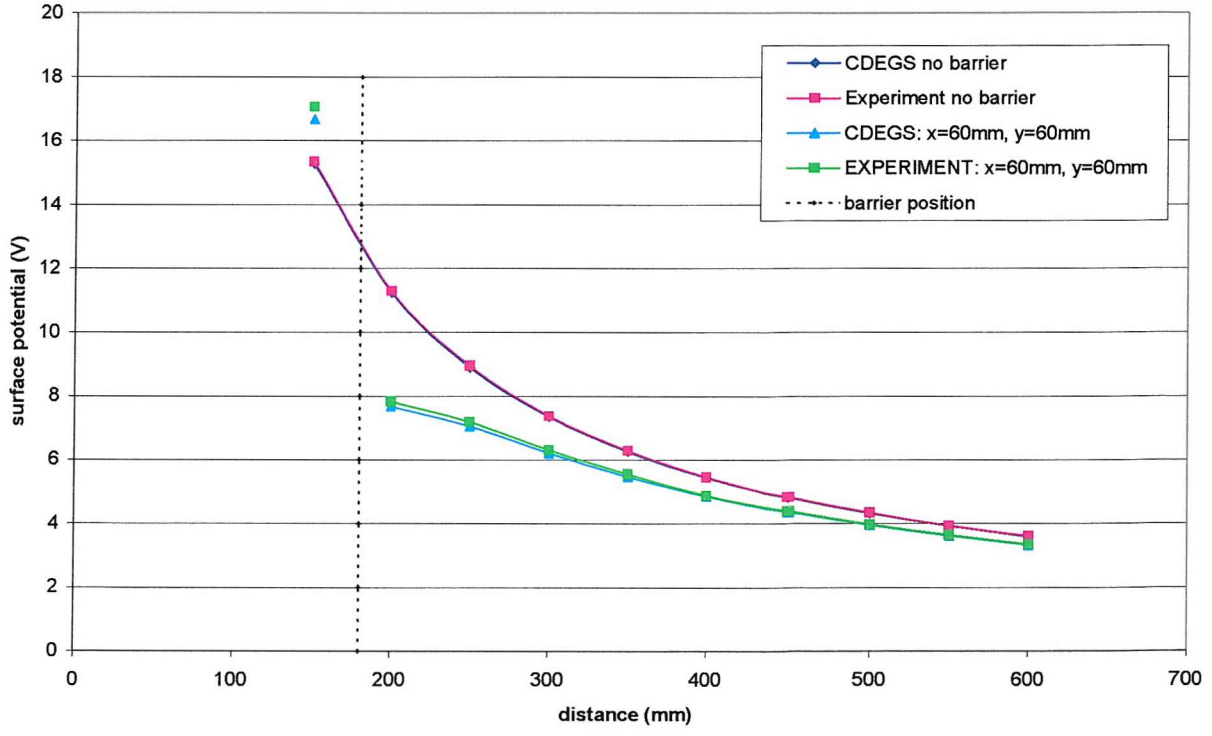

Figure 7.8: CDEGS MALT versus EXPERIMENT: Surface potential, Vs (V) against distance, d (mm) at 0 degree from electrode system with solid barrier x=60mm, y=60mm

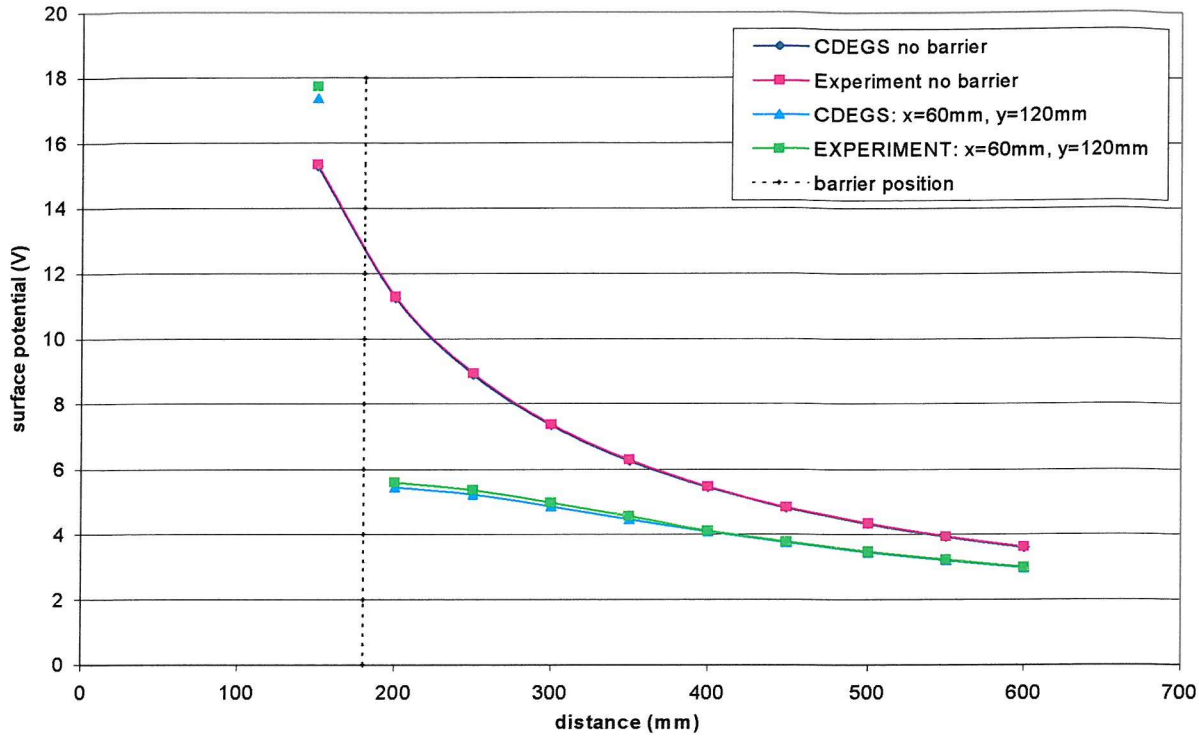

Figure 7.9: CDEGS MALT versus EXPERIMENT: Surface potential, Vs (V) against distance, d (mm) at 0 degree from electrode system with barrier x=60 mm, y=120 mm

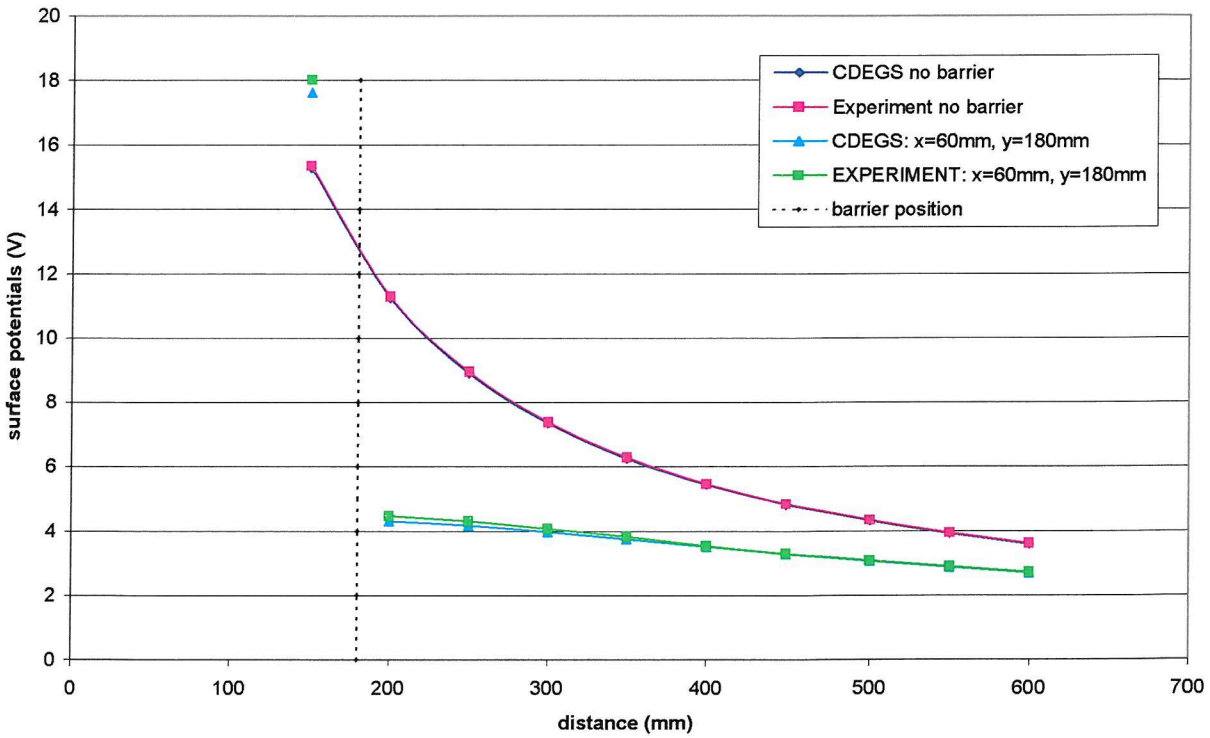

Figure 7.10: CDEGS MALT versus EXPERIMENT: Surface potential, Vs (V) against distance, d (mm) at 0 degree from electrode system with barrier x=60 mm, y=180 mm

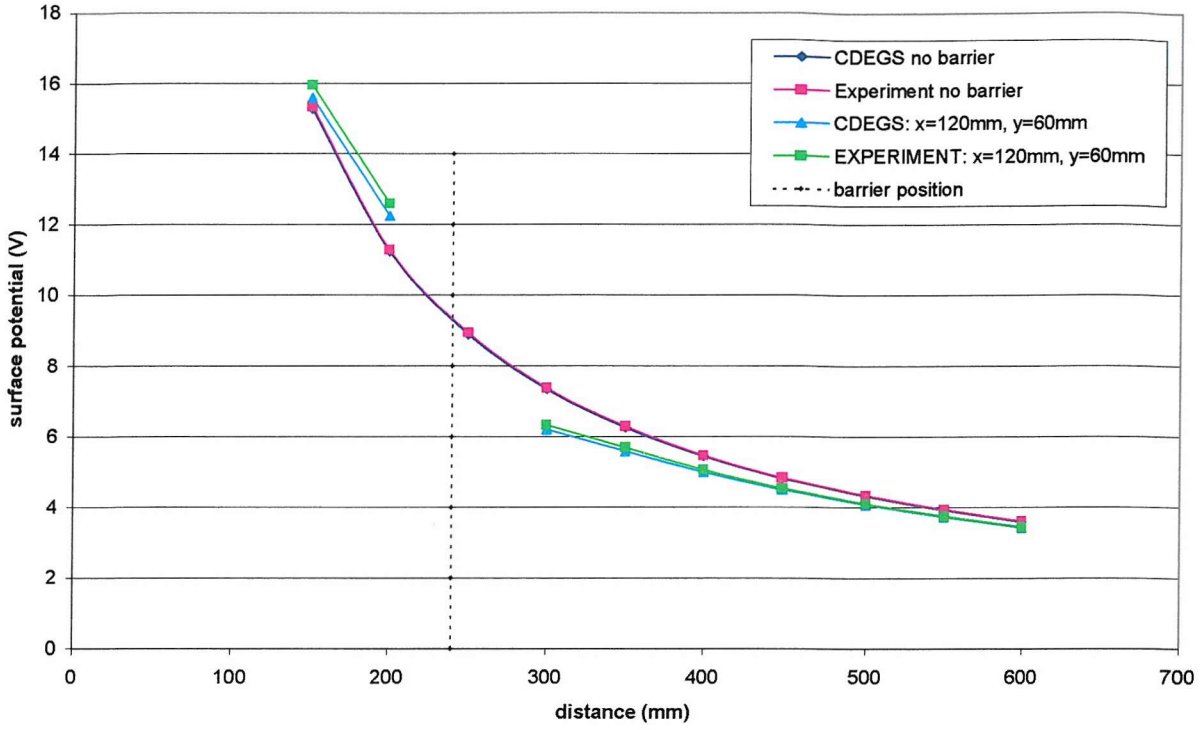

Figure 7.11: CDEGS MALT versus EXPERIMENT: Surface potential, Vs (V) against distance, d (mm) at 0 degree from electrode system with barrier x=120 mm, y=60 mm

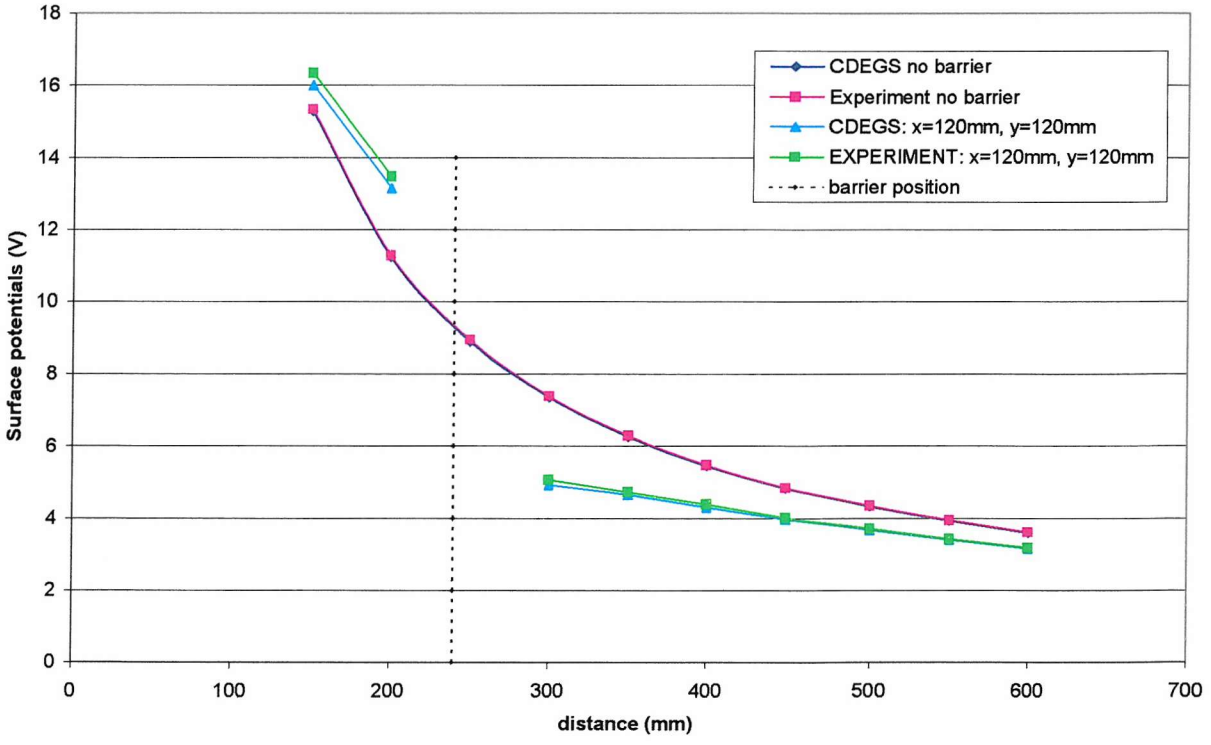

Figure 7.12: CDEGS MALT versus EXPERIMENT: Surface potential, Vs (V) against distance, d (mm) at 0 degree from electrode system with barrier x=120 mm, y=120 mm

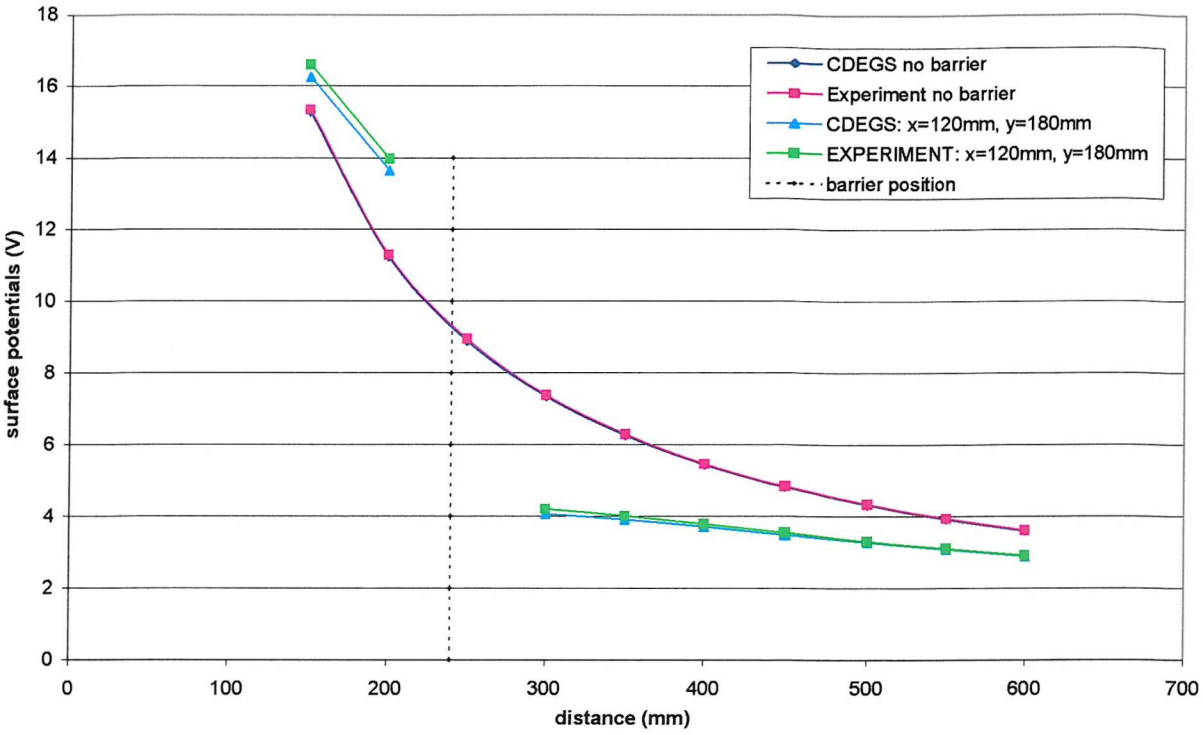

Figure 7.13: CDEGS MALT versus EXPERIMENT: Surface potential, Vs (V) against distance, d (mm) at 0 degree from electrode system with barrier x=120 mm, y=180 mm

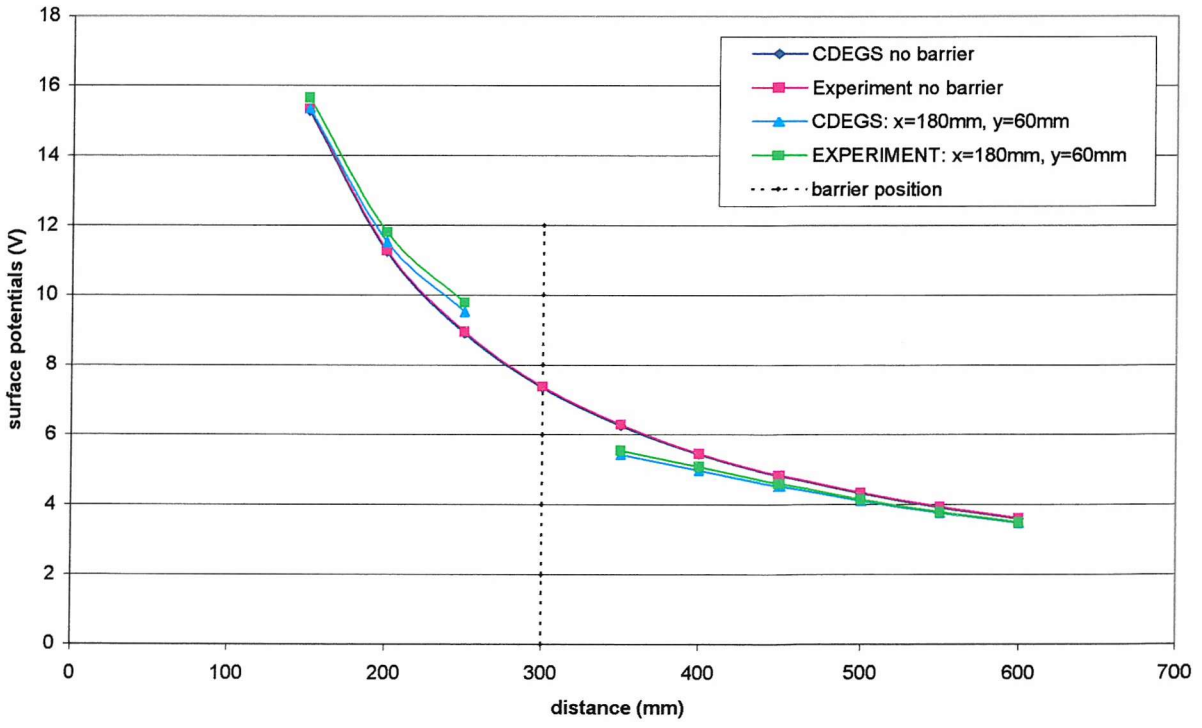

Figure 7.14: CDEGS MALT versus EXPERIMENT: Surface potential, Vs (V) against distance, d (mm) at 0 degree from electrode system with barrier x=180 mm, y=60 mm

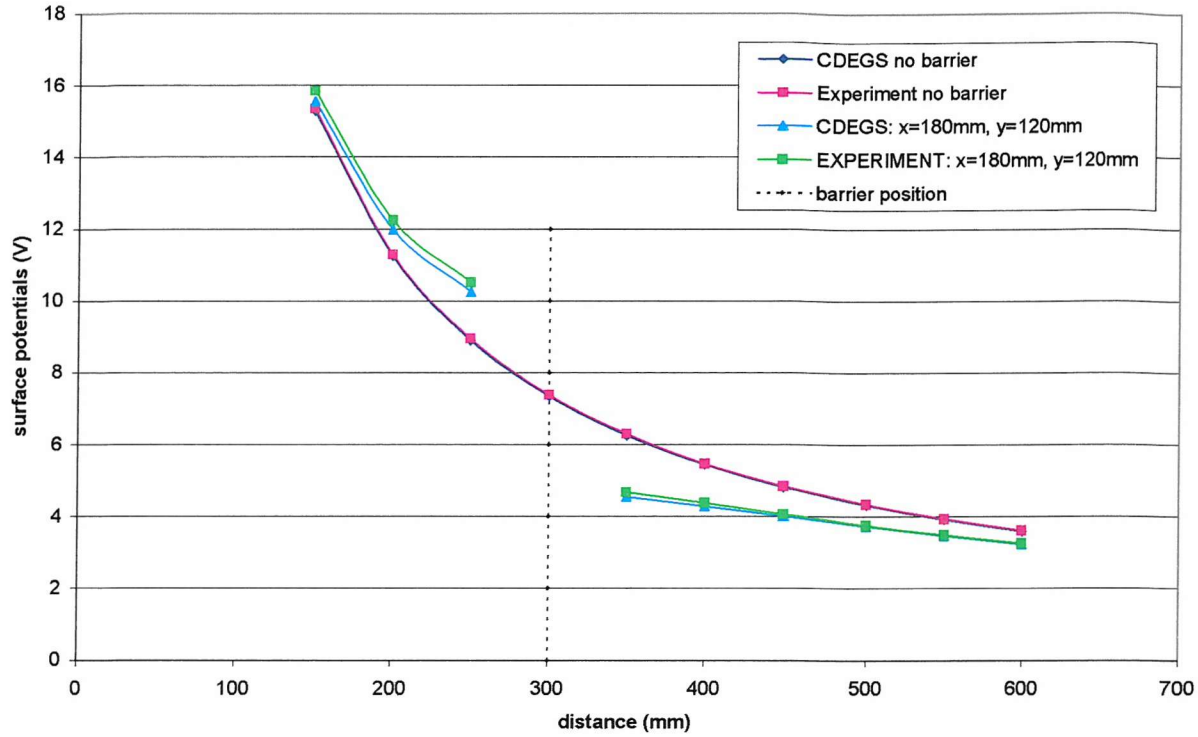

Figure 7.15: CDEGS MALT versus EXPERIMENT: Surface potential, Vs (V) against distance, d (mm) at 0 degree from electrode system with barrier x=180 mm, y=120 mm

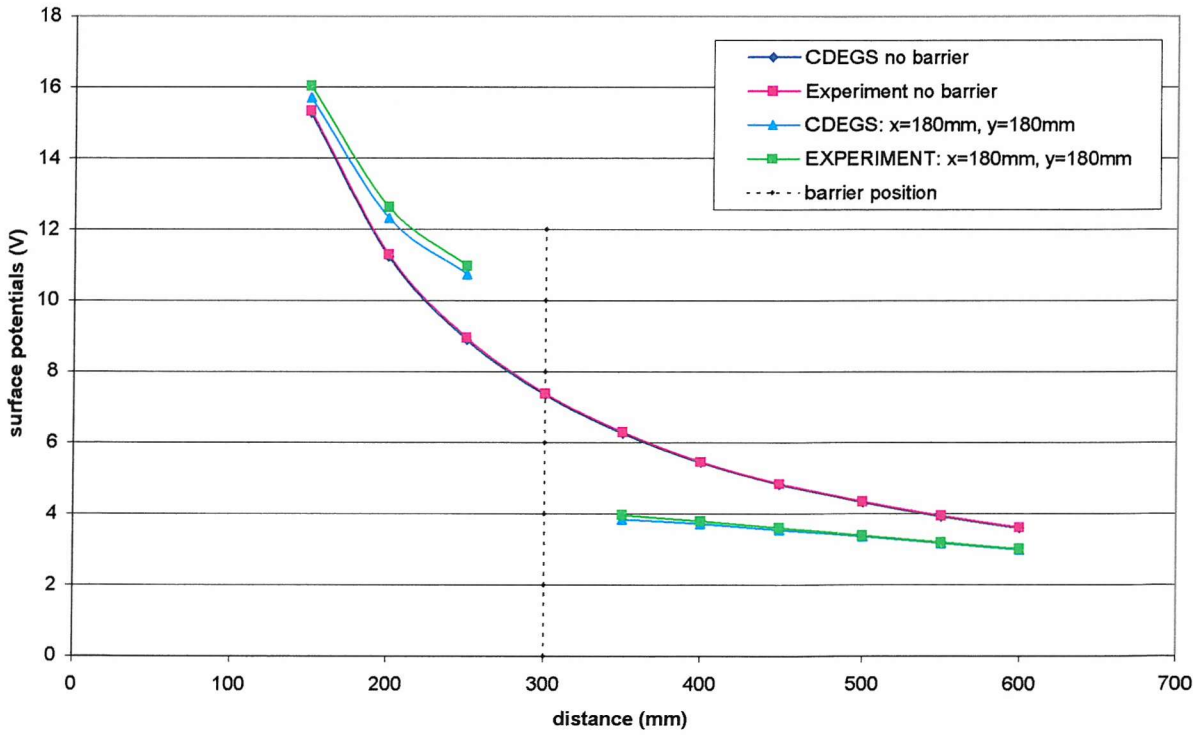

Figure 7.16: CDEGS MALT versus EXPERIMENT: Surface potential, Vs (V) against distance, d (mm) at 0 degree from electrode system with barrier x=180 mm, y=180 mm

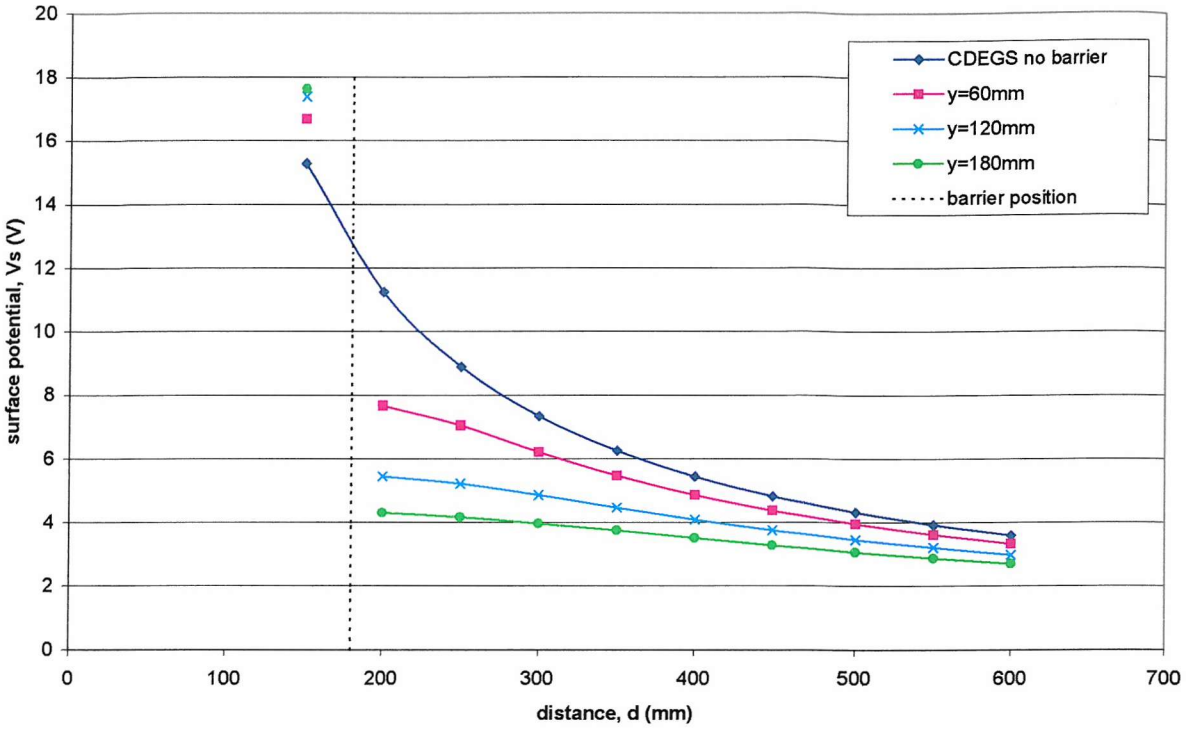

Figure 7.17: CDEGS MALT Surface Potential, Vs (V) against distance, d (mm) at 0 degree from electrode system (x=60 mm, y=variable depth)

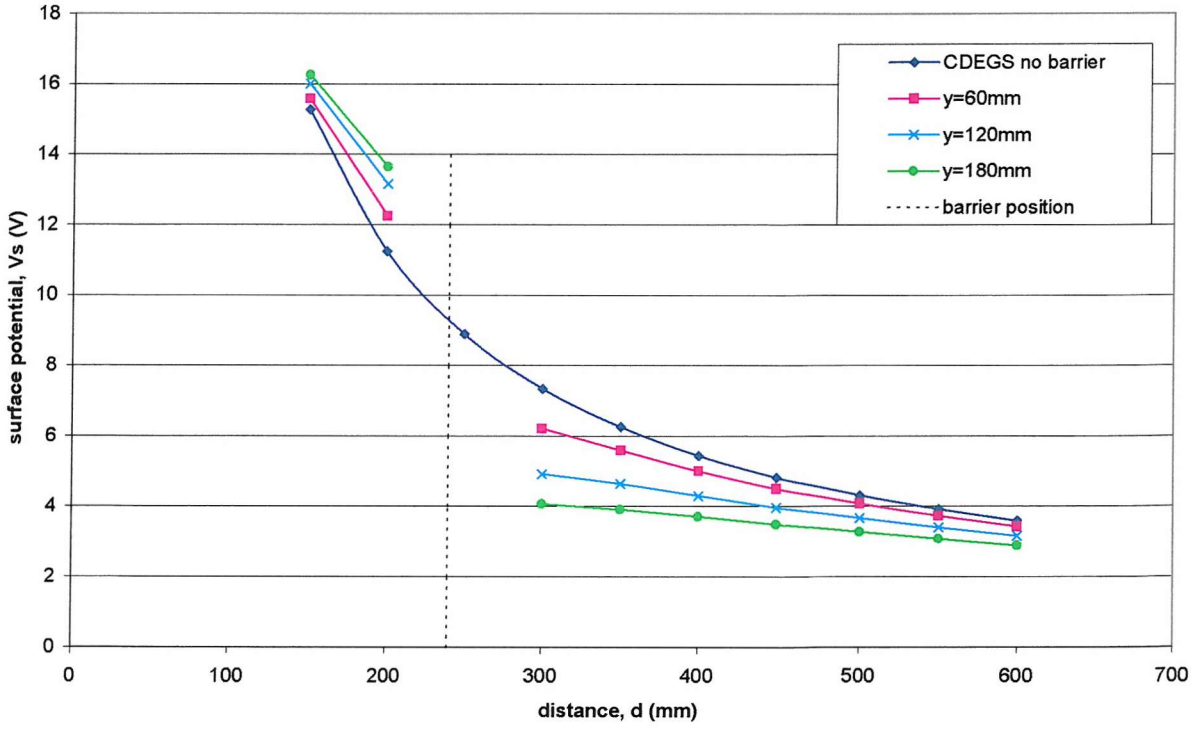

Figure 7.18: CDEGS MALT Surface Potential, Vs (V) against distance, d (mm) at 0 degree from electrode system (x=120 mm, y=variable depth)

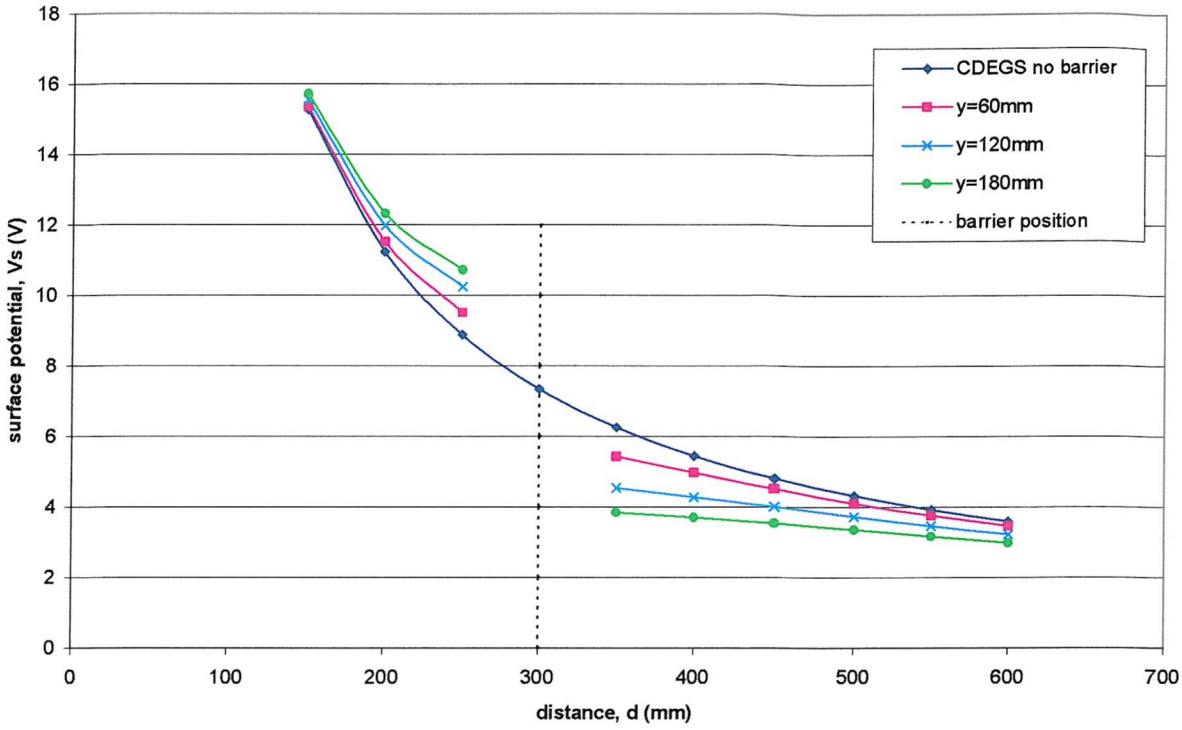

Figure 7.19: CDEGS MALT Surface Potential, Vs (V) against distance, d (mm) at 0 degree from electrode system (x=180 mm, y=variable depth)

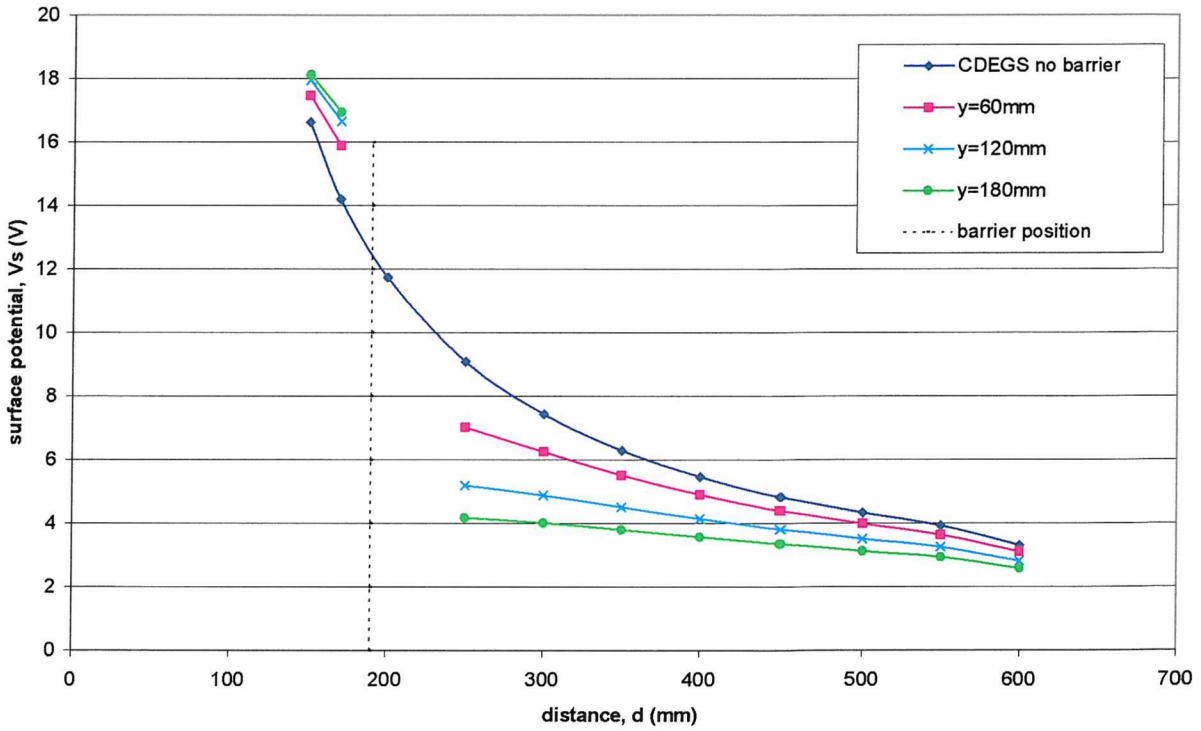

Figure 7.20: CDEGS MALT Surface Potential, Vs (V) against distance, d (mm) at 22.5 degree from electrode system (x=60 mm, y=variable depth)

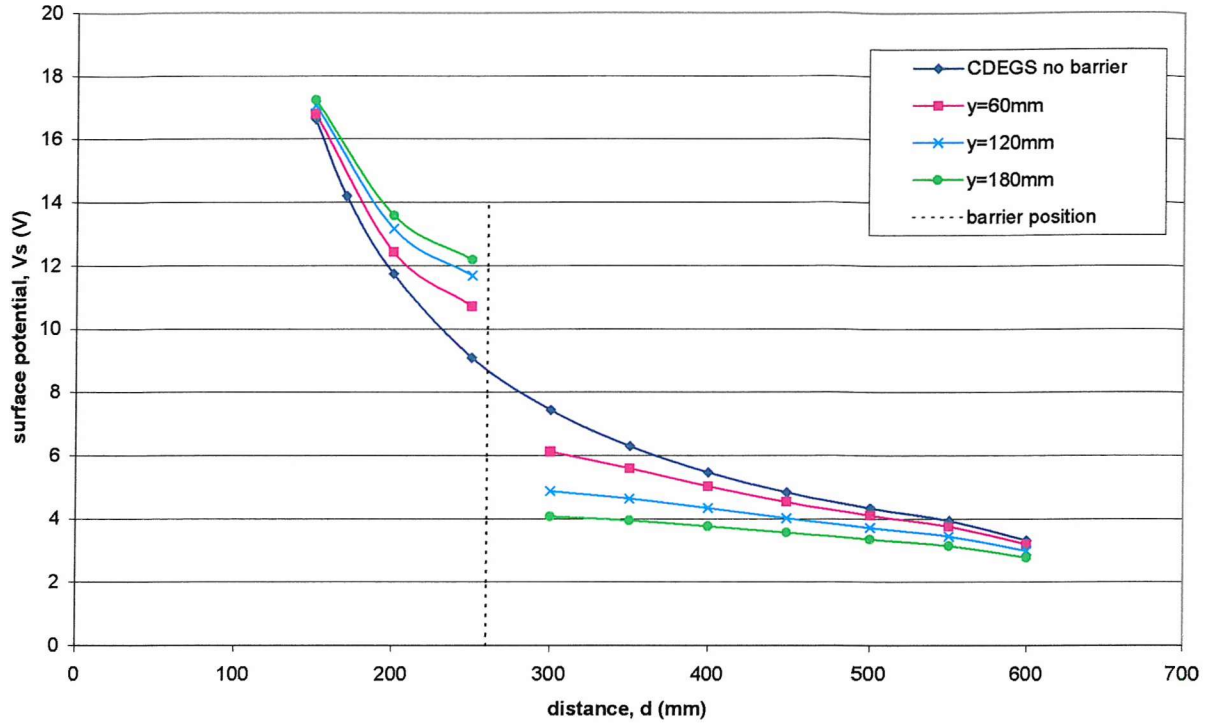

Figure 7.21: CDEGS MALT Surface Potential, Vs (V) against distance, d (mm) at 22.5 degree from electrode system (x=120 mm, y=variable depth)

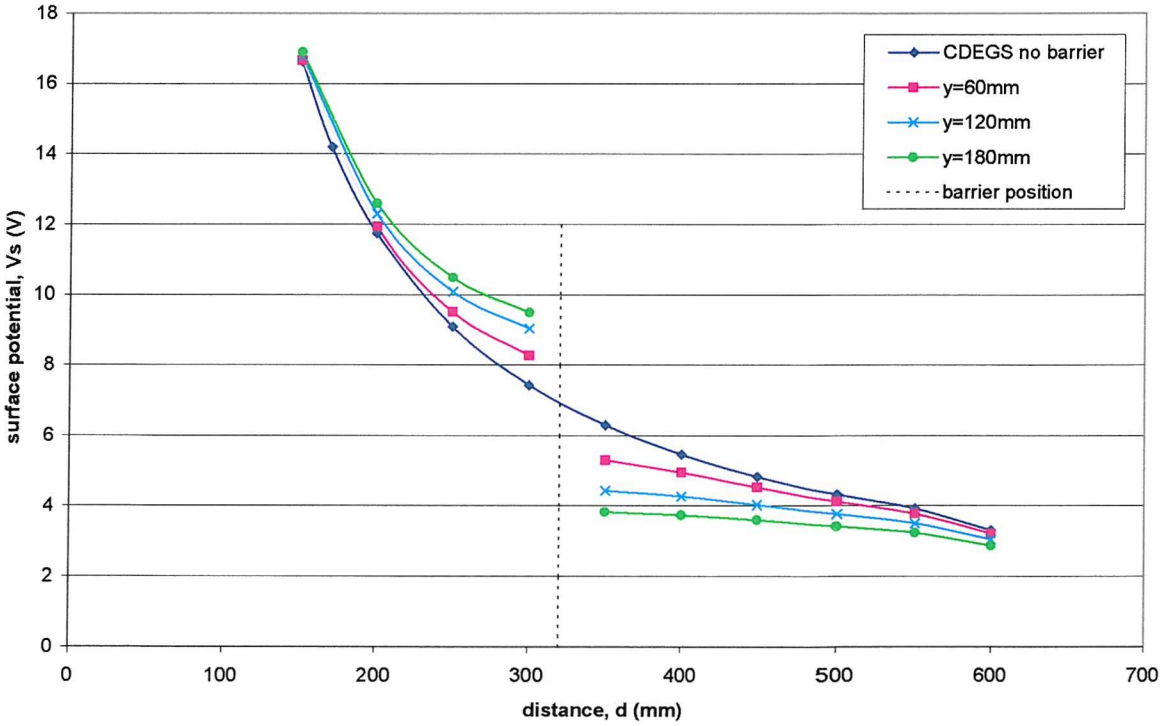

Figure 7.22: CDEGS MALT Surface Potential, Vs (V) against distance, d (mm) at 22.5 degree from electrode system (x=180 mm, y=variable depth)

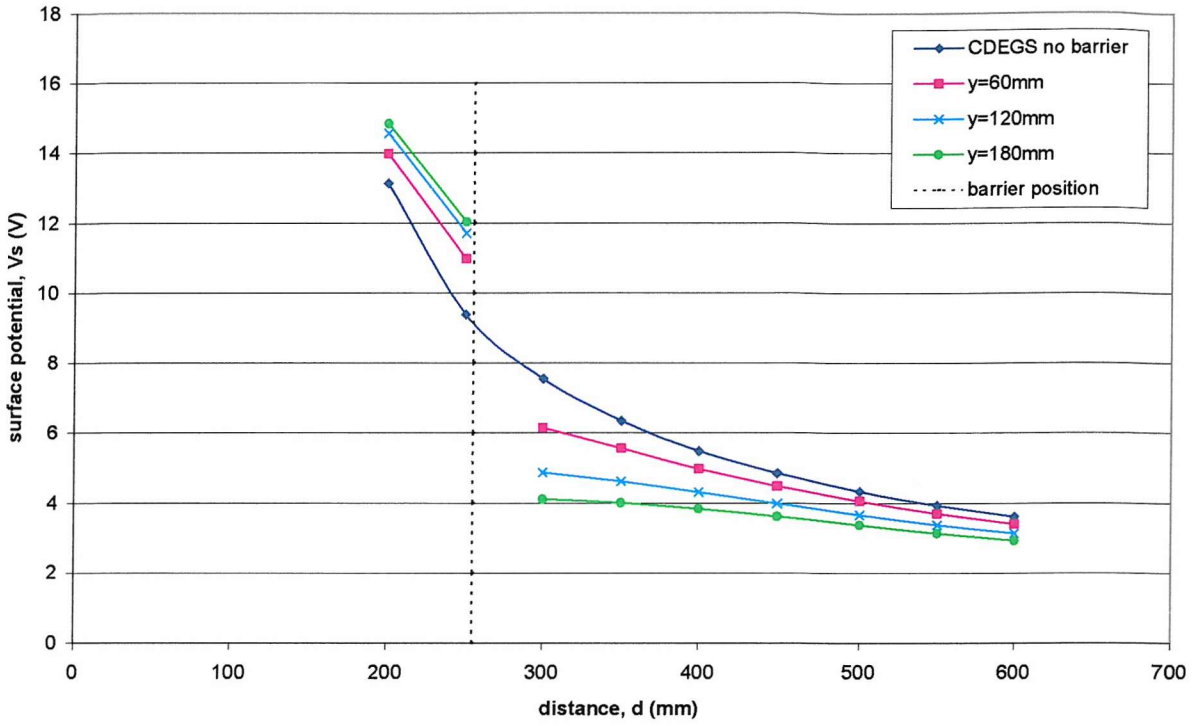

Figure 7.23: CDEGS MALT Surface Potential, Vs (V) against distance, d (mm) at 45 degree from electrode system (x=60 mm, y=variable depth)

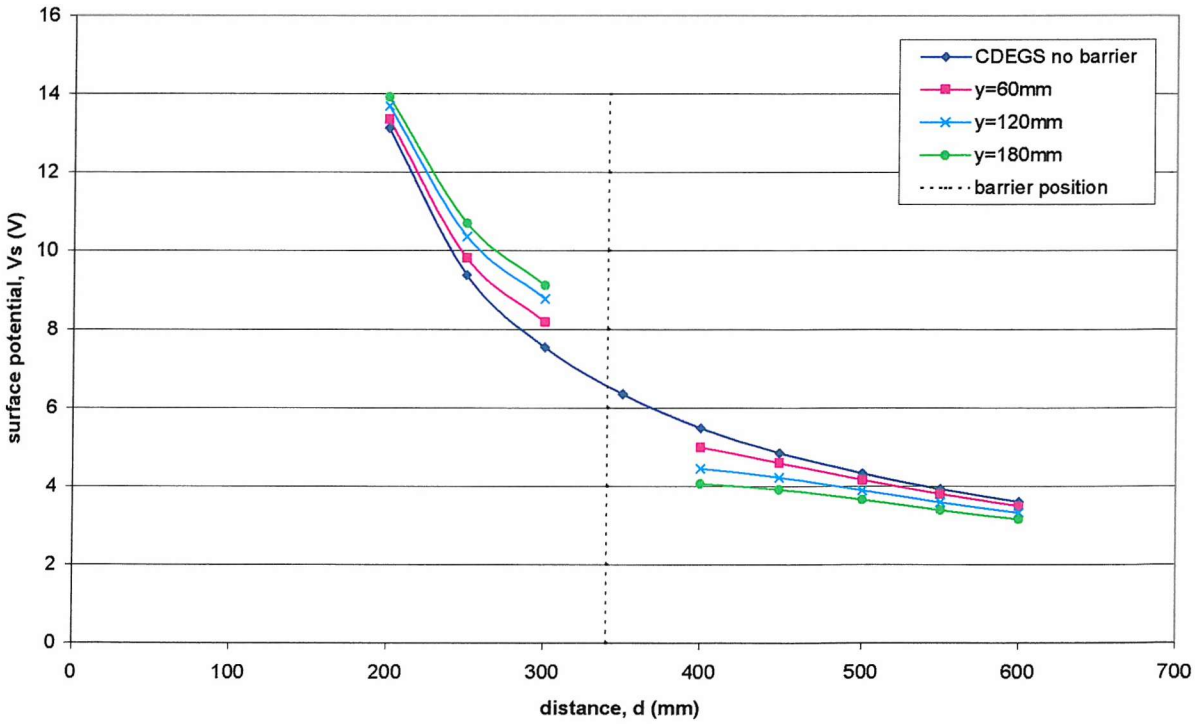

Figure 7.24: CDEGS MALT Surface Potential, Vs (V) against distance, d (mm) at 45 degree from electrode system (x=120 mm, y=variable depth)

Surface potentials at radius 450 mm were also taken at various angles in steps of 15° (around half a circle). This is illustrated in Figure 7.25 below (not to scale). The results are plotted in Figure 7.26. At about 45° the potential probe passes the edge of the barrier, and from Figure 7.26 it can be seen that the surface potential starts to increase and then remains constant at one level. The increase is approximately 21% from 0° to 75° onwards.

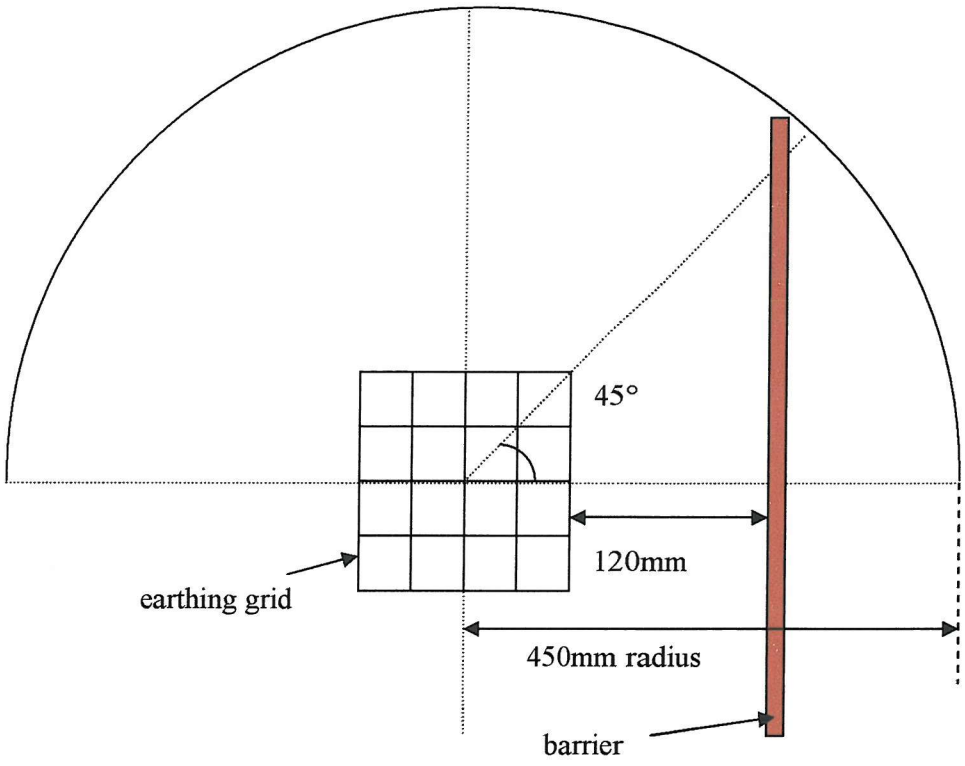

Figure 7.25: Radial Surface Potential measurement (not to scale)

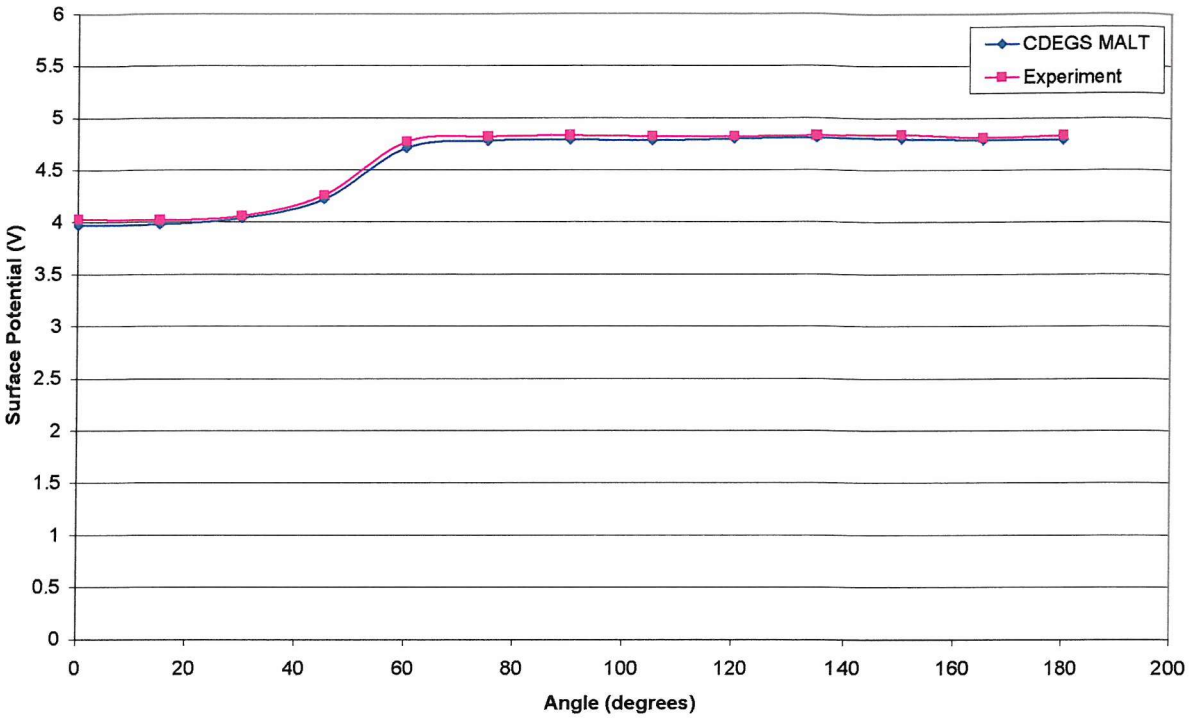

Figure 7.26: Radial surface potential at radius 450 mm for solid barrier position at x=120 mm, y=120 mm

7.2 Plate Barrier

The plate barrier is the same as the solid barrier in terms of its overall dimensions and positions from the earthing grid. The only difference here is that the material used is less because the barrier now has equally spaced gaps formed by a series of plates (refer to Figure 7.2). The gaps or spacing, c, tested are 2 mm, 5 mm and 10 mm, and the plates are arranged such that the total length of the barrier is still the same as the solid barrier, namely 650 mm. The positions and depths of the barrier are still the same as for the solid barrier.

7.2.1 Resistance Measurements for Plate Barrier

The curves of resistance against plate spacing computed by CDEGS MALT are shown in Figures 7.27-7.29, together with the line indicating the original resistance before the barrier was lowered. Figures 7.30-7.32 shows the curves of resistance against barrier depth for CDEGS MALT results for all three plate spacing. The difference between the experimental and CDEGS MALT results are well within experimental error, i.e. less than

1.2% difference. Figures 7.33 and 7.34 show examples of the agreement between the computed and experimented results. Full-tabulated experimental and computed results can be found in Appendix 7(C). All values are scaled to a water conductivity of 0.1 S/m.

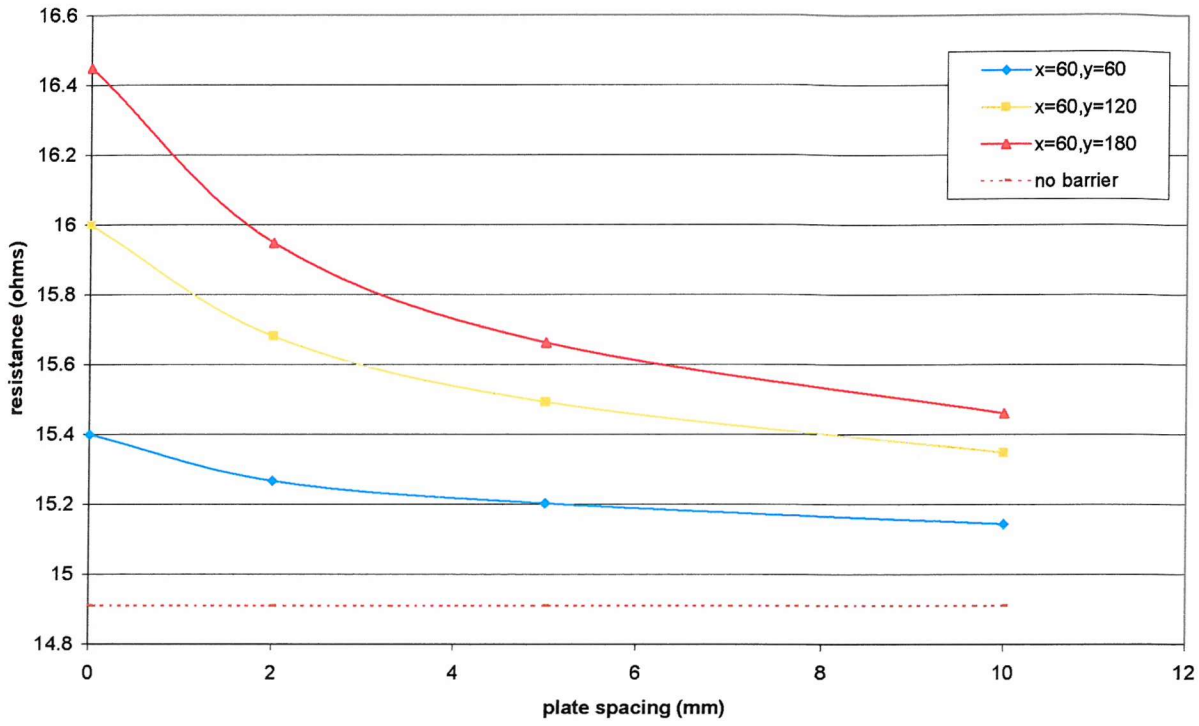

Figure 7.27: CDEGS MALT Resistance of the earthing system with plate barrier at x=60 mm varying y (mm) against plate spacing (mm)

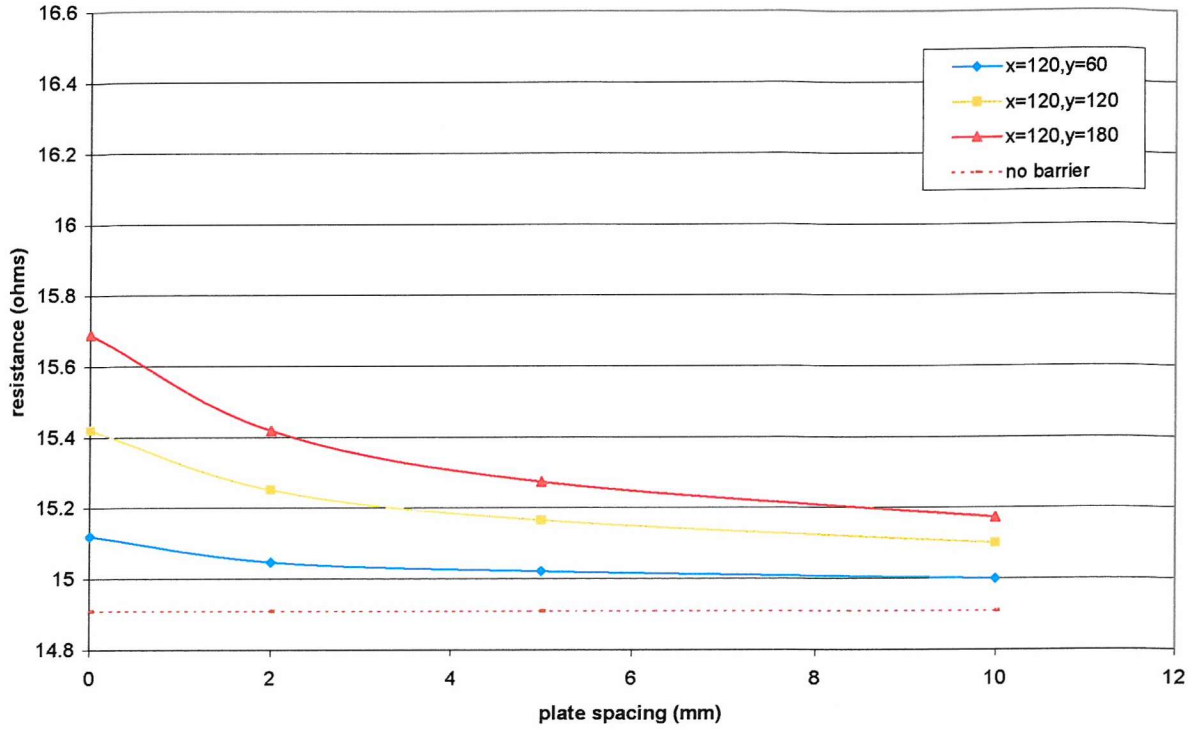

Figure 7.28: CDEGS MALT Resistance of the earthing system with plate barrier at x=120 mm varying y (mm) against plate spacing (mm)

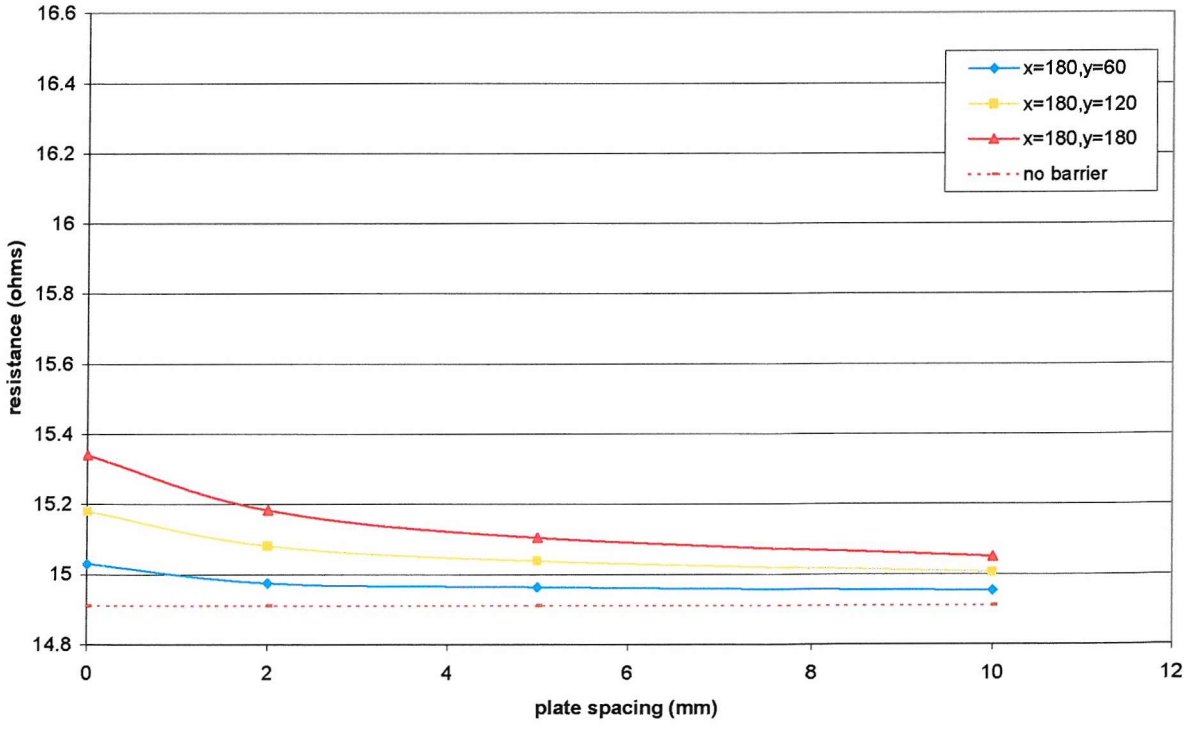

Figure 7.29: CDEGS MALT Resistance of the earthing system with plate barrier at x=180 mm varying y (mm) against plate spacing (mm)

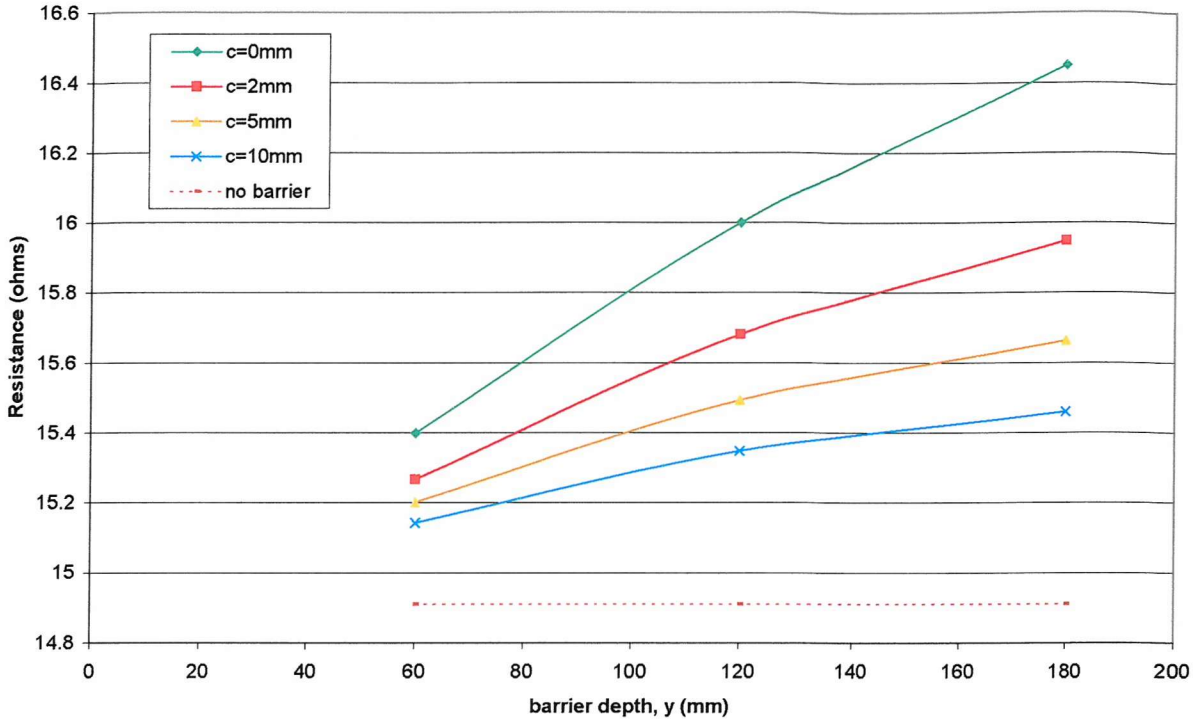

Figure 7.30: CDEGS MALT Resistance of the earthing system with plate barrier at x=60 mm varying plate spacing (mm) against barrier depth (mm)

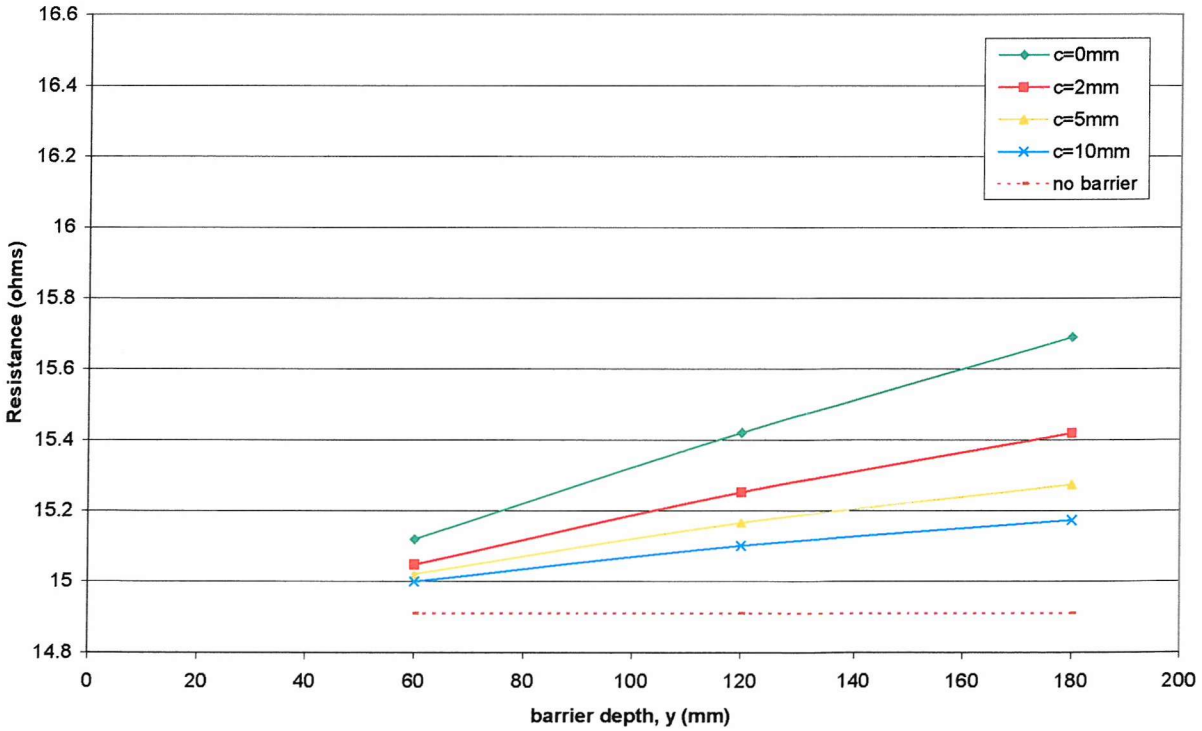

Figure 7.31: CDEGS MALT Resistance of the earthing system with plate barrier at x=120 mm varying plate spacing (mm) against barrier depth (mm)

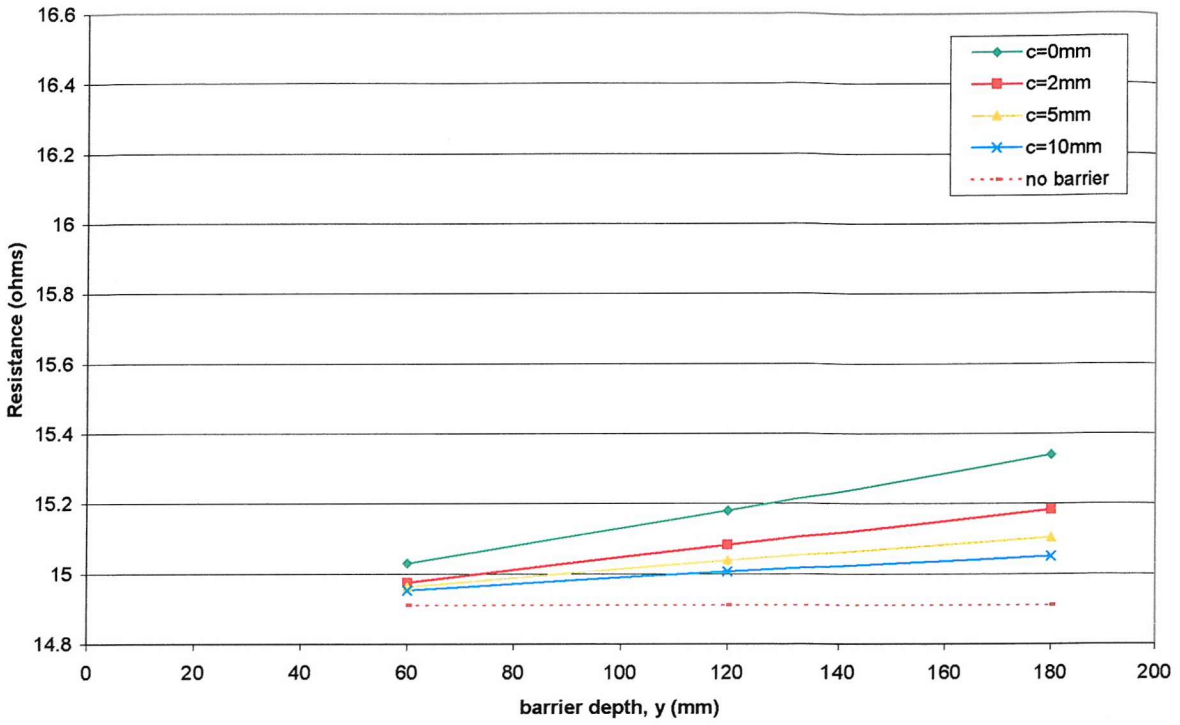

Figure 7.32: CDEGS MALT Resistance of the earthing system with plate barrier at x=180 mm varying plate spacing (mm) against barrier depth (mm)

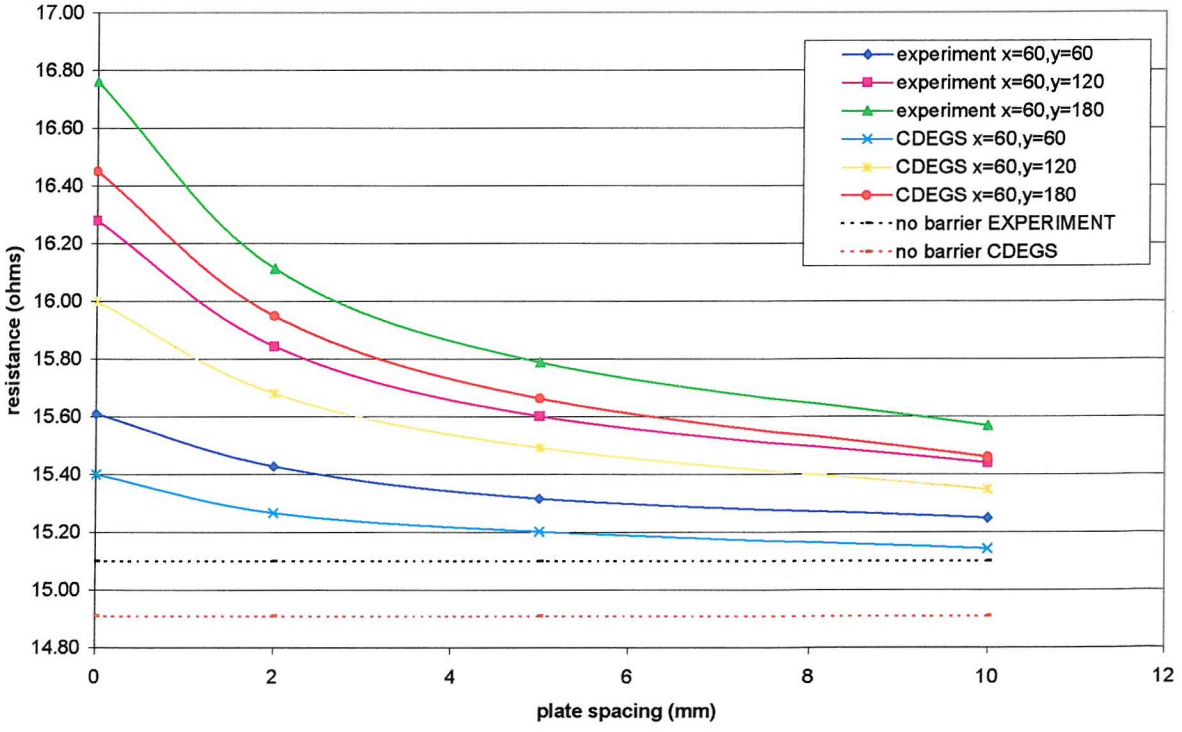

Figure 7.33: CDEGS MALT versus Experimental Resistance for barrier position x=60 varying y (mm) versus plate spacing (mm)

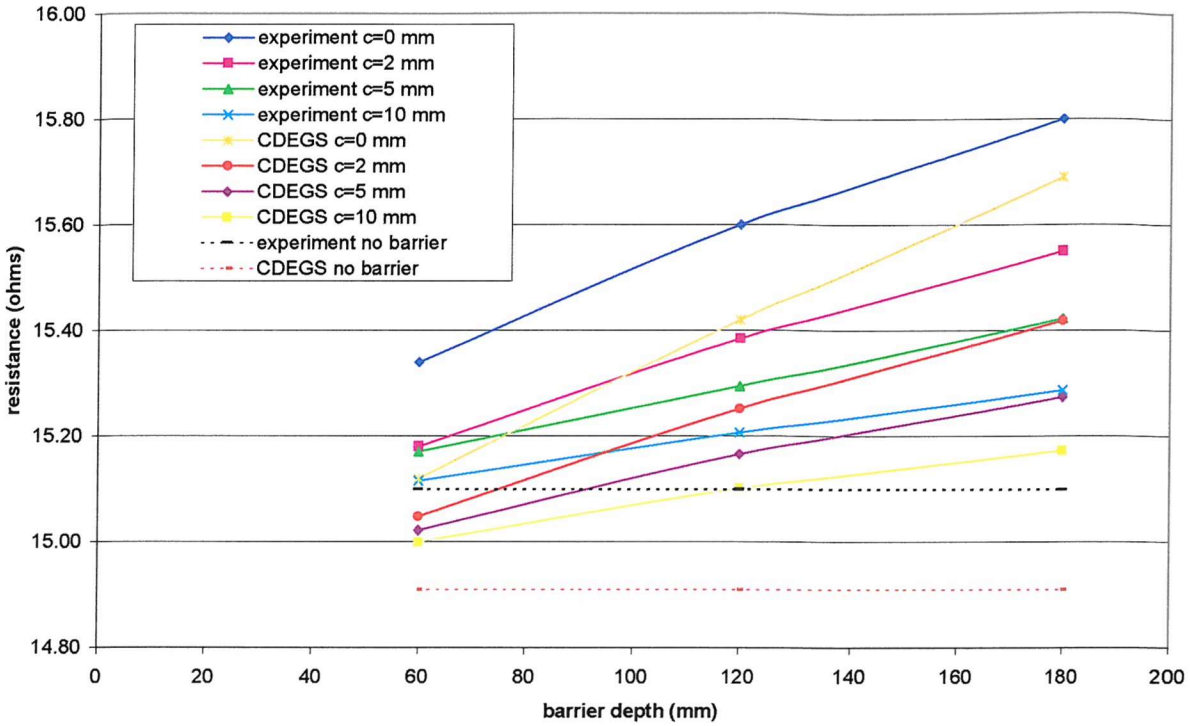

Figure 7.34: CDEGS MALT versus Experimental Resistance for barrier position x=120 mm varying plate spacing, c (mm) versus barrier depth, y (mm)

The increase in earthing resistance when a plate barrier is present is obviously less than with a solid barrier. A plate barrier with the smallest gap tested, which is 1.28 times the rod diameter, gives a rise in earthing resistance (with respect to no barrier present) of about 1.88% and 2.29% for experimental and computed results respectively, for a sensible barrier position and depth in the region of two vertical rod lengths. Even in the worst case tested (a deep barrier close to the array with the smallest gap) the increase is between 6.37% and 6.97% for both cases (CDEGS MALT and experimental results).

Hence, when using plate barriers, the increase in earthing resistance is not so significant when compared to the solid barrier. Also, for the gap sizes tested, the gap size does not have a significant influence on the rise of the earthing resistance. Although using the plate barrier gives a lower percentage increase in the resistance of the overall earthing system, the decrease in percentage with respect to solid barrier is only about 2% for the sensible barrier position (two vertical rod length deep and position) and the widest plate gap of 10mm.

7.2.2 Surface Potential Measurements for Plate Barrier

The surface potentials were investigated in two distinct directions; one being perpendicular to the barrier and the other is parallel to the barrier.

7.2.2.1 Perpendicular Measurements

For the perpendicular traverse (0°), the surface potential measurements were made perpendicular to the edge of the earthing grid and through the centre of the barrier. The important point to note here is that the middle plate of the barrier is always on the axis of the 0° traverse. This is to ensure that when the surface potential measurements are taken, the position of the gaps will not affect the overall conclusion. Only the gap size is investigated here and hence the position of the voltage probe with respect to the plate and its gaps is very important. All the plates making up the barrier are of the same size (width 50 mm). Only the widths of the end plates have to be adjusted to fit the overall barrier length of 650 mm. This is illustrated in Figure 7.35.

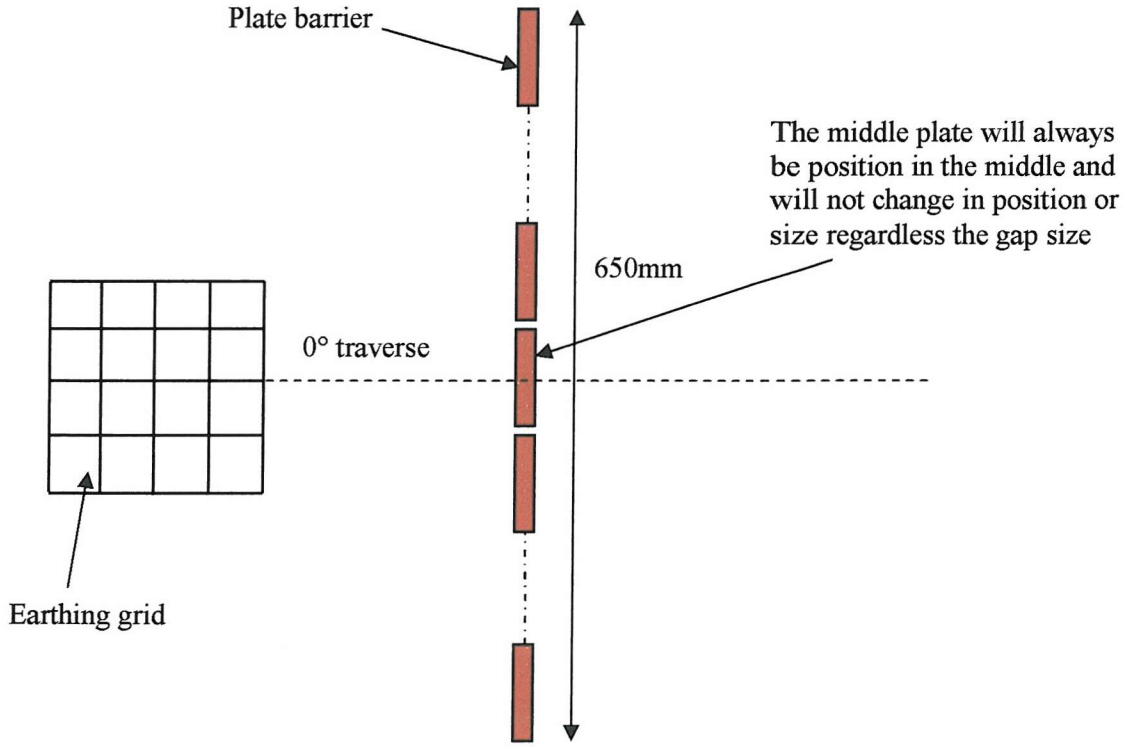

Figure 7.35: Top view of the barrier system with the surface potential measurement perpendicular traverse (not to scale)

Figures 7.36 to 7.38 show the comparison between CDEGS MALT and experimental results for a barrier position of x=120 mm and y=120 mm with varying plate barrier gap spacing. Figures 7.39 to 7.47 show the computed potential distribution in graphical form for all the plate barrier positions with varying gap sizes. Figures 7.48 to 7.56 show the computed potential distribution for all the plate barrier gap sizes with varying positions and burial depths of the barrier. Full detailed tabulated results are in Appendix 7.

For all the different configurations of barrier position and plate spacing, the results obtained from the experiments are well within the computed results. The percentage difference between experimental and computed results is less than 1% (with respect to the energizing voltage, 20V) for readings outside the barrier. Between the barrier and the grid, depending on the position where the reading is taken, the percentage difference between CDEGS MALT and experimental results is between 2-8%. The nearer the reading position is to the grid, the higher the difference. This discrepancy will be discussed further in the next chapter.

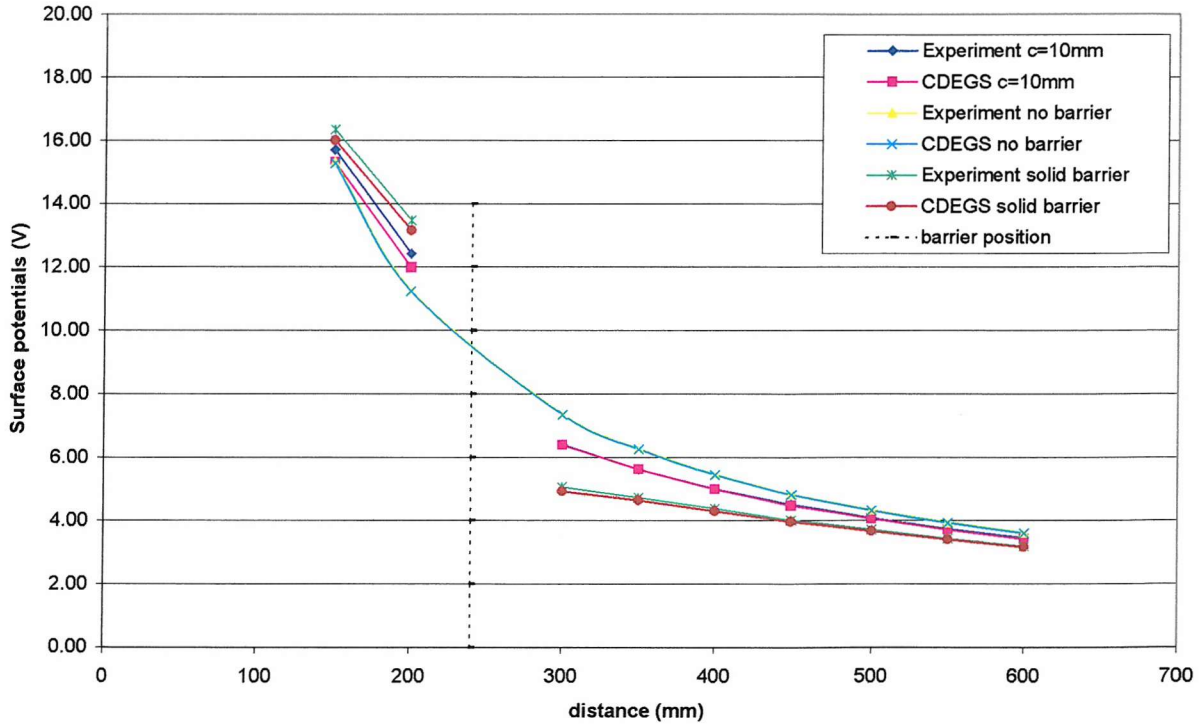

Figure 7.36: CDEGS MALT versus Experiment for surface potentials (V) against distance (mm) for a plate barrier with 10 mm spacing at x=120 mm and y=120 mm

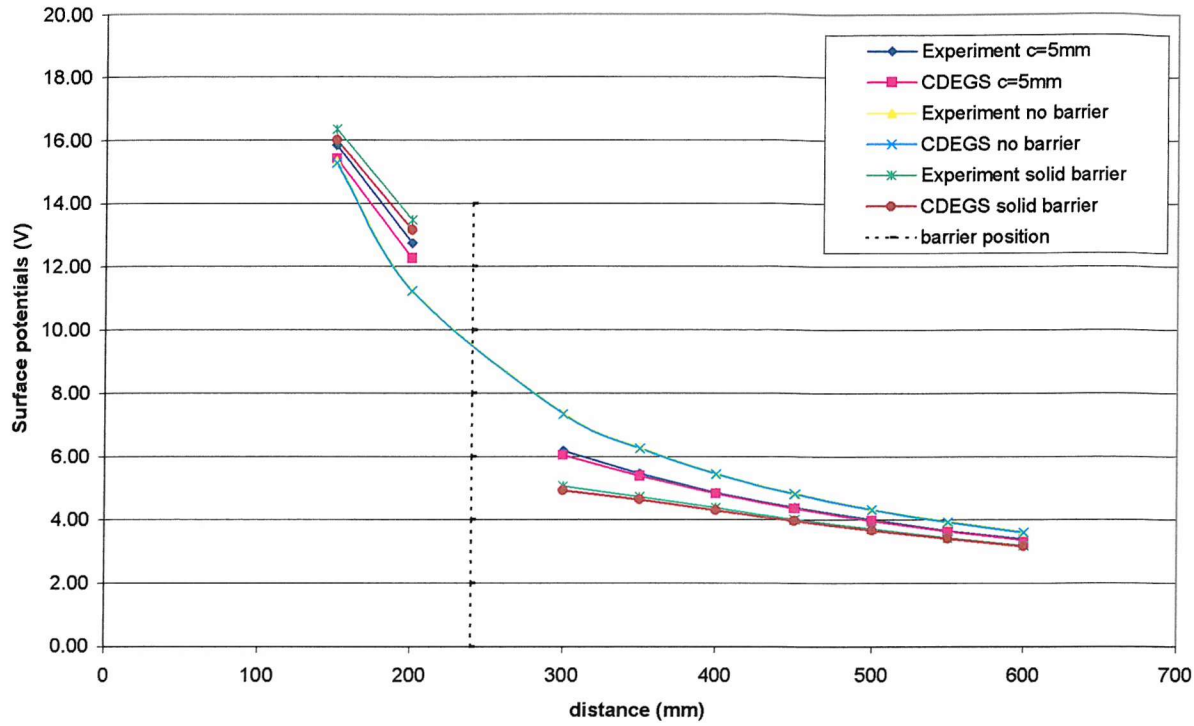

Figure 7.37: CDEGS MALT versus Experiment for surface potentials (V) against distance (mm) for a plate barrier with 5 mm spacing at x=120 mm and y=120 mm

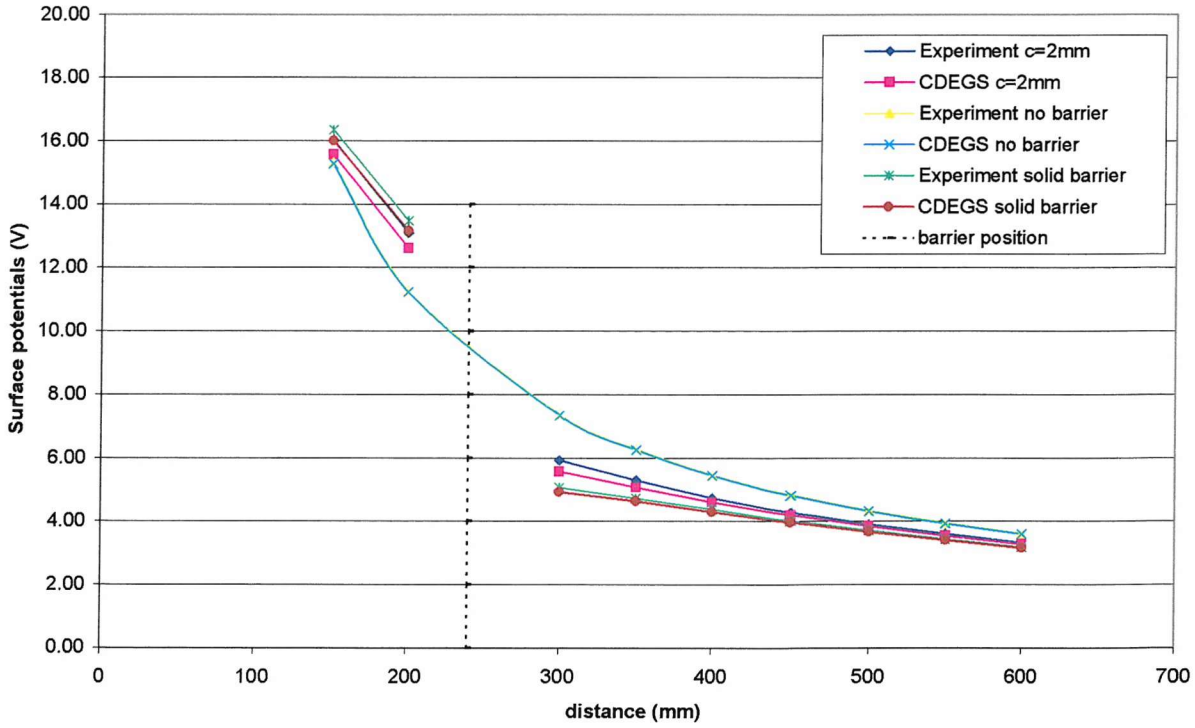

Figure 7.38: CDEGS MALT versus Experiment for surface potentials (V) against distance (mm) for a plate barrier with 2 mm spacing at x=120 mm and y=120 mm

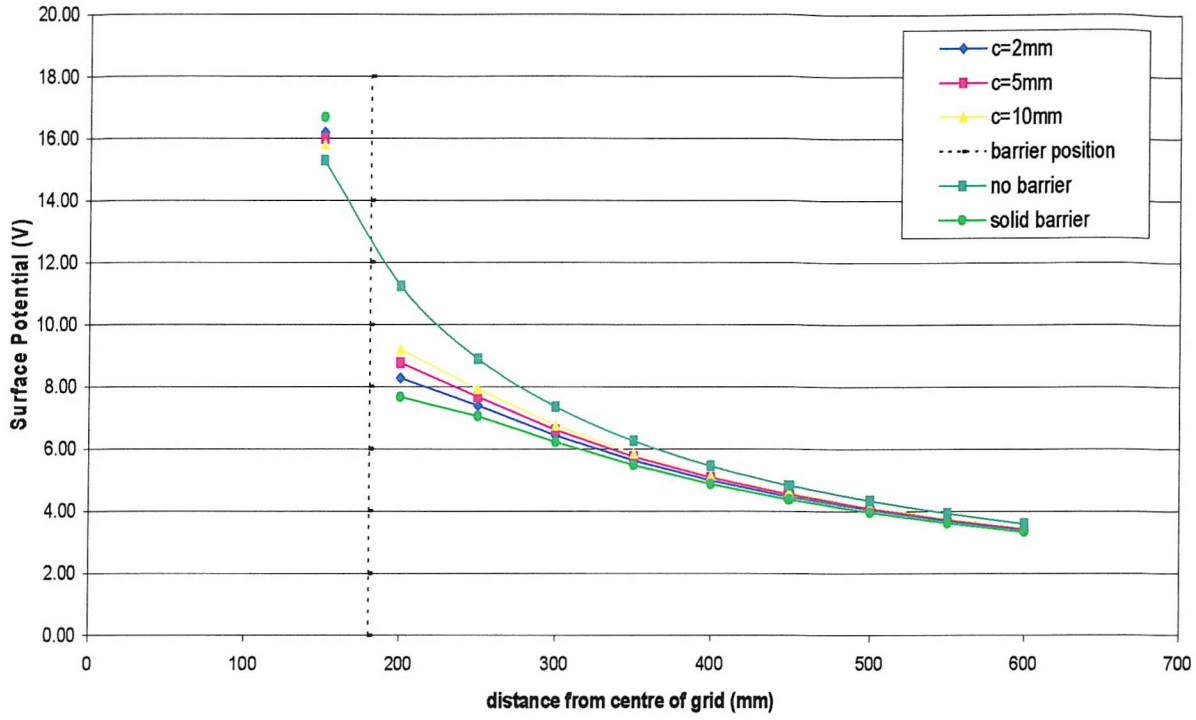

Figure 7.39: CDEGS MALT Surface potentials for plate barrier at position x=60 mm, y=60 mm with varying plate spacing

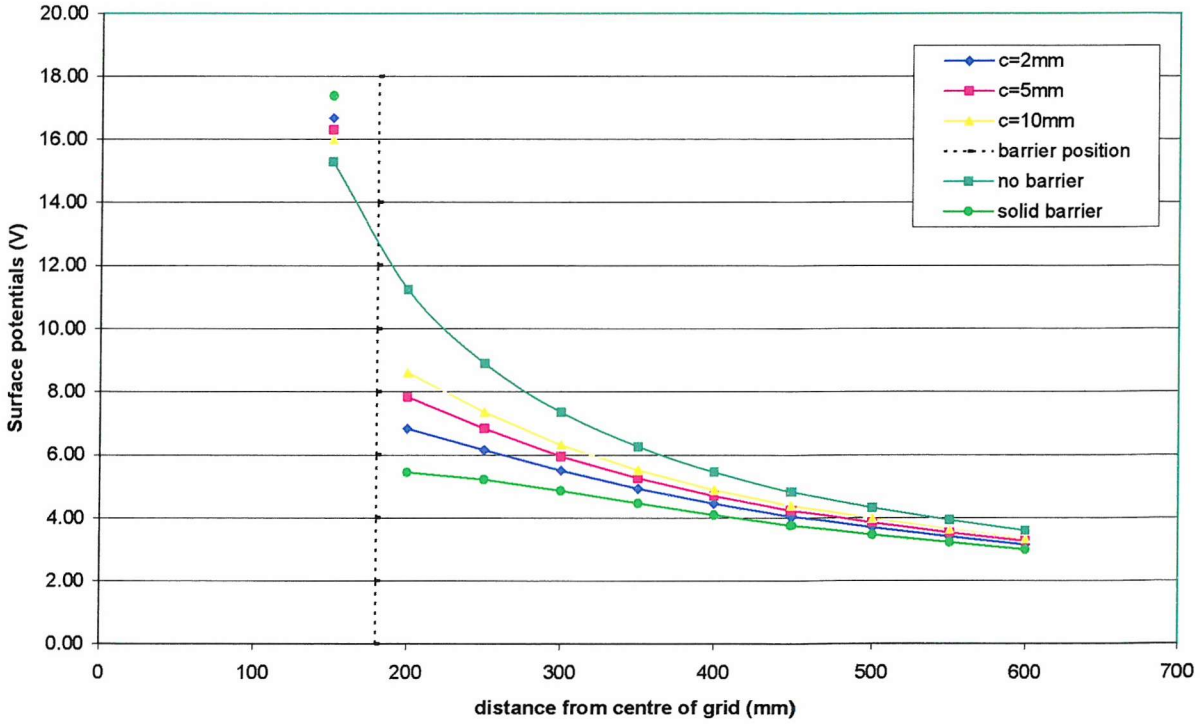

Figure 7.40: CDEGS MALT Surface potentials for plate barrier at position x=60 mm, y=120 mm with varying plate spacing

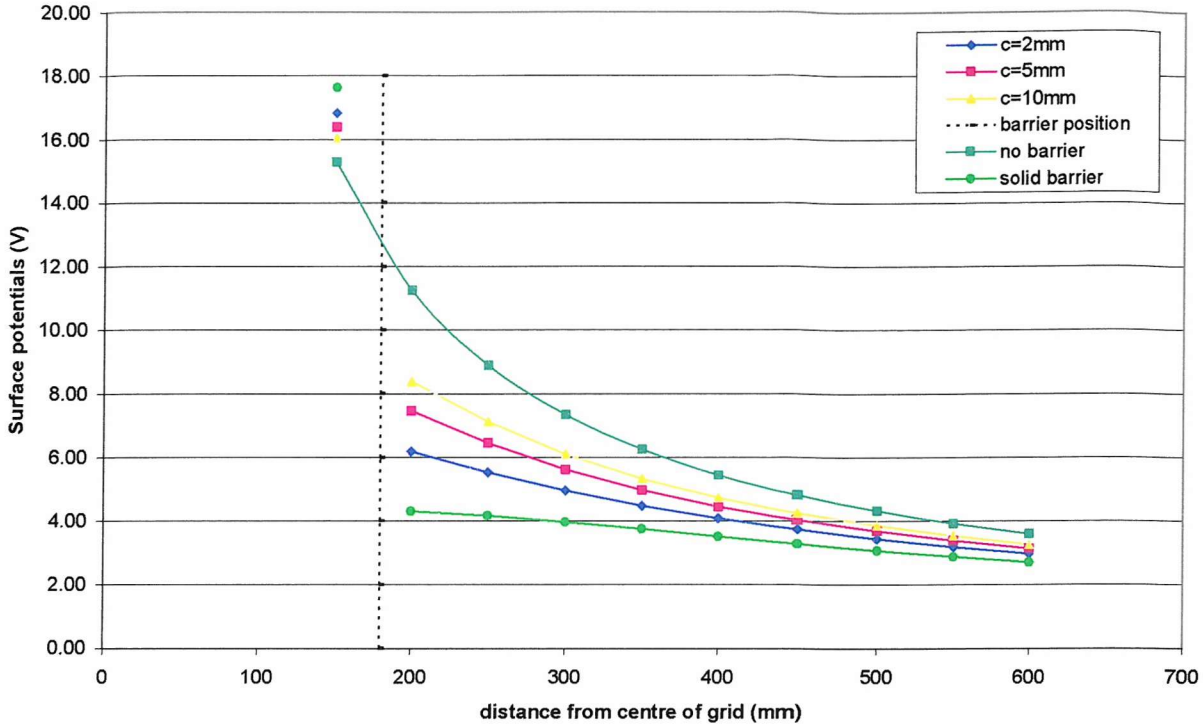

Figure 7.41: CDEGS MALT Surface potentials for plate barrier at position x=60 mm, y=180 mm with varying plate spacing

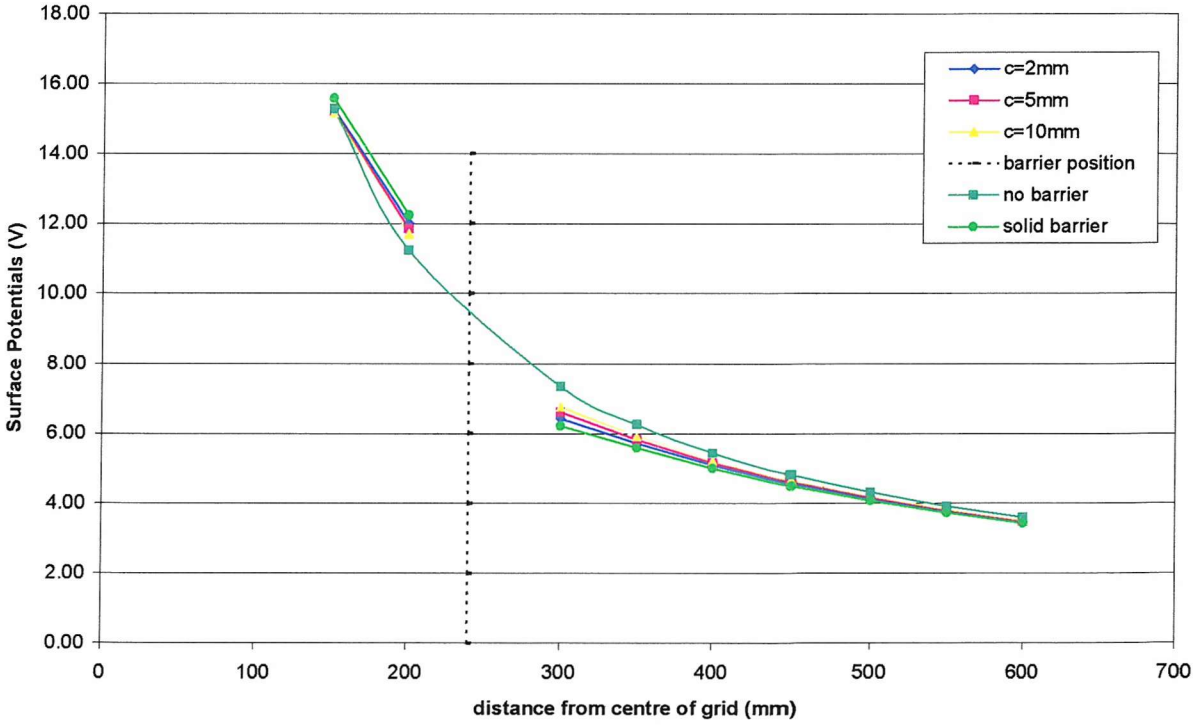

Figure 7.42: CDEGS MALT Surface potentials for plate barrier at position x=120 mm, y=60 mm with varying plate spacing

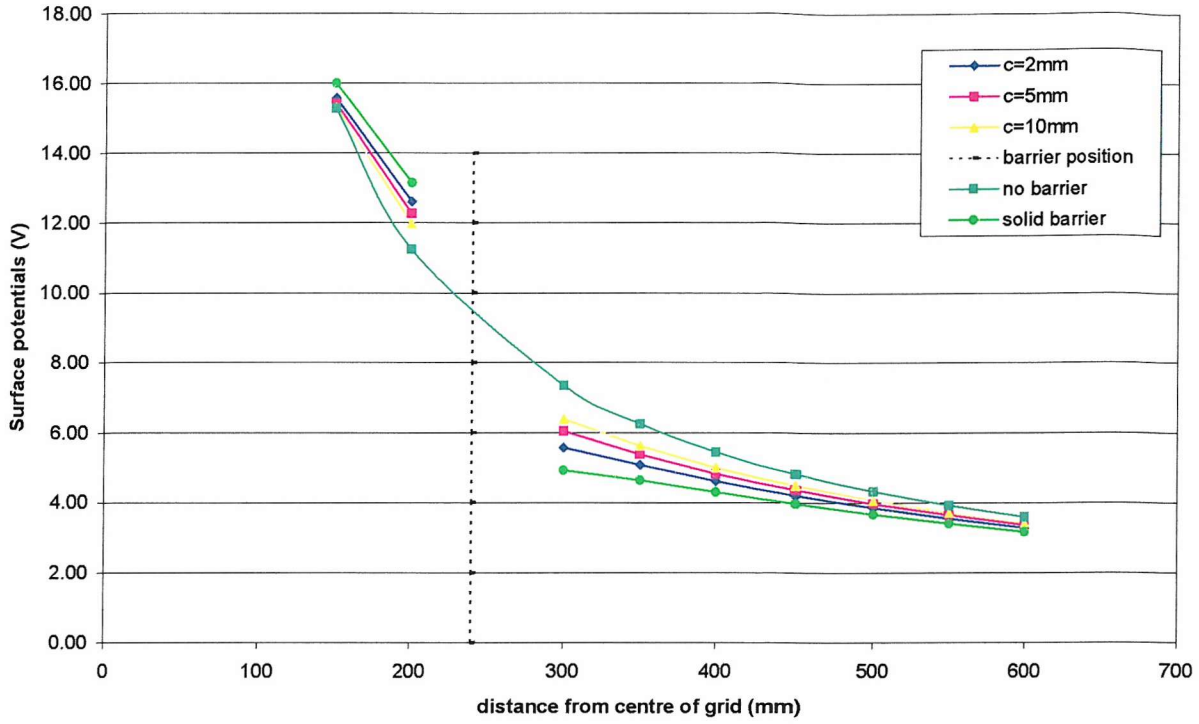

Figure 7.43: CDEGS MALT Surface potentials for plate barrier at position x=120 mm, y=120 mm with varying plate spacing

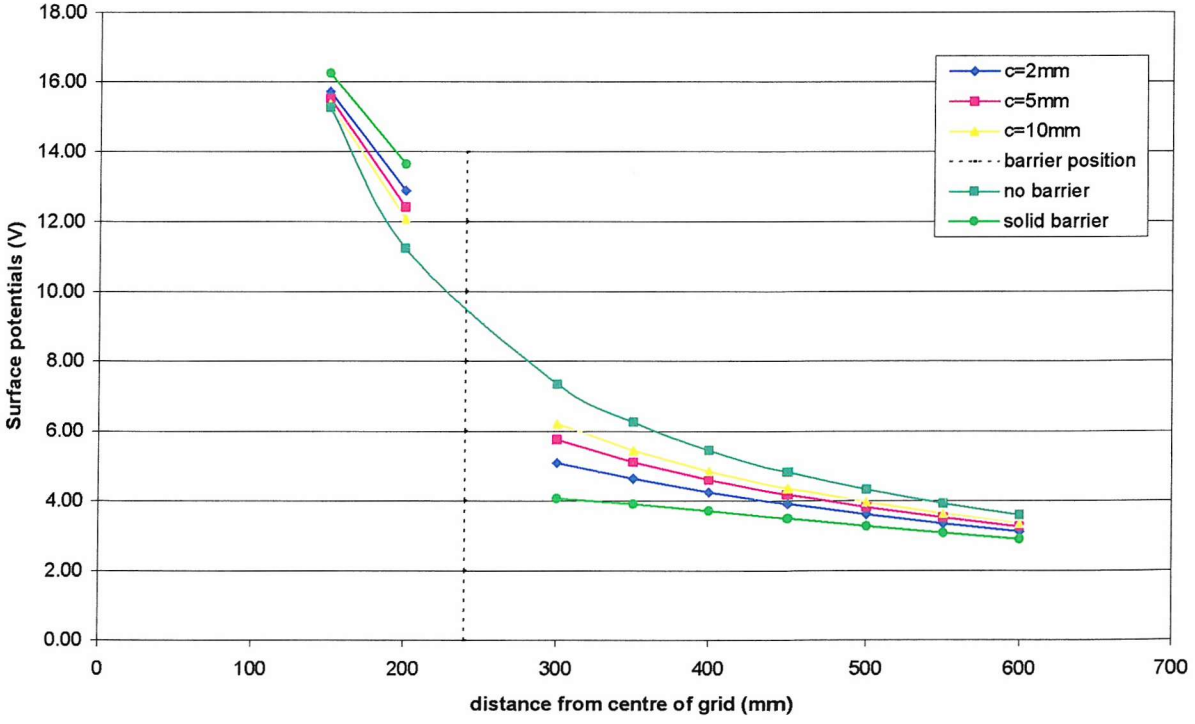

Figure 7.44: CDEGS MALT Surface potentials for plate barrier at position x=120 mm, y=180 mm with varying plate spacing

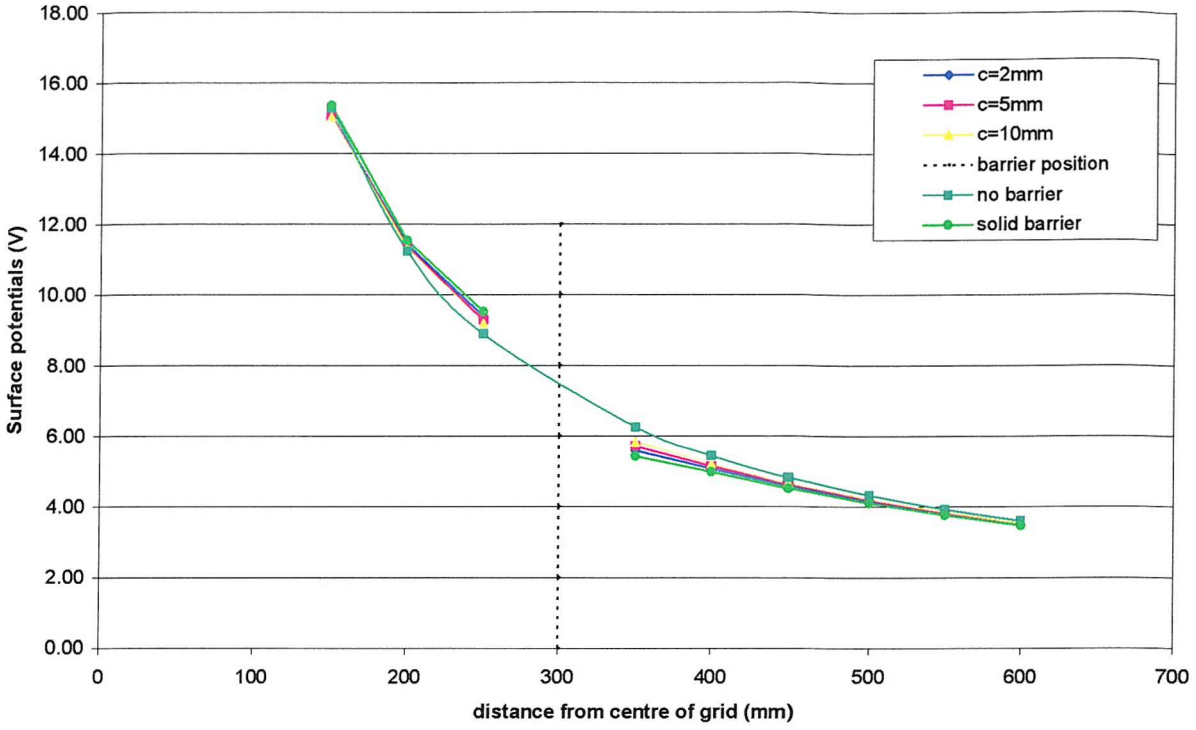

Figure 7.45: CDEGS MALT Surface potentials for plate barrier at position x=180 mm, y=60 mm with varying plate spacing

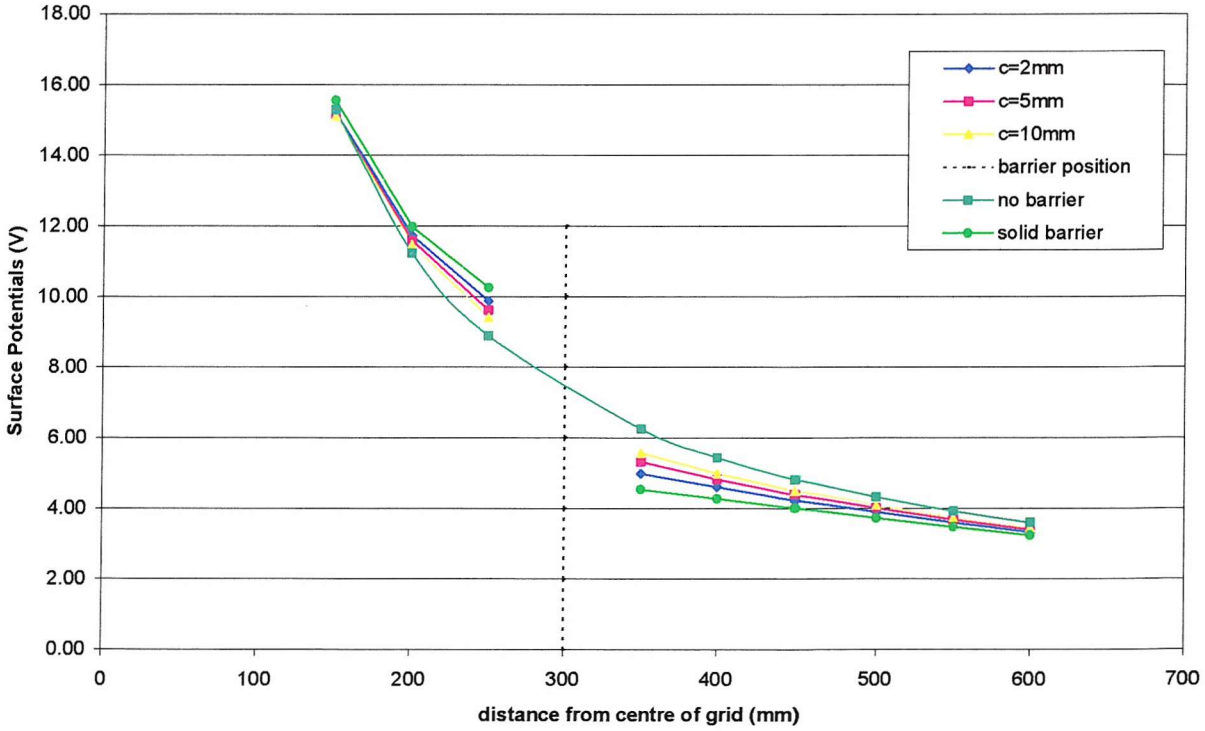

Figure 7.46: CDEGS MALT Surface potentials for plate barrier at position x=180 mm, y=120 mm with varying plate spacing

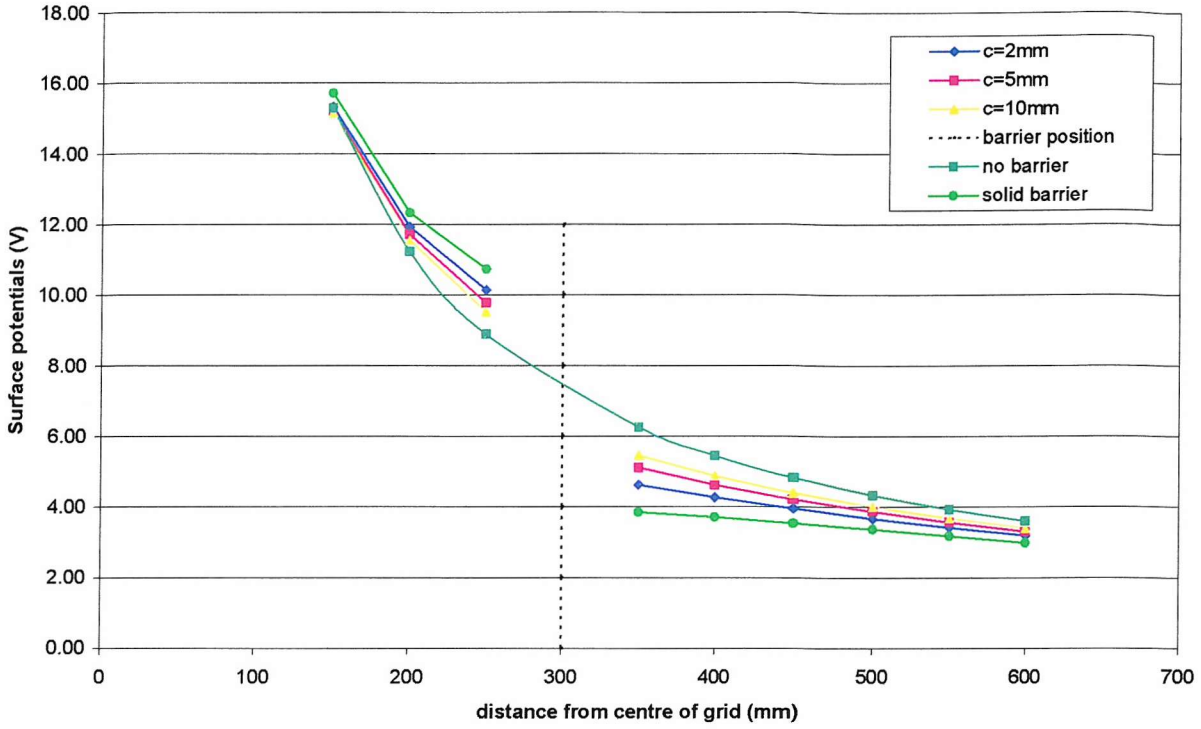

Figure 7.47: CDEGS MALT Surface potentials for plate barrier at position x=180 mm, y=180 mm with varying plate spacing

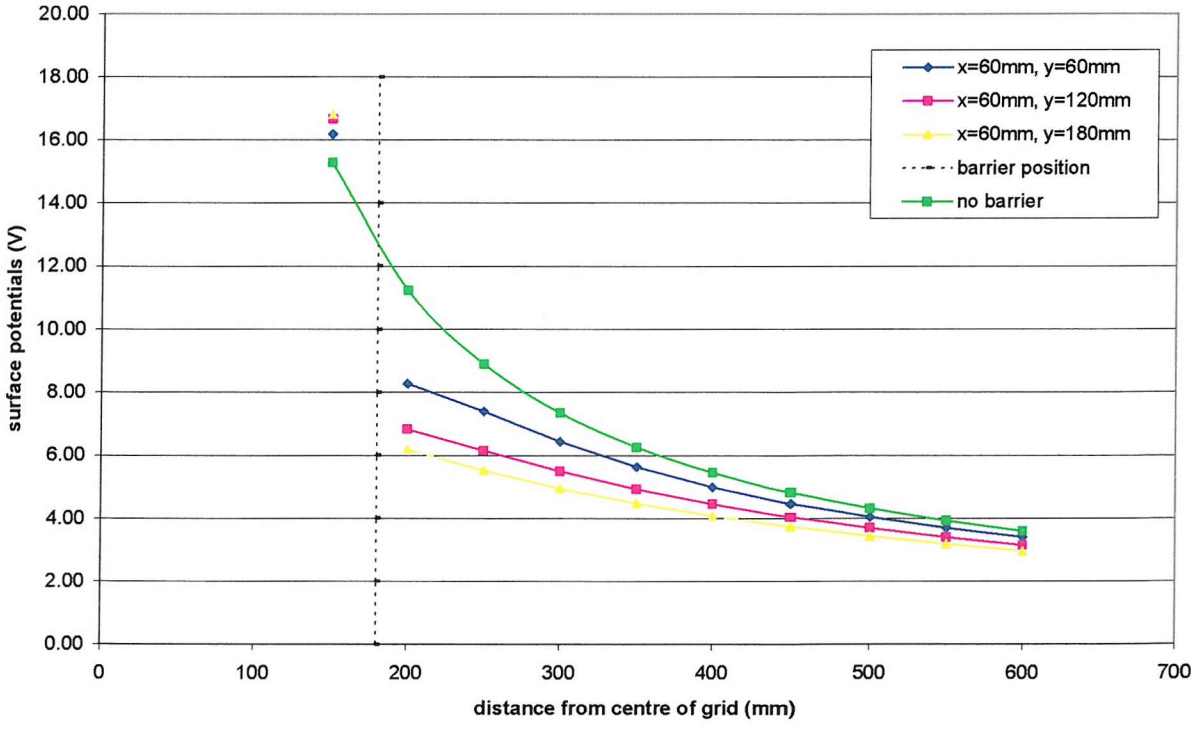

Figure 7.48: CDEGS MALT Surface potentials for plate barrier with gap spacing of 2mm for barrier position of x=60 mm and varying y (mm)

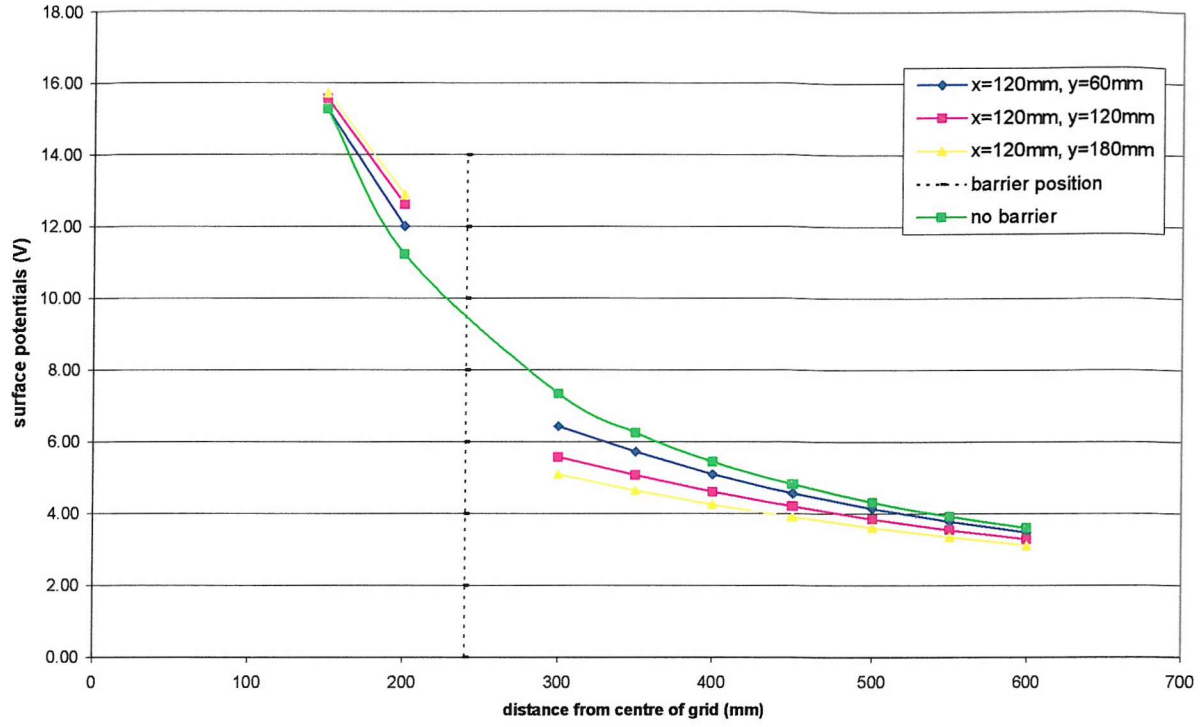

Figure 7.49: CDEGS MALT Surface potentials for plate barrier with gap spacing of 2mm for barrier position of x=120 mm and varying y (mm)

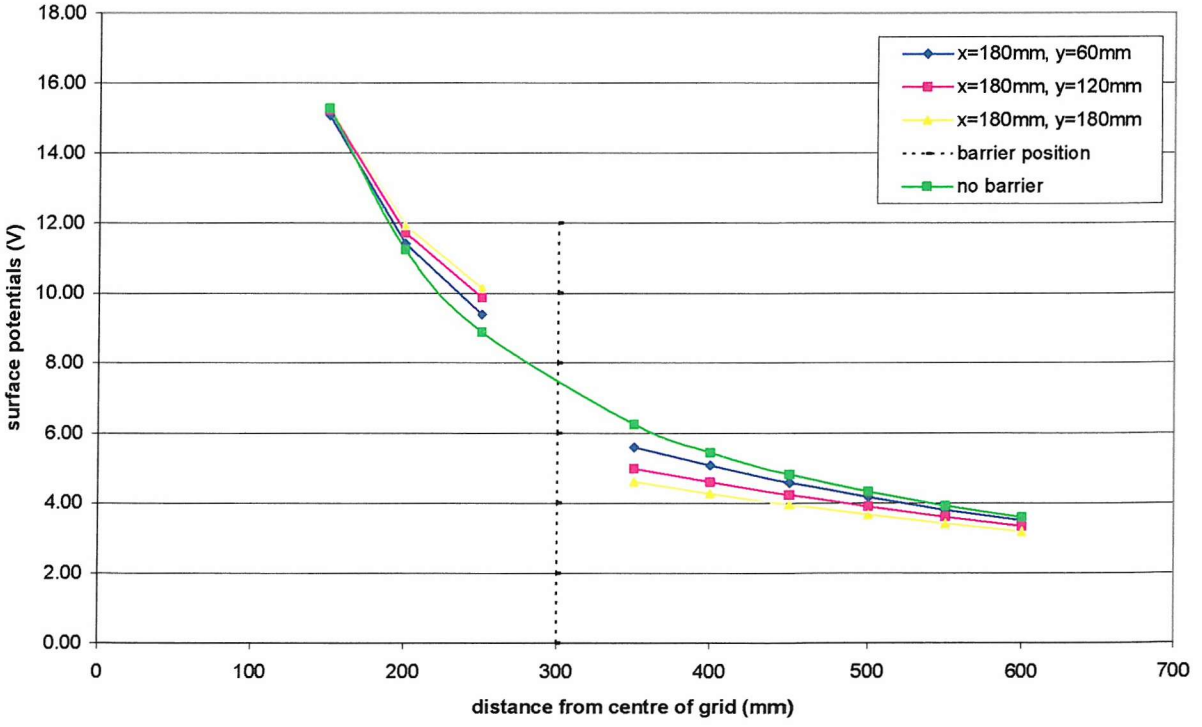

Figure 7.50: CDEGS MALT Surface potentials for plate barrier with gap spacing of 2mm for barrier position of x=180 mm and varying y (mm)

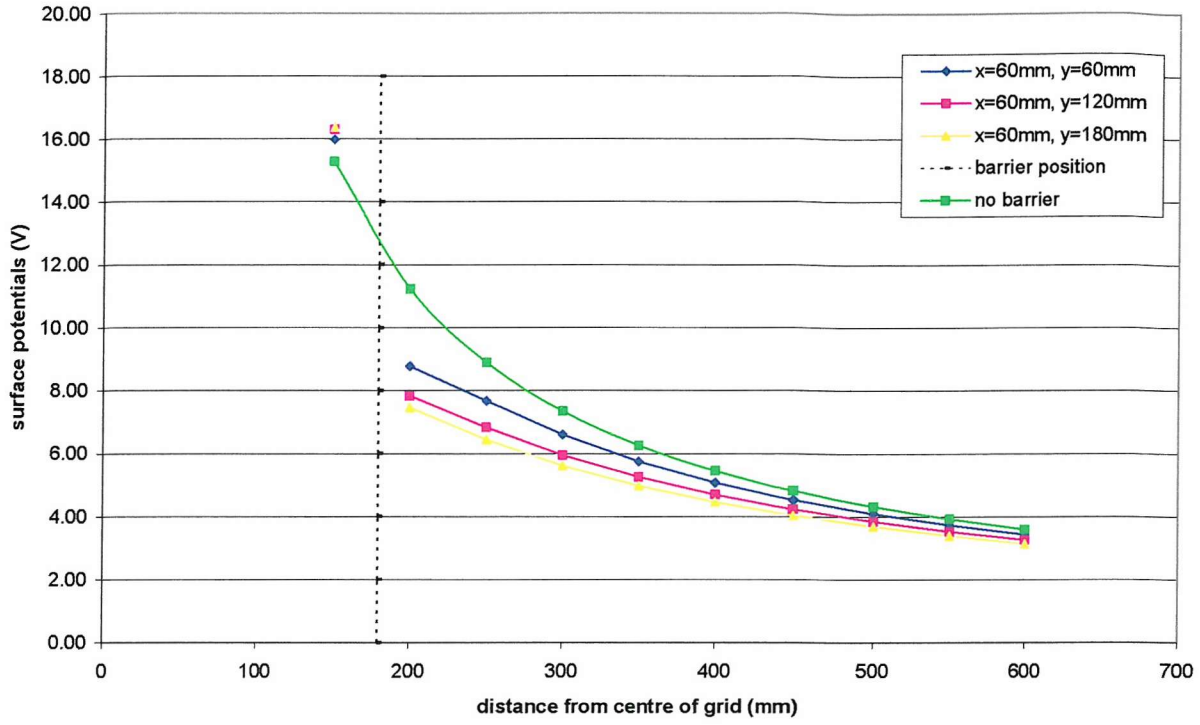

Figure 7.51: CDEGS MALT Surface potentials for plate barrier with gap spacing of 5mm for barrier position of x=60 mm and varying y (mm)

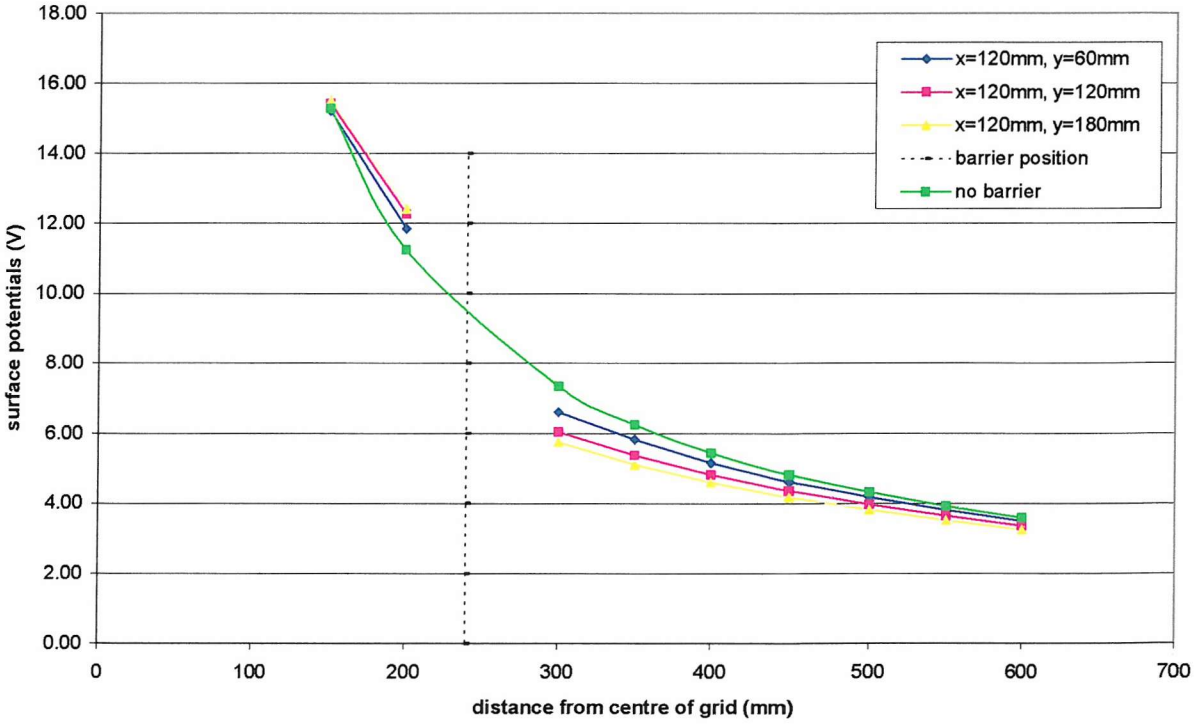

Figure 7.52: CDEGS MALT Surface potentials for plate barrier with gap spacing of 5mm for barrier position of x=120 mm and varying y (mm)

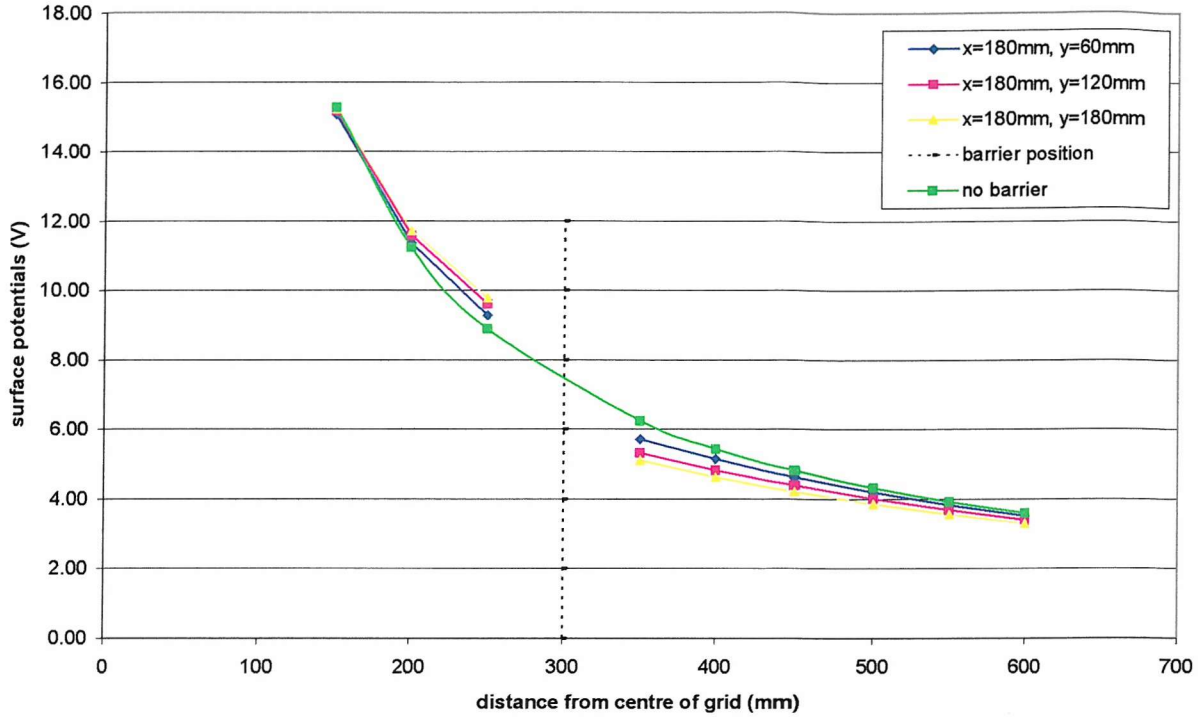

Figure 7.53: CDEGS MALT Surface potentials for plate barrier with gap spacing of 5mm for barrier position of x=180 mm and varying y (mm)

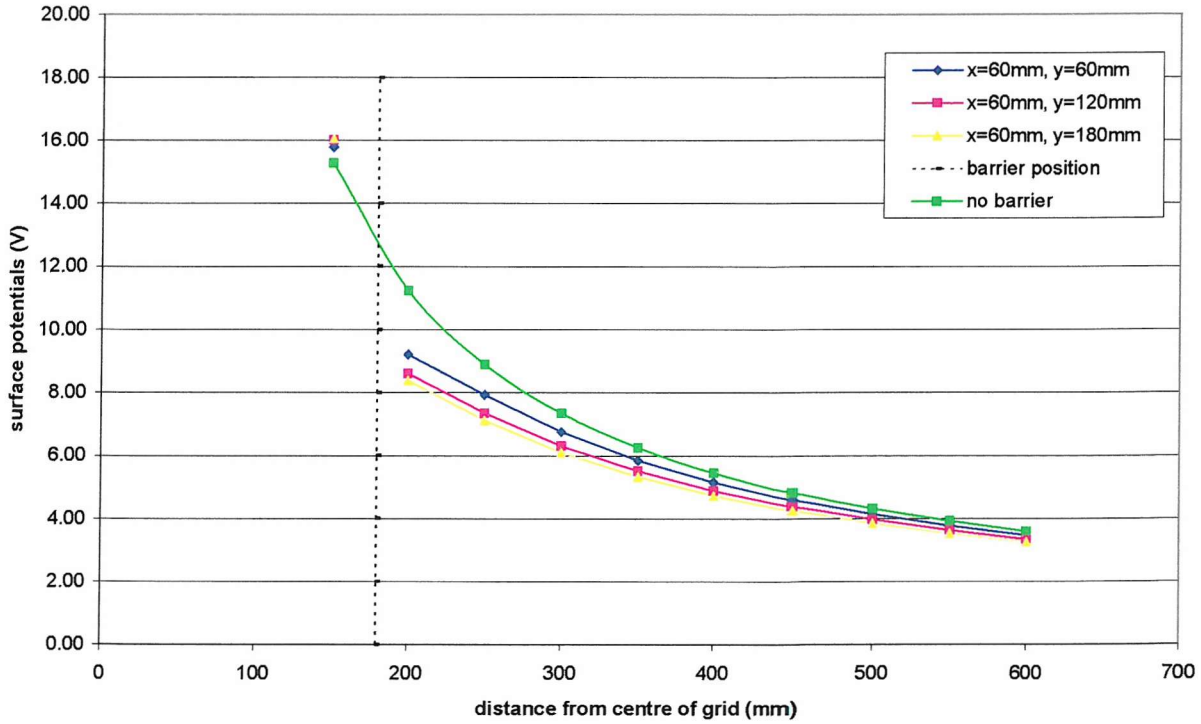

Figure 7.54: CDEGS MALT Surface potentials for plate barrier with gap spacing of 10mm for barrier position of x=60 mm and varying y (mm)

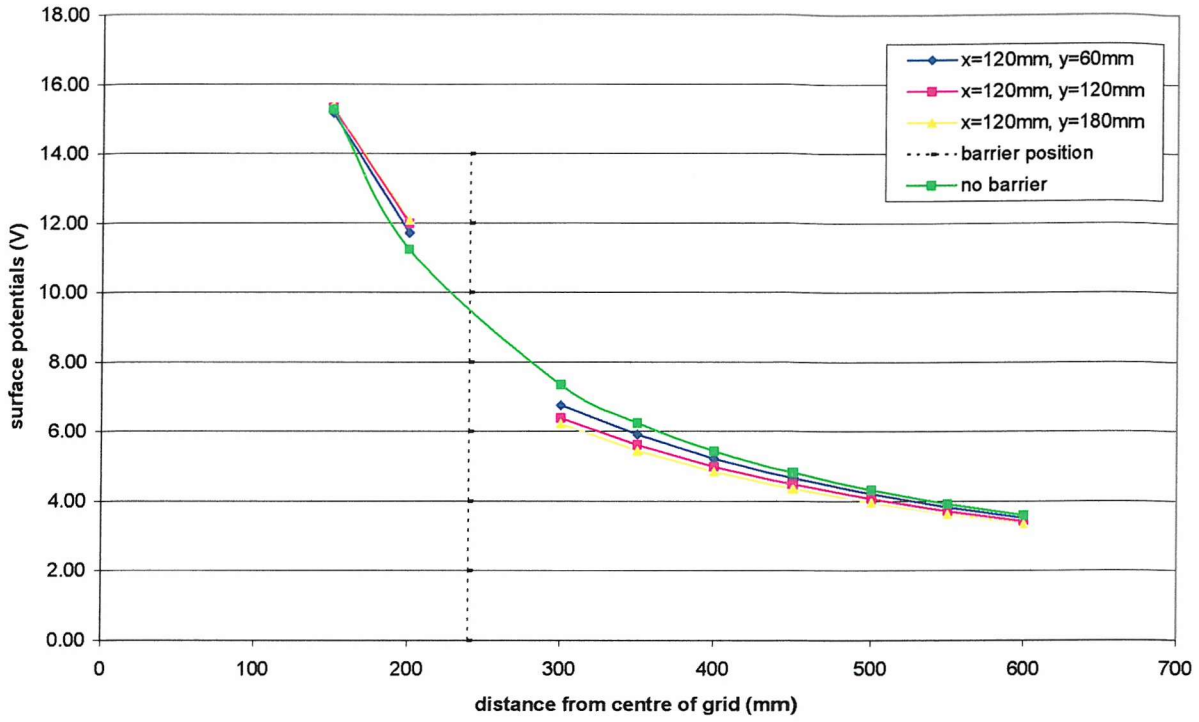

Figure 7.55: CDEGS MALT Surface potentials for plate barrier with gap spacing of 10mm for barrier position of x=120 mm and varying y (mm)

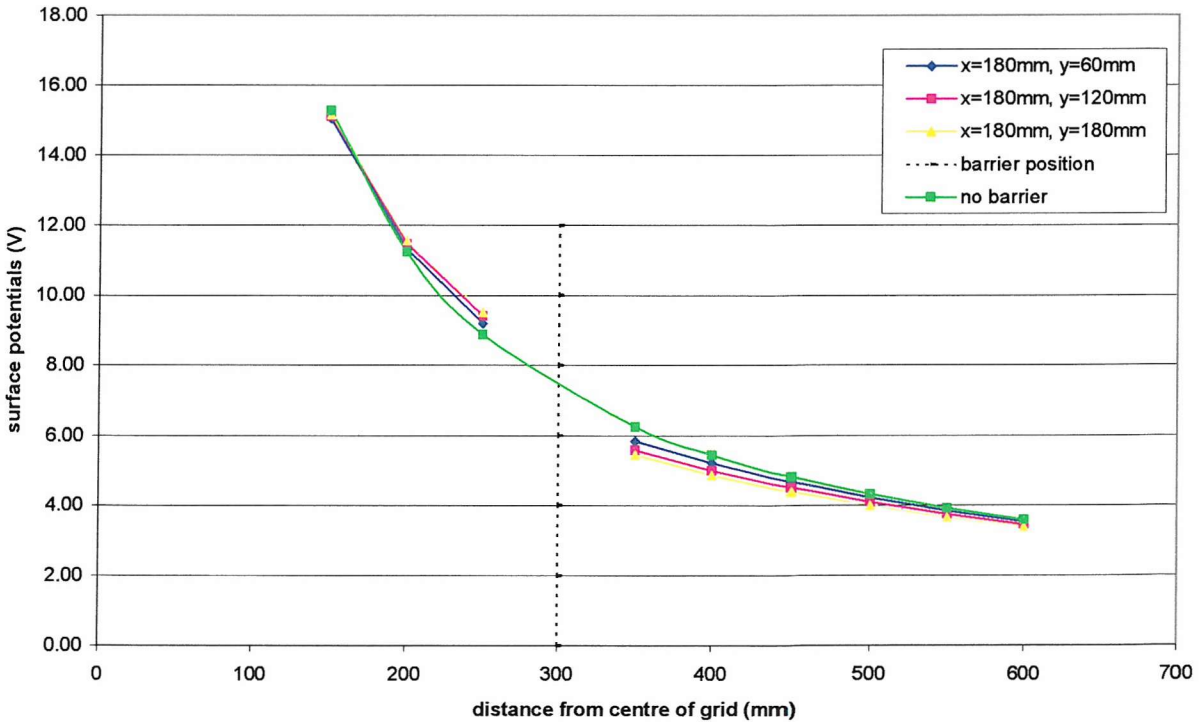

Figure 7.56: CDEGS MALT Surface potentials for plate barrier with gap spacing of 10mm for barrier position of x=180 mm and varying y (mm)

By using a series of plates in a line with relatively small gaps, the screening performance of a barrier is still maintained. As with the solid barrier, it can be seen from Figures 7.39-7.56 that the depth of the plate barrier, for all the gap sizes tested here, has to be at least two rod lengths deep in order for the screening performance of the barrier to be of any significance. For example, for the plate barrier with 2mm gaps positioned at two rod lengths away from the grid edge, the percentage decrease of surface potential when compared to no barrier is almost doubled as the depth of barrier is increased from one rod length to two rod lengths. But, as the depth is increased deeper than two rod lengths, the decrease is no longer linear. See Figure 7.49. Details of the percentage increase and decrease when compared to no barrier present are provided in Appendix 7(D).

When using a plate barrier, the gap size between the plates is very crucial. The percentage increase or decrease in surface potentials when compared to no barrier present, shows that for gaps sizes of 5mm or more, the rate of change is becoming less. Hence, in this case, with gaps sizes of more than 3.2 times the grid rod diameter, the screening performance starts to deteriorate and the percentage difference when compared to no barrier is almost constant as the gap size gets bigger. See Figures 7.39-7.47, 7.52, 7.53, 7.55 and 7.56.

The increase in surface potentials in the vicinity of the substation (in between the grid and the barrier) for a plate barrier with 2mm gap, is about 6% when compared to no barrier present, at the nearest and shallowest burial depth of one rod length. When the gap size is increased to 5mm and 10mm, the increase in surface potential is almost constant at about 3.5-4.7% for both the experimental and computed results. These figures are for potential profile taken at a distance of 30mm from the barrier on the grid side. At position 20mm beyond the barrier, the percentage decrease in surface potential is about 26% for the 2mm gap and 18%-22% for gap sizes of 5mm and 10mm respectively (from CDEGS MALT results). See Figure 7.39.

For the sensible barrier position and depth of two rod lengths (see Figure 7.43), the increase in surface potential 40mm from the barrier (on the grid side) is about 12% for the plate barrier with 2mm spacing. On the other side of the barrier, at a distance 60mm

from the barrier, the decrease in percentage is approximately 24% for the same plate barrier (from computed results).

Overall, even when using the shallowest barrier positioned at the furthest distance (x=180mm, y=60mm), the potential profile relatively far from the grid, i.e. 600mm from the grid, which is about 10 times the rod length, still indicates a reduction in the surface potential outside the vicinity of the substation. See Figure 7.45.

7.2.2.2 Parallel Measurements

Parallel measurements are measurements made at a few positions (with respect to the x-axis) parallel to the barrier. Three selected barrier positions and surface potentials at a few parallel positions to the barrier were investigated. This scenario is illustrated in Figure 7.57 below:

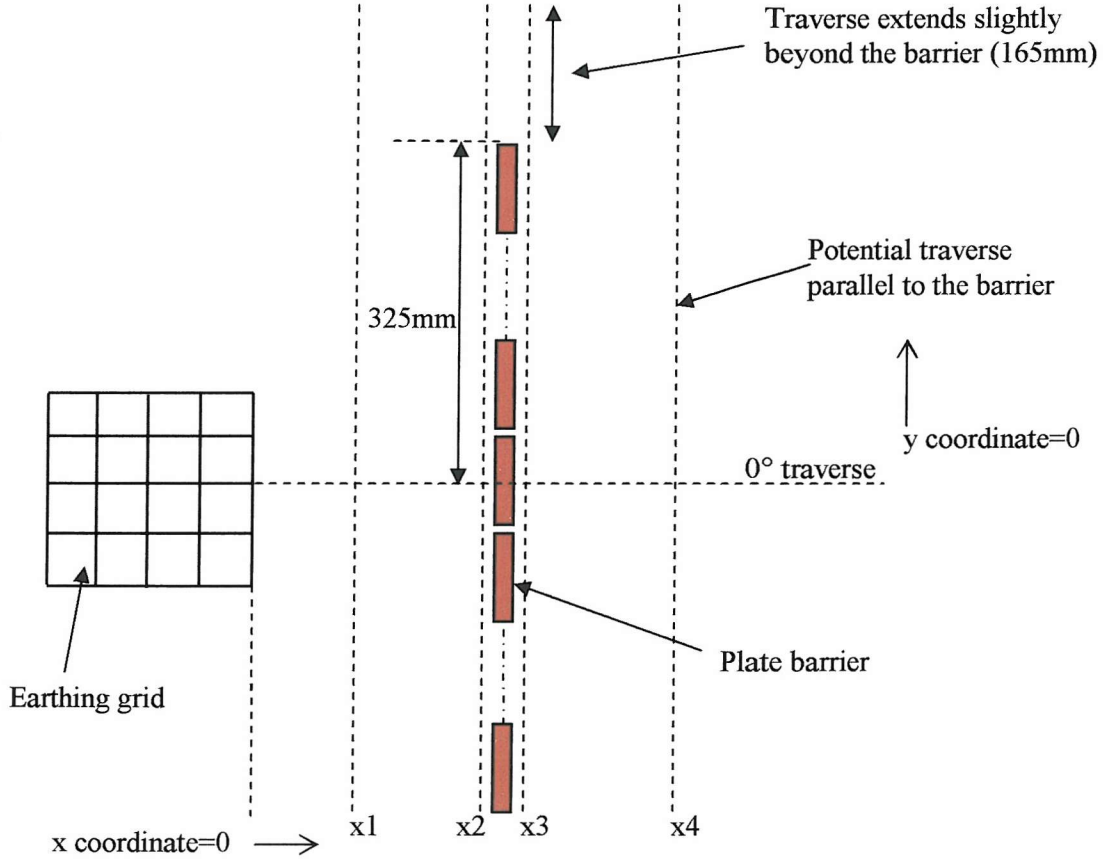

Figure 7.57: Top view of the barrier system with the surface potential measurement parallel traverse (not to scale)

The three barrier positions are:

a) x=60mm, y=60mm

b) x=60mm, y=180mm

c) x=120mm, y=120mm

For barrier position (a) and (b), the potential traverse positions are as follows:

a) x1 = 150mm

b) x2 = 170mm

c) x3 = 200mm

d) x4 = 250mm

For barrier position (c), the potential traverse positions are as follows:

a) x1 = 150mm

b) x2 = 230mm

c) x3 = 260mm

d) x4 = 310mm

The location of interest here is where the gaps are situated, and hence position x2 and x3. x2 and x3 are located just 10mm away from the barrier on either side. x1 and x4 are taken to see the effect as the traverse move further away from the barrier. This parallel measurement section is investigated using the CDEGS MALT computation only.

The next few graphs show the result of the computation for all the above positions. A point to note here is that due to symmetry, the traverses were computed at 1 mm interval for the upper section of the barrier only. 1mm interval is chosen because one of the gaps tested is 2mm wide. Detailed tabulated result is not given because there are up to 500 points for each computation and also it is the shape of the graphs that is of interest.

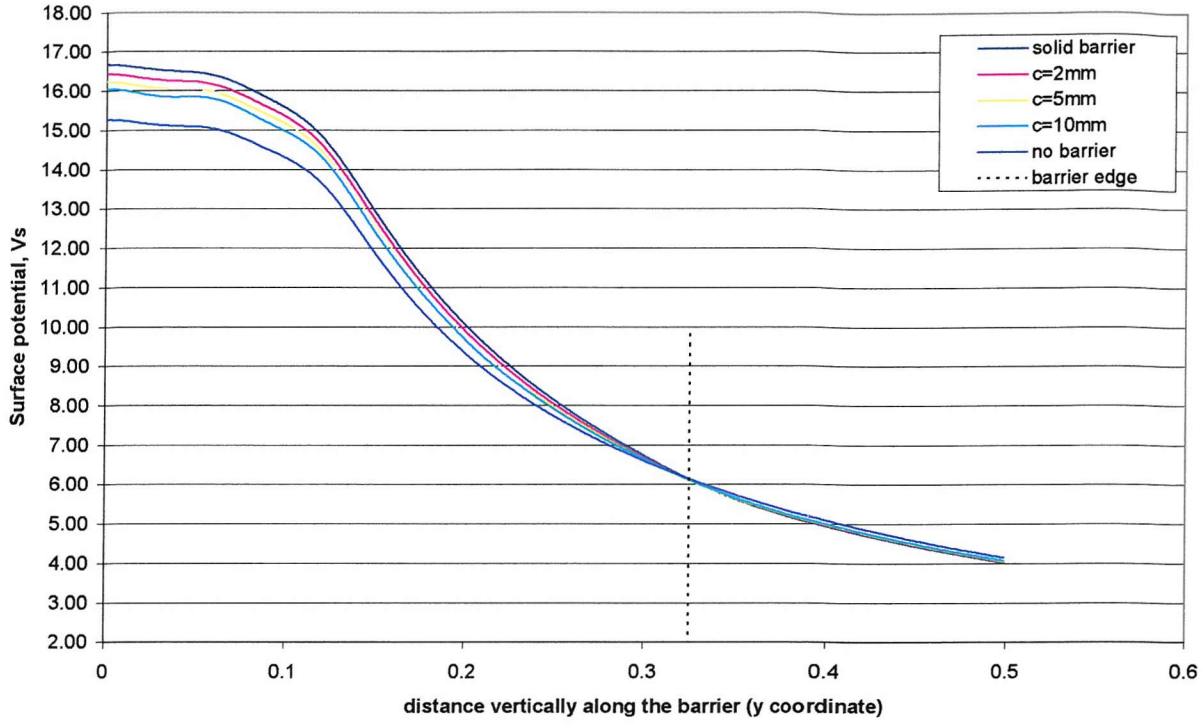

Figure 7.58: Surface potential (Vs) for barrier position x=60mm, y=60mm and the profile traverse at x1=150mm from the grid edge

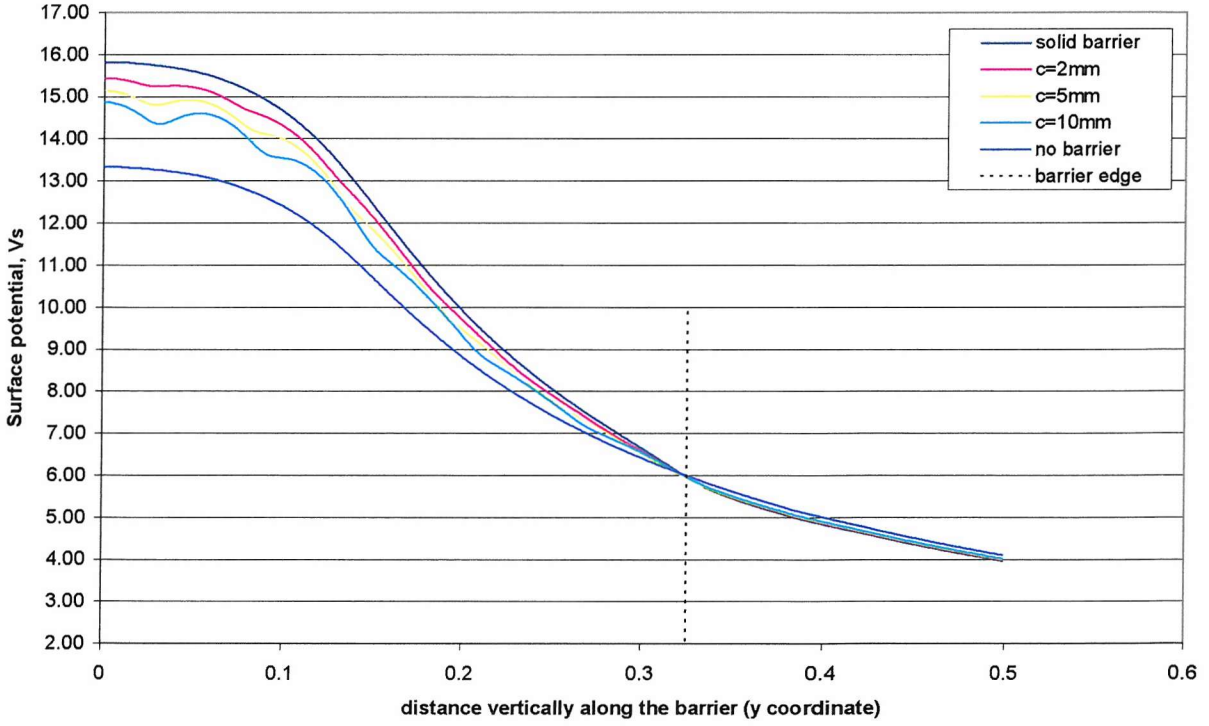

Figure 7.59: Surface potential (Vs) for barrier position x=60mm, y=60mm and the profile traverse at x2=170mm from the grid edge

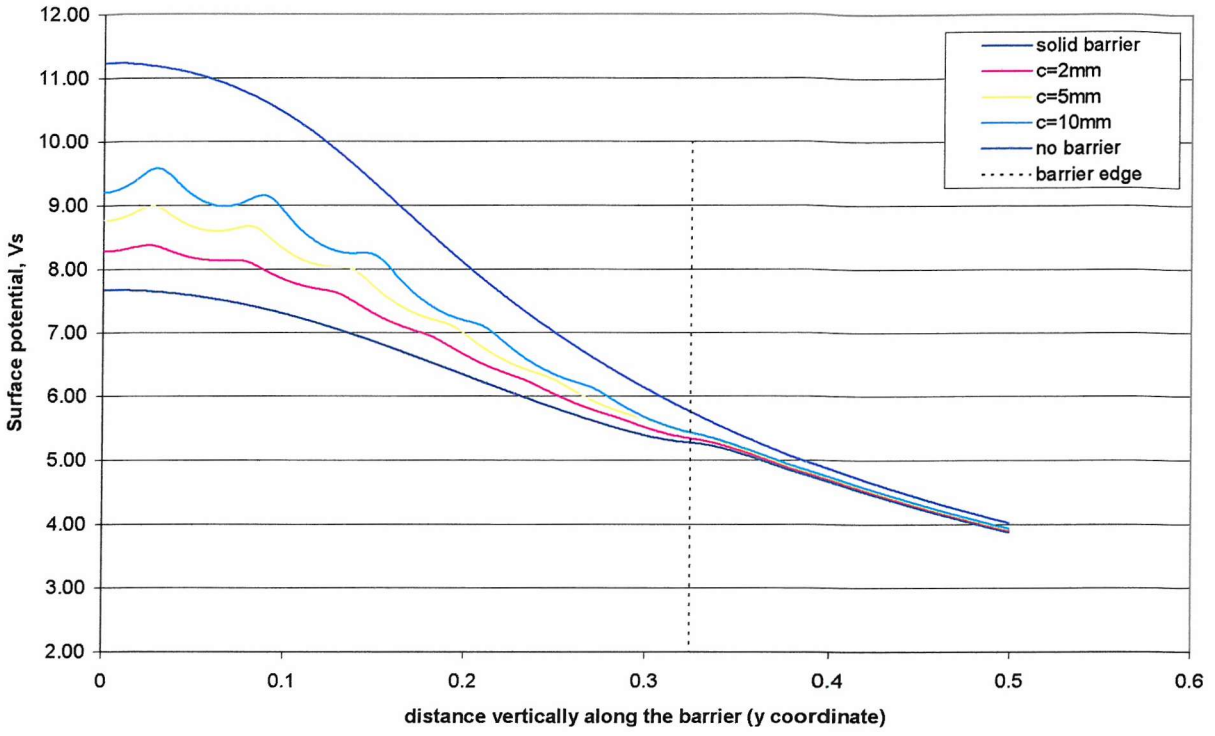

Figure 7.60: Surface potential (Vs) for barrier position x=60mm, y=60mm and the profile traverse at x3=200mm from the grid edge

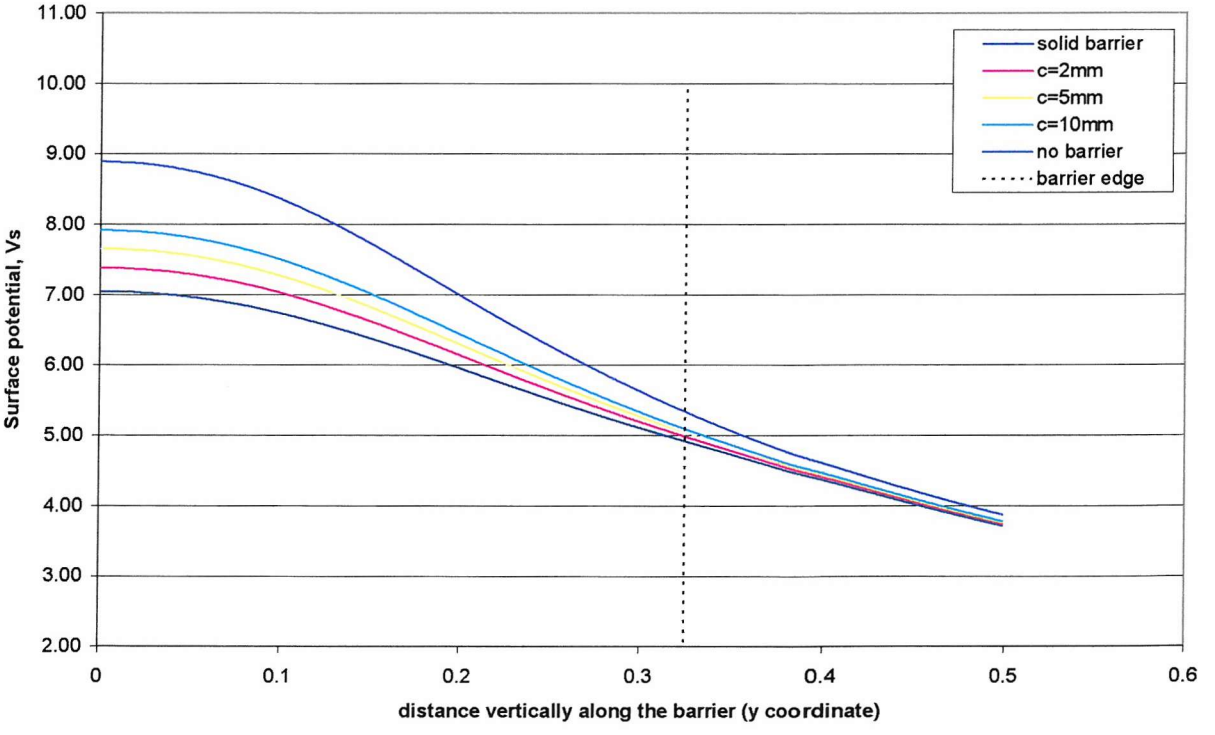

Figure 7.61: Surface potential (Vs) for barrier position x=60mm, y=60mm and the profile traverse at x4=250mm from the grid edge

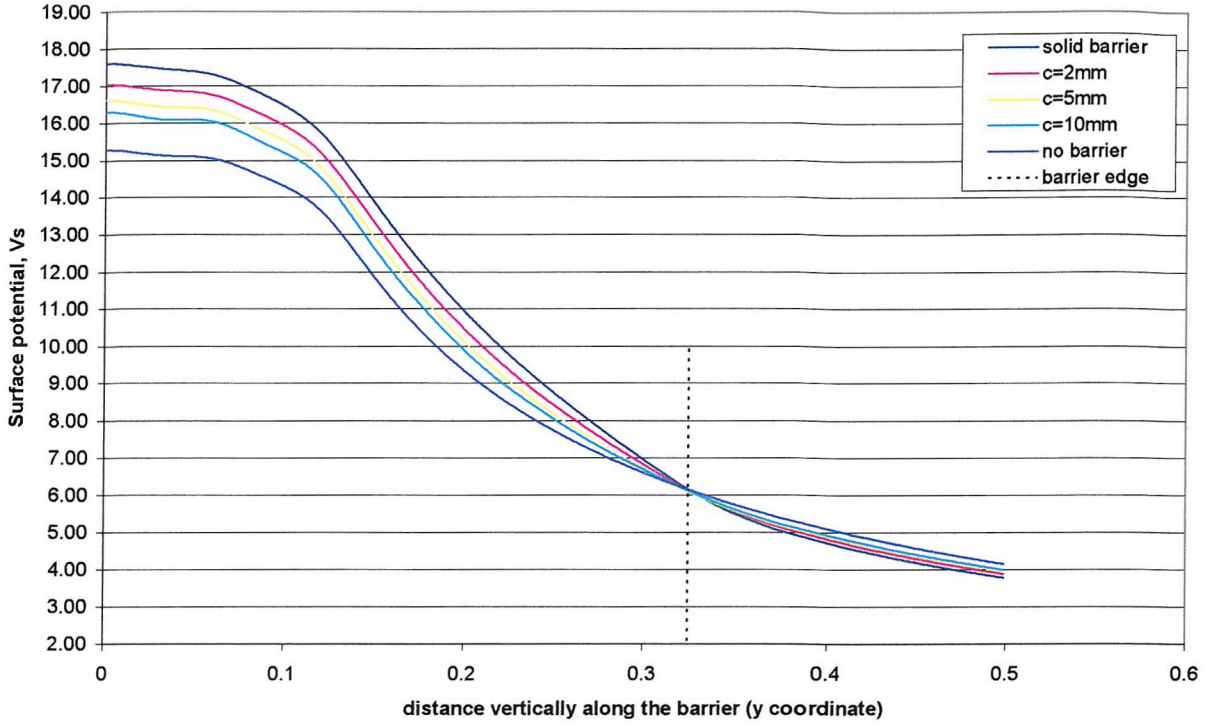

Figure 7.62: Surface potential (Vs) for barrier position x=60mm, y=180mm and the profile traverse at x1=150mm from the grid edge

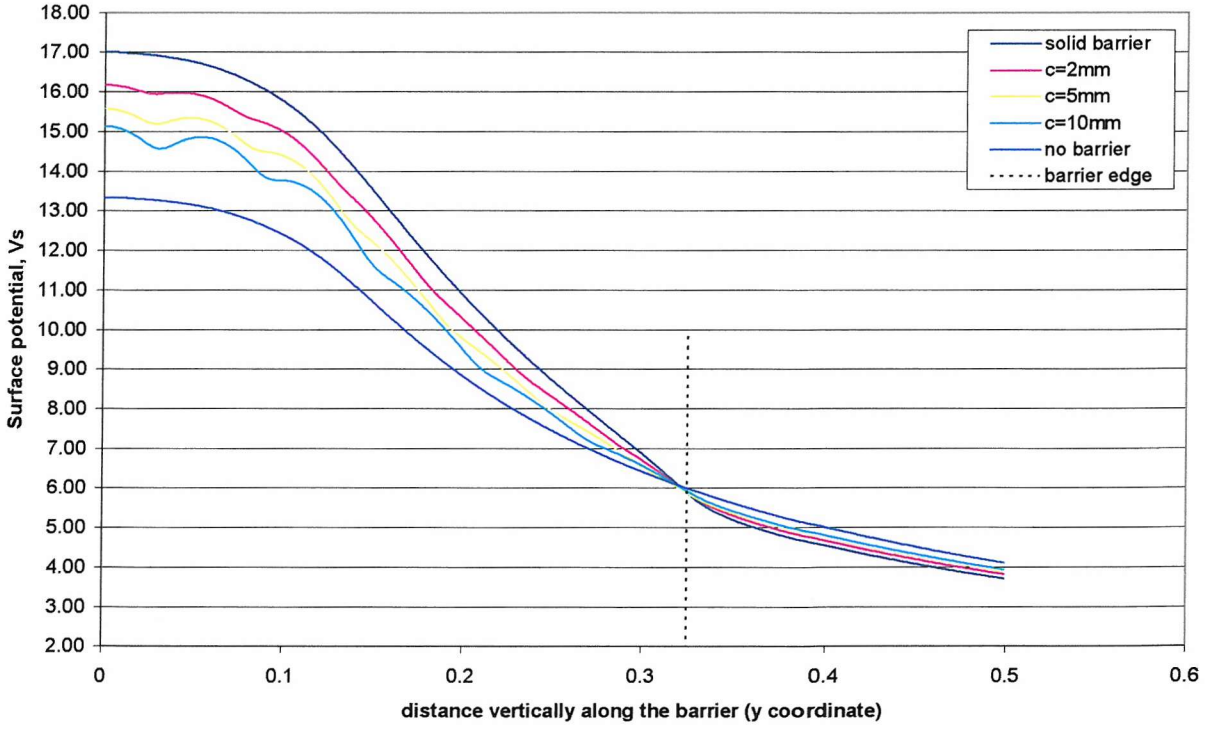

Figure 7.63: Surface potential (Vs) for barrier position x=60mm, y=180mm and the profile traverse at x2=170mm from the grid edge

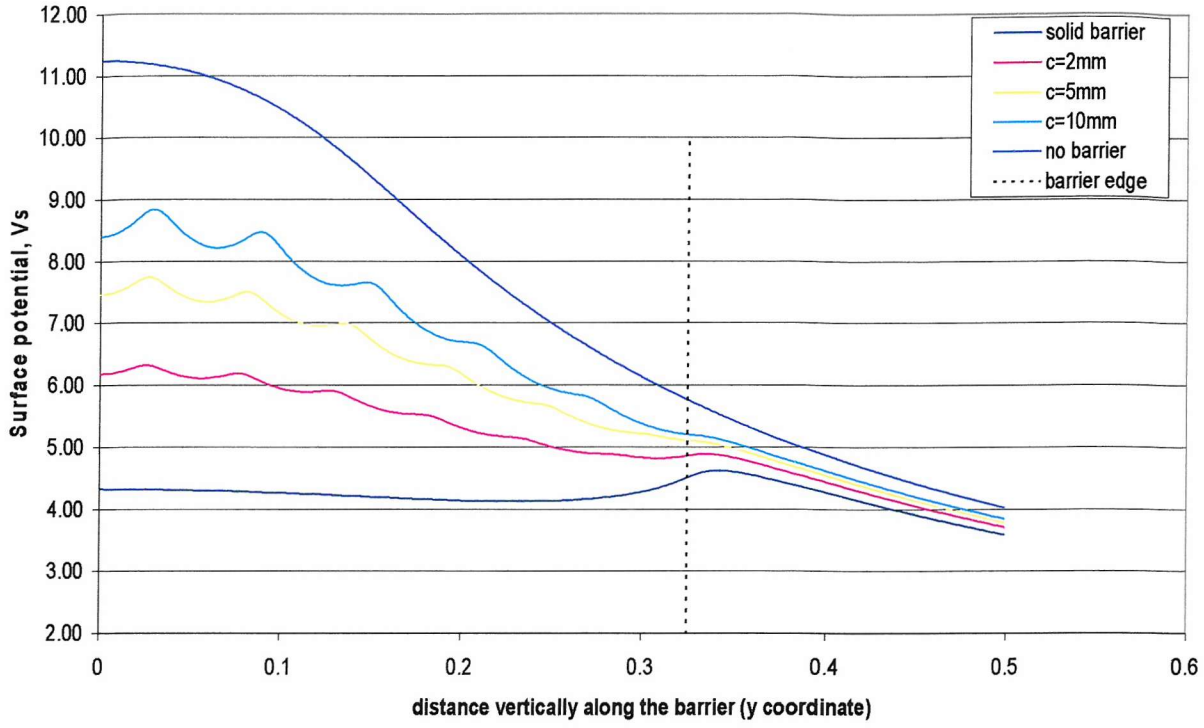

Figure 7.64: Surface potential (Vs) for barrier position x=60mm, y=180mm and the profile traverse at x3=200mm from the grid edge

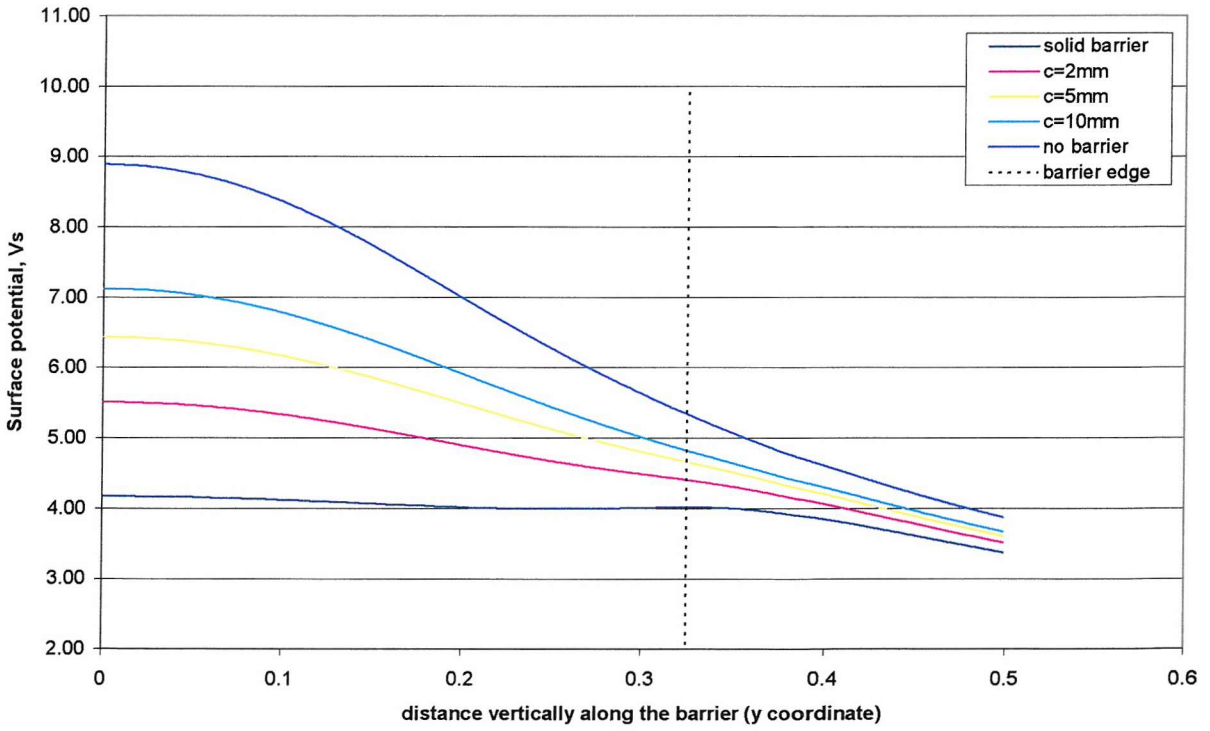

Figure 7.65: Surface potential (Vs) for barrier position x=60mm, y=180mm and the profile traverse at x4=250mm from the grid edge

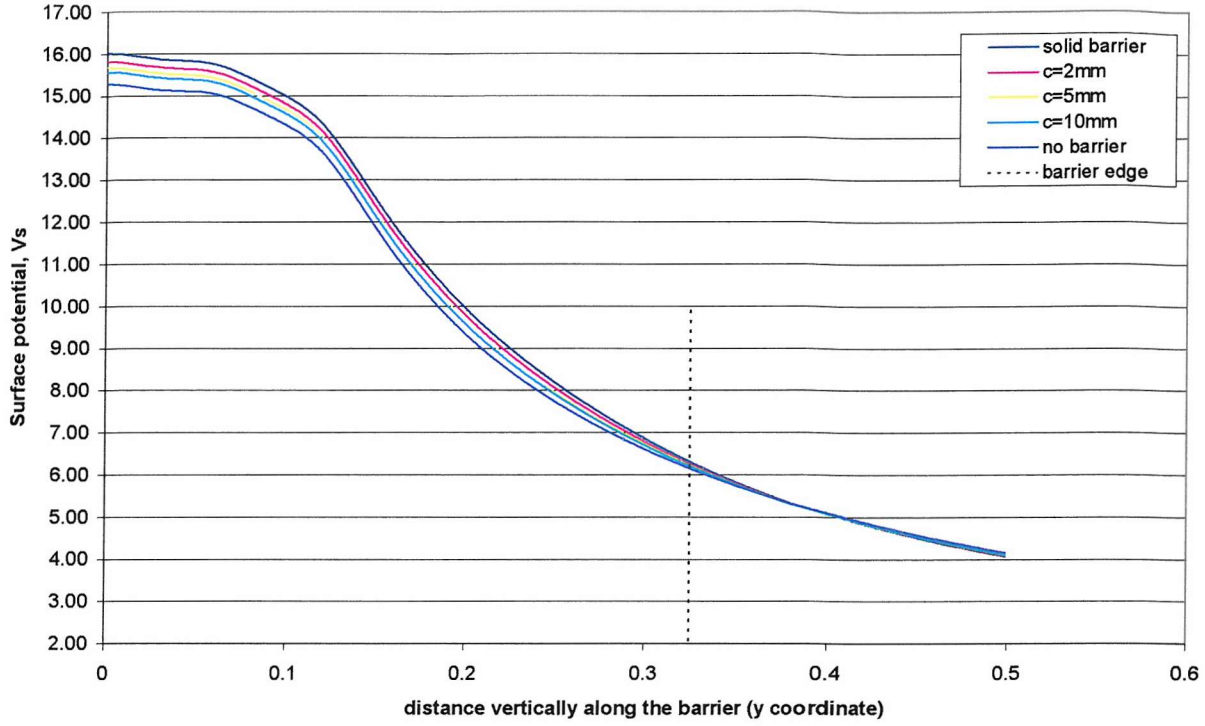

Figure 7.66: Surface potential (Vs) for barrier position x=120mm, y=120mm and the profile traverse at x1=150mm from the grid edge

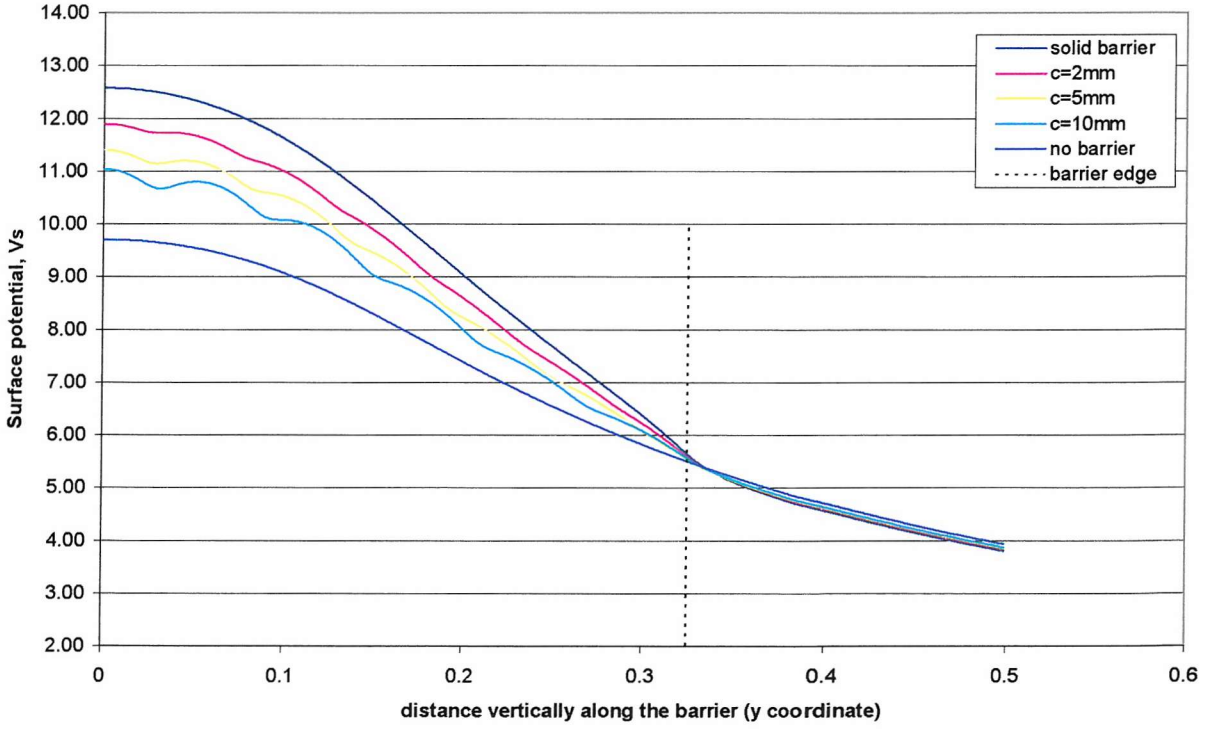

Figure 7.67: Surface potential (Vs) for barrier position x=120mm, y=120mm and the profile traverse at x2=230mm from the grid edge

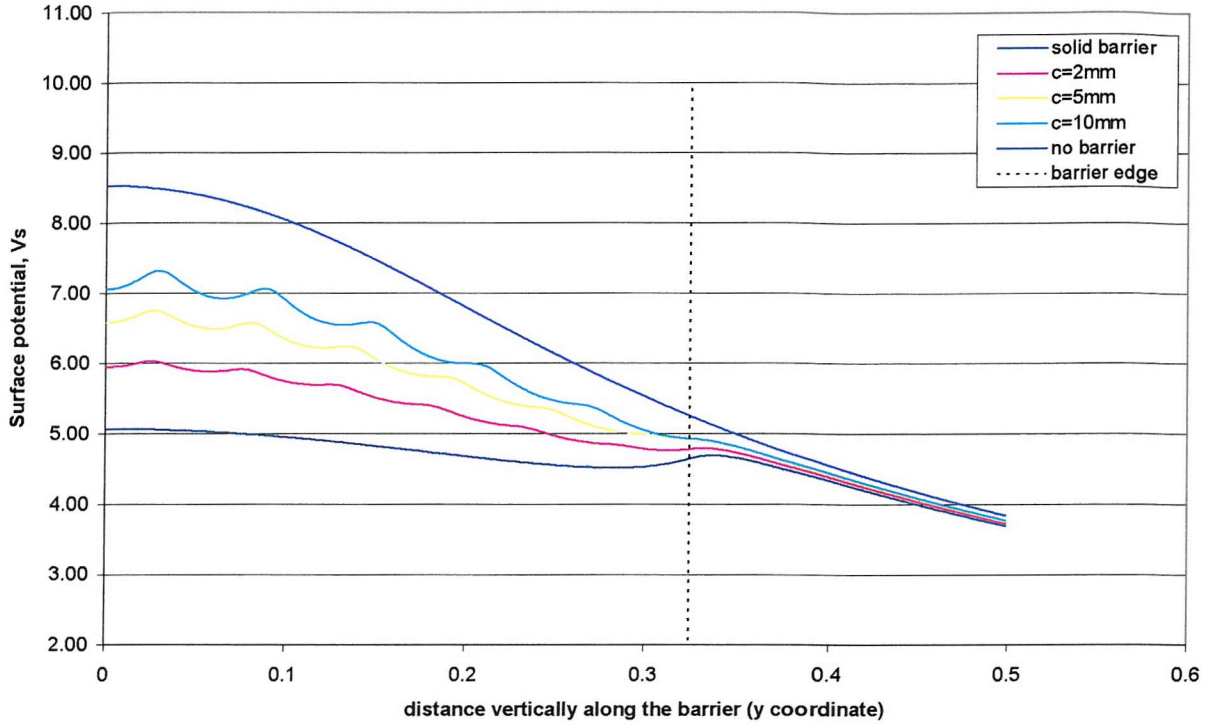

Figure 7.68: Surface potential (Vs) for barrier position x=120mm, y=120mm and the profile traverse at x3=260mm from the grid edge

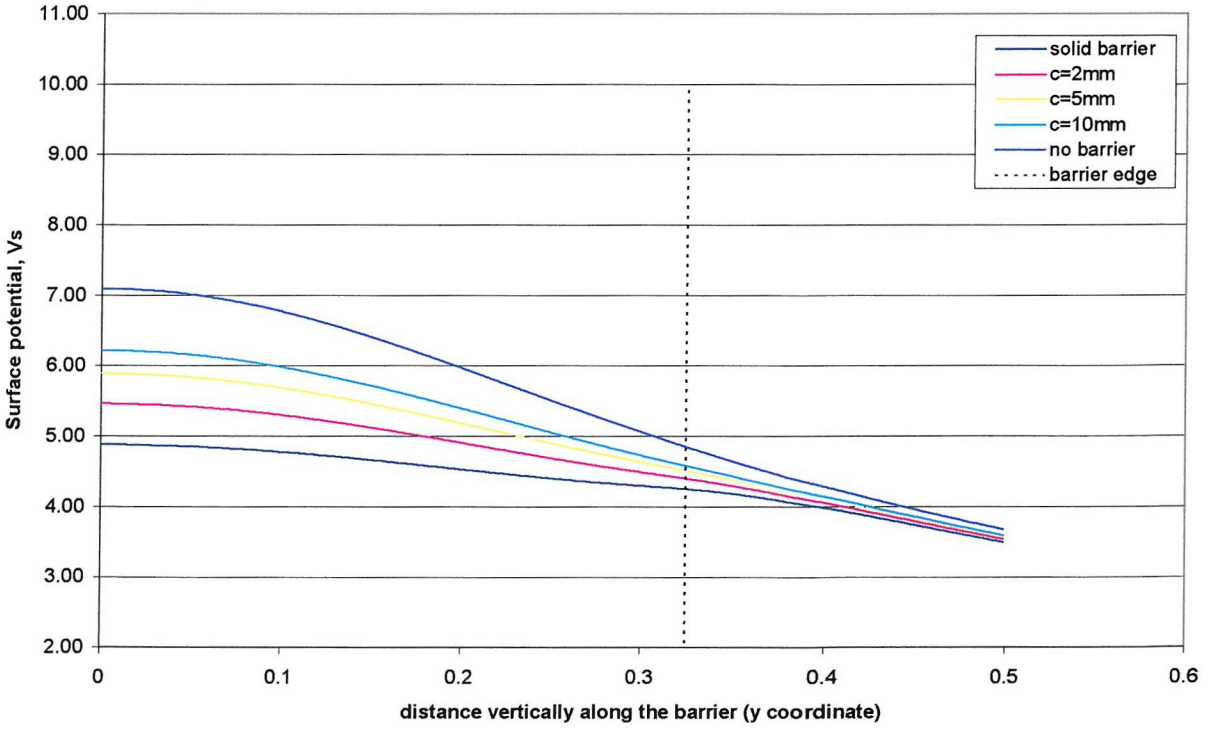

Figure 7.69: Surface potential (Vs) for barrier position x=120mm, y=120mm and the profile traverse at x4=310mm from the grid edge

From all the graphs shown, it can be seen that the gaps in the barrier does not have a significant effect to the surface potential profile, except for the 10 mm gap. However, this only happens at positions very near to the barrier, i.e. in this case about 10 mm either side from the barrier (see Figures 7.59, 7.60, 7.63, 7.64, 7.67, and 7.68). Even so, the slight increase (for position x3) or decrease (for position x2), is about 4.3% and 3.5% respectively. This is for the worst-case scenario, which is a barrier located very close to the grid and at deepest depth (x= 60 mm, y= 180 mm). Also, this maximum glitch only occurs at positions directly along the earthing grid (at 0° traverse), and reduction is seen as the profile moved upwards/downwards towards the 45° traverse.

Furthermore, it can be seen that a barrier with a gap of 2 mm, hardly have any effect on the potential profile distribution (see Figure 7.64). This means that if the gap is small enough, i.e. about 5% from the rod length used, it can safely act as a solid barrier.

Another interesting point to note is that, as the potential profile approaches the barrier edge, the potential will rise slightly before decaying towards 0V. This applies for all the barriers (solid or plate). See Figures 7.60, 7.64 and 7.68. This might be due to the skewed current finding its way to cross the barrier. Hence, that is why the deeper the barrier, the larger the potential rise at the barrier edge (see Figure 7.64).

7.3 Conclusions

A highly resistive barrier is inserted vertically into the ground at a distance from the earthing grid, primarily to lower the surface potentials outside the substation area (beyond the barrier position). However, by doing this, there will be a slight rise in earthing system resistance and the surface potentials within the substation vicinity. Two different types of barriers were investigated, namely are the solid barrier and the plate barrier with various gaps. Both types can be effective. Experimental and computed results agree very well with less than 1% difference in most cases.

When the barrier is inserted very close to the earthing system and at deepest depth (x=60mm, y=180mm), the rise in earthing resistance is quite substantial. On average, for a solid barrier at this position, the rise is approximately 11% and for a plate barrier with the smallest gap (c=2mm) the rise in resistance is about 6.5%. However, as the barrier is moved further away from the grid, say at two rod lengths, the increase in resistance reduces by more than 50%, for both solid and plate barriers. At a sensible barrier position and depth of two rod lengths, the increase in resistance between the two types of barrier is almost constant, with on average 3.1% and 2.1% for solid and plate barrier respectively.

The surface potentials conclusions here are based on 0^{o} traverse for both the solid and plate barrier. On average, for both the solid and plate barrier and for all barrier positions and depths tested here, the decrease in surface potential beyond the barrier is about 50% more compared to the increase in surface potential between the grid and the barrier. Also, at positions very far away from the grid, i.e. 600 mm from the grid, which is about 10 times the rod length, the barrier still has an effect in reducing the surface potential, even though a very shallow barrier is used (one rod length deep). In the vicinity of the substation, the increase in surface potential is greatest at positions very near to the barrier, relatively about one rod length towards the barrier. Midway between the barrier and the grid, the increase is relatively insignificant.

In essence, it all depends on the percentage decrease in surface potentials beyond the barrier that one wants to achieve by using the barrier. A plate barrier of 5mm gap situated at position x=60mm, y=120mm can give a similar result to a solid barrier

situated at x=60mm, y=60mm. In other words, the decrease in surface potential is almost the same for these two types of barrier but at different burial depth. Also, by using a plate barrier of 5mm gap and inserting it nearer by one rod length, it can act as well as a solid barrier situated at two rod lengths away from the grid.

Furthermore, it was shown that the gaps in the barrier do not have any significant effect on the potential profile. However, it is recommended to have small gaps, which is approximately 5% from the rod length used, i.e. in this case about 2 - 5mm plate spacing.

In conclusion, there are advantages and disadvantages when using a highly resistive barrier to reduce surface potentials outside the vicinity of the substation. However, it is shown that the advantages are greater. The increase in resistance and surface potential within the vicinity of the substation is insignificant compared to the reduction in surface potentials that can be achieved outside the vicinity of the substation. One can use barriers made of plates with gaps to achieve almost the same function as a solid barrier. The use of small vertical plates to make up a barrier can save cost and the individual plates can possibly be driven into the ground. In contrast, a solid barrier will require a narrow and deep trench to be dug.

CHAPTER 8

Proximity Effect: Inner Profiles of Surface Potentials

When the elements of an earth electrode system are too close together, the distribution of the fault current will be affected. This influence, or 'proximity' effect, will increase the total earthing impedance, compared with the value obtained when those elements are sufficiently distant [121]. Another very important aspect is when an earthing conductor is very close to the earth surface so that the current dissipating from the top surface of the conductor is much less than that from the bottom surface. This is to say that the leakage current density has a circumferential variation. This will influence the surface potential readings very close to the earthing grid.

In most software packages, this circumferential variation of the leakage current will not be considered. In order to evaluate this further, tests are done using the electrolytic tank to depict the real situation. These results are then compared with the MALT software to study the proximity effect. Various kinds of earthing configuration were investigated. These configurations consist of horizontal and vertical rods. Some of these configurations were experimented with in Chapter 5, but in this chapter, a closer look is taken at the inner potential profiles and profiles close to the earthing conductor. The grids tested are:

i) 8 rods combined grid (horizontal electrodes and vertical rods)
ii) 120mm x 120mm and 240mm x 240mm mesh (horizontal electrodes only)
iii) fat and thin ring

8.1 8 rods combined grid (horizontal electrodes and vertical rods)

This grid was tested at various depths, from 10 mm to 60 mm at intervals of 10 mm below water level. The grid is made of a horizontal mesh with vertical rods connected around the periphery (as illustrated on page 98). All the vertical rods and horizontal electrodes are of the same size (diameter =1.56 mm) and the horizontal mesh is 120 mm

x 120 mm. Figures 8.1 and 8.2 show the surface potential distributions for the shallowest and deepest depths. The results for all the depths can be found in Appendix 8.

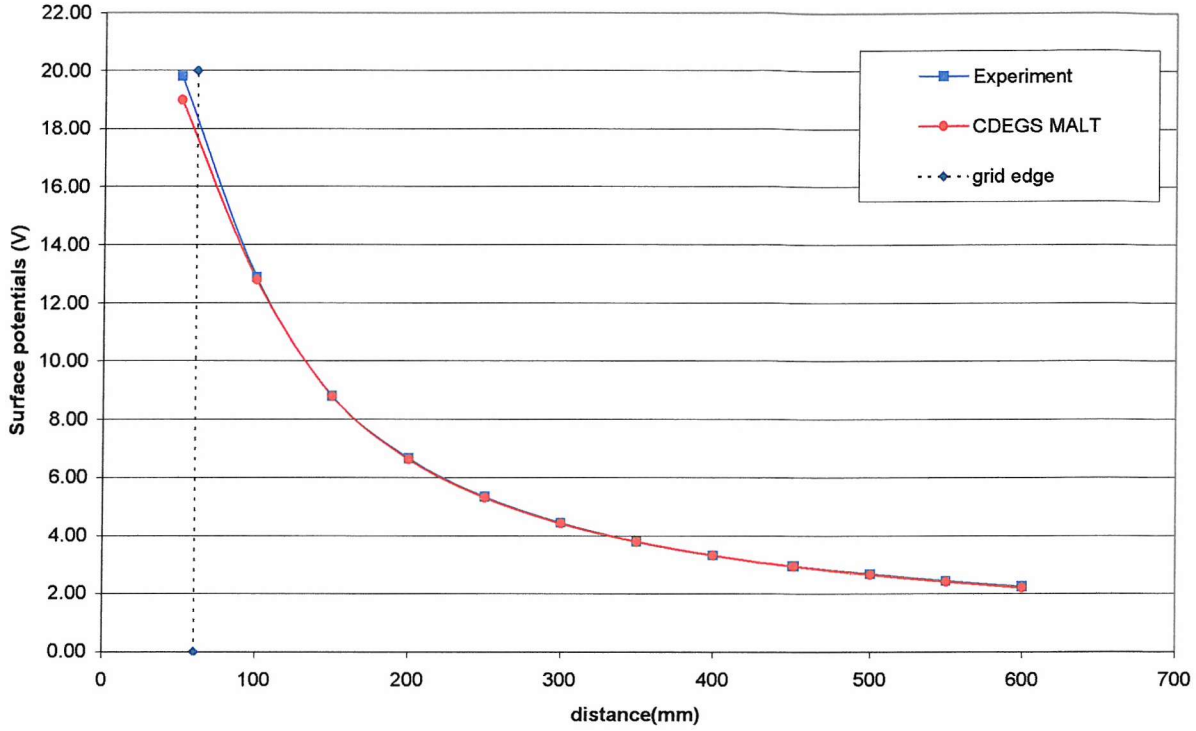

Figure 8.1: Surface potentials against distance for 8 rods combined grid (c=60mm) for buried depth=10mm

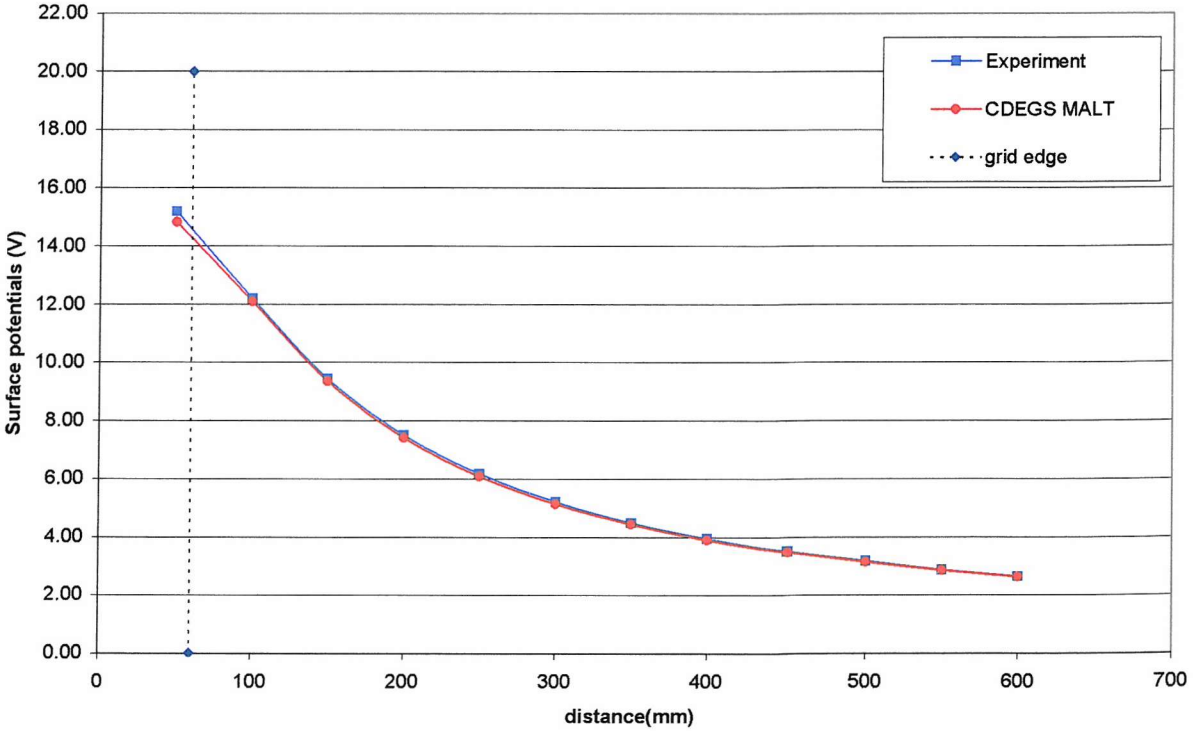

Figure 8.2: Surface potentials against distance for 8 rods combined grid (c=60mm) for buried depth=60mm

From the results obtained, generally both the CDEGS MALT and the experimental results agree very well. As the distance of the surface potential reading (with respect to the middle point of the grid) increases, the difference between the experimental and the computed results decreases. The surface potential reading closest to the earthing grid at distance of 50mm from middle of grid (i.e. the distance to the edge of the grid is 10mm) gives the highest percentage of difference between the two methods.

Furthermore, as the burial depth of the grid increases, the percentage difference between the two methods decreases, particularly very close to the earthing grid. As the burial depth increases from 10mm to 60mm, the percentage difference between experimental and computed results decreases from 4.11% to 1.81%, at the potential profile position very close to the earthing grid. It can be seen also that as the burial depth goes beyond 20mm, the percentage of difference between the experimental and computed result remain almost constant, i.e. between 2.59% and 1.81%.

8.2 120mm x 120mm and 240mm x 240mm mesh (horizontal electrodes only)

The 120 mm x 120mm and 240 mm x 240mm meshes consist of 60 mm x 60 mm mesh (as illustrated on page 98 for 'buried grid'). The rod radius used in this grid is 0.78 mm (the same as the grid in section 8.1).

The 120mm x 120mm mesh grid was tested at various depths, from 10 mm to 60 mm at intervals of 10 mm below water level. The surface potential profiles was taken at 0° traverse from the middle of the mesh. As for the 240mm x 240mm mesh grid, testing was done at depth of 10 mm, 20 mm, 40 mm, and 60 mm below water level. The surface potential profiles were taken at 0° and 45° traverses from the middle of the mesh.

Figures 8.3 - 8.8 show the surface potential distributions for the shallowest and deepest depths for both mesh sizes. The results for all the depths and profiles can be found in Appendix 8.

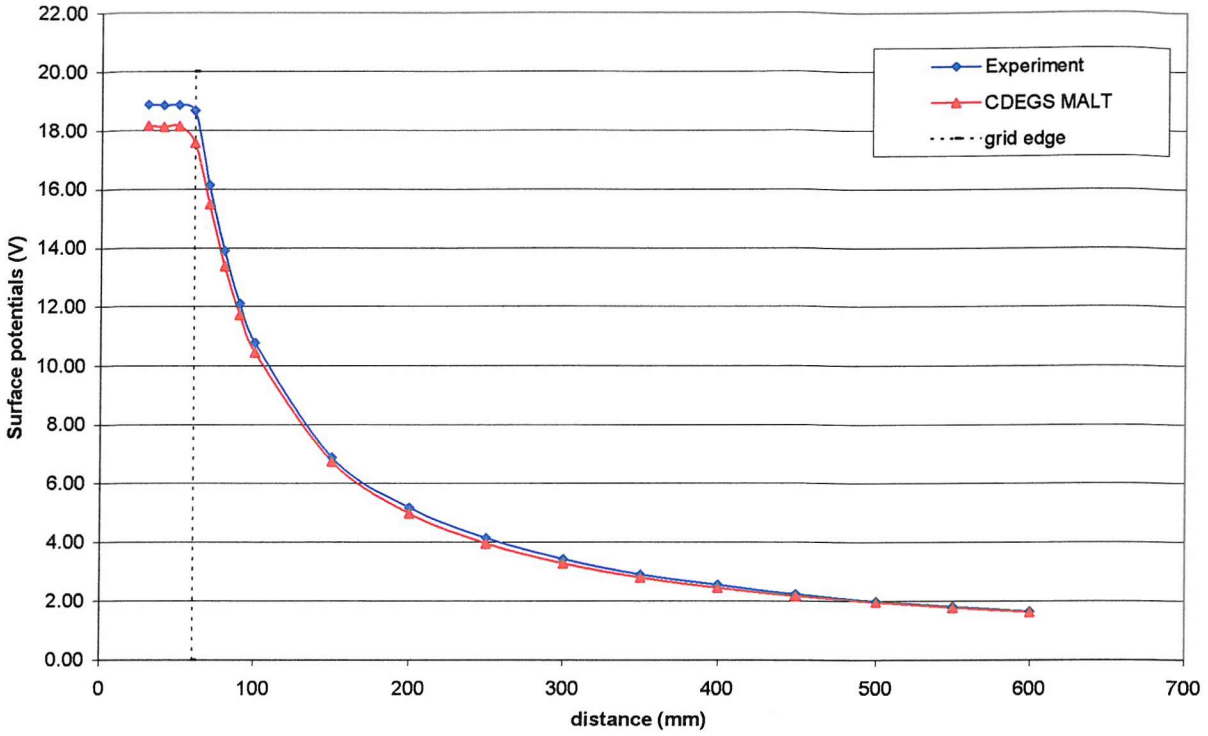

Figure 8.3: Surface potentials (V) against distance (mm) for Buried Grid (120mm x 120mm, c=60mm) at buried depth=10mm

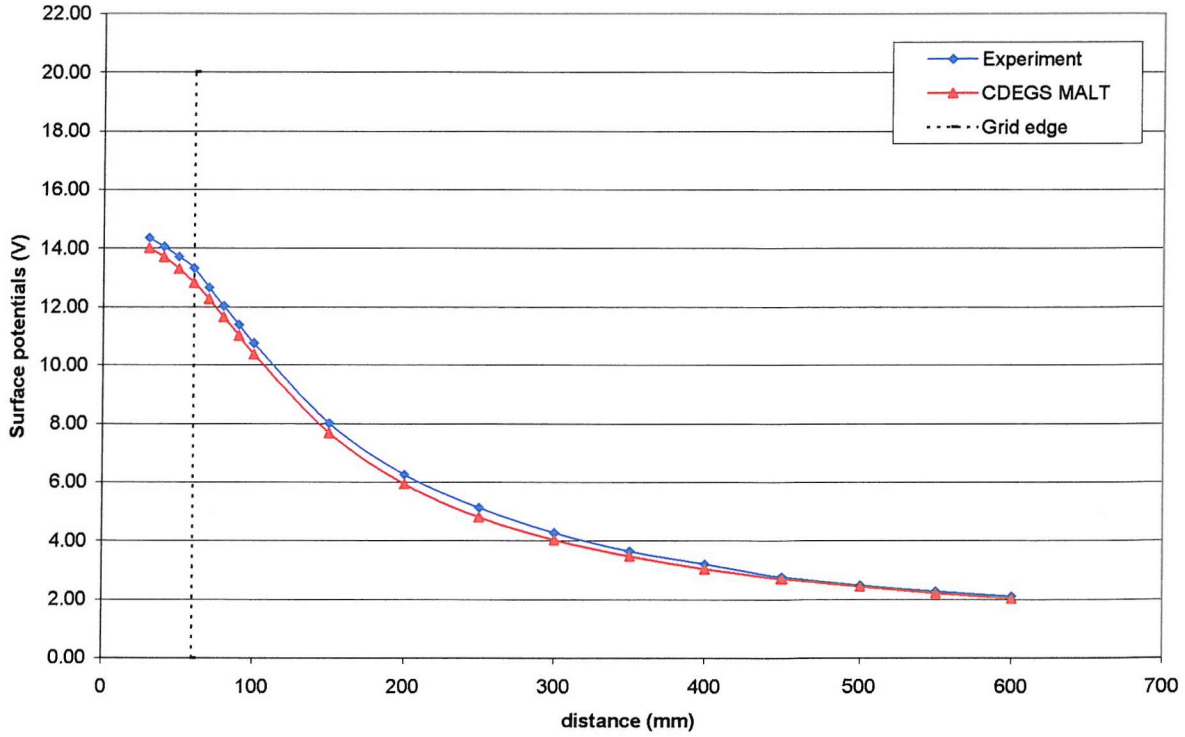

Figure 8.4: Surface potentials (V) against distance (mm) for Buried Grid (120mm x 120mm, c=60mm) at buried depth=60mm

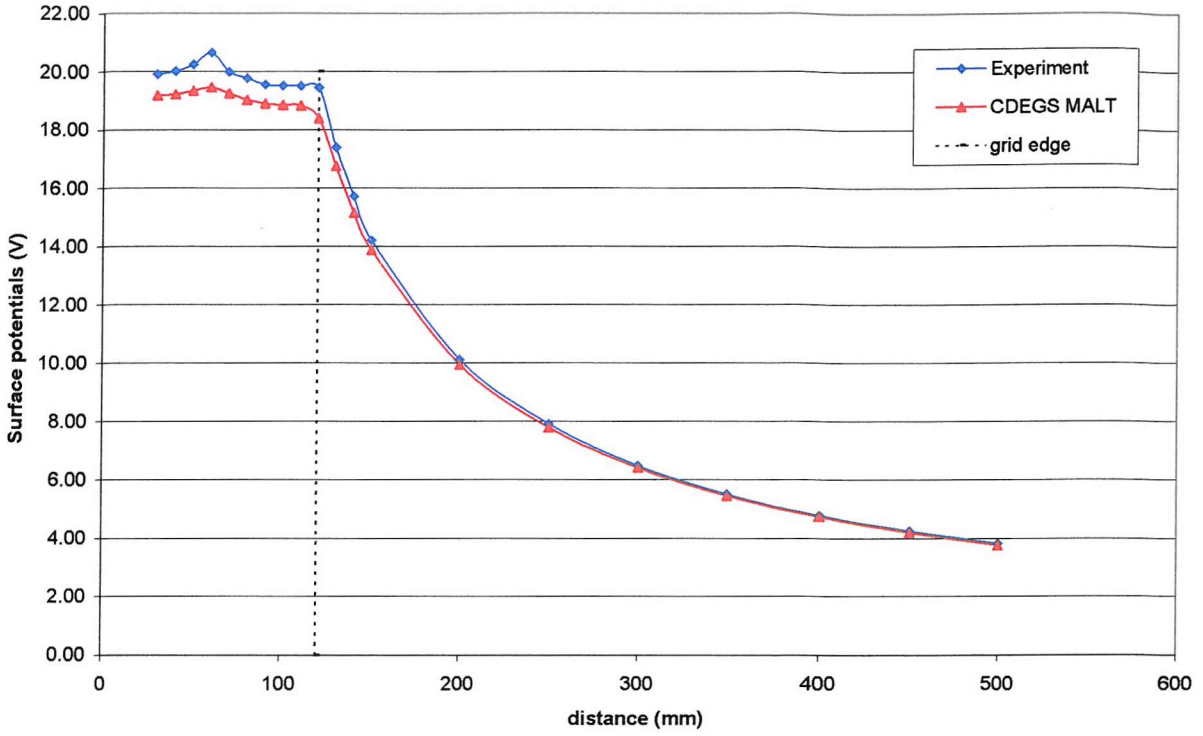

Figure 8.5: Surface potentials (V) against distance (mm) for Buried Grid (240mm x 240mm, c=60mm) at depth=10mm at 0 degree traverse

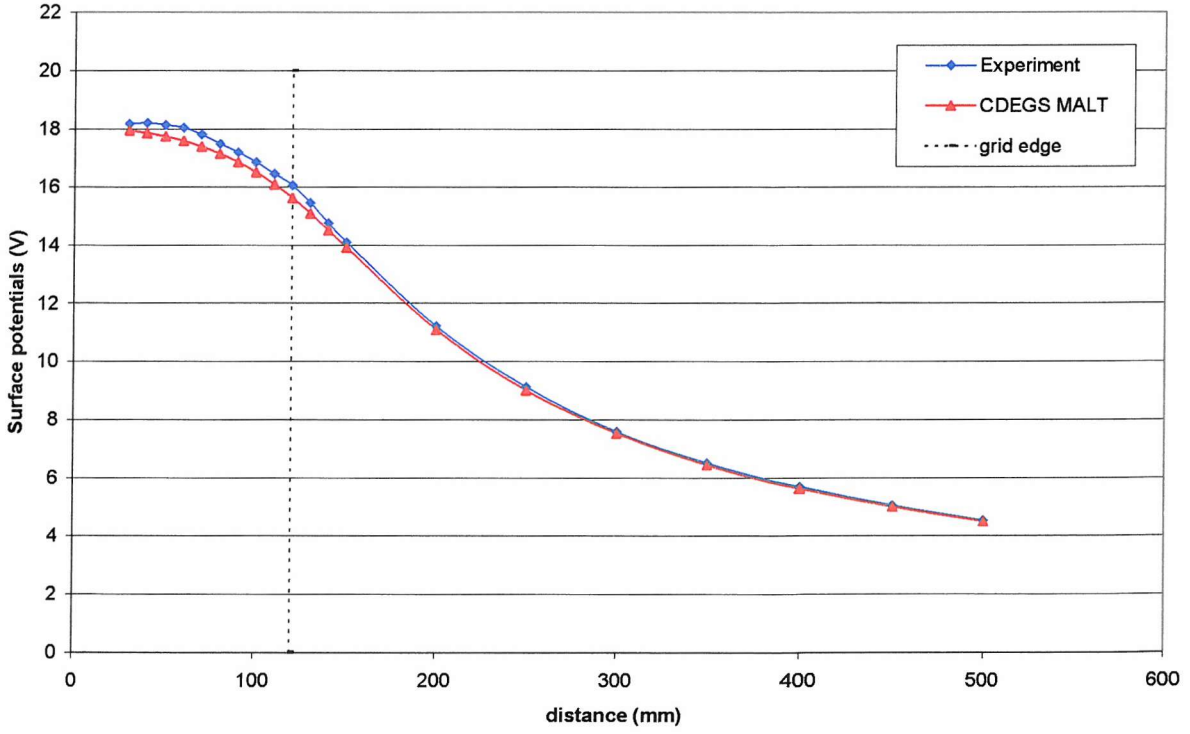

Figure 8.6: Surface potentials (V) against distance (mm) for Buried Grid (240mm x 240mm, c=60mm) at depth=60mm at 0 degree traverse

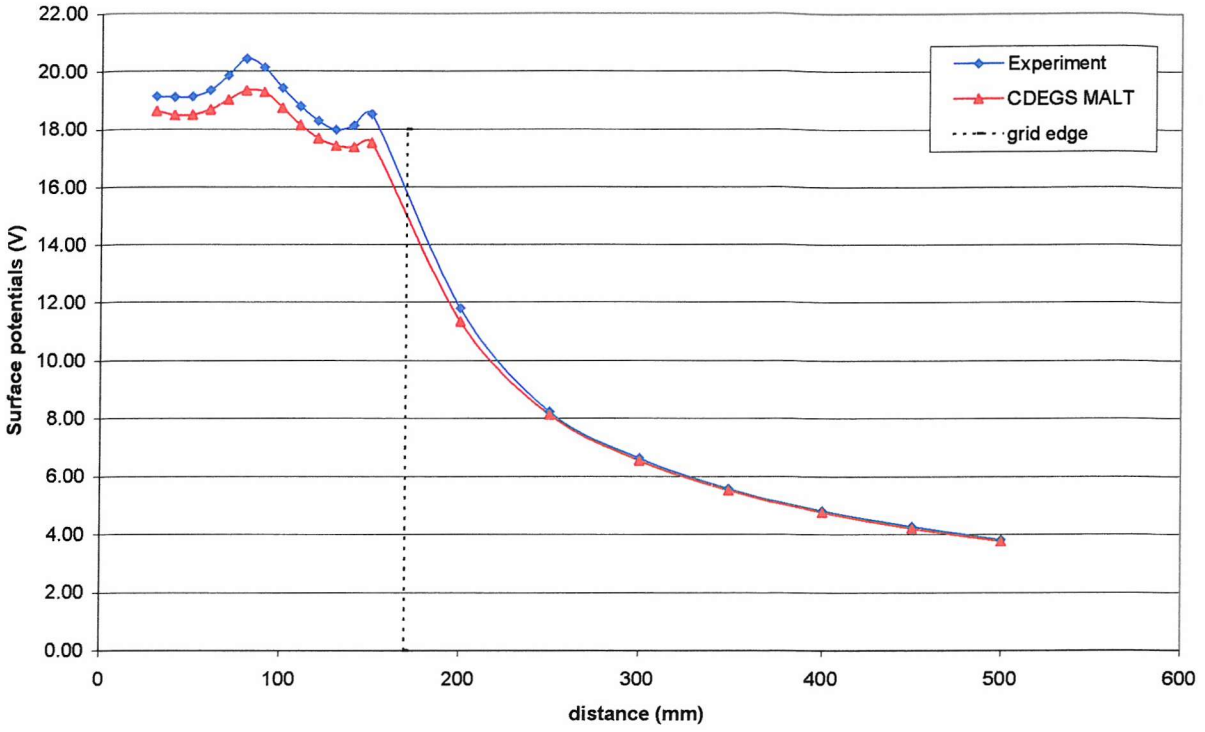

Figure 8.7: Surface potentials (V) against distance (mm) for Buried Grid (240mm x 240mm, c=60mm) at depth=10mm at 45 degree traverse

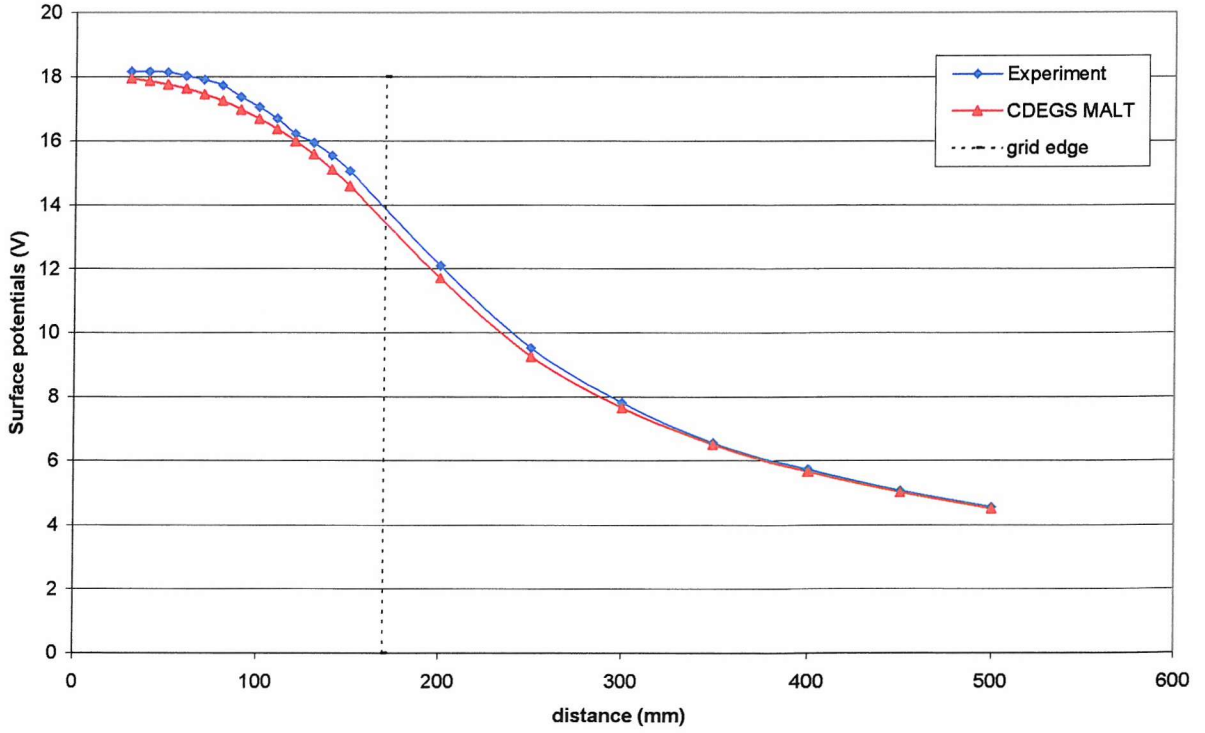

Figure 8.8: Surface potentials (V) against distance (mm) for Buried Grid (240mm x 240mm, c=60mm) at depth=60mm at 45 degree traverse

The same trend as for the 8 rods combined grid can be seen here with the buried grid configuration regardless of the size of the mesh area. When the point of reading is taken immediately above one of the rods in the grid (i.e. at 60 mm from the middle point of the mesh), the percentage difference between experimental and computed result is the highest. As the distance of the surface potential reading (with respect to the middle point of the grid) increases, the difference between the experimental and the computed results decreases. On average, for both grid sizes, the percentage difference between the two methods is less than 0.8% when the reading is taken 300 mm from the grid edge and beyond.

Furthermore, as the burial depth of the grid increases, the percentage difference between the two methods decreases, particularly at the potential profile position very close to the earthing grid. For both mesh sizes, as the burial depth increases from 10 mm to 60 mm, the percentage difference decreases by 40%. For example, for the 120 mm x 120 mm grid, at 10 mm burial depth, the percentage difference is 5.54% at the point closest to the grid, but this value decreases to 2.5% as the burial depth is increased to 60 mm. Also, for both mesh sizes, the maximum percentage difference remains almost constant (~2-3%) at 20 mm burial depth and deeper. This phenomenon was the same as with the 8 rods combined grid case in Section 8.1.

8.3 Fat and Thin Ring

A circular ring when energized will have a uniform leakage current in all directions due to the geometry of the ring. This is ideal to check for the proximity effect. Two different sizes of ring are investigated here. One is a fairly thick ring and the other is a thin ring. The ring dimensions are as illustrated in Figure 8.9.

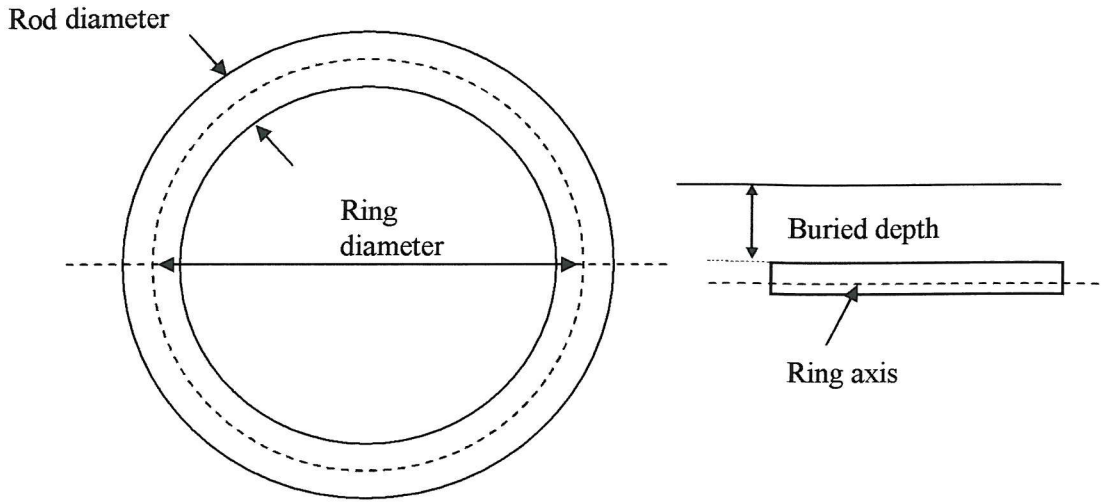

Figure 8.9: Top and side view of the ring electrode

An analytical solution for the potential of a ring is possible due to the circular symmetry of the latter. A full derivation is given in Appendix 9.

8.3.1 Fat Ring

This ring is 57 mm in radius and the thickness of the ring is 8 mm. The ring is buried at depths of 1 mm, 20 mm, 30 mm, 40 mm and 100 mm below water level. Figures 8.10 to 8.12 shows the results for 1 mm, 40 mm and 100 mm buried depths. Full-tabulated results can be seen in Appendix 8.

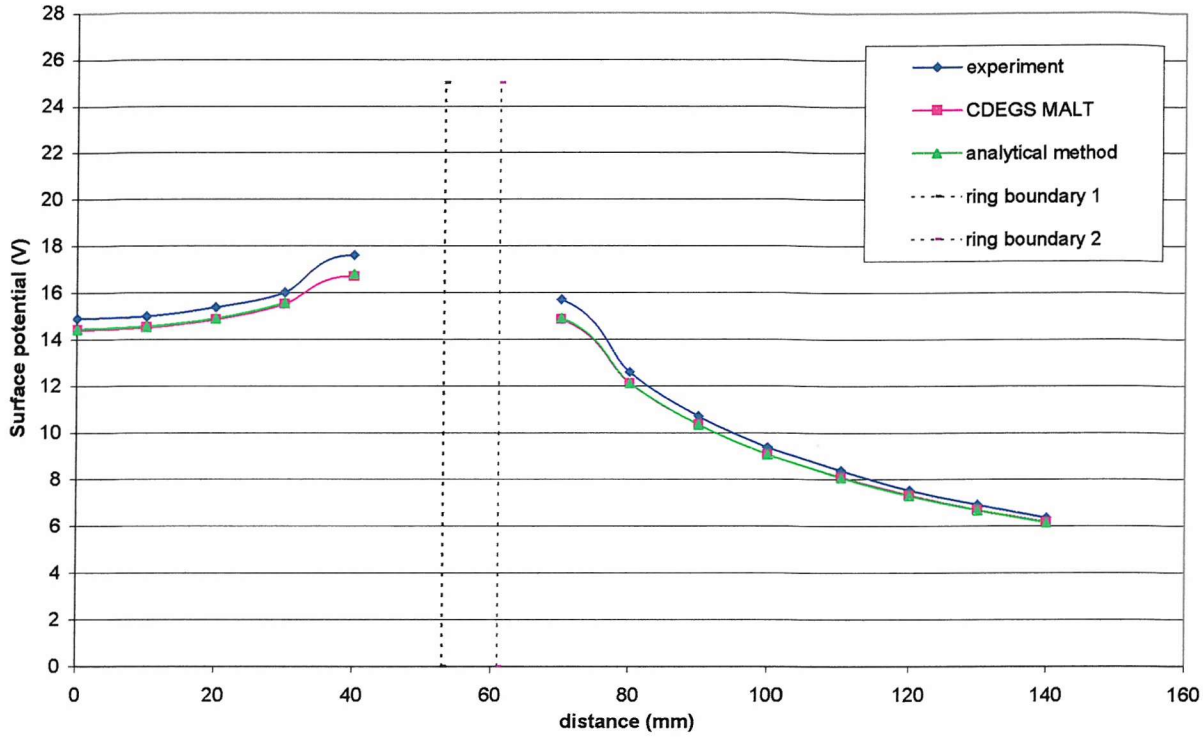

Figure 8.10 : Surface potential (V) against distance from middle of ring (mm) for a fat ring (57mm in radius and 8mm thick) electrode buried at depth of 1mm

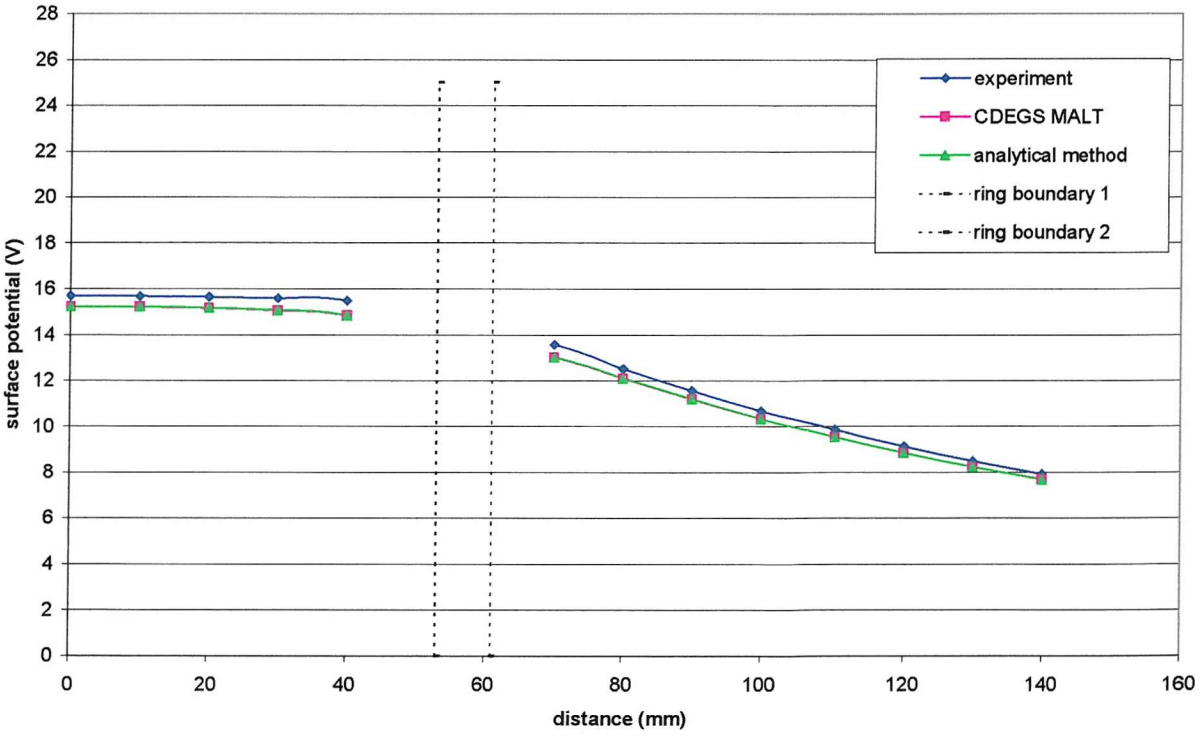

Figure 8.11: Surface potential (V) against distance from middle of ring (mm) for a fat ring (57mm in radius and 8mm thick) electrode buried at depth of 40mm

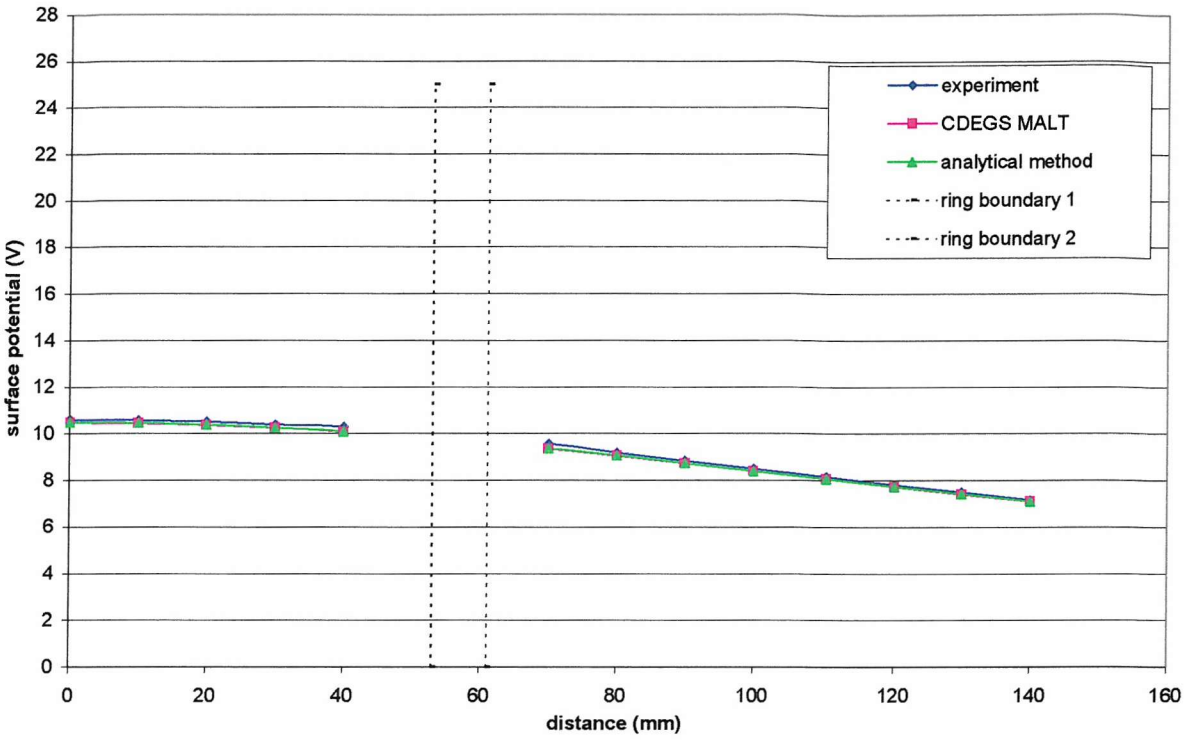

Figure 8.12: Surface potential (V) against distance from middle of ring (mm) for a fat ring (57mm in radius and 8mm thick) electrode buried at depth of 100mm

8.3.2 Thin Ring

This ring is 50 mm in radius and the thickness of the ring is 1.56 mm. The ring is buried at depths of 20 mm, 30 mm and 40 mm below water level. Figures 8.13 and 8.14 show the results for the shallowest and deepest buried depths. Full-tabulated results can be found in Appendix 8.

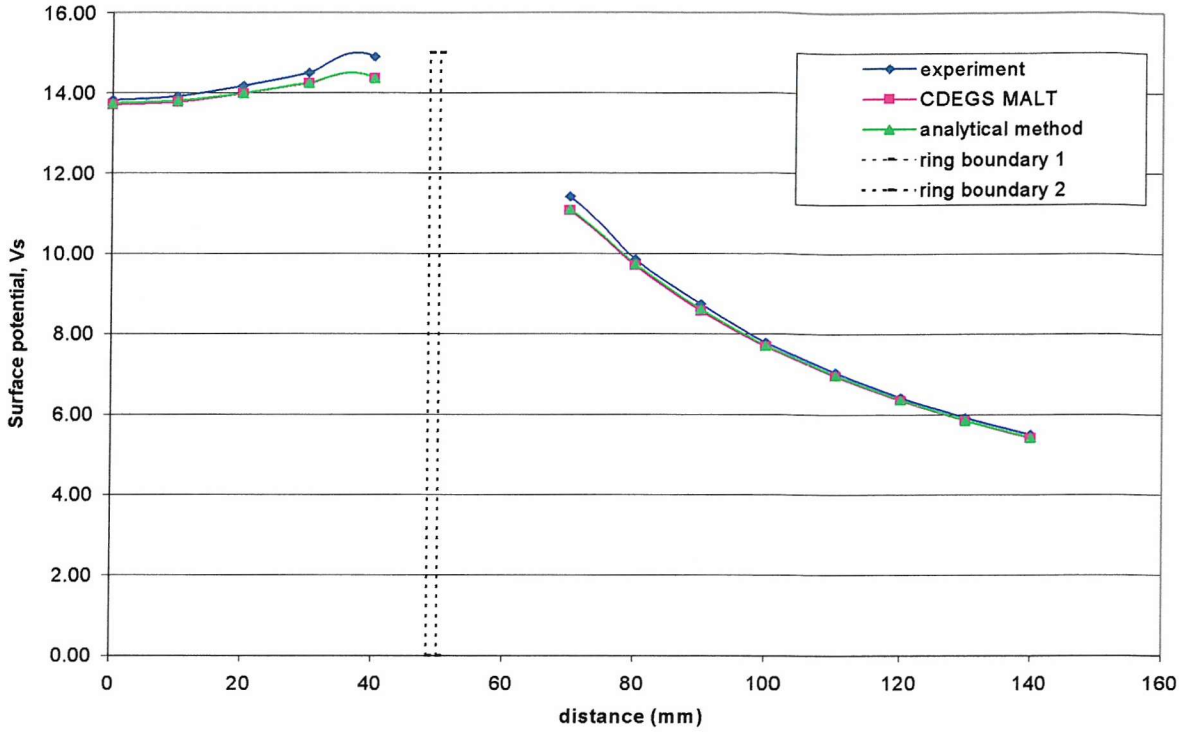

Figure 8.13: Surface potential (V) against distance from middle of ring (mm) for a thin ring electrode buried at depth of 20mm

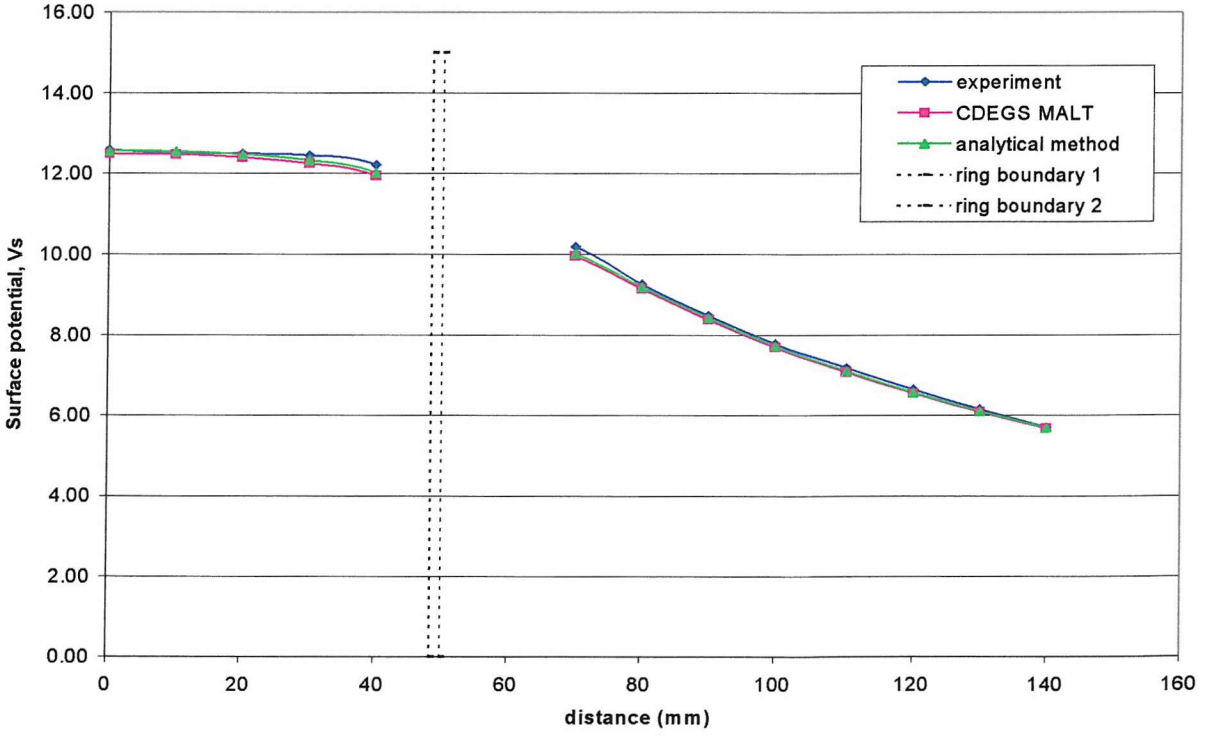

Figure 8.14: Surface potential (V) against distance from middle of ring (mm) for a thin ring electrode buried at depth of 40mm

In MALT, the fat ring is modelled by 8 thinner rings, each of 0.2mm thickness. This is illustrated in Figure 8.15. This is to simulate the proximity effect better because the original ring conductor thickness is relatively large (8 mm thick) compared to the radius of the ring, which is 57 mm. By breaking the fat ring into thinner rings, the current distribution on the surface of the original ring can be better presented. It was found that if the fat ring is computed as a single ring in MALT, the percentage difference (compared to the experimental and analytical results) for the surface potentials is higher compared to when the ring is computed as 8 thinner rings.

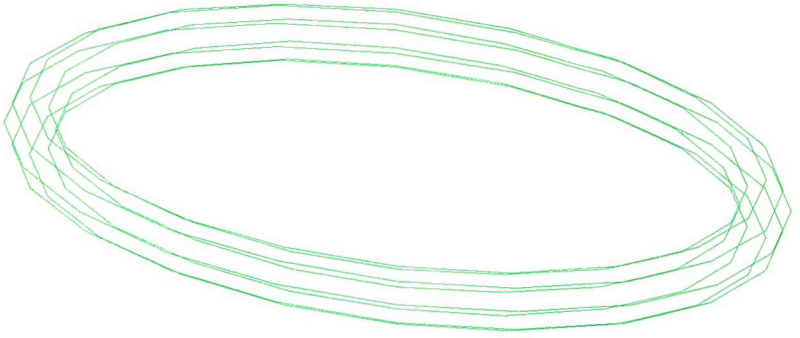

Figure 8.15: 8 thinner rings to simulate the Fat Ring for computations in MALT

For both rings, as the burial depth gets deeper, the proximity effect lessens. This is shown by the decrease in percentage difference between the experimental results and MALT as the burial depth is increased. For the thin ring, its thickness is the same as the radius of the rods used in the previous configurations (see section 8.1 and 8.2). In previous configurations tested, when the burial depth is 20 mm or larger, the agreement between the experimental results and MALT gets closer. The same applied to the thin ring. However, for the fat ring, the percentage difference between experimental results and MALT starts to decrease when the burial depth reach 100 mm.

8.4 Conclusions

In conclusion, leakage current density will have a circumferential variation when the earthing conductor is very close to the earth surface. In other words, the current from the top surface of the conductor is much less than that from the bottom surface of it. This circumferential variation is not considered in CDEGS MALT and analytical solution, which is theoretical. However, in real life situation, this phenomenon is clearly happening as shown in the experimental results.

It is found that for all the three different grid configurations (combined grid, mesh or ring), when the rod size used in the earthing grid is 1.56 mm in diameter, the minimum buried depth is 20 mm in order to reduce the proximity effect. Burial depths less than 20 mm will adversely effect the potential readings in and around the model substation area. When the rods increase in size, the burial depth to reduce the proximity effect increases as well. This is shown by the fat ring, which have a thickness (rod size) of 8 mm. The fat ring has to be buried at least 100mm deep before there is reduction in the proximity effect.

Hence, on any scale we can conclude that the proximity effect reduces as the earthing grid is buried at depths of more than 12 times the rod diameter. This is a precautionary step and is not so critical in real situation as the typical buried depth of an earthing system is 0.6m, and typical rod size is 15 to 16 mm in diameter (refer to Section 2.6, page 38).

CHAPTER 9

Conclusions and Future Work

9.1 Conclusions

Before the completion of the experimental tank, investigations were carried out using some known theoretical formula, from either the standards or the literature and the computer program called CDEGS MALT. Initial study showed that CDEGS MALT seems to agree very well with the theoretical formulas with percentage difference of less than 1.5% for most cases. This is because MALT uses the most commonly used method for earthing analysis, which is based on the method of images and assumes that the earthing system is an equipotential structure. This assumption is incorporated by most of the theoretical formulas.

Part of the initial work also involves the construction of the electrolytic tank, and verifying its accuracy and reliability by comparing with the computer software CDEGS MALT. CDEGS MALT, known to be the most reputable software in earthing and related problems, compares well with not more than 2% difference with the electrolytic tank results for various cases tested here.

Some of the formulas in S34 were investigated, comparing them with the CDEGS MALT and the experimental results. It has been shown that S34 does not give reliable results and many factors have been ignored in the S34 formula. For '*group of rods in hollow square*', it was found that the 'k' factor, which is dependent on the number of rods, has an effect on the accuracy of S34. The higher the 'k' factor, the better the agreement between S34 and MALT. Also, as the rod spacing gets smaller, but the number of rods remains the same (hence, the 'k' factor), the percentage difference between S34 and MALT is less.

For the '*buried grid*' formula, when comparing with CDEGS and experimental results, it was found that as the buried grid area increases, the smaller the difference between CDEGS and S34. Also S34 does not take into account the radius of the vertical rods.

Furthermore, all the formulas given in S34 that were investigated here do not include the depth of the buried grid and the injected current, which are two very important parameters which affect directly the resistance of the earthing system. All the resistance values given by S34 are higher than the computed CDEGS MALT and experimental results.

The variation of the resistance of a disc with varying depth was also investigated briefly. Burying a disc at a depth equal to its radius causes a substantial reduction of the resistance by over 30%. The surface potential is significantly influenced by the depth of the disc only within three or four radii of the axis of symmetry of the disc. Also, the potential close to the disc (up to about three times the radius of the disc) rises as the depth increases before finally decaying.

The next aspect in this work was the effect of an insulating barrier on one side of an earthing system. A highly resistive barrier can be inserted vertically into the ground at a certain distance from the earthing grid to lower the surface potentials in the area beyond where the barrier is situated. In other words, the insertion of a resistive barrier is one of the measures that can be taken to increase public safety. Ideally, the barrier should be buried right below or slightly outside the substation fence for it to achieve its purpose. Two types of barrier were investigated. One is a solid barrier, and the other is a barrier made of rectangular plates arranged at specified spacing such that the dimensions are the same as the solid barrier.

For the solid barrier, some simple scenarios were experimented in the water tank, and the results compared to CDEGS MALT. It was found that for a sensible barrier depth and spacing in the region of two vertical rod lengths, we have an increase of less than 3.5% in the resistance of the earthing system, compared to when no barrier is present. In the worst case tested, which is three rod lengths deep and one rod length away from the grid, the increase in resistance is on average 11%. As for the surface potential measurements,

as expected, the surface potential between the earthing grid and the barrier increases, whilst that outside the barrier will decrease, compared to the values in the absence of a barrier. Although the surface potential within the substation will increase due to the barrier, the increase is not more than 30% (at all three different angles investigated). Furthermore, the percentage increase for the inner surface potential is still less than the decrease in surface potential that can be achieved outside the barrier, even at positions relatively very far away from the barrier.

The plate barrier serves the same function as the solid barrier. When using this type of barrier, the gaps in between the plates are very crucial. It was found that the increase in earthing resistance is not significantly influenced by the gap size. Narrowing the gap size by about 50% increases the resistance by less than 2%. As for the surface potential measurements, it was found that for all the gap sizes tested here, the plate barrier has to be at least two rod lengths deep in order for the barrier to function effectively. This is the case with the solid barrier as well. Also, the screening performance of the plate barrier starts to deteriorate and the percentage difference when compared to no barrier is almost constant as the gap size increases. It was found that, as with the solid barrier, the plate barrier is still effective at positions relatively very far away from the grid, even when using the shallowest barrier positioned at the furthest distance from the grid.

However, the difference between these two types of barrier is that the plate barrier can save cost because the material used to make up the barrier is less. Also, it is easier to drive small plates of material into the ground than to have to dig a deep trench to insert a large solid barrier vertically into the ground. However, due to the gaps between the plates, a plate barrier will not give the same values, either in increase or decrease in earthing resistance or surface potentials respectively. In essence, it all depends on the percentage decrease in surface potentials beyond the barrier that one wants to achieve by using the barrier. A plate barrier of 5mm gap situated at position (x=60mm, y=120mm) can act almost as if it were a solid barrier situated at (x=60mm, y=60mm). In other words, the decrease in surface potential is almost the same for these two different types of barrier but at different burial depths. Also, by using a plate barrier of 5mm gap and inserting it nearer by one rod length, can act as if of a solid barrier situated at two rod lengths away from the grid.

Furthermore, it was shown that the gaps in the barrier do not have any significant effect on the potential profile. However, it is recommended to have small gaps, which is approximately 5% from the rod length used, i.e. in this case about 2 – 5 mm plate spacing.

To conclude, there are advantages and disadvantages when using a highly resistive barrier to reduce surface potentials outside the vicinity of the substation. However, it was shown that the advantages are more. The increase in resistance and surface potential within the vicinity of the substation is insignificant compared to the reduction in surface potentials that can be achieved outside substation. One can use barriers made of plates with gaps to achieve almost the same function as a solid barrier.

Most of the investigations regarding measurement of surface potential were made outside the vicinity of the grid. It is known that when the elements of an earth electrode system are too close together, the distribution of the fault current will be affected. This 'proximity effect' will influence the surface potential readings very close to the earthing grid. Also, when an earthing conductor is very close to the earth surface, the current dissipating from the top surface of the conductor is much less than that from the bottom surface of it. This is to say that the leakage current density has a circumferential variation. In most software packages, this circumferential variation of the leakage current is not taken into account. Hence, experimental results are used to evaluate the extent of the error that can be caused by ignoring this circumferential leakage current variation.

Further investigation on this aspect was carried out using three different types of earthing grid geometry: a combined grid (with vertical rods and horizontal electrodes), a flat mesh (with two different mesh areas), and a ring (with two different ring thickness). It was found that for all the three different grid configurations, the minimum buried depth is 20mm in order to reduce the proximity effect. Burial depths less than 20mm will adversely affect the potential readings in and around the substation area. The grids used in the experiments were made of 1.56 mm diameter rods, regardless of whether horizontal electrodes, vertical rods or ring electrode. Attempting to scale this result to a

grid of any size, we can say that the grid should be buried at a depth of more than 12 times the conductor diameter.

9.2 Future Work

9.2.1 Improvements to the Electrolytic Tank

The present experimental set up is satisfactory but time consuming because the measurements have to be taken manually, i.e. by climbing to a platform above the tank. This can be troublesome especially when there are many measurements to be done. In addition, it is quite dangerous and needs someone who is tall enough to reach up to the middle of the tank in order to take measurements or to change the earthing grids.

The recommendations for future work involving scale models are as follows:

d) Use a motorised arm that can be remote controlled to measure the surface potentials.
e) Use a microprocessor that is connected to the experimental set up to record and store data.
f) Use a motorised remote controlled device that can be used to change the earthing grid and place it in the middle of the tank with known depths and coordinates.
g) Develop a probe that can measure vertical potential profiles.
h) Use a material such as copper for the return mesh, which will not corrode in the water for a long time. The zinc material used in this research does corrode with time. The same applies to the earthing rods. The material used in the experiment for the rods (brass) corrode with time and had to be cleaned or changed from time to time. It is recommended to use other material that will withstand being in the water for a long time without corroding, such as copper or gold plated rods.

9.2.2 Work on the Insulating Barrier

It is recommended to investigate further on the effect of the insulated barrier on the earthing system. In this research, the barrier was positioned only on one side of the

earthing system and the surface potentials were measured only in the area where the barrier was present. It would be useful to investigate the effects of the barrier to the resistance of the earthing system and the surface potential around the grid when the geometry, size, and location of the barrier change. In addition, the effects of the barrier when the earthing system is in two or more layers soil model can be investigated.

9.2.3 Towards a Two Layer Tank Model

The work done used tap water to represent uniform soil. Uniform soil means that we are assuming the soil to have only one layer, and only one resistivity value. In reality, this is not always true. It is recommended to model a two or more layers soil model. *Agar*, a gelatine-like substance frequently used in biological studies can be used to represent the bottom layer and tap water as the top layer. *Agar* is the material used in the study by Caldecott [122]. Since *agar* was not found, the modelling of a two-layer tank was done using sand, jelly, and oil as the bottom layer and tap water as the top layer.

Although it was tedious and troublesome to prepare the required sand, jelly or oil to the required conductivity as mentioned by Caldecott when preparing the *agar*, it was found that sand, jelly and oil increases in resistance and takes sometimes up to a day to settle down to a value. The settling time will decrease as the frequency increases. Due to time constraints, this was not investigated further. It is recommended to pursue this study, and developing a two-layer tank model.

References

1. T. Charlton, *Earthing Practice*. 1997: Copper Development Association.

2. I. Cotton. *Windfarm Earthing*. in *11th International Symposium on High Voltage Engineering Conference Publication*.

3. I. Cotton and N. Jenkins. *The Effects of Lightning on Structures and Establishing The Level of Risk*. in *Lightning Protection Of Wind Turbines, IEE Half-Day Colloquium*. 26 November 1997.

4. N.D. Hatziargyriou, M.I. Lorentzou, I. Cotton, and N. Jenkins. *Transferred Overvoltages by Windfarm Grounding Systems*. in *8th International Conference on Harmonics and Quality of Power ICHQP '98*. 14-16 October 1998. Athens, Greece.

5. G.F. Tagg, *Earth resistances*. 1964: George Newnes Limited London.

6. F. Wenner, *A Method of Measuring Resistivity*. National Bureau of Standards Scientific Paper, S-258, 1916: p. 469.

7. T. Charlton. *Site Measurements*. in *IEE Power Seminar- Substation Earthing: Shedding Light on the Black Art*. Birmingham, UK.

8. J. Ma and F. Dawalibi, *Study of Influence of Buried Metallic Structures on Soil Resistivity Measurements*. IEEE Transactions on Power Delivery, April 1998. **Vol. 13**(No. 2): p. 356-365.

9. F. Dawalibi and C.F. Blattner, *Earth Resistivity Measurement Interpretation Techniques.* IEEE Transactions on Power Apparatus and Systems, February 1984. **Vol. PAS-103**(No. 2): p. 374-382.

10. *CDEGS Manual Book.* 1999: Safe Engineering Services & Technologies Ltd.

11. H.R. Seedher and J.K. Arora, *Estimation of Two Layer Soil Parameters Using Finite Wenner Resistivity Expressions.* IEEE Transactions on Power Delivery, July 1992. **Vol. 7**(No. 3): p. 1213-1217.

12. C.J. Blattner, *Study of Driven Rods and Four Point Soil Resistivity Tests.* IEEE Transactions, 1982. **Vol. PAS-101**(No. 8): p. 2837-2850.

13. J.G. Sverak, W.K. Dick, T.H. Dodds, and R.H. Heppe, *Safe Substation Grounding -Part I.* IEEE Transactions on Power Apparatus and Systems, 1981. **Vol. PAS-100**(No. 9): p. 4281-4290.

14. *IEEE Guide for Measuring Earth Resistivity, Ground Impedance and Earth Surface Potentials of a Ground System, Std. 81-1983.* 1983.

15. G.F. Tagg, *Measurement of Earth Electrode Resistance with Particular Reference to Earth-Electrode Systems Covering A Large Area.* Proc. IEE, 1964. **Vol. 3**(No. 12): p. 2118-2130.

16. M. Datta, A.K. Basu, and M.M. Chowdhury, *Determination of Earth Resistance of Multiple Driven-Rod Electrodes.* Proc. IEE, 1967. **Vol. 114**(No. 7): p. 1001-1006.

17. V. Amoruso, M. Savino, and M.S. Labini. *An Automatic Method for Measuring Earth Resistivity*. in *Third International Symposium on Applied Informatics*. February 1985. Grindelwald, Switzerland.

18. O. Koefoed, *Resistivity Grounding Measurements*. Geosounding Principles 1. 1979, New York: Elsevier Scientific Publishing Co.

19. F. Dawalibi and R. Mukhedkar, *Resistance Measurement of Large Grounding Systems*. IEEE Trans., 1979. **Vol. PAS-98**(No. 6): p. 2348-2354.

20. V. Amoruso, M. Savino, and M.S. Labini, *Analysis of Large Grounding Systems for Earth-Resistance Measurements in Two-Layer Soils*. IEE Proceedings, Pt. C, May 1989. **Vol. 136**(No. 3): p. pp. 182-194.

21. *Power System Earthing Course Notes*. 13th and 14th October 1999: Strategy and Solutions Ltd.

22. B. Allport. *Practical Considerations (Substation Earthing)*. in *IEE Power Seminar - Substation Earthing: Shedding Light on the Black Art*. Birmingham, UK.

23. A. El-Morshedy, A.G. Zeitoun, and M.M. Ghourab, *Modelling of Substation Grounding Grids*. IEE Proceedings Pt. C, July 1986. **Vol. 133**(No. 5): p. 287-292.

24. W.R. Jones, *Bentonite Rods assure ground rod installation in Problem Soils*. IEEE Transactions, 1980. **Vol. PAS-99**(No. 4): p. 1343-1346.

25. M.B. Kostic, Z.R. Radakovic, N.S. Radovanovic, and M.R. Tomasevic-Canovic, *Improvement of Electrical Properties of Grounding Loops by using Bentonite and*

Waste Drilling Mud. IEE Proc. - Generation, Transmission and Distribution, January 1999. **Vol. 146**(No. 1): p. 1-6.

26. Z.R. Radakovic and M.B. Kostic, *Behaviour of Grounding Loop with Bentonite during a Ground Fault at an Overhead Line Tower.* IEE Proc. - Generation, Transmission and Distribution, July 2001. **Vol. 148**(No. 4): p. 275-278.

27. F. Dawalibi, R. Southey, and R. Baishiki, *Validity of Conventional Approaches for Calculating Body Currents Resulting from Electric Shocks.* IEEE Transactions on Power Delivery, April 1990. **Vol. 5**(No. 2): p. 613 -626.

28. *IEEE Guide for Safety in AC Substation Grounding, ANSI/IEEE Std. 80-1996.* August 1996: Institute of Electrical and Electronics Engineers.

29. C.F. Dalziel, *Threshold 60-Cycle Fibrillating Currents.* AIEE Trans. PAS, 1960. **Vol. 79**(No. 3): p. 667-673.

30. *Effects of Current Passing Through the Human Body,*. Second Edition ed. IEC Report, Publication 479-1. 1984: International Electrotechnical Commission.

31. H.R. Amstrong and L.J. Simpkin, *Grounding Electrode Potential Gradients from Model Tests Engineering.* Trans. American Institute Electrical, 1960. **Vol. PAS-79**: p. 618-623.

32. *Practical Applications of ANSI/IEEE Standard 80-1986, IEEE Guide for Safety in AC Substation Grounding Course Text*, in *IEEE Tutorial Course, 86 EH0253-5-PWR.*

33. R.L. Stoll, G. Chen, and A.E. Davies, *Substation Earthing Report (Internal Report)*. May 1999, Department of Electronics and Computer Science, University of Southampton: Southampton.

34. R.L. Stoll, G. Chen, and A.E. Davies, *Substation Earthing Report (Internal Report)*. August 1999, Department of Electronics and Computer Science, University of Southampton: Southampton.

35. *A Guide for Assessing the Rise of Earth Potential at Substation Sites*. EA Engineering Recommendations S34. 1986: Electricity Association Services Ltd.

36. *Code of Practice for Earthing*. BS 7430. 1998.

37. *Code of Practice for Design of High Voltage Open Terminal Stations*. BS 7354. 1990.

38. *Guidelines for the design. Installation, Testing and Maintenance of Main Earthing Systems in Substations*. EA Technical Specification 41-24. 1992: Electricity Association Services Ltd.

39. *IEEE Guide for Safety in AC Substation Grounding, ANSI/IEEE Std. 80-2000*. 2000: Institute of Electrical and Electronics Engineers.

40. http://www.sestech.com, Safe Engineering Services and Technologies Ltd.

41. F. Dawalibi and D. Mukhedkar, *Optimum Design of Substation Grounding in Two-Layer Earth Structure-Part II, Comparison Between Theoretical and Experimental Results*. IEEE Transactions on Power Apparatus and Systems, March/April 1975. **Vol. PAS-94**(No. 2): p. 262-266.

42. D. Mukhedkar, Y. Gervais, and F. Dawalibi, *Modelling of Potential Distribution Around a Grounding Electrode.* IEEE Transactions PAS, Sept/Oct 1973. **Vol. 92**(No. 5): p. 1455-1459.

43. F. Dawalibi, D. Mukhedkar, and D. Bensted, *Measured and Computed Current Densities in Buried Ground Conductors.* IEEE Transactions on Power Apparatus and Systems, August 1981. **Vol. PAS-100**(No. 8): p. 4083-4092.

44. F. Dawalibi and R.S. Baishiki, *Power Frequency Performance of Transmission Line Structure Grounds.* IEEE Transactions on Power Apparatus and Systems, June 1984. **Vol. PAS-103**(No. 6): p. 1295-1303.

45. F. Dawalibi and G.B. Niles, *Measurements and Computations of Fault Current Distribution on Overhead Transmission Lines.* IEEE Transactions on Power Apparatus and Systems, March 1984. **Vol. PAS-103**(No. 3): p. 553-560.

46. F. Dawalibi and J.H. Dunlap. *Analysis of Transmission Line Grounding Systems under Fault Condition.* in *CIGRE Symposium*. 1985. Brussels.

47. F. Dawalibi and N. Barbeito, *Measurements and Computations of the Performance of Grounding Systems Buried in Multilayer Soils.* IEEE Transactions on Power Delivery, October 1991. **Vol. 6**(No. 4): p. 1483-1490.

48. W.K. Daily and F. Dawalibi, *Measurements and Computations of Electromagnetic Fields in Electric Power Substations.* IEEE Transactions on Power Delivery, January 1994. **Vol. 9**(No. 1): p. 324-333.

49. J. Ma, F.P. Dawalibi, W. Ruan, R. Southey, R. Waddell, and J.K. Choi. *Measurement and Interpretation of Ground Impedances of Substation Grounding*

Systems Connected to Ground Wires and Metallic Pipes. in *Proceedings of the American Power Conference: Reliability and Economy Technology Focus for Competition and Globalization*. 1998. Chicago, USA.

50. F. Dawalibi and D. Mukhedkar, *Multi-Step Analysis of Interconnected Grounding Electrodes*. IEEE Transactions on Power Apparatus and Systems, January/February 1976. **Vol. PAS-95**(No. 1): p. 113-119.

51. F. Dawalibi and D. Mukhedkar, *Optimum Design of Substation Grounding in Two layer Earth Structure - Part I, Analytical Study*. IEEE Transactions on Power Apparatus and Systems, March/April 1975. **Vol. PAS-94**(No. 2): p. 252-261.

52. F. Dawalibi and D. Mukhedkar, *Resistance Calculation of Interconnected Grounding Electrodes*. IEEE Transactions on Power Apparatus and Systems, January/February 1977. **Vol. PAS-96**(No. 1): p. 59-65.

53. F. Dawalibi and D. Mukhedkar, *Transferred Earth Potentials in Power Systems*. IEEE Transactions on Power Apparatus and Systems, January/February 1978. **Vol. PAS-97**(No. 1): p. 90-101.

54. M. Bouchard, F. Dawalibi, and D. Mukhedkar. *Survey on Ground Resistance and Earth Resistivity Measurements*. in *IEEE Power Engineering Winter Meeting*. 1977. New York, USA.

55. F. Dawalibi and D. Mukhedkar, *Ground Electrode Resistance Measurements in Nonuniform Soils*. IEEE Transactions on Power Apparatus and Systems, January 1974. **Vol. PAS-93**(No. 11): p. 109-115.

56. F. Dawalibi and D. Mukhedkar, *Parametric Analysis of Grounding Grids.* IEEE Transactions on Power Apparatus and Systems, September/October 1979. **Vol. PAS-98**(No. 5): p. 1659-1668.

57. F. Dawalibi and D. Mukhedkar, *Influence of Ground Rods on Grounding Grids.* IEEE Transactions on Power Apparatus and Systems, November/December 1979. **Vol. PAS-98**(No. 6): p. 2089-2098.

58. F. Dawalibi and W.G. Finney, *Transmission Line Tower Grounding Performance in Nonuniform Soil.* IEEE Transactions on Power Apparatus and Systems, March/April 1980. **Vol. PAS-99**: p. 471-479.

59. F. Dawalibi, M. Bouchard, and D. Mukhedkar, *Survey on Power Systems Grounding Design Practices.* IEEE Transactions on Power Apparatus and Systems, July/August 1980. **Vol. PAS-99**: p. 1396-1405.

60. F. Dawalibi, *Ground Fault Current Distributions Between Soil and Neutral Conductors.* IEEE Transactions on Power Apparatus and Systems, March/April1980. **Vol. PAS-99**: p. 452-461.

61. F. Dawalibi, D. Bensted, and D. Mukhedkar, *Soil Effects on Ground Fault Currents.* IEEE Transactions on Power Apparatus and Systems, July 1981. **Vol. PAS-100**(No. 7): p. 3442-3450.

62. W. Bogajewski, F. Dawalibi, Y. Gervais, and D. Mukhedkar, *Effects of Sustained Ground Fault Current on Concrete Poles.* IEEE Transactions on Power Apparatus and Systems, August 1982. **Vol. PAS-101**(No. 8): p. 2686-2693.

63. F. Dawalibi and A. Pinho, *Computerized Analysis of Power Systems and Pipelines Proximity Effects.* IEEE Transactions on Power Delivery, April 1986. **Vol. PWRD-1**(No. 2): p. 40-48.

64. R.S. Baishiki, C.K. Osterberg, and F. Dawalibi, *Earth Resistivity Measurements Using Cylindrical Electrodes at Short Spacings.* IEEE Transactions on Power Delivery, January 1987. **Vol. 2**(No. 1): p. 64-71.

65. F. Dawalibi, *Electromagnetic Fields Generated by Overhead and Buried Short Conductors, Part I:Single Conductor.* IEEE Transactions on Power Delivery, October 1986. **Vol. 1**(No. 4): p. 105-111.

66. F.Dawalibi, *Electromagnetic Fields Generated by Overhead and Buried Short Conductors, Part 2:Ground Networks.* IEEE Transactions on Power Delivery, October 1986. **Vol. 1**(No. 4): p. 112-119.

67. G. Niles and F. Dawalibi, *Background and Methodology for Analyzing Step and Touch Potentials Near Transmission Structures, Part I - Background.* IEEE Transactions on Power Delivery, April 1986. **Vol. 1**(No. 2): p. 150-157.

68. G. Niles and F. Dawalibi, *Background and Methodology for Analyzing Step and Touch Potentials Near Transmission Structures, Part II - Engineering Evaluation.* IEEE Transactions on Power Delivery, April 1986. **Vol. 1**(No. 2): p. 158-162.

69. F. Dawalibi, R.D. Southey, and R.S. Baishiki, *Validity of Conventional Approaches for Calculating Body Currents Resulting from Electric Shocks.* IEEE Transactions on Power Delivery, April 1990. **Vol. 5**(No. 2): p. 613-626.

70. F. Dawalibi and R.D. Southey, *Analysis of Electrical Interference from Power Lines to Gas Pipelines, Part I - Computation Methods.* IEEE Transactions on Power Delivery, July 1989. **Vol. 4**(No. 3): p. 1840-1846.

71. F. Dawalibi and R.D. Southey, *Analysis of Electrical Interference from Power Lines to Gas Pipelines, Part II - Parametric Analysis.* IEEE Transactions on Power Delivery, January 1990. **Vol. 5**(No. 1): p. 415-421.

72. L. Grcev and F. Dawalibi, *An electromagnetic Model for Transients in Grounding Systems.* IEEE Transactions on Power Delivery, November 1990. **Vol. 5**(No. 4): p. 1773-1781.

73. F. Dawalibi and A. Selby, *Electromagnetic Fields or Energized Conductors.* IEEE Transactions on Power Delivery, July 1993. **Vol. 8**(No. 3): p. 1275-1284.

74. F. Dawalibi, W. Xiong, and J. Ma, *Effects of Deteriorated and Contaminated Substation Surface Covering Layers on Foot Resistance Calculations.* IEEE Transactions on Power Delivery, January 1993. **8**(1): p. 104-113.

75. W.K. Daily and F. Dawalibi, *Cost Reduction and Minimization of Land Based on an Accurate Determination of Fault Current Distribution in Neutral Conductors.* IEEE Transactions on Power Delivery, January 1993. **Vol. 8**(No. 1): p. 97-103.

76. J. Ma, F. Dawalibi, and W.K. Daily, *Analysis of Grounding Systems in Soils with Hemispherical Layering.* IEEE Transactions on Power Delivery, October 1993. **Vol. 8**(No. 4): p. 1773-1781.

77. F. Dawalibi, J. Ma, and R.D. Southey, *Behaviour of Grounding Systems in Multilayer Soils: A Parametric Analysis.* IEEE Transactions on Power Delivery, January 1994. **Vol. 9**(No. 1): p. 334-342.

78. F. Dawalibi and F. Donoso, *Integrated Analysis Software for Grounding, EMF, and EMI.* IEEE Computer Applications in Power, April 1993. **Vol. 6**(No. 2): p. 19-24.

79. R.D. Southey, F. Dawalibi, and W. Vukonich, *Recent Advances in the Mitigation of AC Voltages Occurring in Pipelines Located Close to Electric Transmission Lines.* IEEE Transactions on Power Delivery, April 1994. **Vol. 9**(No. 2): p. 1090-1097.

80. A. Selby and F. Dawalibi, *Determination of Current Distribution in Energized Conductors for the Computations of Electromagnetic Fields.* IEEE Transactions on Power Delivery, April 1994. **Vol. 9**(No. 2): p. 1069-1078.

81. F. Dawalibi, J. Ma, and W.K. Daily. *Electromagnetic Fields and Current Distribution in Electric Power Substations Subject to Unbalanced Currents and Phase to Ground Faults.* in *CIGRE Symposium on Power System Electromagnetic Compatibility.* October 1993. Lausanne, Switzerland.

82. W. Xiong, F. Dawalibi, and A. Selby. *Frequency Response of Substation Ground Systems Subject to Lightning Strikes.* in *CIGRE Symposium on Power System Electromagnetic Compatibility.* October 1993. Lausanne, Switzerland.

83. W.K. Daily, F. Dawalibi, A. Selby, and J. Ma. *Transient Electromagnetic Disturbances and Potential Rises Caused by Capacitor Switching in Power*

Substations. in *CIGRE Symposium on Power System Electromagnetic Compatibility*. October 1993. Lausanne, Switzerland.

84. W. Xiong and F. Dawalibi, *Transient Performance of Substation Grounding Systems Subjected to Lightning and Similar Surge Currents.* IEEE Transactions on Power Delivery, July 1994. **Vol. 9**(No. 3): p. 1412-1420.

85. F. Dawalibi, W. Xiong, and J. Ma, *Transient Performance of Substation Structures and Associated Grounding Systems.* IEEE Transactions on Industry Applications, May/June 1995. **Vol. 31**(No. 3): p. 520-527.

86. J. Ma, F. Dawalibi, and R.D. Southey, *On the Equivalence of Uniform and Two Layer Soils to Multilayer Soils in the Analysis of Grounding Systems.* IEE Proc. - Generation, Transmission and Distribution, January 1996. **Vol. 143**(No. 1): p. 49-55.

87. R.D. Southey, F. Dawalibi, and J. Ma. *Cost-Effective Mitigation of AC Voltages in Pipelines Located Close to Electric Transmission Lines*. in *Proceedings of International Conference on Electromagnetic Compatibility, ICEMC '95 KUL.* 11-13 April 1995. Kuala Lumpur, Malaysia.

88. W. Ruan, F. Dawalibi, and R.D. Southey. *Lightning Transient Response on Communication Towers and Associated Grounding Networks*. in *Proceedings of International Conference on Electromagnetic Compatibility, ICEMC '95 KUL.* 11-13 April 1995. Kuala Lumpur, Malaysia.

89. H.S. Lee, J.H. Kim, F. Dawalibi, and J. Ma, *Efficient Ground Grid Designs in Layered Soils.* IEEE Transactions on Power Delivery, July 1998. **Vol. 13**(No. 3): p. 457-461.

90. F. Dawalibi and D. Mukhedkar, *Optimum Design of Substation Grounding in a Two Layer Earth Structure - Part III, Study of Grounding Grids Performance and New Electrode Configurations.* IEEE Transactions, March/April 1975. **Vol. PAS-94**(No. 2): p. 267-272.

91. A. Selby and F. Dawalibi, *Determination of Current Distribution in Energized Conductors for the Computation of Electromagnetic Fields.* IEEE Transactions on Power Delivery, April 1994. **Vol. 9**(No. 2): p. 1069-1078.

92. J. Ma and F. Dawalibi. *Induced Effects on Parallel Circuits from Lightning Strokes on Transmission Lines.* in *Proceedings of International Conference on Electromagnetic Compatibility, ICEMC '95 KUL.* 11-13 April 1995. Kuala Lumpur, Malaysia.

93. W. Koch, *Grounding Methods for High-Voltage Stations with Grounded Neutrals, (Translated and reprinted as Appendix VI of AIEE-80, 1961).* Elektrotechnische Zeitschrift, February 1950. **Vol. 71**(No. 4): p. 89-91.

94. R.P. Keil, *The History and Future of IEEE-80, Guide for Substation Grounding.* 12-14 May 1982, presented at EPRI Workshop on High Voltage Power System Grounding: Atlanta.

95. A.J. McCrocklin and C.W. Wendlandt, *Determination of Resistance to Ground of Grounding Grids.* AIEE Trans. PAS, 1952. **Vol. 71**(No. 3): p. 1062-1064.

96. H.R. Amstrong, *Grounding Electrode Characteristics from Model Tests.* AIEE Trans. PAS, December 1953. **Vol. 72**(No. 3): p. 1301-1306.

97. H. Schmidt, *Fundamentals of Measuring Techniques for Model Test of Earthing Arrangements.* Elektrotechnische Zeitschrift (Abstract in AIEE Transactions PAS, Vol. 77, April 1960, pp. 56-57), 1954. **Vol. 75**(No. 17): p. 557-559.

98. N. Faletti, C. Rossignani, and G. Malaman, *Some Results of Model test on Earthing Installations for High-Voltage Stations.* Energia Elett., 1955. **Vol. 32**: p. 1109-1116.

99. C. Rossignani and C. Rostagno, *Results of Model Tests on the Earthing of Substations.* Energia Elett., 1958. **Vol. 35**: p. 471-475.

100. B. Thapar and K.K. Puri, *Mesh Potentials in High Voltage Grounding Grids.* IEEE Transactions, 1967. **Vol. PAS-86**: p. 249-254.

101. A.A. Voronina, *Contact Voltages and the Potential of Complex Ground Connections with Homogeneous Soil Model Tests.* Elektrichestvo, 1969(No. 7): p. 52-56.

102. D. Mukhedkar, Y. Gervais, and J. Dejean, *Modelling of a Grounding Electrode.* IEEE TRansactions PAS, Jan/Feb 1973. **Vol. 92**: p. 295-297.

103. P. Kouteynikoff, *Numerical Computation of the Grounding Resistance of Substation and Towers.* IEEE Transactions, May/June 1980. **Vol. PAS-99**(No. 3): p. 957-965.

104. R.P. Keil, *Model Test to Investigate Fence Grounding in a Substation.* April 1973, University of Dayton, Dayton: Ohio.

105. R.L. Boylestad, *Introductory Circuit Analysis.* 5th Edition ed. 1987: Merrill Publishing Co., A. Bell & Howell Co.

106. W.H. Hayt, J.E. Kemmerly, and S.M. Durbin, *Engineering Circuit Analysis*. 6th edition ed. 2002: McGraw Hill.

107. E. Hughes, *Electrical Technology*. 6th edition ed. 1987: Longman Scientific & Technical.

108. H. Cotton, *Electrical Technology*. Seventh ed. 1965: Sir Isaac Pitman & Sons Ltd.

109. C.W. Davies, *The Conductivity of Solutions*. 2nd edition ed. 1933: Chapman & Hall Ltd.

110. R.A. Robinson and R.H. Stokes, *Electrolyte Solutions*. 2nd edition ed. 1959: Butterworths.

111. L. Kirkup, *Experimental Methods: An Introduction to the Analysis and Presentation of Data*. 1994: John Wiley & Sons, Inc.

112. M. Pentz and M. Shott, *Handling Experimental Data*. 1988: Open University Press.

113. B.J. Brinkworth, *An Introduction to Experimentation*. 1973: Hodder and Stoughton.

114. D.C. Baird, *Experimentation: An Introduction To Measurement Theory and Experiment Design*. Third Edition ed. 1995: Prentice Hall Inc.

115. J.R. Taylor, *An Introduction to Error Analysis : The Study of Uncertainties in Physical Measurement*. 1982: University Science Books, Oxford University Press.

116. G.F. Tagg, *Multiple Driven Rod Earth Connection.* IEE Proceedings, 1980. **Vol. 127**(No. 4): p. 240-247.

117. J. Ma and F.P. Dawalibi. *Modern Computational Methods for the Design and Analysis of Power System Grounding.* in *Proceedings of the 1998 International Conference on Power System Technology.* 18-21 August, 1998. Beijing.

118. J.A. Sullivan, *Alternative Earthing Calculations for Grids and Rods.* IEE Proceedings - Generation, Transmission, and Distribution, 1998. **Vol. 45**(No. 3): p. 271-280.

119. E.K.N. Yung and W.Y. Tam, *Analysis of a Circular Earthing Plate.* Proc. IEE, Pt. C, November 1989. **Vol. 136**(No. 6): p. 385-390.

120. R.L. Stoll, *Private communication.* 2002.

121. L.M. Popovic, *Proximity Effect Between an Earthing Grid and External Electrodes in an Earthing System of High-voltage Installations.* IEE Proceedings, Pt. C, 1986. **Vol. 133**(No. 6): p. 346-352.

122. R. Caldecott and D.G. Kasten, *Scale Model Studies of Station Grounding Grids.* IEEE Transactions, 1983. **Vol. PAS-102**: p. 558-566.

APPENDIX 1

Analytical solution for a vertical earthing rod of circular cross-section

The rod is of length l and radius "a" in soil of uniform conductivity σ. If the axis of the rod coincides with the z-axis of a circular-cylindrical co-ordinate system with its origin at depth d below the surface of the earth, the electric potential is defined by Laplace's equation:

$$\frac{\partial^2 V}{\partial r^2}+\left(\frac{1}{r}\right)\frac{\partial V}{\partial r}+\frac{\partial^2 V}{\partial z^2}=0 \qquad (1)$$

$z=d$ is the surface of the earth on which $\partial V/\partial z=0$ (because current can only flow parallel to the surface), and the plane $z=0$ is assumed to be the true earth plane on which $V=0$. The outer radial boundary is allowed to go to infinity with V tending to zero for large values of r. The surface $r=a$ is taken as the inner boundary and over the rod length l a specified current I is injected into the soil. No current is assumed to flow out of the remaining thin column of soil below the tip of the rod (defined by the surface $r=a$, $0<z<c$, where $c=d-l$), because the cross-sectional area of the tip is so much smaller than the cylindrical surface area of the rod.

In the first stage of the work the potential of the rod, not the injected current, was specified and considerable effort was directed towards defining the zone below the tip of the rod as a separate region and solving the resulting two-region problem using appropriate interface conditions. However, the solution was found to be dominated by the outer region, even when the latter was reduced in size by specifying an outer radial boundary at $r=b$, where b was of the same order as the depth d. Not only were the values of the potentials close to the interface in error (as indicated by significant spatial oscillation), but the computed earth resistance of the rod exhibited convergence problems.

With the single region problem, the specification of a potential on the surface of the rod is not possible because the function $V_{r=a}=f(z)$ required for the continuation of this Dirichlet boundary condition on the remainder of the surface below the tip of the rod is unknown (only the end point potentials at $z=0$ and $z=c$ are known). It is however possible to specify $\partial V/\partial r$ by using some reasonable assumption about the way in which the injected current is distributed over the rod surface, together with $\partial V/\partial r=0$ over the lower section $0<z<c$. The more obvious assumption is to specify constant injected current density, so that on $r=a$, $c<z<d$,

$$\left.\frac{\partial V}{\partial r}\right|_{r=a}=-\frac{J_{av}}{\sigma}=-\frac{I}{2\Pi a l\sigma} \qquad (2)$$

since $E_r = J_r/\sigma = -\partial V/\partial r$. Eqn. 2 was used for a large number of solutions but suffers from the disadvantage that the potential of the rod is not constant, the potential at z=d (the surface of the earth) being typically 5% to 10% higher than the average value. The affect on the computed resistance, defined as V_{av}/I, is less than 1%, but the non-uniform potential can be partly rectified by imposing a linear injected current density of the form

$$J_r = \left(\frac{2J_{av}}{l}\right)\left[z(1-x) - \left\{(d-l) - x\left(d - \frac{l}{2}\right)\right\}\right] \qquad (3)$$

where x>1 (typically 1.1) is found to improve the uniformity. J_r now replaces J_{av} in eqn. 2.

The solution of eqn. 1 involves sine functions in z (cosines are eliminated because V=0 at z=o) and zero-order modified Bessel functions of the second kind (K_o), which tend to zero as r goes to infinity as required. Thus we have a series solution of the form

$$V = \sum_m A_m K_o(p_m r) \sin(p_m z) \qquad (4)$$

In order to satisfy $\partial V/\partial z=0$ at $z=d$ the separation constant p_m must satisfy the condition $\cos(p_m d)=0$ or $p_m d = m\pi/2$, where m is an odd integer, giving

$$p_m = m\pi/2d \qquad (5)$$

The interior solution for $\partial V/\partial r$ at r=a is therefore (bearing in mind that $K_o'(x) = -K_1(x)$)

$$\frac{\partial V}{\partial r} = -\sum_m \left(\frac{m\Pi}{2d}\right) A_m K_1\left(\frac{m\Pi a}{2d}\right) \sin\left(\frac{m\Pi z}{2d}\right) \qquad (6)$$

But on the boundary r=a the potential gradient is given by zero over the range 0<z<c, and by eqns. 2 and 3 for c<z<d. The Fourier coefficients for the two solutions must be identical and so we have

$$\int_0^d \sum_m \left(\frac{m\Pi}{2d}\right) A_m K_1\left(\frac{m\Pi a}{2d}\right) \sin\left(\frac{m\Pi z}{2d}\right) \sin\left(\frac{n\Pi z}{2d}\right) dz =$$

$$\int_0^c (0) \sin\left(\frac{n\Pi z}{2d}\right) dz + \int_c^d \left(\frac{-2J_{av}}{\sigma l}\right)\left[z(1-x)\sin\left(\frac{n\Pi z}{2d}\right) - \left\{(d-1) - x\left(d - \frac{l}{2}\right)\right\}\sin\left(\frac{n\Pi z}{2d}\right)\right] dz$$

After some work it can be shown that, with $m\pi/2d$ written again as p_m for brevity,

$$A_m = I\frac{\left[xl\cos(p_m c)+2(1-x)\left\{\sin\left(\frac{m\Pi}{2}\right)-\sin(p_m c)\right\}p_m^{-1}\right]}{\left[\Pi a d l^2 \sigma p_m{}^2 K_1(p_m a)\right]} \tag{7}$$

Thus the potential given by eqn. 4 is now fully defined and, in particular, on the surface of the earth we have

$$V_{z=d} = \sum_m A_m \sin\left(\frac{m\Pi}{2}\right)K_o(p_m r) \tag{8}$$

(with m odd only)

Also the average value of the potential on the surface of the rod is given by

$$V_{av} = I^{-1}\int_c^d \sum_m A_m K_o(p_m a)\sin(p_m z)dz = \sum_m A_m K_0(p_m a)\cos\frac{(p_m c)}{l p_m} \tag{9}$$

The resistance of the rod to true earth is then: $R = V_{av}/I$ (10)

The current distribution flowing into the true earth plane at z=0 is simply given by

$$J_z = \sigma E_z = -\frac{\sigma\partial V}{\partial z} = -\sigma\sum_m A_m p_m K_0(p_m r) \tag{11}$$

A plot of J_z as a function of *r* may be of interest when examining whether the depth *d* selected is sufficiently large, although the decreasing sensitivity of the resistance to *d* as the latter is increased is probably a sufficient test.

APPENDIX 2

Simulation technique for compensating the finite size of the tank

We require to find the resistance between r=b and r $\rightarrow \infty$ assuming the equipotentials have now become hemispheres for r ≥ b, where b is the hemispherical radius representing the cylindrical tank. In this region V(r) obeys Laplaces equation with solution

$V = K_1 r^{-1} + K_2$

As r $\rightarrow \infty$, V $\rightarrow$ 0 so that K_2=0. Also, if the current I crosses r=b with **uniform density,** we have

$$J_r = \frac{I}{2\Pi b^2} = \sigma E_r = -\sigma \frac{\partial V}{\partial r}_{r=b|}$$

Now

$$\frac{\partial V}{\partial r} = -K_1 r^{-2}$$

So that

$$\frac{\partial V}{\partial r}_{r=b} = -K_1 b^{-2}$$

And

$$\sigma K_1 b^{-2} = \frac{I}{2\Pi b^2}$$

$$\therefore K_1 = \frac{I}{2\Pi\sigma}$$

$$\therefore V = \frac{I}{2\Pi\sigma} r^{-1}$$

At r=b,

$$\therefore V_b = \frac{I}{2\Pi\sigma b}$$

This is consistent with taking the resistance of a hemispherical electrode of radius b, ie.

$$\therefore R_e = \frac{I}{2\Pi\sigma b}$$

Experimentally, R_e can be placed in series with the tank. The surface potentials measured will then be approximately compensated.

APPENDIX 3

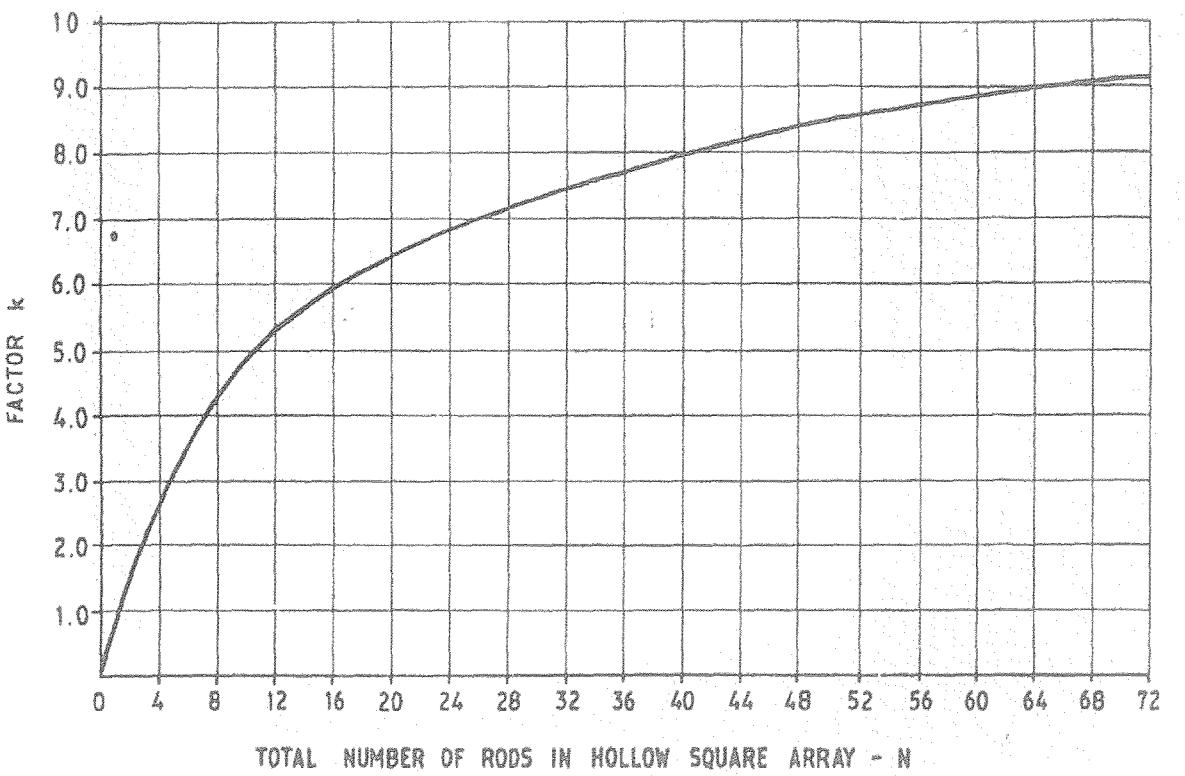

Figure 18 from S34, page 46
Curve for Evaluating Formula in Column 6, Table 1 S34

Electrode Description	Resistance of the electrode systems (ohms)								
	CASE 1			CASE 2			CASE 3		
	CDEGS	S34	Difference= S34 – CDEGS	CDEGS	S34	Difference= S34 – CDEGS	CDEGS	S34	Difference= S34 – CDEGS
Buried Grid	0.4841	0.5264	0.0423	0.7522	0.9973	0.2451	3.9526	5.4311	1.4785
Group of rods in hollow square	**0.6617**	**4.2307**	**3.5690**	0.7318	0.9195	0.1877	**4.4534**	**10.1319**	**5.6785**
Combined grid with rods connected around periphery	0.4817	0.5264	0.0447	0.68108	0.9977	0.31662	3.8606	5.4278	1.5672

Table 1: For cases 1,2, and 3

Electrode Description	Resistance of the electrode systems (ohms)								
	CASE 4			CASE 5			CASE 6		
	CDEGS	S34	Difference= S34 – CDEGS	CDEGS	S34	Difference= S34 – CDEGS	CDEGS	S34	Difference= S34 – CDEGS
Buried Grid	0.5256	0.5264	0.0008	0.8742	0.9973	0.1231	4.7285	5.4311	0.7026
Group of rods in hollow square	**0.7679**	**4.2307**	**3.4628**	0.8351	0.9195	0.0844	**5.5822**	**10.1319**	**4.5497**
Combined grid with rods connected around periphery	0.5221	0.5264	0.0043	0.7678	0.9977	0.2299	4.5719	5.4278	0.8559

Table 2: Depth of buried grid and rods decreased to 0.05m

Electrode Description	Resistance of the electrode systems (ohms)								
	CASE 7			CASE 8			CASE 9		
	CDEGS	S34	Difference= S34 – CDEGS	CDEGS	S34	Difference= S34 – CDEGS	CDEGS	S34	Difference= S34 – CDEGS
Buried Grid	Not applicable : same as Case 4			Not applicable : same as Case 5			Not applicable : same as Case 6		
Group of rods in hollow square	**0.7207**	**1.8741**	**1.1534**	0.6814	0.7812	0.0998	**4.6605**	**5.6974**	**1.0369**
Combined grid with rods connected around periphery	0.5123	0.5257	0.0134	0.6646	1.0030	0.3384	4.1685	5.3597	1.1912

Table 3: Length of rods increased to 3m

Electrode Description	Resistance of the electrode systems (ohms)								
	CASE 10			CASE 11			CASE 12		
	CDEGS	S34	Difference= S34 – CDEGS	CDEGS	S34	Difference= S34 – CDEGS	CDEGS	S34	Difference= S34 – CDEGS
Buried Grid	Not applicable : same as Case 4			Not applicable : same as Case 5			Not applicable : same as Case 6		
Group of rods in hollow square	**0.5948**	**0.8391**	**0.2443**	0.4300	0.6641	0.2341	**3.1479**	**3.6199**	**0.472**
Combined grid with rods connected around periphery	0.4762	0.5169	0.0407	0.42995	1.0250	0.5951	3.0941	6.0609	2.9668

Table 4: Length of rods increased to 10m

APPENDIX 5

Results for rods without links

Experimental water conductivity = 0.0580 S/m
External resistor = 2.74 Ω
S.D. = standard deviation

A) RESISTANCE VALUES (scaled to 0.1 S/m)

Electrode Configuration	Resistance, R (Ω)				
	CDEGS MALT	Ellipsoid	Experiment		
			Resistance (Ω)	Equipment error (±Ω)	S.D. (Ω)
4 rods (c = 60mm)	47.77	47.15	48.50	2.11	0.05
4 rods (c = 120 mm)	40.95	39.78	41.40	1.81	0.05
4 rods (c = 180 mm)	38.27	36.99	38.77	1.70	0.04
8 rods (c = 60 mm)	29.57	29.37	30.10	1.34	0.05
8 rods (c = 90 mm)	25.61	25.14	26.01	1.17	0.05
8 rods (c = 120 mm)	23.44	22.87	23.90	1.08	0.02
12 rods (c = 60 mm)	21.85	21.72	22.03	1.01	0.05
16 rods (c = 60 mm)	17.49	17.39	17.70	0.83	0.04

B) SURFACE POTENTIAL DISTRIBUTION

(1) 4 rods without links (c = 60 mm)

Angle	Distance, d (mm)	Surface Potential, Vs (V)				Distance, d (mm)	Surface Potential, Vs (V)
		CDEGS MALT	Experiment				Ellipsoid
			Vs (V)	Equipment error (±V)	S.D. (Ω)		
0°	0	12.73	12.90	0.30	0.03	0	12.90
	15	12.78	12.95	0.30	0.03	15	12.95
	45	11.28	11.37	0.30	0.03	45	11.43
	75	8.22	8.30	0.30	0.03	75	8.33
	105	6.15	6.21	0.30	0.03	105	6.24
	150	4.39	4.44	0.30	0.03	150	4.45
	250	2.66	2.70	0.30	0.03	250	2.64
	350	1.90	1.93	0.30	0.03	350	1.95
	450	1.48	1.52	0.30	0.03	450	1.50
	550	1.21	1.24	0.30	0.03	550	1.22
	650	1.02	1.04	0.30	0.03	650	1.12
45°	0	12.73	12.88	0.30	0.03	0	12.9
	65	10.14	10.24	0.30	0.03	65	10.53
	107	6.14	6.23	0.30	0.03	107	6.30
	150	4.42	4.49	0.30	0.03	150	4.52
	200	3.32	3.38	0.30	0.03	200	3.17
	300	2.22	2.26	0.30	0.03	300	2.27
	400	1.66	1.71	0.30	0.03	400	1.67
	500	1.33	1.37	0.30	0.03	500	1.33
	600	1.11	1.14	0.30	0.03	600	1.10

(2) 4 rods without links (c =120 mm)

Angle	Distance, d (mm)	Surface Potential, Vs (V)				Distance, d (mm)	Surface Potential, Vs (V)
		CDEGS MALT	Experiment				Ellipsoid
			Vs (V)	Equipment error (±V)	S.D. (Ω)		
0°	0	8.53	8.71	0.33	0.02	0	8.78
	15	8.57	8.73	0.33	0.02	15	8.82
	45	8.66	8.81	0.33	0.02	45	8.92
	75	8.13	8.23	0.33	0.02	75	8.37
	105	6.92	7.01	0.33	0.02	105	7.05
	150	5.19	5.25	0.33	0.02	150	5.34
	250	3.14	3.19	0.33	0.02	250	3.17
	350	2.24	2.29	0.33	0.02	350	2.34
	450	1.73	1.77	0.33	0.02	450	1.79
	550	1.42	1.45	0.33	0.02	550	1.45
	650	1.20	1.22	0.33	0.02	650	1.34
45°	0	8.53	8.68	0.33	0.02	0	8.78
	65	10.64	10.79	0.33	0.02	65	10.79
	107	9.26	9.36	0.33	0.02	107	9.56
	150	5.70	5.79	0.33	0.02	150	5.94
	200	4.08	4.17	0.33	0.02	200	3.99
	300	2.63	2.69	0.33	0.02	300	2.74
	400	1.96	2.02	0.33	0.02	400	2.00
	500	1.56	1.59	0.33	0.02	500	1.58
	600	1.30	1.32	0.33	0.02	600	1.31

(3) 4 rods without links (c = 180 mm)

Angle	Distance, d (mm)	Surface Potential, Vs (V)				Distance, d (mm)	Surface Potential, Vs (V)
		CDEGS MALT	Experiment				Ellipsoid
			Vs (V)	Equipment error (±Ω)	SD (Ω)		
0°	0	6.31	6.48	0.34	0.04	0	6.53
	15	6.33	6.49	0.34	0.04	15	6.55
	45	6.43	6.57	0.34	0.04	45	6.65
	75	6.46	6.59	0.34	0.04	75	6.68
	105	6.19	6.28	0.34	0.04	105	6.41
	150	5.28	5.34	0.34	0.04	150	5.46
	250	3.41	3.45	0.34	0.04	250	3.45
	350	2.42	2.47	0.34	0.04	350	2.54
	450	1.87	1.90	0.34	0.04	450	1.94
	550	1.53	1.56	0.34	0.04	550	1.57
	650	1.29	1.31	0.34	0.04	650	1.35
45°	0	6.32	6.47	0.34	0.04	0	6.53
	65	6.86	7.00	0.34	0.04	65	7.06
	107	9.65	9.78	0.34	0.04	107	9.78
	150	8.72	8.80	0.34	0.04	150	8.89
	200	4.99	5.06	0.34	0.04	200	4.81
	300	2.94	3.01	0.34	0.04	300	3.07
	400	2.14	2.18	0.34	0.04	400	2.19
	500	1.69	1.72	0.34	0.04	500	1.72
	600	1.40	1.43	0.34	0.04	600	1.41

(4) 8 rods without links (c = 60 mm)

Angle	Distance, d (mm)	Surface Potential, Vs (V)				Distance, d (mm)	Surface Potential, Vs (V)
		CDEGS MALT	Experiment				Ellipsoid
			Vs (V)	Equipment error (±Ω)	SD (Ω)		
0°	0	13.7	13.84	0.40	0.03	0	13.77
	15	13.77	13.89	0.40	0.03	15	13.86
	45	15.00	15.12	0.40	0.03	45	15.09
	75	13.77	13.85	0.40	0.03	75	13.86
	105	10.15	10.23	0.40	0.03	105	10.23
	150	7.25	7.33	0.40	0.03	150	7.30
	250	4.34	4.41	0.39	0.03	250	4.29
	350	3.09	3.13	0.39	0.03	350	3.16
	450	2.40	2.44	0.39	0.03	450	2.42
	550	1.96	1.98	0.39	0.03	550	1.96
	650	1.66	1.68	0.39	0.03	650	1.81
45°	0	13.7	13.84	0.40	0.03	0	13.77
	65	14.32	14.46	0.40	0.03	65	14.37
	107	11.44	11.54	0.40	0.03	107	11.69
	150	7.55	7.63	0.40	0.03	150	7.69
	200	5.52	5.58	0.40	0.03	200	5.44
	300	3.62	3.66	0.39	0.03	300	3.69
	400	2.70	2.74	0.39	0.03	400	2.70
	500	2.16	2.18	0.39	0.03	500	2.14
	600	1.80	1.82	0.39	0.03	600	1.77

(5) 8 rods without links (c = 90 mm)

Angle	Distance, d (mm)	Surface Potential, Vs (V)				Distance, d (mm)	Surface Potential, Vs (V)
		CDEGS MALT	Experiment				Ellipsoid
			Vs (V)	Equipment error (±Ω)	SD (Ω)		
0°	0	11.12	11.28	0.44	0.03	0	11.32
	15	11.16	11.3	0.44	0.03	15	11.36
	45	11.61	11.75	0.44	0.03	45	11.82
	75	13.55	13.67	0.44	0.03	75	13.79
	105	12.86	12.94	0.44	0.03	105	13.09
	150	8.58	8.66	0.44	0.03	150	8.74
	250	5.10	5.16	0.43	0.03	250	5.10
	350	3.61	3.67	0.43	0.03	350	3.73
	450	2.79	2.83	0.43	0.03	450	2.84
	550	2.27	2.29	0.43	0.03	550	2.30
	650	1.92	1.94	0.43	0.03	650	2.12
45°	0	11.12	11.26	0.44	0.03	0	11.32
	65	11.53	11.67	0.44	0.03	65	11.73
	107	12.65	12.77	0.44	0.03	107	12.78
	150	10.74	10.82	0.44	0.03	150	10.90
	200	6.91	6.99	0.43	0.03	200	6.80
	300	4.29	4.35	0.43	0.03	300	4.42
	400	3.16	3.20	0.43	0.03	400	3.20
	500	2.51	2.55	0.43	0.03	500	2.51
	600	2.09	2.11	0.43	0.03	600	2.07

(6) 8 rods without links (c = 120 mm)

Angle	Distance, d (mm)	Surface Potential, Vs (V)				Distance, d (mm)	Surface Potential, Vs (V)
		CDEGS MALT	Experiment				Ellipsoid
			Vs (V)	Equipment error (±Ω)	SD (Ω)		
0°	0	9.32	9.48	0.46	0.03	0	9.55
	15	9.34	9.48	0.46	0.03	15	9.57
	45	9.56	9.70	0.46	0.03	45	9.80
	75	10.25	10.37	0.46	0.03	75	10.51
	105	12.63	12.75	0.46	0.03	105	12.94
	150	10.15	10.23	0.46	0.03	150	10.40
	250	5.68	5.76	0.46	0.03	250	5.71
	350	4.00	4.06	0.46	0.03	350	4.16
	450	3.08	3.12	0.46	0.03	450	3.16
	550	2.50	2.52	0.46	0.03	550	2.54
	650	2.11	2.13	0.46	0.03	650	2.16
45°	0	9.32	9.46	0.46	0.03	0	9.55
	65	9.62	9.74	0.46	0.03	65	9.85
	107	9.88	10.00	0.46	0.03	107	10.12
	150	11.65	11.77	0.46	0.03	150	11.78
	200	9.38	9.46	0.46	0.03	200	9.29
	300	4.92	4.98	0.46	0.03	300	5.11
	400	3.53	3.57	0.46	0.03	400	3.59
	500	2.77	2.79	0.46	0.03	500	2.80
	600	2.30	2.32	0.46	0.03	600	2.30

(7) 12 rods without links (c = 60 mm)

Angle	Distance, d (mm)	Surface Potential, Vs (V)				Distance, d (mm)	Surface Potential, Vs (V)
		CDEGS MALT	Experiment				Ellipsoid
			Vs (V)	Equipment error (±Ω)	SD (Ω)		
0°	0	13.24	13.40	0.49	0.03	0	13.31
	15	13.29	13.43	0.49	0.03	15	13.36
	45	13.7	13.82	0.49	0.03	45	13.78
	75	14.47	14.59	0.49	0.03	75	14.55
	105	13.59	13.67	0.49	0.03	105	13.67
	150	10.05	10.13	0.49	0.03	150	10.19
	250	5.98	6.04	0.49	0.03	250	5.90
	350	4.23	4.27	0.49	0.03	350	4.32
	450	3.27	3.29	0.49	0.03	450	3.29
	550	2.66	2.68	0.49	0.03	550	2.66
	650	2.25	2.27	0.49	0.03	650	2.46
45°	0	13.24	13.38	0.49	0.03	0	13.31
	65	14.05	14.19	0.49	0.03	65	14.10
	107	14.72	14.84	0.49	0.03	107	14.77
	150	11.98	12.08	0.49	0.03	150	12.29
	200	7.98	8.06	0.49	0.03	200	7.79
	300	5.01	5.07	0.49	0.03	300	5.10
	400	3.70	3.74	0.49	0.03	400	3.70
	500	2.94	2.96	0.49	0.03	500	2.91
	600	2.44	2.46	0.49	0.03	600	2.40

(8) 16 rods without links (c = 60 mm)

Angle	Distance, d (mm)	Surface Potential, Vs (V)				Distance, d (mm)	Surface Potential, Vs (V)
		CDEGS MALT	Experiment				Ellipsoid
			Vs (V)	Equipment error (±Ω)	SD (Ω)		
0°	0	12.77	12.93	0.58	0.03	0	12.84
	15	12.80	12.94	0.58	0.03	15	12.87
	45	13.07	13.19	0.58	0.03	45	13.14
	75	13.73	13.87	0.58	0.03	75	13.81
	105	15.42	15.54	0.58	0.03	105	15.51
	150	13.02	13.12	0.58	0.03	150	13.10
	250	7.63	7.71	0.57	0.03	250	7.52
	350	5.35	5.41	0.57	0.03	350	5.47
	450	4.12	4.16	0.57	0.03	450	4.15
	550	3.35	3.37	0.57	0.03	550	3.34
	650	2.83	2.85	0.57	0.03	650	3.09
45°	0	12.77	12.91	0.58	0.03	0	12.84
	65	13.36	13.50	0.58	0.03	65	13.39
	107	14.25	14.37	0.58	0.03	107	14.30
	150	14.97	15.09	0.58	0.03	150	15.03
	200	11.53	11.61	0.58	0.03	200	11.47
	300	6.50	6.54	0.57	0.03	300	6.62
	400	4.70	4.74	0.57	0.03	400	4.70
	500	3.71	3.75	0.57	0.03	500	3.67
	600	3.07	3.09	0.57	0.03	600	3.01

APPENDIX 6

Results for rods with horizontal links

A) RESISTANCE VALUES

Electrode Configuration	Resistance, R (Ohm)				
	CDEGS MALT	S34	Experiment		
			Resistance (Ω)	Equipment error (±Ω)	S.D. (Ω)
4 rods in hollow square (c = 120mm)	30.03	39.99	30.52	1.36	0.04
4 rods in hollow square (c = 240mm)	19.33	35.67	19.65	0.92	0.03
8 rods in hollow square (c = 60mm)	26.78	29.95	27.20	1.23	0.04
8 rods in hollow square (c = 120mm)	17.74	22.81	18.01	0.85	0.03
16 rods in hollow square (c = 60mm)	16.02	17.80	16.30	0.78	0.03
Combined grids with 8 rods connected in periphery (c = 60 mm)	26.38	28.61	26.80	1.20	0.04
Combined grids with 8 rods connected in periphery (c = 120 mm)	16.85	19.70	17.11	0.81	0.05
Combined grids with 16 rods connected in periphery (c = 60 mm)	14.42	17.78	14.66	0.71	0.04
Buried grid (120 x 120 mm^2)	38.00	50.82	38.60	1.69	0.02
Buried grid (240 x 240 mm^2)	18.84	22.63	19.16	0.89	0.03
25 rods with 240 x 240 mm^2 grid (c = 60 mm)	14.91	-	15.10	0.73	0.04
21 rods with 240 x 240 mm^2 grid (c = 60 mm)	15.05	-	15.29	0.73	0.04
17 rods with 240 x 240 mm^2 grid (c = 60 mm)	15.20	-	15.45	0.74	0.04

B) SURFACE POTENTIAL DISTRIBUTION

(1) 4 rods in hollow square (c = 120 mm)

Angle (degree)	Distance from centre, d (mm)	Surface potential,Vs (V)			
		CDEGS MALT	Experiment		
			Vs (V)	Equipment error (±V)	S.D. (Ω)
0	150	7.24	7.32	0.40	0.02
	250	4.30	4.36	0.39	0.02
	350	3.05	3.09	0.39	0.02
	450	2.37	2.39	0.39	0.02
	550	1.93	1.95	0.39	0.02
	650	1.63	1.65	0.39	0.02
45	200	5.53	5.57	0.39	0.02
	300	3.59	3.63	0.39	0.02
	400	2.67	2.69	0.39	0.02
	500	2.13	2.15	0.39	0.02
	600	1.77	1.79	0.39	0.02

(2) 4 rods in hollow square (c = 240 mm)

Angle (degree)	Distance from centre, d (mm)	Surface potential,Vs (V)			
		CDEGS MALT	Experiment		
			Vs (V)	Equipment error (±V)	S.D. (Ω)
0	150	11.96	12.04	0.54	0.02
	250	6.93	6.99	0.54	0.02
	350	4.86	4.9	0.53	0.02
	450	3.74	3.76	0.53	0.02
	550	3.04	3.06	0.53	0.02
	650	2.56	2.58	0.53	0.02
45	200	11.73	11.77	0.54	0.02
	300	6.02	6.06	0.54	0.02
	400	4.29	4.31	0.53	0.02
	500	3.38	3.4	0.53	0.02
	600	2.79	2.81	0.53	0.02

(3) 8 rods in hollow square (c = 60 mm)

Angle (degree)	Distance from centre, d (mm)	Surface potential,Vs (V)			
		CDEGS MALT	Experiment		
			Vs (V)	Equipment error (±V)	S.D. (Ω)
0	150	8.08	8.14	0.43	0.02
	250	4.81	4.87	0.43	0.02
	350	3.42	3.46	0.42	0.02
	450	2.65	2.67	0.42	0.02
	550	2.17	2.19	0.42	0.02
	650	1.83	1.85	0.42	0.02
45	200	6.13	6.17	0.43	0.02
	300	4.00	4.04	0.42	0.02
	400	2.99	3.01	0.42	0.02
	500	2.38	2.40	0.42	0.02
	600	1.99	2.01	0.42	0.02

(4) 8 rods in hollow square (c = 120 mm)

Angle (degree)	Distance from centre, d (mm)	Surface potential,Vs (V)			
		CDEGS MALT	Experiment		
			Vs (V)	Equipment error (±V)	S.D. (Ω)
0	150	13.78	13.84	0.57	0.02
	250	7.58	7.64	0.57	0.02
	350	5.29	5.33	0.57	0.02
	450	4.07	4.09	0.57	0.02
	550	3.31	3.33	0.57	0.02
	650	2.79	2.81	0.57	0.02
45	200	12.07	12.11	0.57	0.02
	300	6.47	6.51	0.57	0.02
	400	4.66	4.68	0.57	0.02
	500	3.67	3.69	0.57	0.02
	600	3.03	3.05	0.57	0.02

(5) 16 rods in hollow square (c = 60 mm)

Angle (degree)	Distance from centre, d (mm)	Surface potential,Vs (V)			
		CDEGS MALT	Experiment		
			Vs (V)	Equipment error (±V)	S.D. (Ω)
0	150	14.64	14.72	0.62	0.02
	250	8.37	8.43	0.62	0.02
	350	5.85	5.89	0.62	0.02
	450	4.5	4.52	0.62	0.02
	550	3.66	3.68	0.62	0.02
	650	3.09	3.11	0.62	0.02
45	200	12.73	12.77	0.62	0.02
	300	7.1	7.14	0.62	0.02
	400	5.14	5.16	0.62	0.02
	500	4.05	4.07	0.62	0.02
	600	3.36	3.38	0.62	0.02

(6) Combined grids with 8 rods connected in periphery (c = 60 mm)

Angle (degree)	Distance from centre, d (mm)	Surface potential,Vs (V)			
		CDEGS MALT	Experiment		
			Vs (V)	Equipment error (±V)	S.D. (Ω)
0	150	8.19	8.25	0.43	0.01
	250	4.88	4.94	0.43	0.01
	350	3.47	3.51	0.43	0.01
	450	2.69	2.71	0.43	0.01
	550	2.19	2.21	0.43	0.01
	650	1.86	1.88	0.43	0.01
45	200	6.21	6.25	0.43	0.01
	300	4.06	4.10	0.43	0.01
	400	3.03	3.05	0.43	0.01
	500	2.42	2.44	0.43	0.01
	600	2.02	2.04	0.43	0.01

(7) **Combined grid with 8 rods connected in periphery (c = 120 mm)**

Angle (degree)	Distance from centre, d (mm)	Surface potential,Vs (V)			
		CDEGS MALT	Experiment		
			Vs (V)	Equipment error (±V)	S.D. (Ω)
0	150	14.38	14.44	0.59	0.01
	250	7.94	8.00	0.59	0.01
	350	5.56	5.60	0.59	0.01
	450	4.28	4.30	0.59	0.01
	550	3.48	3.50	0.59	0.01
	650	2.93	2.95	0.59	0.01
45	200	12.32	12.36	0.59	0.01
	300	6.75	6.79	0.59	0.01
	400	4.88	4.90	0.59	0.01
	500	3.85	3.87	0.59	0.01
	600	3.19	3.21	0.59	0.01

(8) **Combined grid with 16 rods connected in periphery (c = 60 mm)**

Angle (degree)	Distance from centre, d (mm)	Surface potential,Vs (V)			
		CDEGS MALT	Experiment		
			Vs (V)	Equipment error (±V)	S.D. (Ω)
0	150	15.14	15.2	0.67	0.01
	250	8.74	8.80	0.67	0.01
	350	6.13	6.17	0.67	0.01
	450	4.72	4.74	0.67	0.01
	550	3.84	3.86	0.67	0.01
	650	3.24	3.26	0.67	0.01
45	200	13.02	13.06	0.67	0.01
	300	7.41	7.45	0.67	0.01
	400	5.38	5.40	0.67	0.01
	500	4.25	4.27	0.67	0.01
	600	3.52	3.54	0.67	0.01

(9) **Buried grid (120 x 120 mm^2)**

Angle (degree)	Distance from centre, d (mm)	Surface potential,Vs (V)			
		CDEGS MALT	Experiment		
			Vs (V)	Equipment error (±V)	S.D. (Ω)
0	150	5.81	5.87	0.34	0.03
	250	3.40	3.46	0.34	0.03
	350	2.41	2.45	0.34	0.03
	450	1.87	1.89	0.34	0.03
	550	1.53	1.55	0.34	0.03
	650	1.29	1.31	0.34	0.03
45	200	4.31	4.35	0.34	0.03
	300	2.82	2.86	0.34	0.03
	400	2.11	2.13	0.34	0.03
	500	1.68	1.70	0.34	0.03
	600	1.40	1.42	0.34	0.03

(10) **Buried grid (240 x 240 mm^2)**

Angle (degree)	Distance from centre, d (mm)	Surface potential,Vs (V)			
		CDEGS MALT	Experiment		
			Vs (V)	Equipment error (±V)	S.D. (Ω)
0	150	12.78	12.84	0.54	0.03
	250	7.09	7.15	0.54	0.03
	350	4.96	5.00	0.54	0.03
	450	3.82	3.84	0.54	0.03
	550	3.11	3.13	0.54	0.03
	650	2.62	2.64	0.54	0.03
45	200	10.14	10.18	0.54	0.03
	300	5.93	5.97	0.54	0.03
	400	4.33	4.35	0.54	0.03
	500	3.43	3.45	0.54	0.03
	600	2.84	2.86	0.54	0.03

(11) 25 rods with 240 x 240 mm^2 grid (c = 60 mm)

Angle (degree)	Distance from centre, d (mm)	Surface potential,Vs (V)			
		CDEGS MALT	Experiment		
			Vs (V)	Equipment error (±V)	S.D. (Ω)
0	150	15.28	15.34	0.65	0.03
	250	8.89	8.95	0.65	0.03
	350	6.25	6.29	0.65	0.03
	450	4.82	4.84	0.65	0.03
	550	3.92	3.94	0.65	0.03
	650	3.31	3.33	0.65	0.03
45	200	13.14	13.18	0.65	0.03
	300	7.54	7.58	0.65	0.03
	400	5.49	5.51	0.65	0.03
	500	4.34	4.36	0.65	0.03
	600	3.59	3.61	0.65	0.03

(12) 21 rods with 240 x 240 mm^2 grid

Angle (degree)	Distance from centre, d (mm)	Surface potential,Vs (V)			
		CDEGS MALT	Experiment		
			Vs (V)	Equipment error (±V)	S.D. (Ω)
0	150	15.21	15.27	0.65	0.03
	250	8.82	8.88	0.64	0.03
	350	6.19	6.23	0.64	0.03
	450	4.78	4.80	0.64	0.03
	550	3.89	3.91	0.64	0.03
	650	3.28	3.30	0.64	0.03
45	200	13.02	13.06	0.65	0.03
	300	7.48	7.52	0.64	0.03
	400	5.44	5.46	0.64	0.03
	500	4.30	4.32	0.64	0.03
	600	3.56	3.58	0.64	0.03

(13) 17 rods with 240 x 240mm^2 grid

Angle (degree)	Distance from centre, d (mm)	Surface potential,Vs (V)			
		CDEGS MALT	Experiment		
			Vs (V)	Equipment error (±V)	S.D. (Ω)
0	150	15.15	15.21	0.64	0.03
	250	8.75	8.81	0.64	0.03
	350	6.14	6.18	0.64	0.03
	450	4.73	4.75	0.64	0.03
	550	3.85	3.87	0.64	0.03
	650	3.25	3.27	0.64	0.03
45	200	13.04	13.08	0.64	0.03
	300	7.42	7.46	0.64	0.03
	400	5.39	5.41	0.64	0.03
	500	4.26	4.28	0.64	0.03
	600	3.53	3.55	0.64	0.03

APPENDIX 7

Results for the earthing system in the presence of a barrier with 25 rods combined grid

(A) NO BARRIER

Electrode configuration	CDEGS MALT	Experiment		
		Resistance (Ω)	Equipment error (±Ω)	S.D. (Ω)
25 rods combined grid with no barrier	14.91	15.10	0.73	0.04

SURFACE POTENTIALS (V)					
Angle	distance, d (mm)	CDEGS MALT (V)	Experiment (V)		
			Vs (V)	Equipment error (±V)	S.D. (Ω)
0°	150	15.27	15.34	0.65	0.03
	200	11.24	11.29	0.65	0.03
	250	8.89	8.95	0.65	0.03
	300	7.34	7.38	0.65	0.03
	350	6.25	6.29	0.65	0.03
	400	5.44	5.46	0.65	0.03
	450	4.82	4.84	0.65	0.03
	500	4.32	4.34	0.65	0.03
	550	3.92	3.94	0.65	0.03
	600	3.59	3.61	0.65	0.03
22.5°	150	16.63	16.69	0.65	0.03
	170	14.20	14.26	0.65	0.03
	200	11.74	11.78	0.65	0.03
	250	9.09	9.13	0.65	0.03
	300	7.43	7.47	0.65	0.03
	350	6.29	6.31	0.65	0.03
	400	5.46	5.48	0.65	0.03
	450	4.83	4.85	0.65	0.03
	500	4.33	4.35	0.65	0.03
	550	3.93	3.95	0.65	0.03
	600	3.31	3.33	0.65	0.03
45°	200	13.14	13.18	0.65	0.03
	250	9.39	9.43	0.65	0.03
	300	7.54	7.58	0.65	0.03
	350	6.35	6.37	0.65	0.03
	400	5.48	5.50	0.65	0.03
	450	4.85	4.87	0.65	0.03
	500	4.33	4.35	0.65	0.03
	550	3.93	3.95	0.65	0.03
	600	3.60	3.62	0.65	0.03

(B) SOLID BARRIER

1) Resistance

Barrier position (x,y) mm	CDEGS MALT (Ω)	Experiment		
		Resistance (Ω)	Equipment error (±Ω)	S.D. (Ω)
60,60	15.40	15.61	0.75	0.04
60,120	16.00	16.28	0.78	0.04
60,180	16.45	16.76	0.80	0.03
120,60	15.12	15.34	0.74	0.04
120,120	15.42	15.60	0.75	0.04
120,180	15.69	15.80	0.76	0.05
180,60	15.03	15.17	0.73	0.05
180,120	15.18	15.32	0.74	0.04
180,180	15.34	15.51	0.74	0.04

2) Surface Potentials

x=60mm, y=60mm

Angle	Distance, d (mm)	CDEGS MALT	Experiment		
			Vs (V)	Equipment error (±V)	S.D. (Ω)
0°	150	16.68	17.06	0.64	0.02
	200	7.67	7.83	0.64	0.02
	250	7.05	7.19	0.64	0.02
	300	6.21	6.31	0.64	0.02
	350	5.47	5.55	0.64	0.02
	400	4.86	4.88	0.64	0.02
	450	4.37	4.39	0.64	0.02
	500	3.96	3.98	0.64	0.02
	550	3.62	3.64	0.64	0.02
	600	3.33	3.35	0.64	0.02
22.5°	150	17.47	17.81	0.64	0.02
	170	15.90	16.20	0.64	0.02
	250	7.03	7.17	0.64	0.02
	300	6.25	6.37	0.64	0.02
	350	5.51	5.61	0.64	0.02
	400	4.90	5.00	0.64	0.02
	450	4.40	4.48	0.64	0.02
	500	3.99	4.036	0.64	0.02
	550	3.64	3.66	0.64	0.02
	600	3.10	3.118	0.64	0.02
45°	200	13.99	14.37	0.64	0.02
	250	10.97	11.31	0.64	0.02
	300	6.15	6.29	0.64	0.02
	350	5.56	5.68	0.64	0.02
	400	4.98	5.06	0.64	0.02
	450	4.48	4.52	0.64	0.02
	500	4.05	4.09	0.64	0.02
	550	3.70	3.72	0.64	0.02
	600	3.40	3.42	0.64	0.02

x=60mm, y=120mm

Angle	Distance, d (mm)	CDEGS MALT	Experiment		
			Vs (V)	Equipment error (±V)	S.D. (Ω)
0°	150	17.38	17.74	0.62	0.02
	200	5.45	5.60	0.62	0.02
	250	5.22	5.36	0.62	0.02
	300	4.86	4.98	0.62	0.02
	350	4.46	4.56	0.62	0.02
	400	4.09	4.11	0.62	0.02
	450	3.76	3.78	0.62	0.02
	500	3.46	3.48	0.62	0.02
	550	3.21	3.23	0.62	0.02
	600	2.98	3.00	0.62	0.02
22.5°	150	17.96	18.32	0.62	0.02
	170	16.66	16.99	0.62	0.02
	250	5.20	5.346	0.62	0.02
	300	4.88	5.016	0.62	0.02
	350	4.51	4.61	0.62	0.02
	400	4.14	4.24	0.62	0.02
	450	3.81	3.87	0.62	0.02
	500	3.51	3.53	0.62	0.02
	550	3.25	3.27	0.62	0.02
	600	2.81	2.824	0.62	0.02
45°	200	14.57	14.93	0.62	0.02
	250	11.71	12.06	0.62	0.02
	300	4.87	4.99	0.62	0.02
	350	4.62	4.72	0.62	0.02
	400	4.31	4.35	0.62	0.02
	450	3.99	4.03	0.62	0.02
	500	3.66	3.68	0.62	0.02
	550	3.38	3.40	0.62	0.02
	600	3.13	3.15	0.62	0.02

x=60mm, y=180mm

Angle	Distance, d (mm)	CDEGS MALT	Experiment		
			Vs (V)	Equipment error (±V)	S.D. (Ω)
0°	150	17.63	18.02	0.61	0.03
	200	4.31	4.47	0.60	0.03
	250	4.17	4.31	0.60	0.03
	300	3.97	4.07	0.60	0.03
	350	3.75	3.83	0.60	0.03
	400	3.51	3.54	0.60	0.03
	450	3.28	3.30	0.60	0.03
	500	3.07	3.09	0.60	0.03
	550	2.88	2.90	0.60	0.03
	600	2.70	2.72	0.60	0.03
22.5°	150	18.13	18.43	0.61	0.03
	170	16.95	17.30	0.61	0.03
	250	4.18	4.32	0.60	0.03
	300	4.01	4.136	0.60	0.03
	350	3.80	3.90	0.60	0.03
	400	3.57	3.67	0.60	0.03
	450	3.35	3.41	0.60	0.03
	500	3.13	3.17	0.60	0.03
	550	2.93	2.97	0.60	0.03
	600	2.58	2.60	0.60	0.03
45°	200	14.84	15.20	0.61	0.03
	250	12.04	12.39	0.61	0.03
	300	4.11	4.25	0.60	0.03
	350	4.01	4.11	0.60	0.03
	400	3.84	3.90	0.60	0.03
	450	3.62	3.68	0.60	0.03
	500	3.37	3.41	0.60	0.03
	550	3.13	3.15	0.60	0.03
	600	2.92	2.94	0.60	0.03

x=120mm, y=60mm

Angle	Distance, d (mm)	CDEGS MALT	Experiment		
			Vs (V)	Equipment error (±V)	S.D. (Ω)
0°	150	15.59	15.95	0.65	0.02
	200	12.25	12.59	0.65	0.02
	300	6.21	6.33	0.65	0.02
	350	5.59	5.69	0.65	0.02
	400	5.00	5.06	0.65	0.02
	450	4.50	4.54	0.65	0.02
	500	4.08	4.10	0.65	0.02
	550	3.73	3.75	0.65	0.02
	600	3.43	3.45	0.65	0.02
22.5°	150	16.8	17.16	0.65	0.02
	200	12.43	12.73	0.65	0.02
	250	10.71	10.99	0.65	0.02
	300	6.12	6.28	0.65	0.02
	350	5.59	5.73	0.65	0.02
	400	5.02	5.12	0.65	0.02
	450	4.52	4.58	0.65	0.02
	500	4.10	4.12	0.65	0.02
	550	3.75	3.79	0.65	0.02
	600	3.19	3.21	0.65	0.02
45°	200	13.36	13.70	0.65	0.02
	250	9.82	10.14	0.65	0.02
	300	8.19	8.49	0.65	0.02
	400	5.00	5.14	0.65	0.02
	450	4.59	4.69	0.65	0.02
	500	4.16	4.20	0.65	0.02
	550	3.80	3.84	0.65	0.02
	600	3.49	3.51	0.65	0.02

x=120mm, y=120mm

Angle	Distance, d (mm)	CDEGS MALT	Experiment		
			Vs (V)	Equipment error (±V)	S.D. (Ω)
0°	150	16.01	16.35	0.64	0.02
	200	13.16	13.48	0.64	0.02
	300	4.92	5.06	0.64	0.02
	350	4.64	4.72	0.64	0.02
	400	4.30	4.38	0.64	0.02
	450	3.97	4.01	0.64	0.02
	500	3.67	3.71	0.64	0.02
	550	3.40	3.42	0.64	0.02
	600	3.16	3.18	0.64	0.02
22.5°	150	17.07	17.16	0.64	0.02
	200	13.17	12.73	0.64	0.02
	250	11.69	10.99	0.64	0.02
	300	4.87	6.28	0.64	0.02
	350	4.63	5.73	0.64	0.02
	400	4.33	5.12	0.64	0.02
	450	4.01	4.58	0.64	0.02
	500	3.71	4.12	0.64	0.02
	550	3.44	3.79	0.64	0.02
	600	2.98	3.21	0.64	0.02
45°	200	13.70	14.04	0.64	0.02
	250	10.36	10.66	0.64	0.02
	300	8.78	9.08	0.64	0.02
	400	4.45	4.55	0.64	0.02
	450	4.22	4.30	0.64	0.02
	500	3.89	3.93	0.64	0.02
	550	3.59	3.61	0.64	0.02
	600	3.32	3.34	0.64	0.02

x=120mm, y=180mm

Angle	Distance, d (mm)	CDEGS MALT	Experiment		
			Vs (V)	Equipment error (±V)	S.D. (Ω)
0°	150	16.26	16.60	0.63	0.03
	200	13.65	13.97	0.63	0.03
	300	4.07	4.21	0.63	0.03
	350	3.91	4.01	0.63	0.03
	400	3.71	3.79	0.63	0.03
	450	3.49	3.55	0.63	0.03
	500	3.28	3.30	0.63	0.03
	550	3.08	3.10	0.63	0.03
	600	2.89	2.91	0.63	0.03
22.5°	150	17.25	17.61	0.63	0.03
	200	13.59	13.89	0.63	0.03
	250	12.19	12.45	0.63	0.03
	300	4.07	4.23	0.63	0.03
	350	3.94	4.06	0.63	0.03
	400	3.76	3.84	0.63	0.03
	450	3.56	3.60	0.63	0.03
	500	3.35	3.39	0.63	0.03
	550	3.14	3.16	0.63	0.03
	600	2.77	2.79	0.63	0.03
45°	200	13.93	14.31	0.63	0.03
	250	10.70	11.04	0.63	0.03
	300	9.12	9.44	0.63	0.03
	400	4.06	4.20	0.63	0.03
	450	3.92	4.04	0.63	0.03
	500	3.66	3.78	0.63	0.03
	550	3.39	3.45	0.63	0.03
	600	3.15	3.21	0.63	0.03

x=180mm, y=60mm

Angle	Distance, d (mm)	CDEGS MALT	Experiment		
			Vs (V)	Equipment error (±V)	S.D. (Ω)
0°	150	15.36	15.66	0.65	0.03
	200	11.53	11.81	0.65	0.03
	250	9.52	9.78	0.65	0.03
	350	5.43	5.55	0.65	0.03
	400	4.98	5.08	0.65	0.03
	450	4.52	4.60	0.65	0.03
	500	4.11	4.15	0.65	0.03
	550	3.76	3.78	0.65	0.03
	600	3.47	3.49	0.65	0.03
22.5°	150	16.66	16.96	0.65	0.03
	200	11.94	12.22	0.65	0.03
	250	9.51	9.79	0.65	0.03
	300	8.27	8.53	0.65	0.03
	350	5.30	5.42	0.65	0.03
	400	4.95	5.05	0.65	0.03
	450	4.53	4.61	0.65	0.03
	500	4.13	4.17	0.65	0.03
	550	3.78	3.80	0.65	0.03
	600	3.22	3.24	0.65	0.03

x=180mm, y=120mm

Angle	Distance, d (mm)	CDEGS MALT	Experiment		
			Vs (V)	Equipment error (±V)	S.D. (Ω)
0°	150	15.55	15.85	0.65	0.02
	200	11.98	12.24	0.65	0.02
	250	10.25	10.51	0.65	0.02
	350	4.54	4.68	0.64	0.02
	400	4.28	4.38	0.64	0.02
	450	4.01	4.07	0.64	0.02
	500	3.73	3.75	0.64	0.02
	550	3.47	3.49	0.64	0.02
	600	3.23	3.25	0.64	0.02
22.5°	150	16.79	17.09	0.65	0.02
	200	12.30	12.60	0.65	0.02
	250	10.09	10.37	0.65	0.02
	300	9.03	9.31	0.65	0.02
	350	4.43	4.57	0.64	0.02
	400	4.27	4.37	0.64	0.02
	450	4.03	4.09	0.64	0.02
	500	3.77	3.79	0.64	0.02
	550	3.51	3.53	0.64	0.02
	600	3.05	3.07	0.64	0.02

x=180mm, y=180mm

Angle	Distance, d (mm)	CDEGS MALT	Experiment		
			Vs (V)	Equipment error (±V)	S.D. (Ω)
0°	150	15.72	16.04	0.64	0.03
	200	12.33	12.63	0.64	0.03
	250	10.73	10.97	0.64	0.03
	350	3.84	3.96	0.63	0.03
	400	3.71	3.79	0.63	0.03
	450	3.54	3.60	0.63	0.03
	500	3.36	3.38	0.63	0.03
	550	3.17	3.19	0.63	0.03
	600	2.98	3.00	0.63	0.03
22.5°	150	16.9	17.22	0.64	0.03
	200	12.59	12.89	0.64	0.03
	250	10.49	10.77	0.64	0.03
	300	9.49	9.75	0.64	0.03
	350	3.83	3.97	0.63	0.03
	400	3.74	3.86	0.63	0.03
	450	3.60	3.68	0.63	0.03
	500	3.42	3.46	0.63	0.03
	550	3.24	3.26	0.63	0.03
	600	2.87	2.89	0.63	0.03

(C) PLATE BARRIER

1) Resistance

PLATE BARRIER (c=2 mm)				
Barrier position (x,y) mm	CDEGS MALT (Ω)	Experiment		
		Resistance (Ω)	Equipment error (±Ω)	S.D. (Ω)
60,60	15.27	15.43	0.74	0.02
60,120	15.68	15.84	0.76	0.03
60,180	15.95	16.11	0.77	0.02
120,60	15.05	15.18	0.73	0.02
120,120	15.25	15.38	0.74	0.04
120,180	15.42	15.55	0.75	0.02
180,60	14.98	15.16	0.73	0.03
180,120	15.08	15.23	0.74	0.03
180,180	15.18	15.33	0.74	0.02

PLATE BARRIER (c=5 mm)				
Barrier position (x,y) mm	CDEGS MALT (Ω)	Experiment		
		Resistance (Ω)	Equipment error (±Ω)	S.D. (Ω)
60,60	15.20	15.32	0.74	0.02
60,120	15.49	15.60	0.75	0.02
60,180	15.66	15.79	0.76	0.02
120,60	15.02	15.17	0.73	0.03
120,120	15.17	15.29	0.74	0.02
120,180	15.27	15.42	0.74	0.03
180,60	14.96	15.14	0.73	0.03
180,120	15.04	15.19	0.73	0.03
180,180	15.10	15.23	0.74	0.03

PLATE BARRIER (c=10 mm)				
Barrier position (x,y) mm	CDEGS MALT (Ω)	Experiment		
		Resistance (Ω)	Equipment error (±Ω)	S.D. (Ω)
60,60	15.14	15.25	0.74	0.03
60,120	15.35	15.44	0.75	0.03
60,180	15.46	15.57	0.75	0.02
120,60	15.00	15.12	0.73	0.02
120,120	15.10	15.21	0.74	0.02
120,180	15.17	15.29	0.74	0.02
180,60	14.95	15.12	0.73	0.02
180,120	15.01	15.14	0.73	0.02
180,180	15.05	15.20	0.74	0.02

2) Surface Potentials: PLATE BARRIER spacing 2 mm

x=60 mm, y=60 mm

PLATE BARRIER spacing 2 mm					
Angle	Distance, d (mm)	CDEGS MALT	Experiment		
			Vs (V)	Equipment error (±V)	S.D. (Ω)
0°	150	16.20	16.70	0.65	0.02
	200	8.28	8.66	0.64	0.02
	250	7.39	7.49	0.64	0.02
	300	6.43	6.43	0.64	0.02
	350	5.63	5.63	0.64	0.02
	400	4.98	4.98	0.64	0.02
	450	4.46	4.47	0.64	0.02
	500	4.04	4.08	0.64	0.02
	550	3.69	3.72	0.64	0.02
	600	3.39	3.42	0.64	0.02

x=60 mm, y=120 mm

PLATE BARRIER spacing 2 mm					
Angle	Distance, d (mm)	CDEGS MALT	Experiment		
			Vs (V)	Equipment error (±V)	S.D. (Ω)
0°	150	16.68	17.20	0.64	0.02
	200	6.84	7.14	0.63	0.02
	250	6.15	6.41	0.63	0.02
	300	5.49	5.65	0.63	0.02
	350	4.92	5.08	0.63	0.02
	400	4.44	4.58	0.63	0.02
	450	4.03	4.23	0.63	0.02
	500	3.69	3.86	0.63	0.02
	550	3.39	3.45	0.63	0.02
	600	3.14	3.22	0.63	0.02

x=60 mm, y=180 mm

PLATE BARRIER spacing 2 mm					
Angle	Distance, d (mm)	CDEGS MALT	Experiment		
			Vs (V)	Equipment error (±V)	S.D. (Ω)
0°	150	16.83	17.35	0.63	0.03
	200	6.19	6.49	0.62	0.03
	250	5.52	5.72	0.62	0.03
	300	4.95	5.13	0.62	0.03
	350	4.48	4.62	0.62	0.03
	400	4.08	4.21	0.62	0.03
	450	3.74	3.87	0.62	0.03
	500	3.44	3.56	0.62	0.03
	550	3.19	3.29	0.62	0.03
	600	2.96	3.06	0.62	0.03

x=120 mm, y=60 mm

PLATE BARRIER spacing 2 mm					
Angle	Distance, d (mm)	CDEGS MALT	Experiment		
			Vs (V)	Equipment error (±V)	S.D. (Ω)
0°	150	15.28	15.76	0.66	0.03
	200	12.02	12.52	0.66	0.03
	300	6.43	6.47	0.65	0.03
	350	5.72	5.82	0.65	0.03
	400	5.09	5.20	0.65	0.03
	450	4.57	4.64	0.65	0.03
	500	4.13	4.20	0.65	0.03
	550	3.77	3.80	0.65	0.03
	600	3.47	3.51	0.65	0.03

x=120 mm, y=120 mm

PLATE BARRIER spacing 2 mm					
Angle	Distance, d (mm)	CDEGS MALT	Experiment		
			Vs (V)	Equipment error (±V)	S.D. (Ω)
0°	150	15.58	16.04	0.65	0.03
	200	12.62	13.10	0.65	0.03
	300	5.58	5.92	0.65	0.03
	350	5.07	5.30	0.65	0.03
	400	4.61	4.73	0.65	0.03
	450	4.20	4.28	0.65	0.03
	500	3.85	3.91	0.65	0.03
	550	3.54	3.60	0.65	0.03
	600	3.28	3.32	0.65	0.03

x=120 mm, y=180 mm

PLATE BARRIER spacing 2 mm					
Angle	Distance, d (mm)	CDEGS MALT	Experiment		
			Vs (V)	Equipment error (±V)	S.D. (Ω)
0°	150	15.73	16.23	0.65	0.03
	200	12.89	13.33	0.64	0.03
	300	5.09	5.29	0.64	0.03
	350	4.64	4.80	0.64	0.03
	400	4.25	4.39	0.64	0.03
	450	3.91	4.03	0.64	0.03
	500	3.61	3.73	0.64	0.03
	550	3.34	3.45	0.64	0.03
	600	3.11	3.21	0.64	0.03

x=180 mm, y=60 mm

PLATE BARRIER spacing 2 mm					
Angle	Distance, d (mm)	CDEGS MALT	Experiment		
			Vs (V)	Equipment error (±V)	S.D. (Ω)
0°	150	15.08	15.52	0.66	0.02
	200	11.42	11.78	0.66	0.02
	250	9.39	9.73	0.65	0.02
	350	5.59	5.63	0.65	0.02
	400	5.07	5.17	0.65	0.02
	450	4.58	4.64	0.65	0.02
	500	4.16	4.22	0.65	0.02
	550	3.80	3.84	0.65	0.02
	600	3.49	3.51	0.65	0.02

x=180 mm, y=120 mm

PLATE BARRIER spacing 2 mm					
Angle	Distance, d (mm)	CDEGS MALT	Experiment		
			Vs (V)	Equipment error (±V)	S.D. (Ω)
0°	150	15.22	15.72	0.66	0.02
	200	11.73	12.21	0.66	0.02
	250	9.87	10.26	0.66	0.02
	350	4.98	5.24	0.66	0.02
	400	4.60	4.75	0.66	0.02
	450	4.23	4.31	0.66	0.02
	500	3.90	3.98	0.66	0.02
	550	3.60	3.68	0.66	0.02
	600	3.33	3.40	0.66	0.02

x=180 mm, y=180 mm

PLATE BARRIER spacing 2 mm					
Angle	Distance, d (mm)	CDEGS MALT	Experiment		
			Vs (V)	Equipment error (±V)	S.D. (Ω)
0°	150	15.33	15.75	0.66	0.03
	200	11.93	12.35	0.66	0.03
	250	10.14	10.64	0.66	0.03
	350	4.62	4.92	0.66	0.03
	400	4.27	4.51	0.66	0.03
	450	3.95	4.17	0.66	0.03
	500	3.67	3.85	0.66	0.03
	550	3.41	3.59	0.66	0.03
	600	3.18	3.33	0.66	0.03

3) Surface Potential: PLATE BARRIER spacing 5 mm

x=60 mm, y=60 mm

PLATE BARRIER spacing 5 mm					
Angle	Distance, d (mm)	CDEGS MALT	Experiment		
			Vs (V)	Equipment error (±V)	S.D. (Ω)
0°	150	15.99	16.45	0.65	0.04
	200	8.78	9.10	0.65	0.04
	250	7.67	7.71	0.64	0.04
	300	6.60	6.61	0.64	0.04
	350	5.74	5.76	0.64	0.04
	400	5.07	5.11	0.64	0.04
	450	4.53	4.55	0.64	0.04
	500	4.09	4.10	0.64	0.04
	550	3.73	3.73	0.64	0.04
	600	3.43	3.44	0.64	0.04

x=60 mm, y=120 mm

PLATE BARRIER spacing 5 mm					
Angle	Distance, d (mm)	CDEGS MALT	Experiment		
			Vs (V)	Equipment error (±V)	S.D. (Ω)
0°	150	16.31	16.77	0.64	0.03
	200	7.84	8.20	0.63	0.03
	250	6.83	7.04	0.63	0.03
	300	5.95	6.13	0.63	0.03
	350	5.25	5.39	0.63	0.03
	400	4.69	4.76	0.63	0.03
	450	4.23	4.30	0.63	0.03
	500	3.85	3.92	0.63	0.03
	550	3.52	3.61	0.63	0.03
	600	3.25	3.34	0.63	0.03

x=60 mm, y=180 mm

PLATE BARRIER spacing 5 mm					
Angle	Distance, d (mm)	CDEGS MALT	Experiment		
			Vs (V)	Equipment error (±V)	S.D. (Ω)
0°	150	16.39	16.85	0.63	0.03
	200	7.47	7.91	0.62	0.03
	250	6.45	6.61	0.62	0.03
	300	5.61	5.83	0.62	0.03
	350	4.97	5.21	0.62	0.03
	400	4.46	4.68	0.62	0.03
	450	4.04	4.23	0.62	0.03
	500	3.69	3.86	0.62	0.03
	550	3.39	3.54	0.62	0.03
	600	3.14	3.28	0.62	0.03

x=120 mm, y=60 mm

PLATE BARRIER spacing 5 mm					
Angle	Distance, d (mm)	CDEGS MALT	Experiment		
			Vs (V)	Equipment error (±V)	S.D. (Ω)
0°	150	15.22	15.68	0.66	0.03
	200	11.86	12.34	0.66	0.03
	300	6.60	6.67	0.65	0.03
	350	5.82	5.91	0.65	0.03
	400	5.16	5.26	0.65	0.03
	450	4.62	4.71	0.65	0.03
	500	4.17	4.24	0.65	0.03
	550	3.80	3.85	0.65	0.03
	600	3.49	3.53	0.65	0.03

x=120 mm, y=120 mm

PLATE BARRIER spacing 5 mm					
Angle	Distance, d (mm)	CDEGS MALT	Experiment		
			Vs (V)	Equipment error (±V)	S.D. (Ω)
0°	150	15.43	15.85	0.65	0.04
	200	12.27	12.75	0.65	0.04
	300	6.04	6.18	0.65	0.04
	350	5.38	5.45	0.65	0.04
	400	4.82	4.85	0.65	0.04
	450	4.36	4.38	0.65	0.04
	500	3.97	4.00	0.65	0.04
	550	3.64	3.65	0.65	0.04
	600	3.36	3.38	0.65	0.04

x=120 mm, y=180 mm

PLATE BARRIER spacing 5 mm					
Angle	Distance, d (mm)	CDEGS MALT	Experiment		
			Vs (V)	Equipment error (±V)	S.D. (Ω)
0°	150	15.53	16.01	0.65	0.03
	200	12.42	12.82	0.64	0.03
	300	5.75	6.11	0.64	0.03
	350	5.11	5.31	0.64	0.03
	400	4.60	4.73	0.64	0.03
	450	4.17	4.27	0.64	0.03
	500	3.82	3.91	0.64	0.03
	550	3.51	3.60	0.64	0.03
	600	3.25	3.33	0.64	0.03

x=180 mm, y=60 mm

PLATE BARRIER spacing 5 mm					
Angle	Distance, d (mm)	CDEGS MALT	Experiment		
			Vs (V)	Equipment error (±V)	S.D. (Ω)
0°	150	15.06	15.48	0.66	0.03
	200	11.37	11.73	0.66	0.03
	250	9.29	9.68	0.65	0.03
	350	5.72	5.85	0.65	0.03
	400	5.15	5.24	0.65	0.03
	450	4.63	4.71	0.65	0.03
	500	4.19	4.25	0.65	0.03
	550	3.82	3.87	0.65	0.03
	600	3.51	3.53	0.65	0.03

x=180 mm, y=120 mm

PLATE BARRIER spacing 5 mm					
Angle	Distance, d (mm)	CDEGS MALT	Experiment		
			Vs (V)	Equipment error (±V)	S.D. (Ω)
0°	150	15.16	15.62	0.66	0.03
	200	11.59	12.05	0.66	0.03
	250	9.62	10.00	0.66	0.03
	350	5.32	5.50	0.66	0.03
	400	4.83	4.91	0.66	0.03
	450	4.39	4.42	0.66	0.03
	500	4.01	4.02	0.66	0.03
	550	3.68	3.71	0.66	0.03
	600	3.40	3.43	0.66	0.03

x=180 mm, y=180 mm

PLATE BARRIER spacing 5 mm					
Angle	Distance, d (mm)	CDEGS MALT	Experiment		
			Vs (V)	Equipment error (±V)	S.D. (Ω)
0°	150	15.23	15.65	0.66	0.03
	200	11.71	12.11	0.66	0.03
	250	9.78	10.22	0.66	0.03
	350	5.11	5.33	0.66	0.03
	400	4.62	4.78	0.66	0.03
	450	4.21	4.33	0.66	0.03
	500	3.86	3.96	0.66	0.03
	550	3.56	3.66	0.66	0.03
	600	3.30	3.37	0.66	0.03

4) Surface Potential: PLATE BARRIER spacing 10 mm

x=60 mm, y=60 mm

PLATE BARRIER spacing 10 mm					
Angle	Distance, d (mm)	CDEGS MALT	Experiment		
			Vs (V)	Equipment error (±V)	S.D. (Ω)
0°	150	15.80	16.20	0.66	0.03
	200	9.21	9.34	0.65	0.03
	250	7.93	7.94	0.65	0.03
	300	6.75	6.79	0.65	0.03
	350	5.85	5.86	0.65	0.03
	400	5.15	5.16	0.65	0.03
	450	4.59	4.60	0.65	0.03
	500	4.14	4.16	0.65	0.03
	550	3.77	3.81	0.65	0.03
	600	3.46	3.51	0.65	0.03

x=60 mm, y=120 mm

PLATE BARRIER spacing 10 mm					
Angle	Distance, d (mm)	CDEGS MALT	Experiment		
			Vs (V)	Equipment error (±V)	S.D. (Ω)
0°	150	16.01	16.43	0.65	0.03
	200	8.61	8.86	0.65	0.03
	250	7.36	7.43	0.65	0.03
	300	6.31	6.31	0.65	0.03
	350	5.51	5.55	0.65	0.03
	400	4.88	4.91	0.65	0.03
	450	4.38	4.41	0.65	0.03
	500	3.97	4.02	0.65	0.03
	550	3.62	3.70	0.64	0.03
	600	3.34	3.44	0.64	0.03

x=60 mm, y=180 mm

PLATE BARRIER spacing 10 mm					
Angle	Distance, d (mm)	CDEGS MALT	Experiment		
			Vs (V)	Equipment error (±V)	S.D. (Ω)
0°	150	16.06	16.46	0.64	0.02
	200	8.39	8.69	0.64	0.02
	250	7.13	7.27	0.64	0.02
	300	6.09	6.20	0.64	0.02
	350	5.33	5.41	0.64	0.02
	400	4.73	4.79	0.64	0.02
	450	4.25	4.35	0.64	0.02
	500	3.86	3.98	0.64	0.02
	550	3.54	3.64	0.64	0.02
	600	3.26	3.37	0.64	0.02

x=120 mm, y=60 mm

PLATE BARRIER spacing 10 mm					
Angle	Distance, d (mm)	CDEGS MALT	Experiment		
			Vs (V)	Equipment error (±V)	S.D. (Ω)
0°	150	15.17	15.613	0.66	0.02
	200	11.72	12.139	0.66	0.02
	300	6.76	6.934	0.66	0.02
	350	5.91	6.058	0.66	0.02
	400	5.22	5.339	0.65	0.02
	450	4.66	4.777	0.65	0.02
	500	4.20	4.287	0.65	0.02
	550	3.83	3.865	0.65	0.02
	600	3.51	3.544	0.65	0.02

x=120 mm, y=120 mm

PLATE BARRIER spacing 10 mm					
Angle	Distance, d (mm)	CDEGS MALT	Experiment		
			Vs (V)	Equipment error (±V)	S.D. (Ω)
0°	150	15.32	15.72	0.66	0.03
	200	11.99	12.43	0.66	0.03
	300	6.39	6.40	0.65	0.03
	350	5.61	5.61	0.65	0.03
	400	4.99	5.00	0.65	0.03
	450	4.48	4.51	0.65	0.03
	500	4.06	4.07	0.65	0.03
	550	3.71	3.73	0.65	0.03
	600	3.42	3.44	0.65	0.03

x=120 mm, y=180 mm

PLATE BARRIER spacing 10 mm					
Angle	Distance, d (mm)	CDEGS MALT	Experiment		
			Vs (V)	Equipment error (±V)	S.D. (Ω)
0°	150	15.38	15.82	0.65	0.03
	200	12.09	12.51	0.65	0.03
	300	6.22	6.31	0.65	0.03
	350	5.45	5.51	0.65	0.03
	400	4.85	4.89	0.65	0.03
	450	4.36	4.41	0.65	0.03
	500	3.96	4.03	0.65	0.03
	550	3.63	3.70	0.65	0.03
	600	3.35	3.42	0.65	0.03

x=180 mm, y=60 mm

PLATE BARRIER spacing 10 mm					
Angle	Distance, d (mm)	CDEGS MALT	Experiment		
			Vs (V)	Equipment error (±V)	S.D. (Ω)
0°	150	15.05	15.45	0.66	0.03
	200	11.33	11.69	0.66	0.03
	250	9.20	9.57	0.66	0.03
	350	5.83	5.91	0.66	0.03
	400	5.21	5.32	0.65	0.03
	450	4.67	4.74	0.65	0.03
	500	4.22	4.30	0.65	0.03
	550	3.84	3.89	0.65	0.03
	600	3.53	3.56	0.65	0.03

x=180 mm, y=120 mm

PLATE BARRIER spacing 10 mm					
Angle	Distance, d (mm)	CDEGS MALT	Experiment		
			Vs (V)	Equipment error (±V)	S.D. (Ω)
0°	150	15.12	15.56	0.67	0.04
	200	11.48	11.94	0.66	0.04
	250	9.42	9.82	0.66	0.04
	350	5.58	5.59	0.66	0.04
	400	5.00	5.00	0.66	0.04
	450	4.51	4.51	0.66	0.04
	500	4.09	4.15	0.66	0.04
	550	3.75	3.77	0.66	0.04
	600	3.45	3.48	0.66	0.04

x=180 mm, y=180 mm

PLATE BARRIER spacing 10 mm					
Angle	Distance, d (mm)	CDEGS MALT	Experiment		
			Vs (V)	Equipment error (±V)	S.D. (Ω)
0°	150	15.16	15.56	0.67	0.03
	200	11.56	11.96	0.66	0.03
	250	9.52	9.92	0.66	0.03
	350	5.46	5.53	0.66	0.03
	400	4.87	4.92	0.66	0.03
	450	4.39	4.45	0.66	0.03
	500	4.00	4.04	0.66	0.03
	550	3.67	3.72	0.66	0.03
	600	3.39	3.45	0.66	0.03

(D) SURFACE POTENTIAL PERCENTAGE INCREASE/DECREASE FROM NO BARRIER

(1) PLATE BARRIER (spacing = 2mm)

x=60mm

PLATE BARRIER (c=2mm) (% increase/decrese from no barrier)							
Angle	distance, d (mm)	depth, y (mm)					
		60		120		180	
		Exp	CDEGS	Exp	CDEGS	Exp	CDEGS
0°	150	8.87	6.02	12.14	9.18	13.08	10.12
	200	-23.29	-26.37	-36.80	-39.19	-42.54	-44.96
	250	-16.31	-16.84	-28.40	-30.84	-36.04	-37.86
	300	-12.87	-12.40	-23.43	-25.19	-30.53	-32.55
	350	-10.46	-9.98	-19.19	-21.23	-26.60	-28.37
	400	-8.72	-8.42	-16.10	-18.36	-22.95	-25.06
	450	-7.71	-7.41	-12.60	-16.33	-20.10	-22.51
	500	-5.99	-6.53	-11.06	-14.63	-17.97	-20.37
	550	-5.58	-5.97	-12.34	-13.42	-16.62	-18.75
	600	-5.26	-5.60	-10.78	-12.51	-15.15	-17.47

x=120mm

PLATE BARRIER (c=2mm) (% increase/decrese from no barrier)							
Angle	distance, d (mm)	depth, y (mm)					
		60		120		180	
		Exp	CDEGS	Exp	CDEGS	Exp	CDEGS
0°	150	2.72	-0.02	4.54	1.94	5.83	2.97
	200	10.85	6.90	16.03	12.28	18.05	14.66
	300	-12.32	-12.47	-19.78	-24.05	-28.36	-30.67
	350	-7.54	-8.51	-15.74	-18.88	-23.70	-25.78
	400	-4.76	-6.43	-13.37	-15.31	-19.62	-21.89
	450	-4.09	-5.27	-11.59	-12.88	-16.80	-18.94
	500	-3.34	-4.33	-10.00	-10.97	-14.12	-16.50
	550	-3.45	-3.78	-8.60	-9.67	-12.51	-14.72
	600	-2.91	-3.43	-8.12	-8.72	-11.02	-13.31

x=180mm

PLATE BARRIER (c=2mm) (% increase/decrese from no barrier)							
Angle	distance, d (mm)	depth, y (mm)					
		60		120		180	
		Exp	CDEGS	Exp	CDEGS	Exp	CDEGS
0°	150	1.19	-1.30	2.50	-0.37	2.66	0.31
	200	4.33	1.56	8.13	4.34	9.41	6.16
	250	8.67	5.58	14.67	11.06	18.89	14.07
	350	-10.45	-10.61	-16.69	-20.26	-21.81	-26.11
	400	-5.27	-6.76	-13.00	-15.40	-17.42	-21.53
	450	-4.11	-4.96	-10.95	-12.18	-13.78	-17.99
	500	-2.83	-3.77	-8.29	-9.84	-11.36	-15.12
	550	-2.59	-3.11	-6.60	-8.29	-8.88	-13.01
	600	-2.69	-2.70	-5.82	-7.21	-7.76	-11.45

(2) PLATE BARRIER (spacing = 5mm)

x=60mm

PLATE BARRIER (c=5mm) (% increase/decrese from no barrier)							
Angle	distance, d (mm)	depth, y (mm)					
		60		120		180	
		Exp	CDEGS	Exp	CDEGS	Exp	CDEGS
0°	150	7.23	4.64	9.30	6.72	9.84	7.26
	200	-19.40	-21.92	-27.35	-30.23	-29.98	-33.59
	250	-13.85	-13.68	-21.34	-23.23	-26.20	-27.50
	300	-10.43	-10.08	-16.94	-18.96	-20.99	-23.56
	350	-8.51	-8.11	-14.31	-16.00	-17.20	-20.51
	400	-6.48	-6.84	-12.82	-13.84	-14.29	-18.11
	450	-6.01	-6.04	-11.16	-12.30	-12.60	-16.29
	500	-5.44	-5.28	-9.68	-11.00	-11.06	-14.70
	550	-5.33	-4.85	-8.38	-10.10	-10.15	-13.55
	600	-4.71	-4.54	-7.48	-9.44	-9.14	-12.67

x=120mm

PLATE BARRIER (c=5mm) (% increase/decrese from no barrier)							
Angle	distance, d (mm)	depth, y (mm)					
		60		120		180	
		Exp	CDEGS	Exp	CDEGS	Exp	CDEGS
0°	150	2.23	-0.38	3.32	0.98	4.36	1.63
	200	9.28	5.50	12.89	9.12	13.58	10.52
	300	-9.65	-10.03	-16.26	-17.72	-17.21	-21.66
	350	-5.98	-6.85	-13.35	-13.95	-15.58	-18.21
	400	-3.74	-5.18	-11.17	-11.32	-13.37	-15.48
	450	-2.64	-4.23	-9.50	-9.54	-11.78	-13.40
	500	-2.24	-3.45	-7.83	-8.10	-9.91	-11.67
	550	-2.21	-3.04	-7.36	-7.14	-8.63	-10.41
	600	-2.13	-2.76	-6.37	-6.46	-7.76	-9.44

x=180mm

PLATE BARRIER (c=5mm) (% increase/decrese from no barrier)							
Angle	distance, d (mm)	depth, y (mm)					
		60		120		180	
		Exp	CDEGS	Exp	CDEGS	Exp	CDEGS
0°	150	0.93	-1.42	1.84	-0.77	2.01	-0.33
	200	3.87	1.13	6.69	3.07	7.30	4.22
	250	8.12	4.47	11.69	8.17	14.17	9.99
	350	-7.01	-8.50	-12.56	-14.82	-15.21	-18.19
	400	-3.99	-5.40	-10.07	-11.29	-12.45	-15.02
	450	-2.77	-3.98	-8.68	-8.96	-10.54	-12.59
	500	-2.00	-2.99	-7.37	-7.22	-8.76	-10.56
	550	-1.85	-2.47	-5.84	-6.10	-7.11	-9.13
	600	-2.11	-2.17	-4.99	-5.32	-6.65	-8.05

(3) PLATE BARRIER (spacing = 10mm)

x=60mm

PLATE BARRIER (c=10mm) (% increase/decrese from no barrier)							
Angle	distance, d (mm)	depth, y (mm)					
		60		120		180	
		Exp	CDEGS	Exp	CDEGS	Exp	CDEGS
0°	150	5.63	3.42	7.12	4.79	7.31	5.11
	200	-17.27	-18.10	-21.52	-23.38	-23.03	-25.32
	250	-11.30	-10.85	-16.98	-17.27	-18.77	-19.85
	300	-8.04	-8.00	-14.50	-14.09	-15.99	-16.98
	350	-6.90	-6.43	-11.76	-11.90	-13.99	-14.78
	400	-5.51	-5.42	-10.07	-10.31	-12.27	-13.07
	450	-4.96	-4.79	-8.88	-9.19	-10.12	-11.78
	500	-4.15	-4.19	-7.37	-8.19	-8.29	-10.63
	550	-3.30	-3.85	-6.09	-7.55	-7.61	-9.80
	600	-2.77	-3.62	-4.71	-7.08	-6.65	-9.19

x=120mm

PLATE BARRIER (c=10mm) (% increase/decrese from no barrier)							
Angle	distance, d (mm)	depth, y (mm)					
		60		120		180	
		Exp	CDEGS	Exp	CDEGS	Exp	CDEGS
0°	150	1.78	-0.70	2.46	0.25	3.14	0.66
	200	7.52	4.26	10.12	6.69	10.80	7.55
	300	-6.04	-7.87	-13.29	-12.93	-14.50	-15.27
	350	-3.69	-5.38	-10.75	-10.21	-12.40	-12.85
	400	-2.22	-4.06	-8.41	-8.29	-10.44	-10.94
	450	-1.30	-3.34	-6.80	-7.03	-8.88	-9.52
	500	-1.22	-2.71	-6.22	-5.95	-7.14	-8.26
	550	-1.90	-2.37	-5.33	-5.26	-6.09	-7.40
	600	-1.83	-2.17	-4.71	-4.79	-5.26	-6.77

x=180mm

PLATE BARRIER (c=10mm) (% increase/decrese from no barrier)							
Angle	distance, d (mm)	depth, y (mm)					
		60		120		180	
		Exp	CDEGS	Exp	CDEGS	Exp	CDEGS
0°	150	0.69	-1.53	1.41	-1.07	1.42	-0.79
	200	3.50	0.76	5.73	2.11	5.90	2.85
	250	6.92	3.48	9.74	5.98	10.86	7.11
	350	-6.07	-6.66	-11.13	-10.74	-12.08	-12.70
	400	-2.56	-4.23	-8.42	-8.18	-9.89	-10.50
	450	-2.09	-3.13	-6.82	-6.54	-8.06	-8.86
	500	-0.94	-2.34	-4.38	-5.25	-6.91	-7.43
	550	-1.17	-1.94	-4.31	-4.44	-5.58	-6.43
	600	-1.41	-1.70	-3.60	-3.90	-4.43	-5.71

APPENDIX 8

1. Surface Potentials for 8 rods combined grid

Rod radius = 0.78mm
Spacing between rods = 60mm
Rod length = 60mm
Water conductivity = 0.1 S/m
Voltage energization = 20V

1) Depth = 10mm

Distance (mm)	Surface Potential (V)			
	Experiment			CDEGS MALT
	Vs (V)	Equipment error (±V)	S.D. (V)	
50	19.80	0.45	0.02	18.98
100	12.88	0.44	0.02	12.79
150	8.80	0.44	0.02	8.79
200	6.66	0.44	0.02	6.63
250	5.32	0.44	0.02	5.30
300	4.43	0.44	0.02	4.42
350	3.79	0.44	0.02	3.78
400	3.31	0.44	0.02	3.31
450	2.94	0.44	0.02	2.94
500	2.68	0.44	0.02	2.65
550	2.43	0.44	0.02	2.41
600	2.24	0.44	0.02	2.20

2) Depth = 20mm

Distance (mm)	Surface Potential (V)			
	Experiment			CDEGS MALT
	Vs (V)	Equipment error (±V)	S.D. (V)	
50	18.61	0.47	0.02	18.09
100	13.07	0.46	0.02	12.99
150	9.14	0.46	0.02	9.11
200	6.95	0.46	0.02	6.92
250	5.60	0.46	0.02	5.55
300	4.69	0.46	0.02	4.63
350	4.02	0.46	0.02	3.97
400	3.51	0.46	0.02	3.48
450	3.12	0.46	0.02	3.09
500	2.80	0.46	0.02	2.78
550	2.54	0.46	0.02	2.53
600	2.34	0.46	0.02	2.32

3) Depth = 30mm

Distance (mm)	Surface Potential (V)			
	Experiment			CDEGS MALT
	Vs (V)	Equipment error (±V)	S.D. (V)	
50	17.67	0.48	0.03	17.24
100	13.02	0.48	0.03	12.94
150	9.34	0.48	0.03	9.30
200	7.15	0.48	0.03	7.12
250	5.80	0.48	0.03	5.74
300	4.85	0.48	0.03	4.80
350	4.15	0.48	0.03	4.13
400	3.65	0.47	0.03	3.61
450	3.25	0.47	0.03	3.21
500	2.91	0.47	0.03	2.89
550	2.64	0.47	0.03	2.63
600	2.42	0.47	0.03	2.41

4) Depth = 40mm

Distance (mm)	Surface Potential (V)			
	Experiment			CDEGS MALT
	Vs (V)	Equipment error (±V)	S.D. (V)	
50	16.82	0.49	0.03	16.41
100	12.80	0.49	0.03	12.74
150	9.48	0.49	0.03	9.39
200	7.29	0.49	0.03	7.27
250	5.94	0.49	0.03	5.89
300	4.95	0.49	0.03	4.94
350	4.29	0.49	0.03	4.25
400	3.75	0.49	0.03	3.73
450	3.34	0.49	0.03	3.32
500	3.00	0.49	0.03	2.99
550	2.73	0.49	0.03	2.72
600	2.50	0.49	0.03	2.49

5) Depth = 50mm

Distance (mm)	Surface Potential (V)			
	Experiment			CDEGS MALT
	Vs (V)	Equipment error (±V)	S.D. (V)	
50	16.00	0.50	0.02	15.61
100	12.54	0.50	0.02	12.45
150	9.49	0.50	0.02	9.41
200	7.47	0.50	0.02	7.36
250	6.09	0.50	0.02	6.00
300	5.13	0.50	0.02	5.05
350	4.40	0.50	0.02	4.35
400	3.87	0.50	0.02	3.82
450	3.43	0.50	0.02	3.40
500	3.08	0.50	0.02	3.07
550	2.80	0.50	0.02	2.79
600	2.56	0.50	0.02	2.56

6) Depth = 60mm

Distance (mm)	Surface Potential (V)			
	Experiment			CDEGS MALT
	Vs (V)	Equipment error (±V)	S.D. (V)	
50	15.18	0.51	0.02	14.82
100	12.21	0.51	0.02	12.10
150	9.45	0.51	0.02	9.36
200	7.50	0.51	0.02	7.41
250	6.17	0.51	0.02	6.08
300	5.21	0.51	0.02	5.13
350	4.48	0.51	0.02	4.43
400	3.93	0.51	0.02	3.90
450	3.50	0.51	0.02	3.47
500	3.17	0.51	0.02	3.13
550	2.86	0.51	0.02	2.85
600	2.63	0.51	0.02	2.62

2. Surface Potentials for 120mm x 120mm and 240mm x 240mm mesh

Rod radius = 0.78mm
Each mesh = 60mm x 60mm
Water conductivity = 0.1 S/m
Voltage energization = 20V

a) 120mm x 120mm buried grid (0° traverse)

120mm x 120mm buried grid (0° traverse)					
Buried depth (mm)	**Distance (mm)**	**Surface Potentials (V)**			
		Experiment	**Equipment error (±V)**	**S.D. (V)**	**CDEGS MALT**
10mm	30	18.87	0.38	0.03	18.16
	40	18.86	0.38	0.03	18.12
	50	18.87	0.38	0.03	18.15
	60	18.68	0.38	0.03	17.57
	70	16.14	0.38	0.03	15.49
	80	13.91	0.38	0.03	13.38
	90	12.11	0.38	0.03	11.74
	100	10.78	0.38	0.03	10.45
	150	6.88	0.38	0.03	6.75
	200	5.18	0.37	0.03	4.99
	250	4.14	0.37	0.03	3.96
	300	3.44	0.37	0.03	3.29
	350	2.91	0.37	0.03	2.81
	400	2.55	0.37	0.03	2.46
	450	2.24	0.37	0.03	2.18
	500	1.99	0.37	0.03	1.96
	550	1.80	0.37	0.03	1.78
	600	1.64	0.37	0.03	1.63
20mm	30	17.97	0.40	0.02	17.48
	40	17.73	0.40	0.02	17.27
	50	17.47	0.40	0.02	16.95
	60	16.88	0.40	0.02	16.24
	70	15.58	0.40	0.02	14.97
	80	13.95	0.39	0.02	13.48
	90	12.50	0.39	0.02	12.10
	100	11.32	0.39	0.02	10.91
	150	7.54	0.39	0.02	7.19
	200	5.67	0.39	0.02	5.34
	250	4.47	0.39	0.02	4.25
	300	3.72	0.39	0.02	3.53
	350	3.13	0.39	0.02	3.02
	400	2.72	0.39	0.02	2.64
	450	2.42	0.39	0.02	2.34
	500	2.15	0.39	0.02	2.11
	550	1.94	0.39	0.02	1.91
	600	1.77	0.39	0.02	1.75

120mm x 120mm buried grid (0° traverse)					
Buried depth (mm)	**Distance (mm)**	**Surface Potentials (V)**			
		Experiment	**Equipment error (±V)**	**S.D. (V)**	**CDEGS MALT**
30mm	30	17.13	0.41	0.03	16.70
	40	16.90	0.41	0.03	16.39
	50	16.49	0.41	0.03	15.94
	60	15.84	0.41	0.03	15.25
	70	14.73	0.41	0.03	14.28
	80	13.61	0.41	0.03	13.16
	90	12.45	0.41	0.03	12.04
	100	11.37	0.41	0.03	11.01
	150	7.65	0.41	0.03	7.47
	200	5.79	0.40	0.03	5.59
	250	4.61	0.40	0.03	4.46
	300	3.87	0.40	0.03	3.71
	350	3.35	0.40	0.03	3.18
	400	2.92	0.40	0.03	2.78
	450	2.58	0.40	0.03	2.47
	500	2.28	0.40	0.03	2.22
	550	2.08	0.40	0.03	2.02
	600	1.90	0.40	0.03	1.85
40mm	30	16.24	0.42	0.03	15.82
	40	15.90	0.42	0.03	15.48
	50	15.50	0.42	0.03	15.01
	60	14.97	0.42	0.03	14.38
	70	14.08	0.42	0.03	13.59
	80	13.16	0.42	0.03	12.70
	90	12.30	0.42	0.03	11.79
	100	11.38	0.42	0.03	10.91
	150	8.00	0.42	0.03	7.63
	200	6.09	0.42	0.03	5.76
	250	4.87	0.42	0.03	4.62
	300	4.07	0.42	0.03	3.85
	350	3.48	0.42	0.03	3.30
	400	3.02	0.42	0.03	2.89
	450	2.64	0.42	0.03	2.57
	500	2.37	0.42	0.03	2.31
	550	2.15	0.42	0.03	2.10
	600	1.96	0.42	0.03	1.92

120mm x 120mm buried grid (0° traverse)					
Buried depth (mm)	**Distance (mm)**	**Surface Potentials (V)**			
		Experiment	**Equipment error (±V)**	**S.D. (V)**	**CDEGS MALT**
50mm	30	15.28	0.43	0.03	14.90
	40	15.00	0.43	0.03	14.57
	50	14.54	0.43	0.03	14.13
	60	14.14	0.43	0.03	13.58
	70	13.35	0.43	0.03	12.92
	80	12.59	0.43	0.03	12.19
	90	11.82	0.43	0.03	11.43
	100	11.05	0.43	0.03	10.68
	150	8.07	0.43	0.03	7.69
	200	6.22	0.43	0.03	5.88
	250	5.01	0.43	0.03	4.73
	300	4.13	0.43	0.03	3.96
	350	3.59	0.43	0.03	3.40
	400	3.15	0.43	0.03	2.97
	450	2.77	0.43	0.03	2.65
	500	2.49	0.43	0.03	2.38
	550	2.27	0.43	0.03	2.17
	600	2.05	0.43	0.03	1.99
60mm	30	14.35	0.44	0.04	14.00
	40	14.06	0.44	0.04	13.69
	50	13.71	0.44	0.04	13.30
	60	13.32	0.44	0.04	12.82
	70	12.66	0.44	0.04	12.27
	80	12.03	0.44	0.04	11.66
	90	11.39	0.44	0.04	11.02
	100	10.76	0.44	0.04	10.38
	150	8.03	0.44	0.04	7.69
	200	6.26	0.44	0.04	5.95
	250	5.14	0.43	0.04	4.82
	300	4.28	0.43	0.04	4.04
	350	3.65	0.43	0.04	3.47
	400	3.21	0.43	0.04	3.05
	450	2.77	0.43	0.04	2.71
	500	2.48	0.43	0.04	2.44
	550	2.27	0.43	0.04	2.22
	600	2.10	0.43	0.04	2.04

b) **240mm x 240mm Buried Grid**

240mm x 240mm Buried Grid (0° traverse)					
Buried depth (mm)	**Distance (mm)**	**Surface Potentials (V)**			
		Experiment	**Equipment error (±V)**	**S.D. (V)**	**CDEGS MALT**
10mm	30	19.90	0.59	0.02	19.18
	40	20.00	0.59	0.02	19.21
	50	20.23	0.59	0.02	19.34
	60	20.64	0.59	0.02	19.45
	70	19.98	0.59	0.02	19.25
	80	19.76	0.59	0.02	19.03
	90	19.54	0.59	0.02	18.90
	100	19.51	0.59	0.02	18.85
	110	19.50	0.59	0.02	18.83
	120	19.44	0.59	0.02	18.39
	130	17.40	0.59	0.02	16.75
	140	15.73	0.59	0.02	15.15
	150	14.21	0.59	0.02	13.88
	200	10.12	0.59	0.02	9.95
	250	7.92	0.59	0.02	7.80
	300	6.49	0.58	0.02	6.42
	350	5.50	0.58	0.02	5.46
	400	4.78	0.58	0.02	4.75
	450	4.25	0.58	0.02	4.20
	500	3.81	0.58	0.02	3.77
20mm	30	19.38	0.62	0.02	18.98
	40	19.44	0.62	0.02	18.99
	50	19.53	0.62	0.02	19.02
	60	19.62	0.62	0.02	19.00
	70	19.44	0.62	0.02	18.87
	80	19.21	0.62	0.02	18.68
	90	18.88	0.62	0.02	18.49
	100	18.79	0.62	0.02	18.30
	110	18.54	0.62	0.02	18.01
	120	18.04	0.62	0.02	17.44
	130	16.94	0.61	0.02	16.47
	140	15.69	0.61	0.02	15.33
	150	14.61	0.61	0.02	14.25
	200	10.77	0.61	0.02	10.42
	250	8.31	0.61	0.02	8.20
	300	6.86	0.61	0.02	6.76
	350	5.84	0.61	0.02	5.75
	400	5.05	0.61	0.02	5.00
	450	4.47	0.61	0.02	4.43
	500	4.02	0.61	0.02	3.97

240mm x 240mm Buried Grid (0° traverse)					
Buried depth (mm)	**Distance (mm)**	**Surface Potentials (V)**			
		Experiment	**Equipment error (±V)**	**S.D. (V)**	**CDEGS MALT**
40mm	30	18.94	0.66	0.03	18.64
	40	18.93	0.66	0.03	18.58
	50	18.86	0.66	0.03	18.50
	60	18.89	0.66	0.03	18.39
	70	18.61	0.66	0.03	18.23
	80	18.28	0.66	0.03	18.01
	90	18.04	0.66	0.03	17.74
	100	17.70	0.66	0.03	17.41
	110	17.31	0.66	0.03	16.98
	120	16.91	0.66	0.03	16.44
	130	16.14	0.65	0.03	15.78
	140	15.31	0.65	0.03	15.04
	150	14.52	0.65	0.03	14.27
	200	11.14	0.65	0.03	10.93
	250	8.84	0.65	0.03	8.72
	300	7.27	0.65	0.03	7.22
	350	6.24	0.65	0.03	6.16
	400	5.43	0.65	0.03	5.37
	450	4.81	0.65	0.03	4.76
	500	4.31	0.65	0.03	4.28
60mm	30	18.17	0.69	0.02	17.95
	40	18.20	0.69	0.02	17.86
	50	18.14	0.69	0.02	17.74
	60	18.04	0.69	0.02	17.59
	70	17.81	0.69	0.02	17.39
	80	17.49	0.69	0.02	17.15
	90	17.20	0.69	0.02	16.86
	100	16.86	0.69	0.02	16.51
	110	16.46	0.69	0.02	16.10
	120	16.06	0.69	0.02	15.63
	130	15.46	0.69	0.02	15.10
	140	14.77	0.69	0.02	14.52
	150	14.11	0.69	0.02	13.93
	200	11.22	0.69	0.02	11.11
	250	9.13	0.69	0.02	9.01
	300	7.58	0.68	0.02	7.53
	350	6.50	0.68	0.02	6.45
	400	5.69	0.68	0.02	5.64
	450	5.05	0.68	0.02	5.01
	500	4.53	0.68	0.02	4.50

240mm x 240mm Buried Grid (45° traverse)					
Buried depth (mm)	**Distance (mm)**	**Surface Potentials (V)**			
		Experiment	**Equipment error (±V)**	**S.D. (V)**	**CDEGS MALT**
10mm	30	19.14	0.59	0.02	18.63
	40	19.11	0.59	0.02	18.48
	50	19.13	0.59	0.02	18.49
	60	19.34	0.59	0.02	18.67
	70	19.85	0.59	0.02	19.01
	80	20.43	0.59	0.02	19.34
	90	20.14	0.59	0.02	19.28
	100	19.43	0.59	0.02	18.74
	110	18.78	0.59	0.02	18.14
	120	18.29	0.59	0.02	17.68
	130	17.97	0.59	0.02	17.42
	140	18.13	0.59	0.02	17.38
	150	18.52	0.59	0.02	17.53
	200	11.81	0.59	0.02	11.36
	250	8.23	0.59	0.02	8.13
	300	6.63	0.58	0.02	6.55
	350	5.57	0.58	0.02	5.52
	400	4.82	0.58	0.02	4.77
	450	4.27	0.58	0.02	4.22
	500	3.81	0.58	0.02	3.77
20mm	30	19.24	0.62	0.03	18.84
	40	19.13	0.62	0.03	18.76
	50	19.11	0.62	0.03	18.74
	60	19.20	0.62	0.03	18.80
	70	19.32	0.62	0.03	18.87
	80	19.50	0.62	0.03	18.89
	90	19.29	0.62	0.03	18.77
	100	18.91	0.62	0.03	18.51
	110	18.52	0.62	0.03	18.15
	120	18.18	0.62	0.03	17.79
	130	17.89	0.62	0.03	17.47
	140	17.65	0.62	0.03	17.2
	150	17.48	0.61	0.03	16.88
	200	12.12	0.61	0.03	11.72
	250	8.86	0.61	0.03	8.54
	300	7.06	0.61	0.03	6.89
	350	5.89	0.61	0.03	5.82
	400	5.09	0.61	0.03	5.03
	450	4.50	0.61	0.03	4.45
	500	4.01	0.61	0.03	3.98

240mm x 240mm Buried Grid (45° traverse)					
Buried depth (mm)	**Distance (mm)**	**Surface Potentials (V)**			
		Experiment	**Equipment error (±V)**	**S.D. (V)**	**CDEGS MALT**
40mm	30	18.85	0.66	0.03	18.63
	40	18.79	0.66	0.03	18.56
	50	18.75	0.66	0.03	18.49
	60	18.76	0.66	0.03	18.4
	70	18.68	0.66	0.03	18.3
	80	18.59	0.66	0.03	18.15
	90	18.31	0.66	0.03	17.93
	100	18.05	0.66	0.03	17.68
	110	17.72	0.66	0.03	17.37
	120	17.25	0.66	0.03	17
	130	16.86	0.66	0.03	16.59
	140	16.44	0.65	0.03	16.11
	150	16.01	0.65	0.03	15.56
	200	12.17	0.65	0.03	11.85
	250	9.19	0.65	0.03	9.02
	300	7.50	0.65	0.03	7.36
	350	6.29	0.65	0.03	6.23
	400	5.45	0.65	0.03	5.4
	450	4.84	0.65	0.03	4.78
	500	4.32	0.65	0.03	4.28
60mm	30	18.16	0.69	0.03	17.95
	40	18.16	0.69	0.03	17.87
	50	18.14	0.69	0.03	17.76
	60	18.02	0.69	0.03	17.63
	70	17.91	0.69	0.03	17.46
	80	17.73	0.69	0.03	17.26
	90	17.37	0.69	0.03	16.98
	100	17.06	0.69	0.03	16.69
	110	16.70	0.69	0.03	16.37
	120	16.23	0.69	0.03	15.99
	130	15.94	0.69	0.03	15.58
	140	15.54	0.69	0.03	15.11
	150	15.06	0.69	0.03	14.6
	200	12.10	0.69	0.03	11.71
	250	9.53	0.69	0.03	9.26
	300	7.81	0.68	0.03	7.65
	350	6.56	0.68	0.03	6.52
	400	5.73	0.68	0.03	5.67
	450	5.07	0.68	0.03	5.03
	500	4.55	0.68	0.03	4.51

3. Surface Potentials for Ring Electrode

a) Fat Ring

radius of ring (from axis)= 57mm
rod radius = 4mm
Thickness of ring = 8mm

Burial depth = 1 mm					
Distance from middle of ring (mm)	**Experiment**	**Equipment error (±V)**	**S.D. (V)**	**MALT Vs (V)**	**Analytical Vs (V)**
0	14.90	0.34	0.03	14.41	14.44
10	14.99	0.34	0.03	14.52	14.55
20	15.38	0.34	0.03	14.86	14.90
30	16.01	0.34	0.03	15.52	15.58
40	17.61	0.34	0.03	16.69	16.81
70	15.70	0.34	0.03	14.85	14.92
80	12.59	0.34	0.03	12.13	12.14
90	10.71	0.34	0.03	10.35	10.35
100	9.37	0.34	0.03	9.07	9.07
110	8.40	0.34	0.03	8.10	8.09
120	7.55	0.34	0.03	7.33	7.32
130	6.92	0.34	0.03	6.70	6.69
140	6.37	0.34	0.03	6.17	6.16

Burial depth = 20 mm					
Distance from middle of ring (mm)	**Experiment**	**Equipment error (±V)**	**S.D. (V)**	**MALT Vs (V)**	**Analytical Vs (V)**
0	16.66	0.38	0.02	16.16	16.19
10	16.70	0.38	0.02	16.21	16.25
20	16.95	0.38	0.02	16.37	16.41
30	17.16	0.38	0.02	16.61	16.66
40	17.60	0.38	0.02	16.81	16.88
70	15.25	0.38	0.02	14.56	14.61
80	13.50	0.38	0.02	13.00	13.03
90	12.01	0.38	0.02	11.59	11.61
100	10.74	0.38	0.02	10.41	10.42
110	9.73	0.38	0.02	9.43	9.43
120	8.87	0.38	0.02	8.61	8.61
130	8.16	0.38	0.02	7.92	7.92
140	7.55	0.38	0.02	7.33	7.33

Burial depth = 30 mm					
Distance from middle of ring (mm)	**Experiment**	**Equipment error (±V)**	**S.D. (V)**	**MALT Vs (V)**	**Analytical Vs (V)**
0	16.37	0.40	0.03	15.87	15.89
10	16.39	0.40	0.03	15.89	15.91
20	16.44	0.40	0.03	15.92	15.95
30	16.48	0.40	0.03	15.94	15.97
40	16.56	0.40	0.03	15.85	15.88
70	14.43	0.40	0.03	13.78	13.81
80	13.08	0.40	0.03	12.62	12.64
90	11.89	0.39	0.03	11.49	11.50
100	10.81	0.39	0.03	10.47	10.48
110	9.90	0.39	0.03	9.58	9.58
120	9.09	0.39	0.03	8.81	8.81
130	8.40	0.39	0.03	8.15	8.15
140	7.79	0.39	0.03	7.57	7.57

Burial depth = 40 mm					
Distance from middle of ring (mm)	**Experiment**	**Equipment error (±V)**	**S.D. (V)**	**MALT Vs (V)**	**Analytical Vs (V)**
0	15.70	0.40	0.03	15.23	15.23
10	15.68	0.40	0.03	15.22	15.22
20	15.65	0.40	0.03	15.17	15.18
30	15.60	0.40	0.03	15.07	15.08
40	15.49	0.40	0.03	14.84	14.86
70	13.57	0.40	0.03	13.01	13.02
80	12.51	0.40	0.03	12.10	12.11
90	11.55	0.40	0.03	11.19	11.20
100	10.67	0.40	0.03	10.33	10.33
110	9.86	0.40	0.03	9.55	9.55
120	9.13	0.40	0.03	8.85	8.85
130	8.49	0.40	0.03	8.23	8.23
140	7.92	0.39	0.03	7.69	7.68

Burial depth = 100 mm					
Distance from middle of ring (mm)	**Experiment**	**Equipment error (±V)**	**S.D. (V)**	**MALT Vs (V)**	**Analytical Vs (V)**
0	10.60	0.44	0.03	10.47	10.48
10	10.58	0.44	0.03	10.45	10.46
20	10.51	0.44	0.03	10.37	10.38
30	10.39	0.44	0.03	10.25	10.26
40	10.30	0.44	0.03	10.09	10.10
70	9.56	0.44	0.03	9.35	9.36
80	9.18	0.44	0.03	9.04	9.05
90	8.83	0.44	0.03	8.72	8.73
100	8.50	0.44	0.03	8.39	8.40
110	8.15	0.44	0.03	8.06	8.07
120	7.80	0.44	0.03	7.73	7.73
130	7.48	0.44	0.03	7.41	7.41
140	7.15	0.44	0.03	7.10	7.10

b) Thin Ring

radius of ring (from axis)= 50mm
rod radius = 0.78mm
Thickness of ring = 1.56mm

Burial depth = 20 mm					
Distance from middle of ring (mm)	**Experiment**	**Equipment error (±V)**	**S.D. (V)**	**MALT Vs (V)**	**Analytical Vs (V)**
0	13.82	0.32	0.03	13.71	13.74
10	13.91	0.32	0.03	13.77	13.81
20	14.18	0.32	0.03	13.98	13.99
30	14.50	0.32	0.03	14.24	14.25
40	14.90	0.32	0.03	14.37	14.37
70	11.41	0.32	0.03	11.07	11.10
80	9.85	0.32	0.03	9.69	9.73
90	8.74	0.32	0.03	8.57	8.61
100	7.78	0.32	0.03	7.68	7.71
110	7.04	0.32	0.03	6.95	6.97
120	6.42	0.32	0.03	6.35	6.36
130	5.92	0.32	0.03	5.85	5.85
140	5.49	0.32	0.03	5.41	5.42

Burial depth = 30 mm					
Distance from middle of ring (mm)	**Experiment**	**Equipment error (±V)**	**S.D. (V)**	**MALT Vs (V)**	**Analytical Vs (V)**
0	13.41	0.33	0.04	13.26	13.31
10	13.40	0.33	0.04	13.27	13.33
20	13.47	0.33	0.04	13.30	13.36
30	13.52	0.33	0.04	13.30	13.33
40	13.49	0.33	0.04	13.10	13.13
70	10.86	0.33	0.04	10.56	10.60
80	9.60	0.33	0.04	9.49	9.54
90	8.66	0.33	0.04	8.56	8.60
100	7.85	0.33	0.04	7.77	7.79
110	7.17	0.33	0.04	7.09	7.11
120	6.58	0.33	0.04	6.51	6.53
130	6.10	0.33	0.04	6.02	6.03
140	5.65	0.33	0.04	5.59	5.60

Burial depth = 40 mm					
Distance from middle of ring (mm)	**Experiment**	**Equipment error (±V)**	**S.D. (V)**	**MALT Vs (V)**	**Analytical Vs (V)**
0	12.59	0.34	0.04	12.50	12.56
10	12.50	0.34	0.04	12.48	12.55
20	12.49	0.34	0.04	12.41	12.48
30	12.45	0.34	0.04	12.25	12.33
40	12.22	0.34	0.04	11.96	12.03
70	10.19	0.34	0.04	9.95	10.02
80	9.25	0.34	0.04	9.14	9.19
90	8.48	0.34	0.04	8.38	8.42
100	7.78	0.34	0.04	7.69	7.72
110	7.18	0.34	0.04	7.08	7.10
120	6.64	0.34	0.04	6.55	6.57
130	6.15	0.34	0.04	6.08	6.10
140	5.70	0.34	0.04	5.68	5.69

APPENDIX 9

Derivation of the Potential Generated by a Ring

Note: This derivation was developed by Dr. Jinxi Ma, Manager, of Analytical R&D from Safe Engineering Services & Technologies Ltd.

The following is the derivation of the potential due to a ring of radius a buried at a depth of h in a uniform soil with a resistivity ρ. Let us first assume the soil type is an infinite space with a resistivity ρ instead of a uniform soil (half space). Figure A9.1 shows the configuration. Assuming the total current injected into the ring is I, then the per unit length leakage current along the ring is $I/(2\pi a)$. Therefore for a short length dl ($=ad\varphi$), the leakage current dI is

$$dI = dl\frac{I}{2\pi a} = (ad\varphi)\frac{I}{2\pi a} = \frac{Id\varphi}{2\pi} \tag{A9.1}$$

When the observation point is on the axis of the ring (see Figure 1), the potential due to dl is

$$dV = \frac{\rho dI}{4\pi}\frac{1}{\sqrt{h^2+a^2}} = \frac{\rho}{4\pi}\frac{Id\varphi}{2\pi}\frac{1}{\sqrt{h^2+a^2}} = \frac{\rho I d\varphi}{8\pi^2}\frac{1}{\sqrt{h^2+a^2}} \tag{A9.2}$$

Integrating along the ring will give us the potential at the observation point due to the whole ring:

$$V = \frac{\rho I}{8\pi^2}\frac{1}{\sqrt{h^2+a^2}}\int_0^{2\pi} d\varphi = \frac{\rho I}{4\pi}\frac{1}{\sqrt{h^2+a^2}} \tag{A9.3}$$

Now, for the practical uniform soil (half space), we can use the method of image. Basically, we consider that there is another ring above the earth surface with a height h, and that the air above the earth surface is replaced with soil having the same resistivity ρ. This is an equivalent problem of the original one because it satisfies the same boundary conditions and has the same source in the soil as the original problem. The solution is simple. At the observation point, we have twice the contribution as due to one ring in an infinite space.

Therefore, for a ring of radius a buried at a depth of h in a uniform soil with resistivity ρ, the potential at the observation point which is on the axis of the ring and on the earth surface is

$$V = \frac{\rho I}{2\pi} \frac{1}{\sqrt{h^2 + a^2}} \tag{A9.4}$$

If the observation is not on the axis of the ring, then in (2) the distance factor $\sqrt{h^2 + a^2}$ should be replaced by $\sqrt{h^2 + a^2 + r^2 - 2ra\sin\varphi}$, where r is the distance between the observation point on the earth surface and the axis of the ring. Therefore, the potential due to the whole ring in this case is

$$V = \frac{\rho I}{8\pi^2} \int_0^{2\pi} \frac{d\varphi}{\sqrt{h^2 + a^2 + r^2 - 2ra\sin\varphi}} \tag{A9.5}$$

For uniform soil (half space), V should be twice as shown in Equation (5). We can rewrite the potential due to the ring in a uniform soil as

$$V = \frac{\rho I}{4\pi^2 R} \int_0^{2\pi} \frac{d\varphi}{\sqrt{1 - A\sin\varphi}} \tag{A9.6}$$

where

$$R = \sqrt{r^2 + h^2 + a^2} \text{ and } A = \frac{2ra}{r^2 + h^2 + a^2} \tag{A9.7}$$

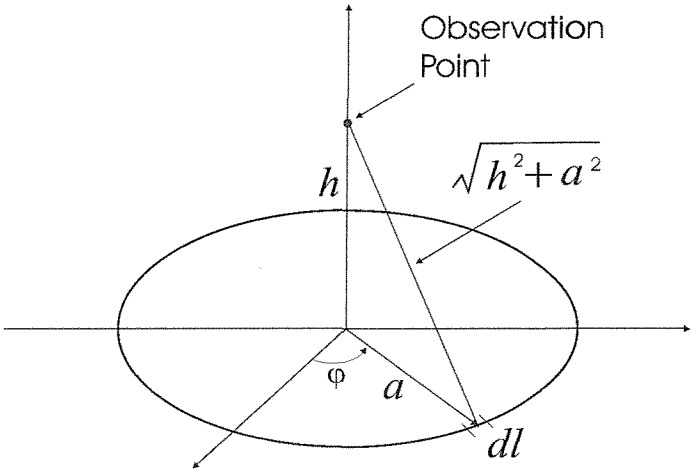

Figure A9.1